جامعة سيدي محمد بن عبد الله بفاس
ⵜⴰⵙⴷⴰⵡⵉⵜ ⵙⵉⴷⵉ ⵎⵓⵃⵎⴷ ⴱⵏ ⵄⴱⴷⵍⵍⴰⵀ ⴱ ⴼⴰⵙ
UNIVERSITÉ SIDI MOHAMED BEN ABDELLAH DE FES

كلية العلوم والتقنيات فاس
ⵜⴰⵖⵡⵍⵓⵎⵜ ⵏ ⵜⵙⵏⵜⵉⵙⵉⵏ ⴷ ⵜⵙⵙⵏⵉⵡⵉⵏ ⴼⴰⵙ
FACULTÉ DES SCIENCES ET TECHNIQUES DE FÈS

Centre d'Études Doctorales : Sciences et Techniques et Sciences Médicales

N° d'ordre 102 / 2021

THÈSE DE DOCTORAT

Présentée par

Mr. Naoufal EL YOUSSFI

Spécialité : Génie Électrique

Sujet de la thèse :

"Estimation and control of the lateral dynamics of an automotive vehicle"

Thèse présentée et soutenue le 25/12/2021 devant le jury composé de :

Prénom Nom	Titre	Établissement	
Pr. Najia ES-SBAI	PES	Faculté des Sciences et Techniques, Fès	Présidente
Pr. Abdelhamid RABHI	PH	Université de Picardie Jules Verne, MIS, Amiens	Rapporteur
Pr. Ahmed KHALLAAYOUN	PH	Université Al Akhawayn, Ifrane	Rapporteur
Pr. Ismail BOUMHIDI	PES	Faculté des Sciences Dhar El Mahraz, Fès	Rapporteur
Pr. Houcine CHAFOUK	PES	Université de Rouen Normandie, ESIGELEC, Rouen	Examinateur
Pr. Karima EL HAMMOUMI	PH	École Supérieure de Technologie, Fès	Examinatrice
Pr. Rachid EL BACHTIRI	PES	École Supérieure de Technologie, Fès	Directeur de thèse

Laboratoire d'accueil : Technologies et Services Industriels (TSI)

Établissement d'accueil : École Supérieure de Technologie de Fès

Estimation and control of the lateral dynamics of an automotive vehicle

Naoufal El Youssfi

Résumé

Cette thèse s'inscrit dans la thématique de la sécurité routière pour aborder les questions liées à l'évolution des moyens de transport, leur gestion et leur sécurité. Les véhicules d'aujourd'hui sont de plus en plus équipés de divers systèmes (passifs ou actifs) destinés à améliorer la sécurité, le confort des passagers et l'aide à la conduite. Cependant, malgré la mise en place de ces dispositifs dans la majorité des véhicules actuels, une proportion importante des accidents mortels est due à la perte de contrôle des véhicules automobiles. Ce constat nous amène à réfléchir sur la fiabilité des différents composants et sur le besoin potentiel d'améliorer et de développer ces systèmes de sécurité pour détecter et corriger en temps réel les problèmes liés à la perte de contrôle et à la stabilité des véhicules automobiles. En s'appuyant sur les outils existant en mathématiques et en automatique, l'évolution des techniques et des connaissances actuelles offre de nouvelles solutions pour améliorer et modifier les systèmes de commande automobile. L'objectif de notre thèse est de synthétiser des techniques de Commande Tolérante aux Défauts (FTC) qui prennent automatiquement en compte l'effet de certains types de défauts pouvant survenir sur les capteurs ou les actionneurs tout en gardant le véhicule automobile stable et en évitant les situations de conduite critiques. Ces techniques de commande sont conçues à partir de données sur les états et les défauts fournies par les observateurs. Le système de la dynamique latérale du véhicule automobile est globalement représenté par le modèle flou Takagi-Sugeno (T-S). Cette représentation est largement utilisée dans les problèmes de commande et d'estimation des systèmes non linéaires. Elle est basée sur la décomposition du comportement dynamique du système non linéaire en un nombre fixe de régions, et chaque région est caractérisée par un sous-modèle linéaire. Le comportement général du système est représenté en considérant la contribution de chaque sous-modèle à l'aide des fonctions d'appartenance. La stabilité du modèle flou T-S est analysée par l'approche de Lyapunov ; les conditions appropriées pour la conception des commandes et des observateurs sont fournies sous forme des Inégalités Matricielles Linéaires (LMIs), qui peuvent être résolues aisément par des outils spécifiques (solveurs de LMI).

Mots clés: Véhicule automobile, dynamique latérale, Modèle flou Takagi-Sugeno (T-S), Estimation de Défaut (FE), Commande Tolérante aux Défauts (FTC).

Abstract

This thesis is part of the road safety topic. It addresses issues related to the evolution of transport means, their management and their safety. Today, vehicles are increasingly equipped with various systems (passive or active) designed to improve safety, passenger comfort and driving assistance. Despite installing these devices in most current vehicles, a significant proportion of fatal accidents are due to the loss of control of automotive vehicles. This observation leads us to reflect on the reliability of the various components and the potential need to improve and develop these safety systems to detect and correct the problems inherent in the loss of control and stability of automotive vehicles in real-time. Building on existing tools in mathematics and automation, the evolution of current techniques and knowledge offers new solutions to improve and modify automotive control systems. The objective of our thesis is to synthesise Fault-Tolerant Control (FTC) techniques that automatically take into account the effect of some types of faults that may occur on sensors or actuators while keeping the automotive vehicle stable and avoiding critical driving situations. These control techniques are designed using state and fault data provided by observers. The lateral dynamics system of the automotive vehicle is globally represented by the Takagi-Sugeno (T-S) fuzzy model. This representation is widely used in control and estimation problems of non-linear systems. It is based on the decomposition of the dynamic behaviour of the non-linear system into a fixed number of regions. Each region is characterised by a linear sub-model. The overall behaviour of the system is represented by considering the contribution of each sub-model using membership functions. The stability of the T-S fuzzy model is analysed using the Lyapunov approach. The appropriate conditions for the design of controls and observers are provided in the form of Linear Matrix Inequalities (LMIs), which can be solved simply by specific tools (LMI solvers).

Keywords: Automotive vehicle, lateral dynamics, Takagi-Sugeno (T-S) fuzzy model, Fault Estimation (FE), Fault-Tolerant Control (FTC).

Acknowledgements

I would like to express my gratitude and sincere thanks to my thesis director, **Mr Rachid El Bachtiri**, for taking me under his responsibility during these years. His calmness, good humour, and support in difficult moments allowed me to work in very pleasant conditions. He was always present to answer my questions and gave me great autonomy in my work. I am also very grateful for his moral and human support and his precious help in writing this thesis manuscript.

I would like to thank **Mrs Najia Es-Sbai**, Professor at the Faculty of Sciences and Techniques of Fez, for having accepted to chair the jury of this thesis and participate in the examination of this work.

I am very grateful to **Mr Ismail Boumhidi**, Professor at the Faculty of Sciences Dhar El Mahraz of Fez, **Mr Abdelhamid Rabhi**, Professor at the University of Picardie Jules Verne of Amiens and **Mr Ahmed Khallaayoun**, Professor at the University of Al Akhawayn of Ifrane, for having agreed to report on this work and for having honoured me with their participation in the jury. I have no doubt that their criticisms and remarks to bring to this manuscript.

I also address my sincere thanks to **Mrs Karima El Hammoumi**, Professor at the Higher School of Technology of Fez and **Mr Houcine Chafouk**, Professor at the University of Rouen Normandy, for having accepted to participate in this jury and to examine this work.

Many thanks to all the professors who have taught me during my university career. My thanks also go to my colleagues, friends and PhD students that I worked with during my thesis years, especially Redouane Chaibi, Imane Idrissi, Taha Zoulagh, Hicham El Aiss and Yassine Fadili. Thank you for helping me in my research, sharing useful ideas and information, and supporting me morally during my studies.

I would like to thank Mr Ahmed El Hajjaji, Professor at the University of Picardie Jules Verne of Amiens, for hosting me in his team COVE "Control and Vehicles" of the Modelling, Information & Systems laboratory (MIS-Lab) to perform a research internship in 2018.

Finally, I would like to express my gratitude to my beloved parents, Malika and Ali, for their encouragement and unconditional support since I was born. To my darling wife Najlae, for her patience and support throughout this thesis. To my dear sisters Asmae and Ilham and my dear brothers Soufiane and Mohamed for their daily support and immense availability. You have been, for me, a strength of mind, a true source of inspiration and an example of love to accomplish this thesis.

Thank you all !!

Dedicated to
my parents Ali and Malika,
my wife Najlae,
my sisters Asmae & Ilham,
my brothers Soufiane & Mohamed,
all my family . . .

Contents

List of Figures

List of Tables

List of Abbreviations

FTC	**F**ault-**T**olerant **C**ontrol
FDD	**F**ault **D**etection and **D**iagnosis
FD	**F**ault **D**etection
AFTC	**A**ctive **F**ault-**T**olerant **C**ontrol
PFTC	**P**assive **F**ault-**T**olerant **C**ontrol
FDI	**F**ault **D**etection and **I**solation
FL	**F**uzzy **L**ogic
FLS	**F**uzzy **L**ogic **S**ystems
LPV	**L**inear **P**arameter-**V**arying
PIM	**P**seudo-**I**nverse **M**ethod
AI	**A**rtificial **I**ntelligence
ANN	**A**rtificial **N**eural **N**etwork
UIO	**U**nknown **I**nput **O**bserver
EsA	**E**igen **s**tructure **A**ssignment
T-S	**T**akagi-**S**ugeno
PDC	**P**arallel **D**istributed **C**ompensation

List of Notations

I	Identity matrix of appropriate dimension
0	Null matrix of appropriate dimension
$X > 0$	Symmetric positive definite X-matrix
$X \geq 0$	Symmetric positive semi-definite X-matrix
X^T	Transpose of the matrix X
$X^\dagger$	Pseudo-inverse of X
X^{-1}	Inverse of matrix X
$sym(X)$	$X + X^T$
$diag\{X_1, \ldots, X_m\}$	Diagonal block matrix
$\begin{bmatrix} X_{11} & X_{12} \\ * & X_{22} \end{bmatrix}$	Symmetric matrix, symbol "$*$" represents X_{12}^T

List of Symbols

β	side-slip angle	[rad]
δ_f	steering angle	[rad]
ψ	suspended mass yaw angle	[rad]
ϕ	suspended mass roll angle	[rad]
α_f / α_r	front/rear wheel side-slip angle	[rad]
m_v / m_s	total/suspended mass of the vehicle	[kg]
l_f / l_r	front/rear axle distance from the vehicle's centre of gravity	[m]
h_ϕ	height of the centre of gravity with respect to the roll axis	[m]
v_v	vehicle speed	[m/s]
v_x	vehicle longitudinal velocity ($\approx v_v$)	[m/s]
v_y	vehicle lateral velocity ($\approx \beta.v_x$)	[m/s]
F_f^x / F_r^x	front/rear wheel longitudinal force	[N]
F_f^y / F_r^y	front/rear wheel lateral force	[N]
I_x	roll axis moment of inertia	[kg m^2]
I_z	inertia moment at the vehicle's centre of gravity	[kg m^2]
C_ϕ	combined roll damping coefficient	[N m s/rad]
K_ϕ	combined roll stiffness coefficient	[N m/rad]
g	earth's gravity acceleration	[m s^{-2}]

General introduction

1 Framework

This work has been carried out during the thesis preparation at the Industrial Technologies and Services Laboratory (Lab-TSI), Higher School of Technology (EST-Fez) in order to obtain Doctorate degree from the Doctoral Studies Centre in Engineering Sciences and Techniques (CED-STI), Faculty of Sciences and Techniques (FST-Fez), Sidi Mohammed Ben Abdellah University (USMBA), under the direction of Professor Rachid El Bachtiri.

2 Background and problematic

This thesis entitled **"Estimation and control of the lateral dynamics of an automotive vehicle"** is a part of the road safety research area. Works relating to road transport are the subject of careful attention and present an increasing interest for laboratories, researchers, and automotive manufacturers. Indeed, several national and international research projects have been carried out to address challenges related to the development and evolution of transport means, their management, and their safety.

The automotive vehicle is an indispensable element in improving our daily life, allowing everyone to move more freely. It is therefore easy to imagine the economic and commercial stakes involved. Since its appearance in the 19^{th} century during the industrial revolution, the automotive vehicle has undergone tremendous changes in all areas; from the improvement of mechanical structures and mechanisms to the rapid development of energy, microelectronics, computer and communication technologies during the recent years. The numerous automakers and their capacity for innovation generate intense technological competition. Nowadays, the transformation of automotive vehicles is important so that they have the characteristics of being electric, intelligent and networked.

From the road safety point of view, since the introduction of electronics in automotive vehicles at the end of the 20^{th} century, many new systems and devices were designed to improve safety, passenger comfort, and driver assistance have been incorporated in new automotive vehicles. These systems can be divided into two groups:

- Passive safety systems are all automotive vehicle elements that reduce the effects of an accident and are triggered without control. Among these elements, we can find Airbags, which are bags containing an expansive gas designed to inflate extremely quickly in the event of a crash. Their purpose is to protect

passengers and prevent them from violently hitting some vehicle accessories. The seat belt that was first introduced and installed on Volvo cars in 1959 is also a passive safety system (Håland, 2006); it is a device that limits the uncontrollable motions of a vehicle's occupants during an impact and prevents them from being ejected. Recently, the European Commission aimed to introduce the E-call system in all vehicles distributed in the European Union (Guilbot, 2014), which is an automatic emergency call system that allows a crashed vehicle to contact the emergency services immediately and inform them of its precise location, whether its passengers are conscious or not. In general, the vehicle body structure's deformation is designed to absorb the maximum amount of energy during a collision. Thus, the front, rear and side parts of a vehicle are bumpers that absorb shocks. Also, the dashboard, steering wheel and all controls are made of shock-absorbing materials to avoid injuring the driver and passengers in case of impact. Furthermore, the windshields are designed to keep in place during a collision and crumble to reduce the risk of serious cuts.

- Active safety systems are all equipment that intervene during the use of a vehicle to prevent an accident before it occurs, this equipment is permanently monitored. Therefore, it requires actuators to perform the action and sensors to adjust it. Various electronic active safety systems have been developed to assist the driver. In this aspect, we can cite the Anti-lock Braking System (ABS) (Aly et al., 2011), which ensures that the wheels do not lock during emergency braking, especially when driving in low adhesion conditions, to maintain the vehicle's steering while avoiding an obstacle. In the case without ABS, loss of control would be very rapid, not to mention the impossibility of undertaking an avoidance manoeuvre. The Adaptive Cruise Control (ACC) is also an active safety system (Marsden et al., 2001), it is an advanced version of the cruise control. It not only allows the vehicle to maintain a fixed speed, but also to control speed according to the safe distance from the vehicle that precedes it in the same track. Using radar or laser, the ACC measures the distance to the vehicle in front and adapts the speed to keep a safe distance. The Electronic Stability Program (ESP) is another successful active safety system (Farmer, 2004), also known as Electronic Stability Control (ESC), it works when the vehicle is taking a turn at high speed or when there is a sudden change in trajectory. This system keeps the vehicle on the road by braking one or more wheels. It can also reduce engine torque if the driver continues to accelerate. Recently, the Driver Drowsiness Monitoring System (DDMS) (Saini and Saini, 2014), also known as an anti-sleep system, is an electronic system that indicates to the driver when it's time to take a break. At each moment, the different data are compared in real-time with databases to detect or not a drop in concentration. The information is usually displayed by an icon such as a coffee cup, a message or a sound signal.

There are a dozen other active security systems that we cannot all present. However, despite the presence of all these systems in the majority of today's vehicles, a significant percentage of fatal accidents are due to loss of vehicle stability and control. This observation leads us to reflect on the reliability of the different components and the potential need to improve and develop these safety systems to detect and correct real-time problems related to loss of control and vehicle stability. Taking advantage of existing tools in linear and non-linear automation, the evolution of current techniques and knowledge offers new solutions to improve and modify automotive vehicles' monitoring and control systems.

The design of such in-vehicle safety control systems requires precise knowledge of the dynamic parameters and their evolution in real-time. Instrumental sensors can directly determine these parameters. However, the use of these sensors is subject to some constraints, namely their lack of reliability, their high cost, the degradation and loss of signals in particular weather conditions, and, in some cases, the unavailability of these sensors. Therefore, vehicle parameters can be estimated using only accessible and available measurements. Furthermore, the vehicle is a complex system subject to many uncertainties, disturbances, and sometimes faults in actuators, sensors, or the system itself. It is well-known that conventional control strategies such as PID or fixed gain cannot adapt when these abnormalities occur. Thus, the controller must be designed to assist the driver in the presence of uncertainties and disturbances and to ensure that the vehicle remains stable even when various faults occur. This last task is commonly referred to as Fault-Tolerant Control (FTC) (Isermann, 2006; Shen et al., 2017).

3 Objective

Our main objective in this thesis is to propose, develop and apply methods to accurately estimate and control the non-linear system of automotive vehicle lateral dynamics. In addition, Fault-Tolerant Control (FTC) laws are generated using the information provided by observers, which aim to maintain the automotive vehicle's stability and automatically limit the impact of some faults that may occur on sensors or actuators in order to avoid critical driving situations. Two models of the lateral dynamics of the automotive vehicle are used in this thesis, the first only takes in consideration lateral speed and yaw angle as state variables, while the second also takes into account roll motions (Doumiati et al., 2012; Rajamani, 2011). With these models, the advantage is related to the simplicity and linearity of the structure. However, the vehicle is generally subject to strong parametric variations (mass, tyre/ground contact, slip angle, tyre forces, etc.), making the tyres' behaviour non-linear (Oudghiri, 2008). Therefore, the linear model becomes unsuitable for predicting the system's outputs and for analysing its behaviour. To overcome this, the solution is to use complete models where the automotive vehicle is represented globally by Takagi-Sugeno (T-S) fuzzy models. This representation is widely used in the problems of control and estimation of non-linear

systems, which consists of a set of linear models linked by an interpolation structure represented by non-linear membership functions (Takagi and Sugeno, 1985; Wang, 1994; Tanaka et al., 1998; Babuška, 2012; Bede, 2013; Chadli and Borne, 2013; Benzaouia and Hajjaji, 2016). The stability of T-S models is analysed using the Lyapunov function (Tanaka et al., 2003). The appropriate conditions for the design of controllers and observers are provided as Linear Matrix Inequalities (LMIs), which can be solved simply by specific tools (LMI toolbox or YALMIP).

4 Thesis structure

The works developed in this thesis are structured in five chapters, as follows:

- **Chapter I:** This chapter outlines an overview of Fault Detection (FD) and Fault-Tolerant Control (FTC) techniques. After recalling some terminologies and classifications of faults, some methods for residue generation and fault isolation are presented. Then, some important approaches to FTC are discussed, classified into active and passive methods.

- **Chapter II:** This chapter presents the basic results of T-S fuzzy models for continuous systems. First of all, T-S fuzzy models and the process of obtaining them are described. Then, a set of results concerning the stability of T-S fuzzy systems is presented. Afterwards, some fuzzy observers and control laws are considered.

- **Chapter III:** This chapter is devoted to the modelling of automotive vehicle dynamics. Initially, the necessary elements for the modelling of the automotive vehicle are introduced. Then, some models of tyre/ground contact forces are presented. After that, based on a set of assumptions, some well-known automotive vehicle models are presented. This chapter contains a section on the T-S fuzzy representation of the nonlinear automotive vehicle system.

- **Chapter IV:** In this chapter, the problem of fault and state estimation for the automotive vehicle lateral dynamics system represented by T-S fuzzy model is addressed. Observers are designed in this chapter to simultaneously estimate faults and states of the system. First, using a descriptor approach, an observer is designed to estimate a perturbed system affected by actuator faults. Then, another method based on the unknown input observer is proposed to estimate an uncertain vehicle system affected by sensor and actuator faults.

- **Chapter V:** This chapter is devoted to the application of different fault tolerant control laws to assist driving. Starting with a H_∞ static output-feedback control that is robust to disturbances. Then, active fault-tolerant control laws are proposed that can automatically compensate for the impact of faults that may occur in the sensors or actuators of the automotive vehicle's lateral dynamics system, with consideration of the roll motion. These laws have the ability to maintain stability and avoid critical driving situations.

5 Contributions and publications

During this thesis, publications in various journals and conferences have been carried out and some others are in progress.

Peer-reviewed book chapter

– N. El Youssfi and R. El Bachtiri (May 19^{th}, 2020). "T-S fuzzy observers to design actuator fault-tolerant control for automotive vehicle lateral dynamics" [Online First], IntechOpen, DOI: 10.5772/intechopen.92582.

Peer-reviewed and indexed journal articles

– N. El Youssfi, T. Zoulagh, H. El Aiss, R. El Bachtiri and Z. Feng (under review). "T-S fuzzy observer and actuator fault-tolerant controller designs for descriptor systems", IEEE Transactions on Systems, Man, and Cybernetics: Systems. (Manuscript ID SMCA-20-05-1011)

– N. El Youssfi, R. El Bachtiri, T. Zoulagh and H. El Aiss (2021). "Unknown input observer design for vehicle lateral dynamics described by T–S fuzzy systems", Optim Control Appl Methods, vol. 2021, p. 01-15.
DOI:10.1002/oca.2808

– N. El Youssfi, R. El Bachtiri and H. El Aiss (2021). "T-S fuzzy observers design and actuator fault-tolerant control applied to vehicle lateral dynamics", Int. J. Digital Signals and Smart Systems, vol. 5, no. 2, p. 105-124.
DOI: 10.1504/IJDSSS.2020.10032267

– N. El Youssfi, R. El Bachtiri, T. Zoulagh and H. El Aiss (2020). "Relaxed state and fault estimation for vehicle lateral dynamics represented by T–S fuzzy systems", Journal of Control Science and Engineering, vol. 2020.
DOI: 10.1155/2020/8797482.

– N. El Youssfi, R. El Bachtiri, R. Chaibi and E. H. Tissir (2020). "Static output-feedback H_∞ control for T–S fuzzy vehicle lateral dynamics", SN Applied Sciences, vol. 2, no. 1, p. 101.
DOI: 10.1007/s42452-019-1897-y.

– N. El Youssfi, M. Oudghiri and R. El Bachtiri (2019). "Vehicle lateral dynamics estimation using unknown input observer", Procedia computer sciences, vol. 148, p. 502-511.
DOI: 10.1016/j.procs.2019.01.063.

– N. El Youssfi, M. Oudghiri and R. El Bachtiri (2018). "Control design and sensors fault-tolerant for vehicle dynamics (a selected paper from SSD'17)", Int. J. Digital Signals and Smart Systems, vol. 2, no. 1, p. 50-67.
DOI: 10.1504/IJDSSS.2018.090874

Peer-reviewed international conference articles (Indexed in Scopus and WoS)

- N. El Youssfi, M. Oudghiri, A. Aitouche and R. El Bachtiri. "Fuzzy sliding-mode observer for lateral dynamics of vehicles with consideration of roll motion". IEEE - 26th Mediterranean Conference on Control and Automation, p. 861-866, Zadar, Croatia, 2018.
  DOI: 10.1109/MED.2018.8442946

- N. El Youssfi, M. Oudghiri, R. El Bachtiri and H. Chafouk. "H_∞ yaw and roll sensors fault-tolerant control for vehicle lateral dynamics". IEEE - International Conference on Electronics, Control, Optimization and Computer Science (ICECOCS), p. 01-06, Kenitra, Morocco, 2018.
  DOI: 10.1109/ICECOCS.2018.8610653

- N. El Youssfi, R. El Bachtiri and R. Chaibi. "Fuzzy state and output feedback control for vehicle lateral dynamics". Proceeding of International Meeting on Advanced Technologies in Energy and Electrical Engineering, Hamad bin Khalifa University Press, vol. 2019, no. 1, p. 26, Fez, Morocco.
  DOI: 10.5339/qproc.2019.imat3e2018.26

- N. El Youssfi, M. Oudghiri and R. El Bachtiri. "Actuator fault estimation and fault-tolerant control for vehicle lateral dynamics". 2nd International Conference on Applied Mathematics (ICAM), AIP Conference Proceeding, vol. 2074, no. 1, p. 020027, Fez, Morocco, 2018.
  DOI: 10.1063/1.5090644

- N. El Youssfi, M. Oudghiri and R. El Bachtiri. "Observer-based fault-tolerant control for vehicle lateral dynamics". IEEE - 14th International Multi-Conference on Systems, Signals & Devices (SSD), p. 70-75, Marrakech, Morocco, 2017.
  DOI: 10.1109/SSD.2017.8166922

National conferences

- N. El Youssfi, R. El Bachtiri, R. Chaibi, I. Idrissi and M. Khanfara. "Commande et Estimation des Systèmes T-S : Application au Véhicule Automobile". Quatrième Rencontre Nationale des Jeunes Chercheurs en Sciences de l'Ingénieur RNJC-SI'18, Fez, Morocco, December, 2018.

- N. El Youssfi, M. Oudghiri and R. El Bachtiri. "État de l'art sur le contrôle multi-modèle de la dynamique du véhicule automobile". Rencontre Scientifique des Jeunes Chercheurs en Énergies Renouvelables, Fez, Morocco, October, 2018.

- N. El Youssfi, M. Oudghiri and R. El Bachtiri. "H_∞ sensor fault-tolerant control of nonlinear T-S systems : application to vehicle dynamics". Workshop on Innovation and Emergent Technologies (WIET), Fez, Morocco, December 2017.

– N. El Youssfi, M. Oudghiri and R. El Bachtiri. "Une stratégie de commande tolérante aux défauts basée sur les observateurs de Luenberger, appliquée aux véhicules automobiles". Journée de Recherche Inter-Laboratoire JRIL'17, Fez, Morocco, December, 2017.

Chapter I

Overview of fault detection and fault-tolerant control techniques

I.1 Introduction

With the development of industrial equipment and the abundance of advanced engineering systems in various fields (e.g. finance, aerospace, automotive, bio-medical, telecommunications, etc.), modern technology systems have become more and more complex, which means that there is an increased risk that faults will lead to undesirable behaviour. These faults affect a system and change its functional properties; they can eventually produce degradation of the process performances and sometimes even lose its stability (Chen and Patton, 2012). Therefore, it is important to consider the operational safety aspect, not only for systems used in sensitive sectors such as nuclear power plants, chemical installations and aeronautics in which damage caused by faults can lead to loss of life, material, economics and environment, but also for any system used in other fields.

Accordingly, online Fault Detection and Isolation (FDI) play an indispensable role in any industry-wide process, whatever their security levels and costs. Indeed, early detection of process faults can help to avoid abnormal progression of events. In this context, many researchers have dedicated their work to FDI in industrial systems. We mention the following main books: In (Isermann, 2006), the author presented an introduction to advanced methods for fault detection. He discussed both model-free fault detection methods, such as limit and trend checking, and model-based methods, such as Fourier analysis, correlation and wavelets. Whereas, the authors in (Meskin and Khorasani, 2011) have discussed the design and development of FDI algorithms based on a geometric approach for driverless vehicles. In (Zhang et al., 2012), the authors examined the theory and technology of fault estimation for dynamic systems; they provided a comprehensive and systemic framework of fault estimation together with accommodation for continuous and discrete systems. While in (Chen and Patton, 2012), the authors discussed many important robust approaches to model-based FDI and their applications. Thus, although online fault detection and monitoring are of great interest and necessary to improve safety-critical systems' reliability, they do not

guarantee safe and reliable functioning. To overcome this restriction, a control strategy called Fault-Tolerant Control (FTC) law is required to achieve the correct operation and keep an acceptable level of performance (Stetter et al., 2020). FTC's purpose is to adjust immediately after a fault occurrence with optimal feedback to ensure that a small defect in one subsystem does not become a serious fault in the whole system. For non-critical systems, online fault detection and FTC techniques can improve system efficiency, maintainability, availability and reliability (Shen et al., 2017). Hence, the issue of the FTC has been widely covered in numerous publications. Authors presented the model-based analysis and design methods for FTC in (Blanke et al., 2006). They suggested these methods for processes described by analytical models, discrete event models, or those considered as quantified systems. A demonstration of FTC techniques and basics for real systems is presented in (Noura et al., 2009). In (Stetter et al., 2020), authors proposed some innovative FTC methods that can take over uncertainties and share redundant and flexible elements applied to vehicles and automated processes. Alwi et al. (2011) presented a sliding mode control design that can directly deal with actuator failures by exploiting redundancy in the aircraft. In (Shen et al., 2017), authors outlined theoretical developments and practical applications of FTC by combining adaptive control with other control methods. They applied the obtained results to complex dynamical systems, including uncertain non-linear systems with delay. In fact, many scientific articles published in literature deal with FTC and FDI's problems, some of which will be quoted throughout this chapter.

This chapter provides an overview of FD and FTC techniques. It includes a section with a reminder of some concepts and terminologies related to fault detection and diagnosis, followed by a part on fault classifications according to their modelling, location, and time evolution. The third section is dedicated to fault detection and isolation, mentioning some approaches to residual generation and fault isolation techniques. The fourth section introduces some important FTC approaches classified into active and passive methods. A chapter conclusion is included in the last section.

I.2 Diagnosis terms and fault classifications

I.2.1 Terminologies

This sub-section will clarify some of the terms needed in the diagnosis area to deepen our discussion. These terms will be defined based on these references (Isermann and Ballé, 1997; Ichalal, 2009; Sallem, 2013).

- **Fault:** is an inadmissible departure of at least one characteristic of the system from its nominal behaviour, it may affect the sensors, the actuators or the process itself. Generally, the fault is denoted by $f(t)$.
- **Failure:** is a functional fault that degrades or prevents the system's ability to accomplish its desired function(s). Indeed, it is a dysfunction of the system that makes the process operate unacceptably from the performance point of view.

- **Malfunction:** is the inability of a system to perform its required function (total shutdown), it is always the result of a failure which is itself the result of a fault:

$$Fault \longrightarrow Failure \longrightarrow Malfunction$$

- **Residual:** is a signal designed to be an indicator of functional or behavioural abnormalities, substantially zero in the absence of faults and not zero in their presence and is often denoted by $r(t)$.

- **Error:** is the difference between measured or estimated values of a variable and a theoretically correct model value.

- **Fault detection:** is the determination of system faults and the time of their occurrence.

- **Fault diagnosis:** is the determination of the type, nature, and duration of a fault. The diagnosis of process faults is the interpretation of the installation's actual situation based on sensor readings and knowledge of the system.

- **Fault isolation:** is synonymous with fault diagnosis; it can refer to hardware or software and consists of finding the source of a fault by isolating the device(s) of the faulty system.

- **Fault identification:** is the real-time estimation of the size and behaviour of an isolated fault.

- **Supervision:** is the monitoring of the correct operation of a system or activity. Process supervision can be an advanced control and diagnostic application.

- **Protection:** signifies that the system's potentially dangerous behaviour is removed and thus avoid their effects.

- **Safety:** is the confident and peaceful feeling that results from the sense that we are free from all danger. Physically, safety is the capacity of a system to present the minimum risk and not cause trouble to the persons, the equipment or the environment.

- **Reliability:** is the probability that a system will function correctly under given conditions, within a precise perimeter, and over a specific period. During this correct operation, the system adequately fulfils the required function, so that no repairs are necessary.

- **Fault tolerance:** is also known as "fault insensitivity", it is a design technique that allows a system to operate continuously without breaking down completely when a fault has occurred.

I.2.2 Fault classifications

Faults are characterised by a deviation from the system's regular operation. Generally, they are classified according to their modelling, their location and their temporal characteristics.

a. Fault modelling

Depending on its modelling, the faults can occur as additive or multiplicative faults (see Fig. I.1), due to malfunction or equipment ageing (Noura et al., 2009).

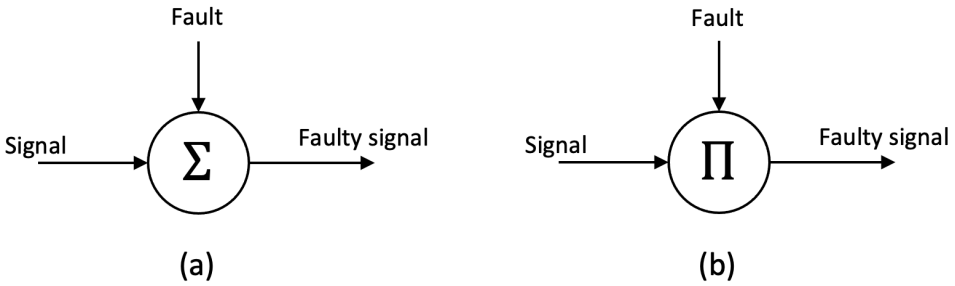

FIGURE I.1: Fault models
a- additive fault; b- multiplicative fault

Additive faults are interference signals that are added to a point in the block diagram. Normally, sensor and actuator faults are modelled as additive faults. However, component faults are modelled as multiplicative faults that introduce changes in the correlation of system output signals and modify the system's dynamic characteristics (Isermann, 2005).

b. Fault location

As can be seen in Fig. I.2, the faults are generally classified according to their location into three types (Jain et al., 2018):

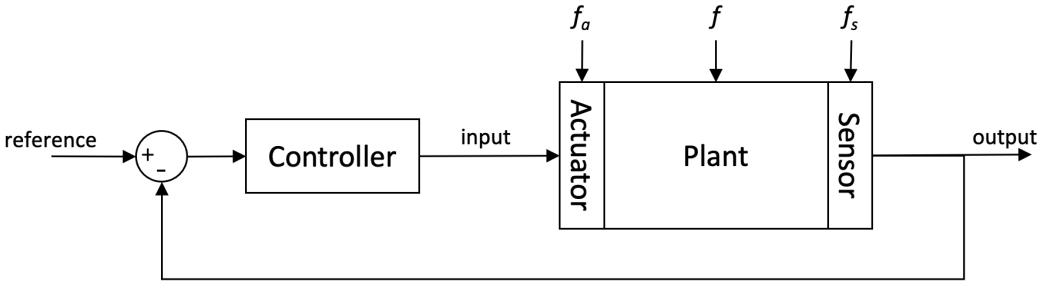

FIGURE I.2: Faults in automatic control systems

- **Sensor faults:** represent the incorrect sensor reading; they are characterised by an error in measuring a physical parameter, and sensor faults can be total or partial. A partial sensor fault (loss of precision) produces a signal with more or

less adequacy with the variable's real value to be measured, and it appears as a bias, deviation or decrease of efficiency. However, in the case of a total sensor fault (blockage), the sensor signal evaluation is impossible. This kind of fault is often noted by f_s.

- **Actuator faults:** affect the operating part and deteriorate the system's input signal. Similar to sensor faults, actuator faults represent partial or total control loss actions. In the first case, the actuator is characterised by degenerative operation, i.e. it functions nominally, but its action is barely partial. A loss of energy often characterises this phenomenon. However, a total control loss means that the actuator has become unable to control the system, for example, a valve that remains stuck in its initial position or a break/interruption of an electrical thread connecting the actuator to the system. Actuator faults are noted by f_a.

- **Plant faults:** are the faults that affect the system itself; they represent all other faults that cannot be characterised as sensor or actuator faults. They reflect a change in the system's physical parameters due to structural damage. System faults cover a large category of situations. Therefore, diagnosis of these types of faults is considered the most difficult.

c. Time characteristics of faults

Faults can be classified based on their shape and temporal characteristics, as shown in Fig. I.3, in three different forms (Alrowaie, 2015).

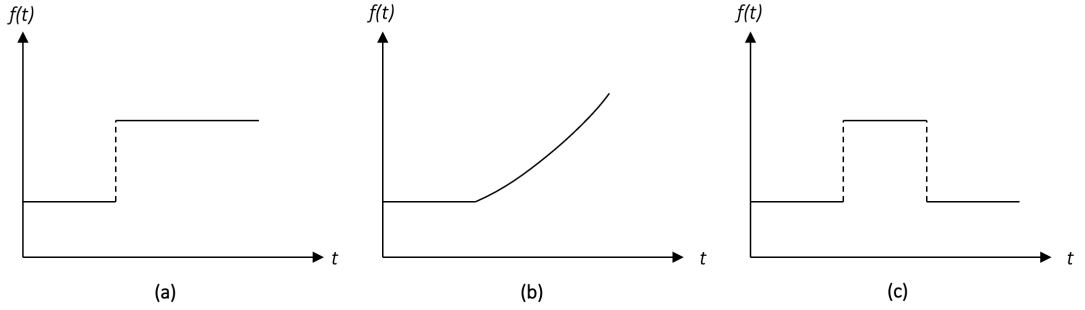

FIGURE I.3: Time evolution of a fault
a- abrupt; b- incipient; c- intermittent

- **Abrupt (or hard):** this type of fault is characterised by a discontinuous temporal reaction, which often occurs suddenly due to material damage. It is a grave fault as it usually affects the controlled system's performance and/or stability. Mathematically, it is described as follows:

$$f(t) = \begin{cases} \alpha, & t \geq t_f \\ 0, & t < t_f \end{cases} \tag{I.1}$$

where t_f is the fault occurrence time, $f(t - t_f)$ is the fault's temporal behaviour and α is the constant threshold.

- **Incipient (or soft):** this fault type has a low impact on the system, but it is difficult to detect it due to its slow temporal evolution. The following relation can express the development of this kind of fault:

$$f(t) = \begin{cases} \alpha \left(e^{\beta(t-t_f)} - 1 \right), & t \geq t_f \\ 0, & t < t_f \end{cases} \tag{I.2}$$

  β is a positive constant.

- **Intermittent:** is a sequence of abrupt faults with the particular characteristic that the signal returns to its nominal value, it randomly appears and disappears. It is often difficult to determine whether it is a fault or a disruption.

I.3 Fault detection and isolation

Today's industrial processes require a high level of availability, reliability, operational safety, and environmental protection. Hence, a fault diagnosis system is needed to detect various faults as soon as they occur and then identify them to isolate the faulty component before affecting the overall system.

In general, when speaking of fault diagnosis for monitoring dynamic systems, it refers to the FDI procedure, which necessitates obtaining characteristic signals of the monitored process operation and analysing them to deduce the system status. Signals are always determined based on the available knowledge of healthy behaviour. In recent years, the FDI problem has been the subject of a large number of results and research studies (see, for example, (Patton and Chen, 1997; Lin and Horng, 2006; Blanke et al., 2006; Isermann, 2006; Alwi et al., 2011; Meskin and Khorasani, 2011; Chen and Patton, 2012; Patton et al., 2013; Wang et al., 2013; Martinez-Guerra and Mata-Machuca, 2016; Li, 2016), and the references therein). The classification of FDI techniques is generally made according to several criteria, including the complexity of the system, the nature of the available information (quantitative or qualitative), the FDI implementation online and/or offline, the system dynamics (continuous, discrete or hybrid), the decision-making structure (centralised, decentralised or distributed), etc. From the modelling point of view, non-model-based techniques do not require any form of model information and depend only on system data. These techniques are also known as "signal-based techniques", they detect faults by testing specific properties (e.g. frequency analysis) of different measurement signals. On the other hand, there are techniques based on mathematical models that require a thorough knowledge of the system. These techniques have a wider range of application than signal-based methods. As illustrated in Fig. I.4 (Danancher et al., 2011), they include two steps: residuals generation and residuals evaluation using a decision-making scheme

(Frank, 1996; Yoon and MacGregor, 2000; Isermann, 2005; Oudghiri, 2008; You et al., 2017). In this thesis, we focus only on model-based FDI methods.

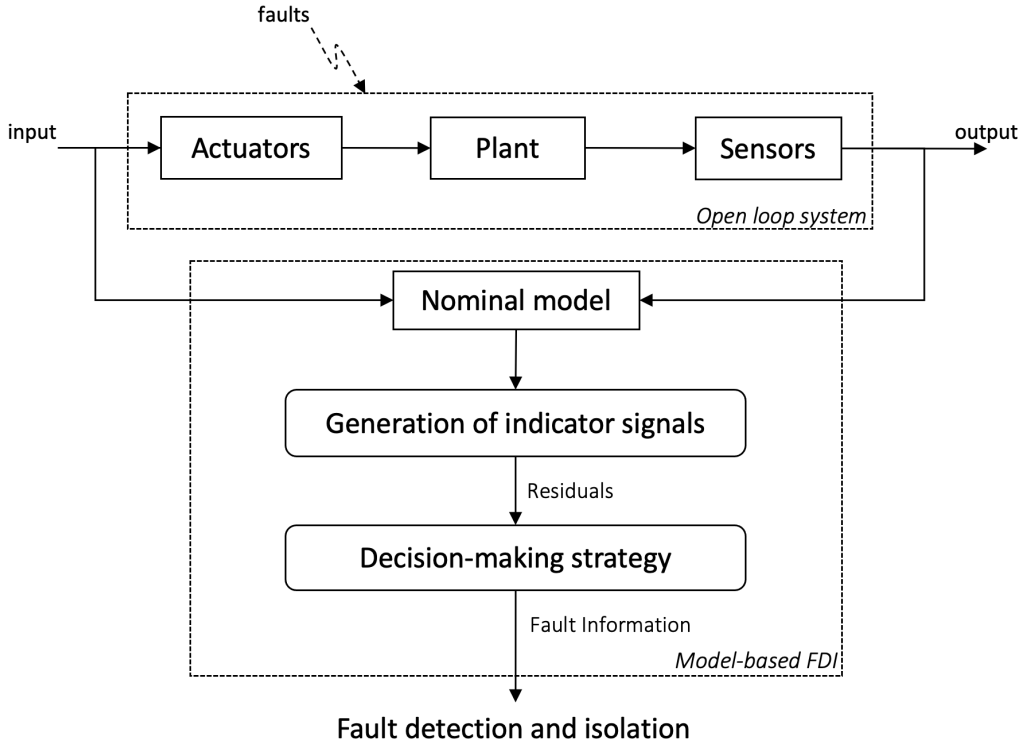

FIGURE I.4: FDI principle scheme

In the remainder of this section, the steps of the model-based FDI methods are outlined, starting with the residual generation, then fault detection, followed by fault isolation with its types.

I.3.1 Residuals generation

The residual generation is the first step in the FDI procedure. It is identified as a key problem in model-based FDI as an information processing procedure. If not designed correctly, it could lose some fault information. Several strategies have been used for the residual generation; hardware redundancy is the most traditional, consisting of doubling sensitive equipment or devices (machines, appliances, instruments, etc.) for the same vital function. This approach aims to identify, in the case of a fault, its appearance time and its precise location among all redundant elements. Although this approach is very successful in several industrial areas, it has the disadvantage of additional redundant components that require additional space to support them, plus the additional cost issue. An alternative approach to residuals generation is based on analytical redundancy, which uses redundant analytical relationships between the inputs and measured outputs of the system to generate residual signals. This approach's application necessitates a mathematical model (static or dynamic, linear or non-linear, deterministic or stochastic) of the supervised system connecting the measured inputs and outputs. These methods are often referred to as the model-based approach.

Several model-based residue generation techniques exist in literature (Basseville et al., 1993; Gertler, 1998; Patton et al., 2013), these include, observer-based approach, parity equation, and parameter identification & estimation. A comparison of these three model-based methods can be found in (Chen and Patton, 2012). The success of state-space models and the extensive use of observers in modern surveillance theory and applications make the FDI observer-based approach the most successful in this field. Therefore, particular interest will be given to this approach, which involves using state observers or filters to construct residual signals, which represent the deviations between the observed behaviour and the expected reference behaviour when the system is operating normally. Ideally, a residual should stay at zero in the absence of faults and move significantly away from zero in the presence of faults (Meskin and Khorasani, 2011; Methnani, 2012; You et al., 2017).

The residue is an indicator of system failure. For observers, the residue $r(.)$ represents the difference between the real output $y(.)$ and the estimated one $\hat{y}(.)$; it is defined for continuous systems as follows:

$$r(t) = y(t) - \hat{y}(t) \tag{I.3}$$

In practice, the residue is not exactly equal to zero in the absence of faults. This is because, during the modelling phase, several simplifying assumptions are introduced, leading to a model that does not accurately represent the real system. Besides, measurements carried out on the system are most often affected by noises. Consequently, the residual vector is written as follows:

$$r(t) = y_m(t) - \hat{y}(t) \tag{I.4}$$

with $y_m(t)$ is the measured output of the system.

Observer approaches are widely used in literature about residual generation. In this context, fault detection for uncertain linear systems is discussed in (Han et al., 2018). The authors assumed that the residual generator is perfectly realized as designed. This study considered the imprecision and uncertainty on the residual generator implementation. Authors in (Li et al., 2016) developed a universal residual generator based on the T-S fuzzy observer via Lyapunov fuzzy functions. An approach to identify faults by deriving information about fault signals, based on a defined relationship between a fault signal and the observer theory is proposed in (Jeong et al., 2019). In (Li et al., 2020), the authors examined optimal observation-based fault detection and estimation schemes for T-S fuzzy systems with process faults. The issue of fault detection based on the sliding-mode observer for a class of T-S fuzzy singular systems is investigated in (Li and Yang, 2020).

I.3.2 Fault detection

After generating the residuals, the next step in the FDI procedure is the detection, which determines the presence or absence of a fault. The detection is carried out

by evaluating the residues that are directly related to variations from inputs (actuator faults, unknown inputs, disturbances) and outputs (measurement noise, sensor faults). The fault detection process consists of residue evaluation, threshold selection, and decision making.

The residual is the signal that contains information on the duration and occurrence of the fault; it is based on the deviation between the measurements and the model's calculations. The fault detection method consists of comparing the residual value to a predefined threshold ι_{th}; if the residue exceeds the threshold value, an alarm is triggered, indicating a fault. The challenge in fault detection is defining the residuals threshold for detecting any changes without causing false alarms.

$$\begin{cases} |r(t)| \geq \iota_{th} \Longrightarrow f(t) \neq 0 \\ |r(t)| < \iota_{th} \Longrightarrow f(t) = 0 \end{cases} \tag{I.5}$$

with $f(t)$ is the fault vector.

Under ideal conditions (no model uncertainties, no noises), the residues are assumed to be zero, and they deviate from zero in the presence of faults.

A high threshold can lead to the risk of not detecting faults. Conversely, a low threshold can lead to false alarms. For this reason, several research works focus on the problem of choosing an optimal threshold that is the best compromise between a rate of non-detection and a minimum rate of false alarms. Some research in this context proposes methods using an adaptive threshold, including the following (Hashemi and Pisu, 2011; Yoon and MacGregor, 2000; Zhang et al., 2002; Casavola et al., 2005)

I.3.3 Fault isolation

When a fault is successfully detected, the next step serves to separate the others' specific fault. While one residual may be enough to detect a fault, a set of residuals (or residual vector) is often necessary for fault isolation. In literature (Patton and Chen, 1994, 1991; Chen and Patton, 2012), the following two main types of residues are obtained:

a. Structured residual sets

The set of structured residuals presents residuals sensitive to a sub-set of faults and robust to others. Let us consider for example a residual vector $r(t) \in \mathbb{R}^{n_r}$ and a fault vector $f(t) \in \mathbb{R}^{n_f}$. The m elements of $r(t)$ (denoted $r_m(t)$) are sensitive just to the l elements of the faults (denoted $f_l(t)$):

$$\begin{cases} |r_m(t)| \geq \iota_{th} \Longrightarrow \text{presence of faults } f_l(t) \\ |r_m(t)| < \iota_{th} \Longrightarrow \text{no faults } f_l(t) \text{ detected} \end{cases}, \forall t \tag{I.6}$$

where ι_{th} is the predefined threshold.

Following this procedure, a set of residues is generated to consider all possible combinations to locate each fault. The residual sensitivities are listed in a binary table called the theoretical signature table. If a residue is sensitive to a fault, the corresponding box in the table is marked with a "1", and if it is not, with a "0". Once the theoretical signature table is created, the generated residuals are compared with this table at any time to trigger the alarm corresponding to the occurrence of a fault on the affected system component (Gertler, 1992).

Several schemes are proposed in literature to design structured residuals (Gertler, 1998; Chen and Patton, 2012; Patton et al., 2013), among them are the following:

Dedicated Observer Scheme (DOS). In this scheme, the idea is to build enough observers as shown in Fig. I.5 to detect faults, the i^{th} observer is driven by the i^{th} input and all outputs, then each observer generates a residue insensitive to all faults except one. Therefore, the observer receiving a faulty measurement provides a wrong variable estimate, whereas other observers' estimates converge to the corresponding output measurements except on the faulty output. In this structure, all faults can be detected simultaneously. However, although this structure sometimes gives good results, its design remains very restricted because it does not achieve desirable performance requirements such as robustness against uncertainties and modelling noises.

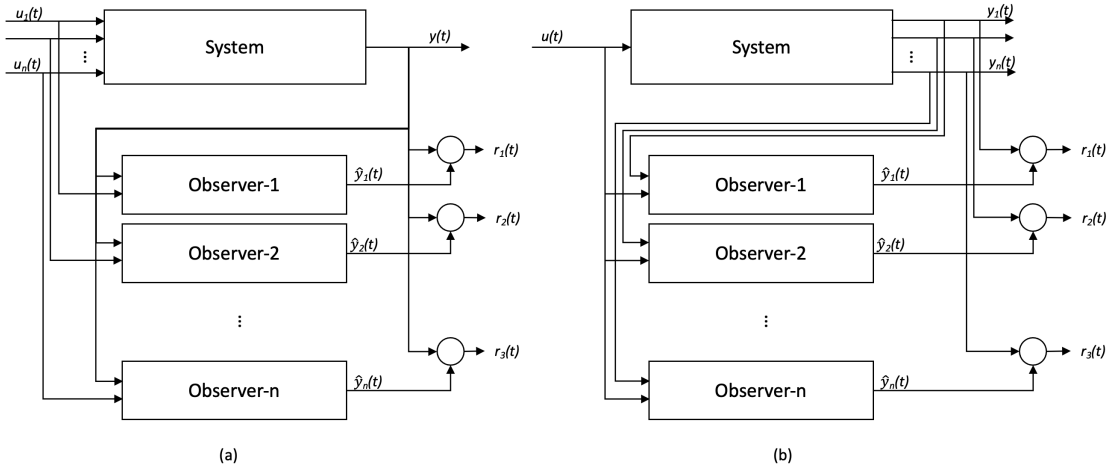

FIGURE I.5: Dedicated observer scheme to detect and isolate
(a) actuator faults; (b) sensor faults

Generalized Observer Scheme (GOS). In this scheme, the idea is to synthesize several observers as seen in Fig. I.6 to be insensitive to a specific fault. If a fault appears, all state estimates will be erroneous except those from the observer insensitive to this single fault. In this type of structure, a generalized residual set is introduced that can only detect a single fault. Despite having degrees of freedom to achieve robustness against uncertainties and model noises, this approach's problem remains in the interactions between the sub-systems. Indeed, if these interactions are weak or null, a fault will only affect the corresponding local observer's estimation. It is then possible to isolate the faulty component. On the other hand, if the interactions are high, a fault in one of the components will affect the other components' observers.

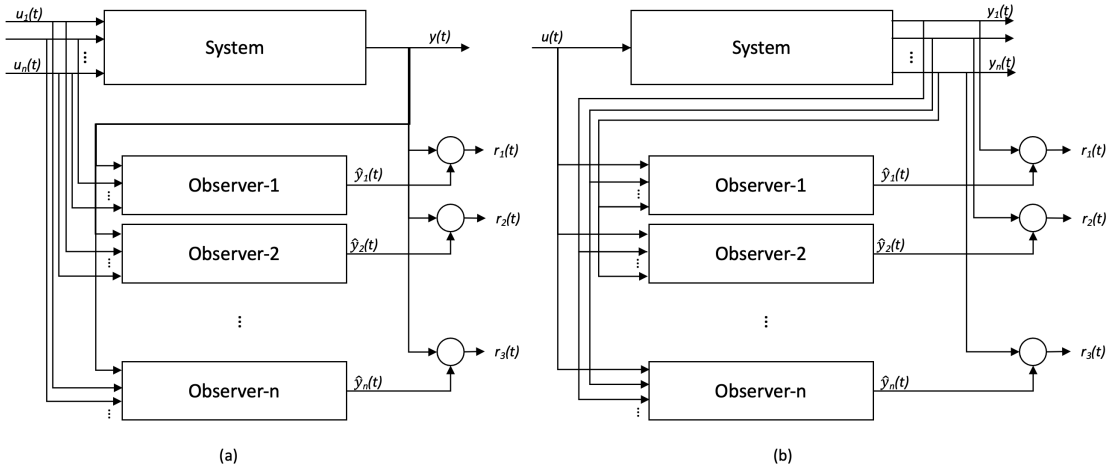

FIGURE I.6: Generalized observer scheme to detect and isolate (a) actuator faults and (b) sensor faults

The structured residual set's main benefit is that the diagnostic analysis is simplified to identify which residuals have crossed their thresholds. The threshold test can be performed separately for each residue, giving a Boolean decision table, and then the isolation task can be performed using this table.

b. Fixed direction residuals

The fixed direction residuals set is an alternative approach to isolating faults consisting of generating a residual in the vector form (directional residue vector). The residual vector is oriented in the residual space's specific direction to react to a fault that occurs (see Fig. I.7).

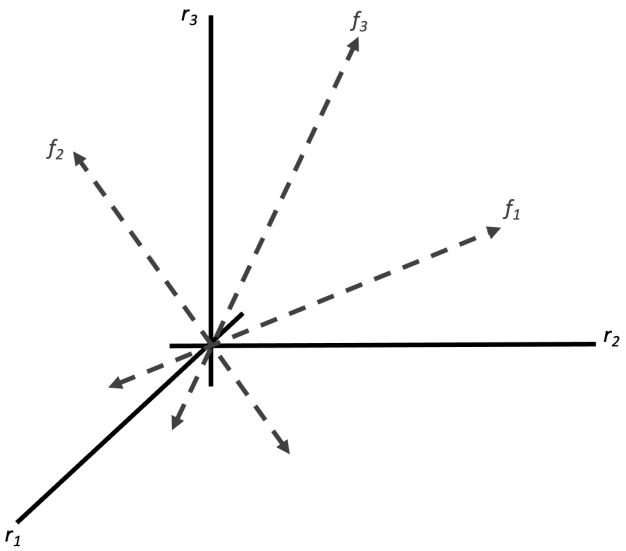

FIGURE I.7: Fixed direction residuals

The vector of fixed directional residuals $\vec{r}(t)$, for a fault $f_i(t)$, is expressed as follows:

$$\vec{r}(t|f_i) = \eta_i(t)\vec{v}_i\,, \qquad i = 1, 2, ..., n \tag{I.7}$$

where $\vec{v}_i$ is a vector named directional signature of the fault f_i in residual space and $\eta_i(t)$ is a scalar function that depends on the amplitude of the fault dynamics (Gertler, 1998; Sobhani-Tehrani and Khorasani, 2009).

The problem of fault isolation is identifying the theoretical signature closest to the real signature obtained by the residual vector calculation. In Fig. I.8, an example of a fault isolation problem using fixed direction residuals is shown. The actual residual signatures are represented by black solid lines and the theoretical directional signatures by red dotted lines.

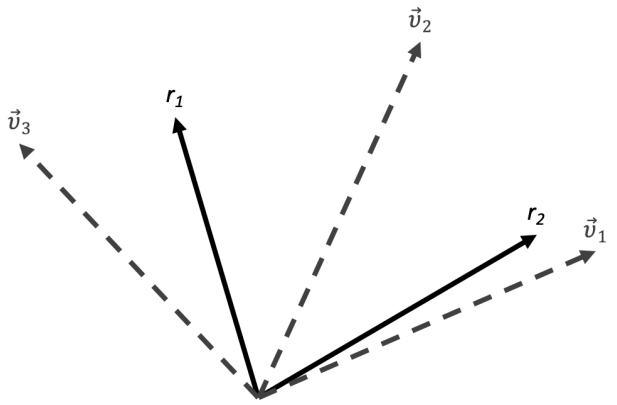

FIGURE I.8: Fault isolation using fixed direction residuals

It can be seen on Fig. I.8 that the real signature r_2 is very close to the theoretical signature of the fault f_1. This means the probability that this fault is present on the system when r_2 was calculated. Therefore, r_2 does not exactly overlap with the vector $\vec{v_1}$, perhaps because of the perturbations, which are considered less impact than the faults. On the other hand, it is harder to evaluate the residue r_1 because it is close to $\vec{v_2}$ and $\vec{v_3}$ simultaneously.

To summarize, the solvency conditions for generating a structured residual set are generally more relaxed than those for the directional residual vector, since the design objective in the latter approach is to generate a residual vector with the fault isolation condition. In contrast, in the first approach, a set of residuals is generated, and it is possible to have more design degrees of freedom (Meskin and Khorasani, 2011).

I.4 Fault-tolerant control systems

The FTC systems aim to improve reliability, availability, and safety while ensuring a permanently satisfactory performance level. For this reason, the control algorithms must be able to maintain stability and performance regardless of the occurring faults. The FTC has received tremendous attention from the research community and remains a widely followed topic of publications in recent decades. One of the first review articles in the FTC field was published in 1991 by Stengel (Stengel, 1991), which introduced the basic FTC concepts for continuous dynamical systems and also presented its applications that include artificial intelligence. In (Blanke et al., 1997), authors treated

FTC from a wider angle, covering the whole design process from interface engineering to structural implementation. A literature review on reconfigurable FTC is presented in (Zhang and Jiang, 2008), where the authors made a brief comparison of the various existing approaches to active FTC and classified them according to different criteria including design approaches and implementations. The authors examined the similarities and differences between active and passive FTCs from a philosophical and practical point of view in (Jiang and Yu, 2012), discussing the advantages and limitations of each method. FTC's strategy based on a bank of observers performing detection and isolation of sensor faults is presented in (El Youssfi et al., 2018b). This control is applied to the vehicle lateral dynamics with consideration of roll motions represented by the T-S fuzzy models. In (Sami and Patton, 2013), a description of a fault-tolerant tracking control law for non-linear systems based on robust fault estimation, the objective of this control is to compensate both actuator and sensor faults simultaneously. Generally, hundreds of references in the literature have documented FTC's problem, which cannot be fully cited.

I.4.1 Definition of fault-tolerant control systems

A system is said to be fault-tolerant when it can return to its original function with identical or degraded performances in the event of a failure. In general, a fault-tolerant system represents a more advanced function than the diagnostic unit. It consists of determining a control strategy that can maintain the nominal objectives, despite a fault's occurrence and accommodate it automatically. This type of control has the property of minimizing or even eliminating the fault effects on the system's performances to guarantee its stability and correct operation.

The general scheme of the FTC system is illustrated in the Fig. I.9 (Jain et al., 2018), it is divided into two blocks. The first is the FDI block, which monitors the system and provides the supervisor with information on the system status. It performs the tasks of detection, isolation (location determining) and identification (estimation of the size and nature) of faults. The second is the supervisor block, which in the event of a fault, evaluates the previous information and redefines the set-points and changes to be made to all actuators, sensors or control law (Achbi, 2012).

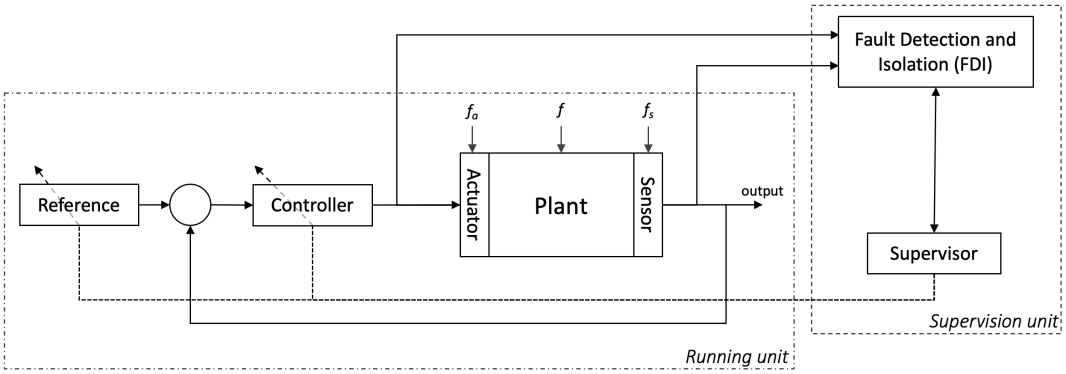

FIGURE I.9: Fault-tolerant control system principle

I.4.2 Classification of fault-tolerant control methods

The FTC is generally classified according to two different approaches: The first is the Passive Fault-Tolerant Control (PFTC). It is a robust control that may be sufficient to achieve nominal performance in the presence of a low severity fault. The second is the Active Fault-Tolerant Control (AFTC), which requires an FDI block to detect and isolate the fault. In the latter, a distinction is made between adaptation, reconfiguration and restructuring according to the quality of performance after the fault. The diagram in Fig. I.10 illustrates FTC methods classification, based on passive and active approaches (Stetter et al., 2020).

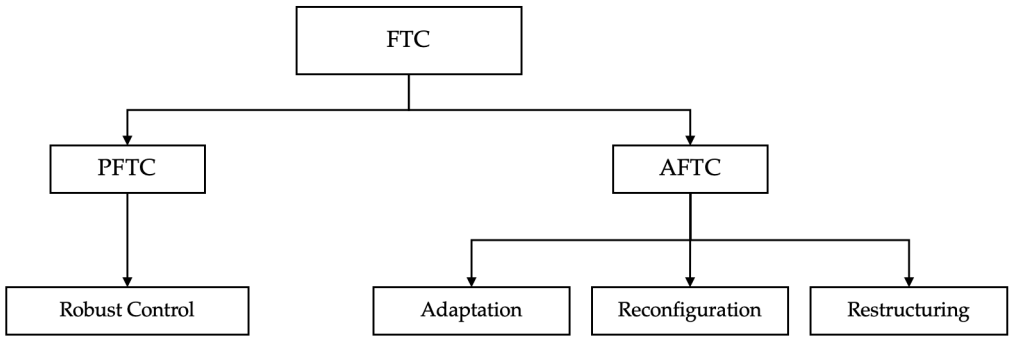

FIGURE I.10: Classification of FTC approaches

a. Passive fault-tolerant control methods

The PFTC methods are based on the control synthesis that makes the system insensitive to specific known faults. This control is robust against parametric uncertainties and external disturbances (e.g. H_∞ control, sliding-mode control, etc.) and does not require any online fault information or controller reconfiguration strategy. Under these control types, the modified system continues to operate with the original controller, making it a more attractive approach from a computational point of view (Jain et al., 2018). In practice, the major drawback of these techniques is that in the case of occasional faults, it is not desired to significantly and permanently modify the system performance to be insensitive to these types of faults. Thus, the PFTC systems generally guarantee a low level of performance. However, in some applications where faults are known and restricted, these techniques may be sufficient. For an overview of robust control methods, the reader can consult (Zhou and Doyle, 1998; Mackenroth, 2013).

b. Active fault-tolerant control methods

Compared to PFTC methods, the AFTC methods are adaptive and react to the fault occurrence via real-time reconfiguration. AFTCs maintain stability and ensure adequate performance, not only when all control elements are functioning correctly, but

also in the event of a malfunction of sensors, actuators or other system components (Kanev, 2004; Jiang and Yu, 2012). These methods strongly require a FDI block to provide precise and real-time information on possible faults (time of occurrence, type and magnitude of fault). The general architecture of the AFTC is as shown in Fig. I.9. The supervision unit's FDI block uses the system's measured inputs and outputs to detect and locate faults. Afterwards, information on the estimated faults is transmitted on-line to the supervision block. Thus, it is possible to modify the parameters and/or controller design depending on the mechanism used and the fault type that occurred. The major disadvantage of active approaches is the limitation of the time available to recalculate the new control law at each moment of detecting a fault. However, active FTC methods are more developed in the literature than passive methods because they offer better performance and the possibility to handle a large class of faults (Kanev, 2004; Du et al., 2015).

As shown in Fig. I.10, AFTC is divided into three different classes: The first is fault adaptation where only low amplitude faults are taken into account. This class's control law is generated by on-line adjustment of the controller parameters and the system inputs/outputs. The second class is system reconfiguration, which is used if the faulty parts cannot be adapted. The modification of the system structure characterises it in order to compensate for the fault. The third class is restructuring, which is the synthesis of a new control law by changing its structure and parameters. It is necessary if the control problem has no solution with adaptation and reconfiguration (Blanke et al., 2006; Jain et al., 2018). Several methods of AFTC are available in literature (Staroswiecki, 2005; Youmin Zhang and Jin Jiang, 2001; Oudghiri, 2008; Seron et al., 2008; Ikeda et al., 1993; Patan, 2014). In the following, some active strategies of the FTC are presented.

Pseudo-Inverse Method (PIM). The PIM was originally proposed for aircraft control systems in (Caglayan et al., 1988) and developed in (Gao and Antsaklis, 1992). It is one of the most widely cited methods and has been largely addressed by many researchers in the field of AFTC (Huang and Stengel, 1990; Staroswiecki, 2005; Blanke et al., 2006). This method is used in linear systems and minimises the deviation between the faulty system's closed-loop model and the reference model. Its principle is to modify the constant feedback gain matrix in the state feedback control law such that the reconfigured system closely approximates the nominal model.

Let us consider the closed-loop system, where the following state representation defines the nominal model:

$$\begin{cases} \dot{x}(t) = Ax(t) + Bu(t) \\ y(t) = Cx(t) \end{cases} \tag{I.8}$$

where $x(t) \in \mathbb{R}^{n_x}$, $u(t) \in \mathbb{R}^{n_u}$ and $y(t) \in \mathbb{R}^{n_y}$ are the state, input and output vectors of the system, respectively. The matrices A, B and C are system matrices in the nominal case with appropriate dimensions.

Let us consider the state feedback control law $u(t) = -Kx(t)$, $K \in \mathbb{R}^{n_u \times n_x}$, and under the assumption that the state vector is known, the closed-loop system is

$$\begin{cases} \dot{x}(t) = (A - BK)\, x(t) \\ y(t) = Cx(t) \end{cases} \tag{I.9}$$

The occurrence of a fault leads to a change of model, and the faulty system is then represented as follows:

$$\begin{cases} \dot{x}_f(t) = A_f x_f(t) + B_f u_f(t) \\ y_f(t) = C_f x_f(t) \end{cases} \tag{I.10}$$

with the subscript f indicates the fault situation of the system.

The new reconfigured control law is formulated in the same form as the previous one:

$$u_f(t) = -K_R x_f(t) \tag{I.11}$$

The objective is to find the new feedback gain K_R such that the state matrices of the nominal and faulty systems are approximated.

$$K_R = B_f^+ \left(A_f - A + BK\right) \tag{I.12}$$

where $B_f^\dagger$ denotes the pseudo-inverse of B_f.

The resulting input to the faulty system is

$$u_f(t) = -B_f^+ \left(A_f - A + BK\right) x_f(t) \tag{I.13}$$

This approach has the advantage of being simple, which makes it very suitable for on-line implementation. On the other hand, changes on the system caused by a fault are computed directly by (I.12). However, no guarantee of closed-loop system stability is the main disadvantage of PIM. This method has been developed in (Gao and Antsaklis, 1991, 1992) by adding constraint such that the closed-loop system remains stable. However, this additional constraint considerably increases the computation time. Another major disadvantage of this method is the need to know the faulty system's mathematical model (A_f, B_f and C_f) to calculate the new gain K_R.

Eigenstructure Assignment (EsA). The EsA method for control law reconfiguration is considered a more powerful approach than PIM. This method was initially introduced in (Andry et al., 1983) and has been the subject of several publications (for instance, see (Konstantopoulos and Antsaklis, 1996; Sauter et al., 2006)). Its main principle is to coincide, via feedback control laws, the eigenstructure (vectors and eigenvalues) of the matrices of nominal and faulty systems in a closed-loop. The EsA technique synthesizes the feedback gain matrix to make the closed-loop eigenvalues of the reconfigured system similar to those of the pre-fault system, and at the same time,

minimizes the 2-norm of the difference between the corresponding eigenvectors. This method has been developed using both state feedback control (Zhang and Jiang, 2000) and output feedback control (Konstantopoulos and Antsaklis, 1996).

Considering v_i as eigenvectors of the closed-loop system state matrix corresponding to the eigenvalues λ_i ($i = 1, 2, ..., n$). The EsA method allows to compute the state feedback gain matrix K_R of the faulty model as a solution of the following optimization problem:

$$\begin{cases} \textit{Find} & K_R \\ \textit{such that} & \left(A_f - B_f K_R\right) v_i^f = \lambda_i v_i^f,\ i = 1, 2, \ldots, n \\ \textit{and} & v_i^f = \arg\min_{v_i^f} \left\| v_i - v_i^f \right\|_{W_i}^2 \end{cases} \tag{I.14}$$

where

$$\left\| v_i - v_i^f \right\|_{W_i}^2 = (v_i - v_i^f)^T W_i (v_i - v_i^f) \tag{I.15}$$

with W_i is a positively defined weighting matrix serving an additional degree of freedom.

This is the least-squares optimization problem, but it does not impose any computational burden in this approach. Besides, the fact that the computational load does not seem to be necessary since the solution of the analytical expression (I.14) is available. Moreover, another benefit of EsA approach is that the performance specifications are given in terms of the system eigenstructure. The closed-loop system's eigenstructure can be accurately determined to perform stability analysis and specified dynamic performance analysis. However, integrating model mismatch issues and fault diagnosis uncertainties into this optimization framework remains an important challenge (Jain et al., 2018).

Reference model approach. This is often called the following approach. The reference model approach for AFTC systems is interesting for designing an on-line control law, in such a way that the performances of the controlled faulty system approximate as closely as possible to those of a reference model. Classically, this approach considers the following reference model:

$$\begin{cases} \dot{x}_r(t) = A_r x_r(t) + B_r r(t) \\ y_r(t) = C_r x_r(t) \end{cases} \tag{I.16}$$

where $r(t)$ corresponds to the reference trajectory signal, $x_r(t)$ and $y_r(t)$ are the state and the output of the reference model, respectively.

Considering the open-loop system (I.8), the state feedback control $u(t)$ composed of the matrices K_r and K_x is given by:

$$u(t) = K_x x(t) + K_r r(t) \tag{I.17}$$

Based on the above control gains, the reference model and the closed-loop system can be written as follows:

$$\begin{cases} \dot{y}_r(t) = C_r A_r x_r(t) + C_r B_r r(t) \\ \dot{y}(t) = (CA + CBK_x)\, x(t) + CBK_r r(t) \end{cases} \tag{I.18}$$

The objective is to match precisely the two models mentioned above ((I.8) and (I.16)). The following selection allows to obtain a perfect follow-up of the model :

$$\begin{cases} K_r = (CB)^{-1} C_r B_r \\ K_x = (CB)^{-1} (C_r A_r - CA) \end{cases} \tag{I.19}$$

The solutions (I.19) exist if the system is square (i.e. $\dim(y(t)) = \dim(u(t))$) and the CB matrix is invertible.

When the system matrices are unknown, they can be replaced by estimated matrices $(\hat{A}, \hat{B}, \hat{C})$, from the indirect (explicit) method (Bodson and Groszkiewicz, 1997). This method does not always guarantee the stability of the closed-loop system. To avoid this problem, the direct (implicit) technique has been used to directly compute controller gain-matrices (K_r & K_x) from an adaptive method (Tao et al., 2002). An advantage of using this approach is that it does not require any FDI scheme. However, this method has a limited ability to adapt to on-line faults due to the necessity of a perfect faulty model, which introduces difficulties in dealing with uncertainties (Jain et al., 2018).

Multiple-model approach. The multiple-model approach is also among the important methods of AFTC. It allows controlling a non-linear system over a large operating area divided into several linearized areas around different operating points, making linear techniques usable in non-linear conditions. In this way, considering a bank of models, the principle is based on the idea that there is a bank of controllers (calculated in real time for all possible system situations) for each operating mode. In this method, each fault scenario can be described by a different model. All system models are implemented in parallel, where each one has its controller as shown in Fig. I.11. The first controller corresponds to the nominal operation of the system. However, the others consider the occurrence of a particular fault causing the system to operate outside its nominal operating range.

The controller's selection associated to the active operating mode is carried out by a supervisor, which comprises a set of estimators and a switching logic scheme as shown in Fig. I.12. At each moment, the estimator closest to the active system is determined by calculating the errors $e_i(t)$ between the estimated outputs $y_i(t)$ and the measured ones $y(t)$ at the moment t. The estimator corresponding to the minimum error is chosen. The corresponding controller is then applied to the system using a switching logic with a delay $\tau_{min} > 0$ imposed to prevent fast switching.

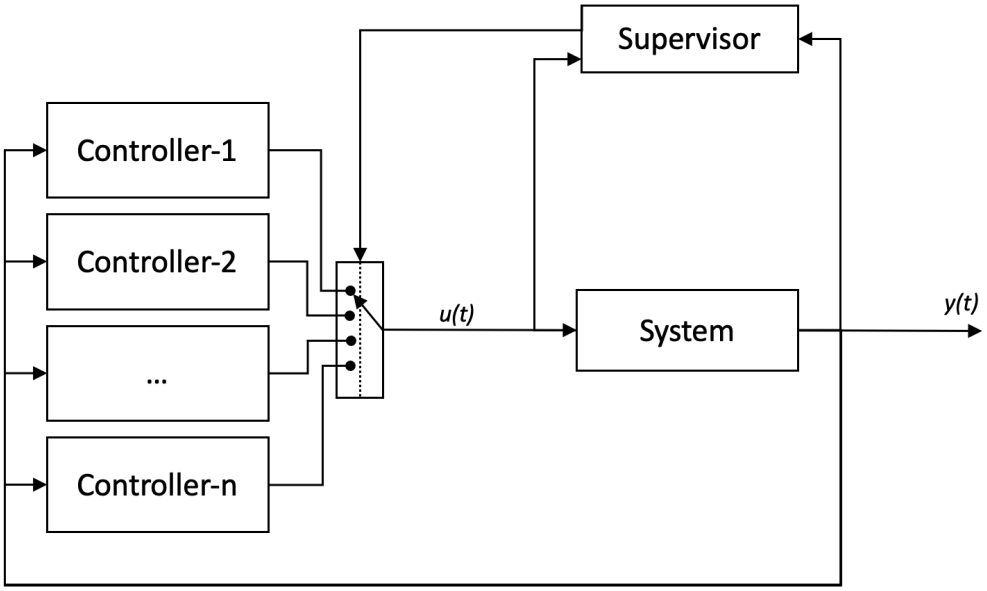

FIGURE I.11: Multiple-model control approach to FTC

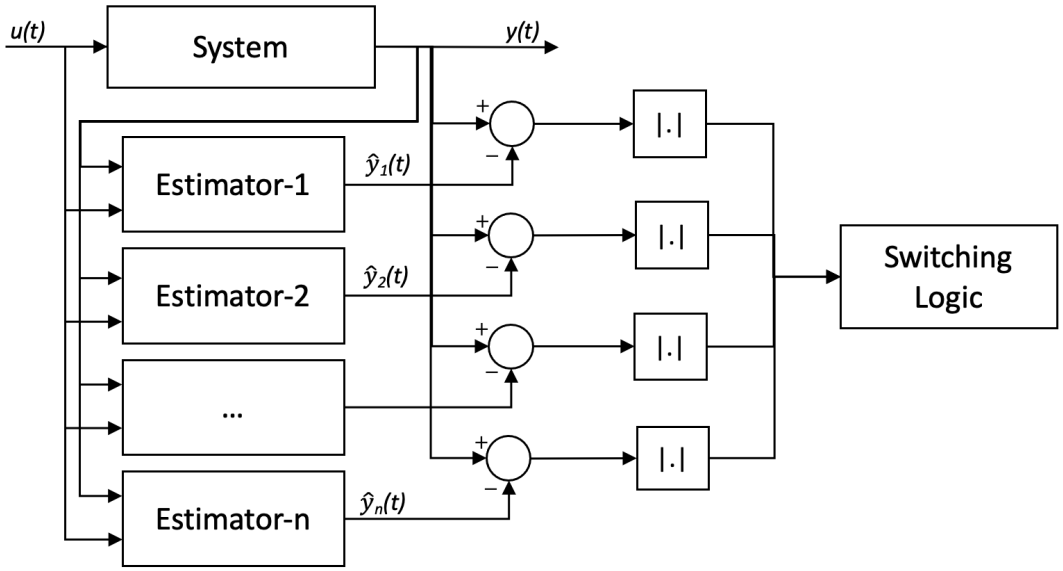

FIGURE I.12: Supervisor structure

Many studies have used the multiple model concept for FTC application. In (Maybeck and Pogoda, 1989), a multi-model adaptive controller that tolerates sensor and/or actuator faults is designed for an approach and landing profile for F-15 short take-off and landing aircraft. In (Jung et al., 2009), the authors used a fault-tolerant multi-model adaptive control to apply it to the aircraft. In this study, a switching scheme and a new decision logic are suggested to improve adaptability in the system's transient state dynamics. A design of a fault-tolerant controller with periodic feedback for autonomous underwater vehicles using a multi-model approach is presented in (Joshi and Talange, 2016).

This method is proving to be an exciting tool for modelling and controlling nonlinear systems. For available model systems, switching between multiple models has the advantage of being very fast and stable. However, the main disadvantage of these methods is that unrecorded faults can still occur and the number of models can explode with the number of simultaneous faults considered. Another limitation is the calculation a priori of the controller gains corresponding to each system situation. To deal with this limitation, a method based on the principle of interacting multiple models has been developed for sensor and actuator faults (for more details the reader can refer to (Yang et al., 2000).

It should be noted that there are other AFTC methods in literature, we do not claim to cover all them, such as: model predictive control, data-driven approaches, neural networks, fuzzy logic as well as approaches based on LPV modelling, and so on.

I.5 Conclusion

In this chapter, we have presented an overview of fault detection and fault-tolerant control techniques. First, we have defined some concepts and terms related to fault diagnosis and then presented different fault classifications according to their modelling, location, and evolution over time. Next, we described the model-based FDI method's steps, starting with the residual generation, followed by fault detection, and finally fault isolation with their types. Subsequently, FTC systems were studied and illustrated as an emerging and attractive topic in automatic control. Both passive and active approaches to the FTC were discussed, as well as their benefits and drawbacks. Besides, the reasons for the growing interest of researchers in active FTC were summarised. It can also be concluded that the problem with FDI is, on the one hand, to generate residuals that should be zero in normal operation and sufficiently sensitive to any fault in the system to be monitored and, on the other hand, to analyse these residuals to detect the presence of a fault and locate the faulty element. At the end of this step, a FTC strategy is launched to determine a control scenario that will cancel, or at least limit, the effects of the faults on the system's stability and performances.

As mentioned in the general introduction, automakers have, over the last decades, introduced new safety systems for vehicles, either passive or active. These products are now commonplace in today's vehicles and are being investigated to increase vehicle safety. However, in the case of a fault, they can lead to serious situations. This observation motivates us to study fault detection and fault-tolerant control of automotive vehicle systems. The techniques presented in this chapter will be the subject of Chapters IV-V of this manuscript, where they are applied to an automotive vehicle lateral dynamics system.

Chapter II

Basic concepts on Takagi-Sugeno fuzzy systems

II.1 Introduction

A real system's study requires a fundamental step, namely modelling, to obtain a mathematical representation describing its functioning. Historically, modelling is considered as the double conjunction between understanding the nature and behaviour of a system on one side and the appropriate mathematical treatment on the other side (Jensen, 2007). It aims to establish the relationships that link the system characteristic variables and accurately represent its behaviour in a specific operational area. The linear systems modelling has been studied in-depth for a long time (Markovsky et al., 2006; Schoukens and Pintelon, 2014). Actually, the input-output relations of a linear system allow building a model approximating its behaviour. This type of model has been widely studied in different contexts, including estimation, control and diagnosis. However, many models can only represent a system's behaviour around a specific operating point.

The assumption of linearity is verified only within a limited operating range around a system equilibrium point. Since real systems are non-linear in nature, control and diagnostic systems developed based on linear models provide degraded performance as soon as one moves away from the equilibrium point. For overcoming this issue, fuzzy logic theory in automation is famous for designing accommodation techniques and describing complex non-linear systems' behaviour. In literature, there are two main classes of fuzzy models, namely Mamdani models (or fuzzy linguistic models) (Mamdani and Assilian, 1975) and Takagi-Sugeno (T-S) fuzzy models (Takagi and Sugeno, 1985; Sugeno and Kang, 1988). This last class is the most popular and is known as multi-model (Chadli and Borne, 2013). It has been successfully applied in several automation areas such as identification, control and diagnosis.

The T-S fuzzy models provide a suitable tool for modelling complex and non-linear systems, allowing any non-linear system, whatever its complexity, to be represented by a finite number of local linear subsystems within different regions of operation. Non-linear functions interpolate these subsystems. T-S fuzzy models have the advantage of providing an efficient design strategy for dealing with non-linearities without

any assumptions about their nature, tolerating model uncertainties and compensate their effect and reducing the effect of external perturbations. For a broader study of the T-S fuzzy models, we invite readers to refer to the following books: (Wang, 1994; Klir and Yuan, 1995; Tanaka and Wang, 2004; Lendek et al., 2011b; Driankov et al., 2013; Chadli and Borne, 2013; Benzaouia and Hajjaji, 2016).

This chapter is devoted to the presentation of basic results on T-S fuzzy models for continuous systems. In the first part, we define T-S fuzzy models and present three methods for obtaining them from a non-linear model, namely methods of parametric optimisation, linearisation and non-linear sectors. In the third part, we describe the stability conditions of T-S fuzzy systems. The fourth section studies the observer design for T-S fuzzy systems. Next, we present an unknown input observer. Finally, we examine the quadratic stabilisation of T-S fuzzy systems with different control laws, which are state feedback, static output feedback and estimated state feedback controls.

II.2 Definition and presentation of T-S fuzzy models

The multi-model approach is based on the decomposition of the dynamic behaviour of the non-linear system into a fixed number of active regions, and a linear sub-model characterises each region. Fig. II.1 illustrates the principle of the multi-model approach in a two-dimensional case (Orjuela et al., 2009).

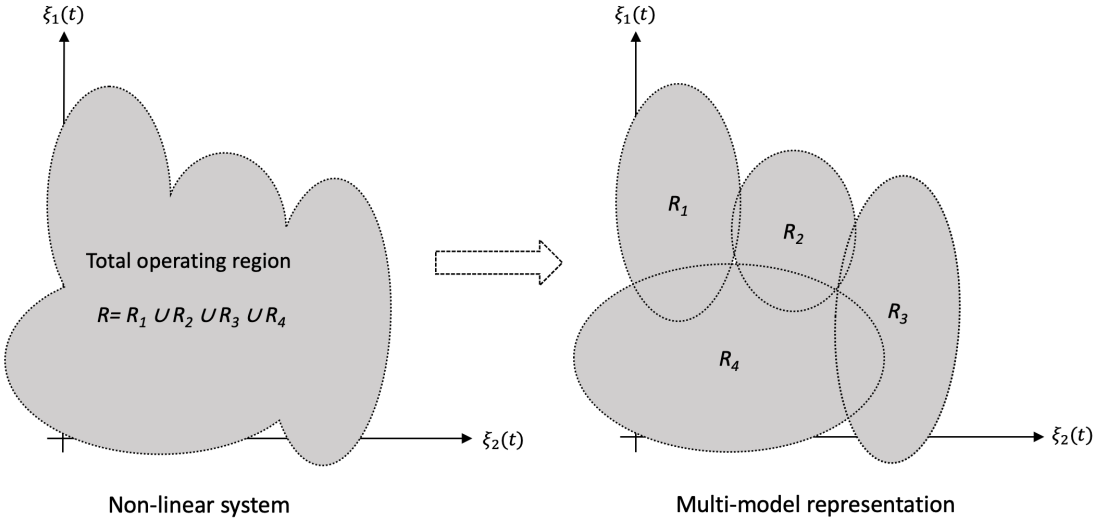

FIGURE II.1: Principle of the multi-model approach

In Fig. II.1, the set of operating points of the system is decomposed into four operating regions (noted R_1, R_2, R_3 and R_4). The total operating region is defined by the combination of the local regions ($R = R_1 \cup R_2 \cup R_3 \cup R_4$). For each of the local regions, a linear sub-model can be constructed. The overall behaviour of the non-linear system is represented by considering the relative contribution of each sub-model using a weighting function for each operating region. Then, a multi-model can be considered as a set of assembled sub-models via an interpolation mechanism.

Several structures are used to interconnect the different sub-models to generate the overall output of the multi-model. Two multi-model structures can be distinguished. The first is the T-S model structure and is the most common in multi-model analysis and synthesis. The sub-models in this structure are homogeneous, sharing the same structure and state space. The second is the decoupled multi-model structure. The sub-models in this structure are heterogeneous, and they have a different structure and state space. Only the coupled state multi-model (T-S model) is considered in the remainder of this document. This choice is motivated by the fact that the T-S fuzzy model representation is the best regarding the constraints imposed for the synthesis of control laws and observers (robustness/performance). This model is used to approximate the non-linear system of automotive vehicle lateral dynamics and the synthesis of the control laws and observers in chapters III-V.

Let us consider the following state representation of a non-linear continuous dynamic system:

$$\begin{cases} \dot{x}(t) = f(x(t), u(t)) \\ y(t) = g(x(t)) \end{cases} \tag{II.1}$$

where $f(.)$ and $g(.)$ are continuously varying non-linear functions with appropriate dimensions. $x(t) \in \mathbb{R}^{n_x}$, $y(t) \in \mathbb{R}^{n_y}$ and $u(t) \in \mathbb{R}^{n_u}$ denote state, output and input vectors, respectively.

It is sometimes necessary or useful to use a more general form of model that can take into account, in addition to the previous differential relations, algebraic constraints linking the different quantities of the system (Luenberger, 1977). These models are called descriptor systems and are of the form :

$$\begin{cases} E(x(t))\dot{x}(t) = f(x(t), u(t)) \\ y(t) = g(x(t)) \end{cases} \tag{II.2}$$

where $E(x(t)) \in \mathbb{R}^{n_x \times n_x}$.
When the matrix $E(x(t))$ is non-invertible, the system is said to be singular (Dai et al., 1989). Otherwise, the system is called regular. In this case, it is then possible to return to the standard form given by a state representation of the form (II.1). However, it is often advantageous to keep the descriptor form for the analysis or synthesis of a control law (Taniguchi et al., 2000; Guelton et al., 2008).

The non-linear system (II.1) can be described by a set of "If-Then" fuzzy rules, which locally represent the linear input-output relations of a non-linear system. The i^{th} rule is described as follows:

$$\begin{aligned} &\textbf{If } \theta_1(t) \text{ is } \Omega_i^1 \text{ and, } \ldots, \text{ and } \theta_p(t) \text{ is } \Omega_i^p, \\ &\textbf{Then} \begin{cases} \dot{x}(t) = A_i x(t) + B_i u(t) \\ y(t) = C_i x(t) \end{cases} \qquad i = 1, \ldots, m. \end{aligned} \tag{II.3}$$

where the vectors $\theta_j(t)$, with $j = 1, 2, \ldots, p$ are the premise variables which can be dependent of the state, the input or a combination of both. The sets Ω_i^j, with $j = 1, 2, \ldots, p$; $i = 1, 2, \ldots, m$, where m is the number of rules, are the membership functions of the fuzzy sets. $A_i \in \mathbb{R}^{n_x \times n_x}$, $B_i \in \mathbb{R}^{n_x \times n_u}$ and $C_i \in \mathbb{R}^{n_y \times n_x}$ are the state, the input and the output matrices, respectively. For each rule, a weight $\omega_i(\theta(t))$ is attributed which depends on the vector $\theta(t) = \left[\theta_1(t), \theta_2(t), \ldots, \theta_p(t)\right]$ and the choice of the logical operator.

The logical operator "and" is often chosen as the product:

$$\begin{cases} \omega_i(\theta(t)) = \prod_{j=1}^{p} \Omega_i^j(\theta_j(t)) \\ \omega_i(\theta(t)) \geq 0 \end{cases} \qquad i = 1, \ldots, m. \tag{II.4}$$

The non-linear system (II.1) can be represented by the following:

$$\begin{cases} \dot{x}(t) = \sum_{i=1}^{m} h_i(\theta(t)) \left(A_i x(t) + B_i u(t)\right) \\ y(t) = \sum_{i=1}^{m} h_i(\theta(t)) C_i x(t) \end{cases} \tag{II.5}$$

with:

$$h_i(\theta(t)) = \frac{\omega_i(\theta(t))}{\sum_{i=1}^{m} \omega_i(\theta(t))} \tag{II.6}$$

The membership function $h_i(\theta(t))$ (also known as activation function) indicates the degree of activation of the i$^{\text{th}}$ associated local model. It indicates the contribution of the local model corresponding to the global model. This function allows a gradual transition from the current model to the neighbouring local models.

The functions $h_i(\theta(t))$ have a triangular, sigmoidal or Gaussian form and satisfy the following convex properties:

$$\begin{cases} \sum_{i=1}^{m} h_i(\theta(t)) = 1 \\ 0 \leq h_i(\theta(t)) \leq 1 \end{cases} \tag{II.7}$$

II.3 Obtaining T-S fuzzy models

The T-S fuzzy model represents the non-linear system as an interpolation between local linear models. Each local model is a valid linear time-invariant dynamic system around a specified operating point. Therefore, obtaining a fuzzy model is a fundamental procedure in this approach. In literature, three main approaches can be found to get a non-linear model of a system in T-S form. These different approaches are parametric identification, linearisation and sector non-linearity approach.

II.3.1 Obtaining T-S fuzzy models by identification

The parametric identification method makes it possible to identify the local model parameters corresponding to the different operating points from inputs and outputs

data. This method is generally based on minimising the deviation function between the fuzzy model estimated output and the system measured output (Gasso et al., 1999; Gasso, 2000). In this case, the problem of identification of the nonlinear model is reduced to the identification of the local models (Babuška, 2012). Note that this method is often used in the case of systems with dynamics that are difficult to describe using an analytical model. The most commonly used criterion is the criterion that represents the squared deviation between the two indicated outputs:

$$J(\theta) = \frac{1}{2}\sum_{t=1}^{M}\epsilon^2(t,\theta) = \frac{1}{2}\sum_{t=1}^{M}\big(y_m(t) - y(t)\big)^2 \tag{II.8}$$

Where M is the observation horizon, and θ is the vector of local model and activation function parameters.

Methods for minimising the criterion $J(\theta)$ are based on a limited development of the criterion $J(\theta)$ around a particular value of the parameter vector θ and an iterative procedure for incrementally modifying the solution. If the iteration index of the search method is denoted by k and the value of the solution at iteration k is denoted by $\theta(k)$, the update of the estimate is performed as follows:

$$\theta(k+1) = \theta(k) - \eta D(k) \tag{II.9}$$

where η represents an adjustment factor to adjust the speed of convergence to the solution. $D(k)$ is the search direction in the parameter space. Depending on how $D(k)$ is calculated, different numerical optimisation methods can be distinguished, the main ones being: Levenberg-Marquardt algorithm, gradient algorithm, Newton algorithm and Gauss-Newton algorithm.

II.3.2 Obtaining T-S fuzzy models by linearisation

This method assumes the availability of a non-linear mathematical model of the physical process, which is linearised around different accurately selected operating points. Indeed, this linearisation is a Taylor series expansion, which may or may not be equilibria.

The purpose is to represent the non-linear system (II.1) as a set of m rules. The linearization around an arbitrary operating point $(x_i, u_i) \in \mathbb{R}^{n_x} \times \mathbb{R}^{n_u}$ is as follows:

$$\begin{cases} \dot{x}(t) = A_i(x(t) - x_i) + B_i(u(t) - u_i) + \tilde{f}(x_i, u_i) \\ y(t) = C_i(x(t) - x_i) + D_i(u(t) - u_i) + \tilde{g}(x_i, u_i) \end{cases} \tag{II.10}$$

The i$^{\text{th}}$ fuzzy model rule (II.10) can be rewritten as follows:

$$\begin{cases} \dot{x}(t) = A_i x(t) + B_i u(t) + R_i \\ y(t) = C_i x(t) + D_i u(t) + S_i \end{cases} \tag{II.11}$$

where the matrices and biases of the local linear models are the following:

$$A_i = \frac{\partial f(x,u)}{\partial x}\Big|_{\substack{x=x_i \\ u=u_i}}, \quad B_i = \frac{\partial f(x,u)}{\partial u}\Big|_{\substack{x=x_i \\ u=u_i}}, \quad C_i = \frac{\partial g(x,u)}{\partial x}\Big|_{\substack{x=x_i \\ u=u_i}}, \quad D_i = \frac{\partial g(x,u)}{\partial u}\Big|_{\substack{x=x_i \\ u=u_i}}$$

$$R_i = \tilde{f}(x_i,u_i) - (A_i x_i + B_i u_i)\,, \qquad S_i = \tilde{g}(x_i,u_i) - (C_i x_i + D_i u_i)$$

Assuming that local models result from linearization around m operating points (x_i, u_i), then the T-S fuzzy models are formulated by:

$$\begin{cases} \dot{x}(t) = \sum_{i=1}^{m} h_i(\theta(t))\,(A_i x(t) + B_i u(t) + R_i) \\ y(t) = \sum_{i=1}^{m} h_i(\theta(t))\,(C_i x(t) + D_i u(t) + S_i) \end{cases} \tag{II.12}$$

where $h_i(\theta(t))$ and $\theta(t)$ are the same defined in the section II.2. Note that number of local models m depends on the modelling's desired accuracy, the complexity of the non-linear system, and the choice of the structure of the activation functions.

This method's main benefit for obtaining T-S fuzzy models is to preserve the important properties of the non-linear system at the linearisation points. However, this method has the drawback that there are no general guidelines for selecting the linearisation points. Besides, depending on the non-linearity, a precise approximation may require many points, which implies high calculation costs.

II.3.3 Obtaining T-S fuzzy models by sector non-linearity

The sector non-linearity approach provides a T-S representation of a non-linear model. The idea of using this method for T-S fuzzy modelling was first introduced in the (Kawamoto et al., 1992) and then extended by (Wang et al., 1996) and (Tanaka and Ohtake, 2001). It should be noted that this is not an approximation, but the T-S model obtained is identical to the non-linear model in a compact set of the state space (Ohtake et al., 2003).

Let us consider the state representation of a non-linear dynamic system as (II.1). The goal is to determine global sector such that $a_1 x(t) \leq \dot{x}(t) \leq a_2 x(t)$, with $\dot{x}(t) = f(x(t), u(t))$ representing a non-linear system. Figure II.2-(a) represents the global sector non-linearity approach (Wang et al., 1996). Here, the T-S fuzzy models can be accurately derived. However, it is sometimes hard to find global sectors for non-linear systems. Then, local non-linear sectors can be considered (Tanaka and Wang, 2004). This assumption is logical since the variables of physical systems are always bounded. Figure II.2-(b) illustrates the local sector non-linearity where the fuzzy model can accurately represent the non-linear system in the local area $-d < x(t) < d$.

The sector non-linearity approach makes it possible to associate the T-S models for a non-linear system according to the distribution of non-linearities obtained. The linking membership functions are calculated using Lemma 1.

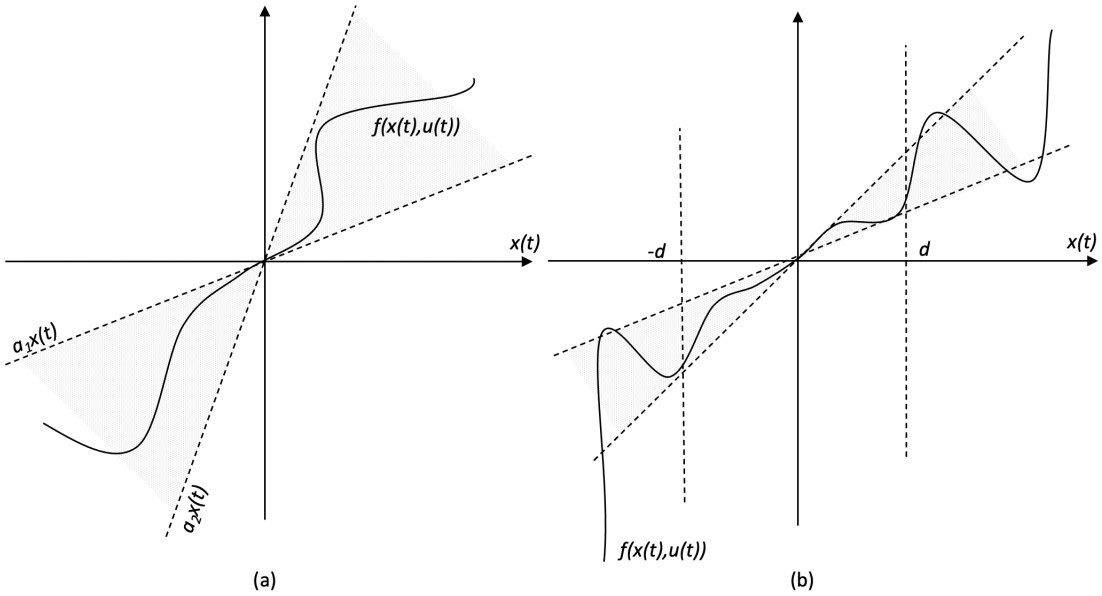

FIGURE II.2: Global(a) and local(b) Sector non-linearities

The approach by sector non-linearity offers advantages regarding precision and knowledge of the membership functions that ensure the LTI local models' interconnection. Indeed, this method does not introduce approximation errors, and the number of local models is reduced compared to the linearisation method. It should be noted that reducing the number of LTI models decreases the number of constraints related to stability and/or stabilisation. To better understand, the following example illustrates the approach by sector non-linearity to obtain T-S fuzzy models.

Example. II. 1 *Let the following non-linear system (Chadli and Coppier, 2013):*

$$\begin{cases} \dot{x}_1(t) = -x_1(t) + sin(x_2(t))x_2(t) + u(t) \\ \dot{x}_2(t) = 2x_1(t) - 3x_2(t) + x_1^2(t)u(t) \\ y(t) = x_1^3(t) \end{cases} \tag{II.13}$$

The non-linear system (II.13) *can be rewritten as follows:*

$$\begin{cases} \dot{x}(t) = A(x(t))x(t) + B(x(t))u(t) \\ y(t) = C(x(t))x(t) \end{cases} \tag{II.14}$$

where $x(t) = \begin{bmatrix} x_1^T(t) & x_2^T(t) \end{bmatrix}^T$, *and*

$$A(x(t)) = \begin{bmatrix} -1 & \sin(x_2(t)) \\ 2 & -3 \end{bmatrix}, \quad B(x(t)) = \begin{bmatrix} 1 \\ x_1^2(t) \end{bmatrix}, \quad C(x(t)) = \begin{bmatrix} x_1^2(t) & 0 \end{bmatrix}$$

The system (II.14) *presents the following two non-linearities:*

$$\theta_1(x(t)) = \sin(x_2(t)), \qquad \theta_2(x(t)) = x_1^2(t) \tag{II.15}$$

Note that $\theta_1(x(t))$ is bounded regardless of the value of $x(t)$ in the state space, in contrast to $\theta_2(x(t))$ which can only be bounded on a limited compact. So let's assume that $x_1(t)$ is bounded on $[-\gamma, \gamma]$, with $\gamma > 0$. Thus the two non-linearities can be rewritten as follows:

$$\begin{cases} \theta_1(x(t)) = M_1(x(t)) \times 1 + M_2(x(t)) \times (-1) \\ \theta_2(x(t)) = N_1(x(t)) \times \gamma^2 + N_2(x(t)) \times 0 \end{cases} \tag{II.16}$$

where

$$\begin{cases} M_1(x(t)) + M_2(x(t)) = 1 \\ N_1(x(t)) + N_2(x(t)) = 1 \end{cases} \tag{II.17}$$

Therefore, the membership functions can be calculated in the following way:

$$\begin{aligned} M_1(x(t)) = \frac{\theta_1(x(t)) + 1}{2}, \quad M_2(x(t)) = 1 - M_1(x(t)) \\ N_1(x(t)) = \frac{\theta_2(x(t))}{\gamma^2}, \quad N_2(x(t)) = 1 - N_1(x(t)) \end{aligned} \tag{II.18}$$

The non-linear system (II.14) *can be precisely represented using the sector non-linearity approach by the following 4-rules fuzzy system:*

$$\textit{If } \theta_1(x(t)) \textit{ is } M_1 \textit{ and } \theta_2(x(t)) \textit{ is } N_1, \textbf{ Then } \begin{cases} \dot{x}(t) = A_1 x(t) + B_1 u(t) \\ y(t) = C_1 x(t) \end{cases} \tag{II.19}$$

$$\textit{If } \theta_1(x(t)) \textit{ is } M_1 \textit{ and } \theta_2(x(t)) \textit{ is } N_2, \textbf{ Then } \begin{cases} \dot{x}(t) = A_2 x(t) + B_2 u(t) \\ y(t) = C_2 x(t) \end{cases} \tag{II.20}$$

$$\textit{If } \theta_1(x(t)) \textit{ is } M_2 \textit{ and } \theta_2(x(t)) \textit{ is } N_1, \textbf{ Then } \begin{cases} \dot{x}(t) = A_3 x(t) + B_3 u(t) \\ y(t) = C_3 x(t) \end{cases} \tag{II.21}$$

$$\textit{If } \theta_1(x(t)) \textit{ is } M_2 \textit{ and } \theta_2(x(t)) \textit{ is } N_2, \textbf{ Then } \begin{cases} \dot{x}(t) = A_4 x(t) + B_4 u(t) \\ y(t) = C_4 x(t) \end{cases} \tag{II.22}$$

with the following local matrices :

$$A_1 = \begin{bmatrix} -1 & 1 \\ 2 & -3 \end{bmatrix}, \; A_2 = \begin{bmatrix} -1 & 1 \\ 2 & -3 \end{bmatrix}, \; A_3 = \begin{bmatrix} -1 & -1 \\ 2 & -3 \end{bmatrix}, \; A_4 = \begin{bmatrix} -1 & -1 \\ 2 & -3 \end{bmatrix}$$

$$B_1 = B_3 = \begin{bmatrix} 1 & \gamma^2 \end{bmatrix}^T, \; B_2 = B_4 = \begin{bmatrix} 1 & 0 \end{bmatrix}^T, \; C_1 = C_3 = \begin{bmatrix} \gamma^2 & 0 \end{bmatrix}, \; C_2 = C_4 = \begin{bmatrix} 0 & 0 \end{bmatrix}$$

Hence, the equivalent T–S fuzzy system of non-linear system (II.13) *is:*

$$\begin{cases} \dot{x}(t) = \sum_{i=1}^{4} h_i(\theta(t)) \left(A_i x(t) + B_i u(t)\right) \\ y(t) = \sum_{i=1}^{4} h_i(\theta(t)) C_i x(t) \end{cases} \tag{II.23}$$

where the T-S fuzzy system activation functions are the following:

$$\begin{aligned} h_1(\theta(t) &= M_1(\theta(t)) \times N_1(\theta(t)), & h_2(\theta(t) &= M_1(\theta(t)) \times N_2(\theta(t)) \\ h_3(\theta(t) &= M_2(\theta(t)) \times N_1(\theta(t)), & h_4(\theta(t) &= M_2(\theta(t)) \times N_2(\theta(t)) \end{aligned} \tag{II.24}$$

The simulation results of the non-linear system and its corresponding T-S fuzzy model for $u(t) = 2$ *are presented in Fig. II.3. It is clear that the T-S fuzzy model* (II.23) *represents well the nonlinear system* (II.13) *in the region* $[-\gamma, \gamma]$*, with* $\gamma > 0$*.*

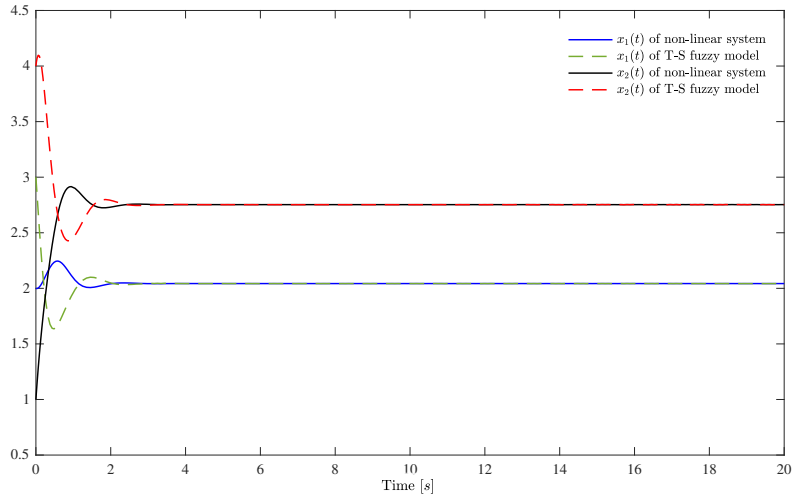

FIGURE II.3: States of the non-linear model and of its corresponding T-S fuzzy model

II.4 Stability analysis

The stability concept is a key factor in studying the dynamic systems' behaviour and synthesising their control laws. Thus, the dynamic system's stability problem remains a subject of great attention by automation engineers. The stability is often related to the systems studied, their environments, specifications, and desired performances.

Several works present stability notions that solve several practical system study cases summarised and discussed extensively in (Leine, 2010). The best known is the Lyapunov stability, introduced by the Russian mathematician Alexander Lyapunov in 1892 (Mawhin, 2005). His contribution consists of a qualitative characterisation of stability by studying dynamic systems' trajectories, using auxiliary functions nowadays called Lyapunov functions. This method is based on the idea that if a function with the energy form is dissipated in time, it tends towards an equilibrium point (Wen, 1990; Najim et al., 2004). Therefore, the Lyapunov method is a distance measure between the state variables and the equilibrium point. In the following, some definitions and theorems relating to stability will be presented based on these references (Khalil and Grizzle, 2002; Zak, 2003; Sastry, 2013; Bhiri, 2017). Then, the stability conditions of the T-S models will be discussed.

II.4.1 Stability definitions and theorems

Let us consider time-invariant autonomous systems, which are described by the following differential equation:

$$\begin{cases} \dot{x}(t) = f(x,t) \\ x(t_0) = x_0 \end{cases} \tag{II.25}$$

Definition. II. 1 *(Equilibrium point) The state x^* is said to be an equilibrium point of the system* (II.25)*, if $x(t_1) = x^*$ implies $x(t) = x^*$ for any $t \geq t_1$. Or simply that the state x^* checks the equation $f(x^*) = 0$.*

Definition. II. 2 *(Intuitive definition of stability) When a dynamic system is slightly disturbed with respect to its equilibrium point and remains close to it. The equilibrium point is then said to be stable.*

As an illustrative example, let us take a ball on a spherical surface, as shown in Fig. II.4 (Danglot et al., 2018). The ball is stable in the left-hand case, where if it moved away from its equilibrium position under a slightly disturbing action; it remains close to its equilibrium position. But the ball is unstable in the right-hand case, meaning that if it moved away from its equilibrium position under a slightly disturbing action; it moves away from its initial position.

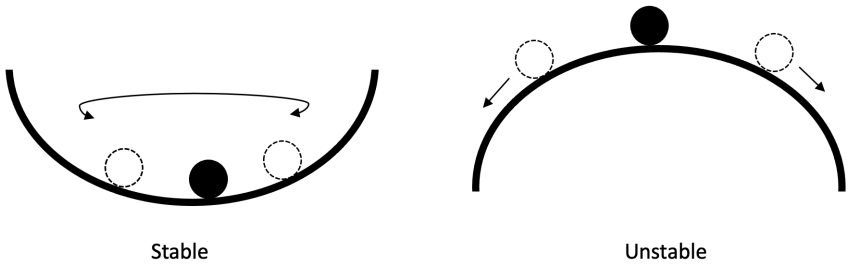

FIGURE II.4: Stable and unstable equilibria

The mathematical expression of this intuitive definition of stability is given by the following definition.

Definition. II. 3 *(Lyapunov stability) The equilibrium point x^* is said to be stable if $\forall \epsilon > 0$ and $\forall t_0 > 0$, there exists a function $\delta(\epsilon, t_0) > 0$ such as:*

$$||x_0 - x^*|| < \delta \implies ||x(t) - x^*|| < \epsilon, \forall t \geq t_0 \tag{II.26}$$

In other words, Stability in the sense of Lyapunov means that the trajectory $x(t)$, with the initial condition $x_0 = x(t_0)$, must remain close to the equilibrium point x^*, for any $t \geq t_0$. For this, the solutions $x(t)$ must remain within the region bounded by $||x(t) - x^*|| < \epsilon$, i.e. remain in a "tube" of radius ϵ around the trajectory $x(t) = x^*$ (see Fig. II.5).

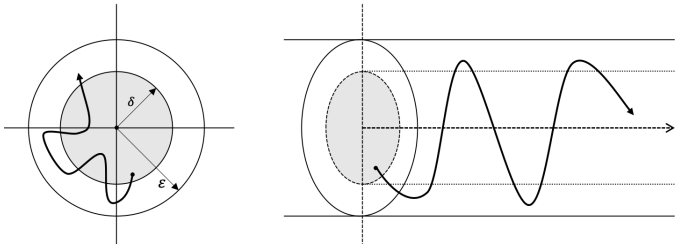

FIGURE II.5: Concept of stability in the sense of Lyapunov

Definition. II. 4 *The equilibrium point x^* is said to be attractive if there is $\rho > 0$ such that:*

$$||x_0 - x^*|| < \delta \implies \lim_{t \to \infty} ||x(t) - x^*|| = 0 \tag{II.27}$$

The attractiveness means that if the state is initialized close to the equilibrium state, then this initial state's trajectory will converge to the equilibrium state over time.

Definition. II. 5 *(Asymptotic stability) The equilibrium point x^* is asymptotically stable if it is stable and attractive.*

The asymptotic stability implies the existence of proximity to the equilibrium point, such that for any initial condition belonging to this proximity, the state $x(t)$ converges towards x^* when time tends to infinity (see Fig. II.6).

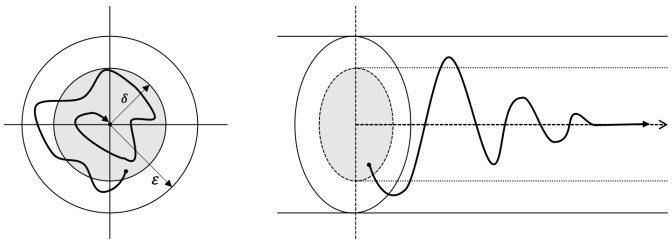

FIGURE II.6: Concept of asymptotic stability in the sense of Lyapunov

Definition. II. 6 *(Global asymptotic stability) If the condition of asymptotic stability is satisfied in all $\mathbb{R}^n$, then the equilibrium point is globally asymptotically stable.*

Definition. II. 7 *(Lyapunov candidate) Any defined positive and continuous function $V(x)$ is called candidate of Lyapunov.*

Definition. II. 8 *(Lyapunov function) A Lyapunov function is a Lyapunov candidate having the following property:*

$$\begin{cases} \dot{V}(x,t) \leq 0 \; \forall x \neq 0 \\ \dot{V}(x,t) = 0 \; if \; x = 0 \end{cases} \tag{II.28}$$

In the following, we present some theorems that are essential for studying a dynamic system's stability.

Theorem. II. 1 *(Lyapunov stability) Let $x^* = 0$ an equilibrium point of the system* (II.25) *and $\mathcal{I} \subset \mathbb{R}^n$ a proximity of this equilibrium point. If there is a Lyapunov function $V(x,t)$ defined on $\mathcal{I}$ satisfying $V(x,t) \leq 0$, $\forall x \in \mathcal{I}_{\neq 0}$, then the equilibrium point x^* is stable in the Lyapunov sense.*

Theorem. II. 2 *(Asymptotic stability) Let $x^* = 0$ an equilibrium point of the system* (II.25) *and $\mathcal{I} \subset \mathbb{R}^n$ a proximity of this equilibrium point. If there is a Lyapunov function $V(x,t)$ defined on $\mathcal{I}$ satisfying in addition $V(x,t) < 0$, $\forall x \in \mathcal{I}_{\neq 0}$, the equilibrium point x^* is then asymptotically stable.*

Note that Theorems II.1 and II.2 give sufficient conditions to ensure the Lyapunov sense stability and asymptotic stability, respectively. The non-existence of a Lyapunov function for a dynamic system does not mean that the latter is unstable (Bhiri, 2017).

It should be noted that the conditions of these two theorems are only true in proximity around the equilibrium point x^*. In the case where the field of attraction is the whole state space $\mathbb{R}^n$, the equilibrium point x^* will be said to be globally asymptotically stable. Then, the property of the non-radial boundaryitude must be added to the conditions of Theorem. II.2 to ensure global asymptotic stability. The following theorem summarises these conditions.

Theorem. II. 3 *(Global asymptotic stability) Let $x^* = 0$ an equilibrium point of the system* (II.25) *and the function, such as:*

$$V(0) = 0 \quad and \quad V(x) > 0, \ \forall x \in \mathbb{R}_{\neq 0} \tag{II.29}$$

$$||x|| \to 0 \implies V(x) \to \infty \tag{II.30}$$

$$\dot{V}(x) < 0, \ \forall x \in \mathbb{R}_{\neq 0} \tag{II.31}$$

then x^* is globally asymptotically stable.

The condition (II.29) guarantees the non-radial boundary of the function V on $\mathbb{R}$.

II.4.2 Stability of T-S models

The stability of continuous non-linear systems represented by the T-S fuzzy models has been the subject of several studies, initially inspired by techniques developed in the linear field (Boyd et al., 1994; Tanaka et al., 1998). In general, the stability analysis of T-S fuzzy models is carried out using the Lyapunov method. In this context, the choice of Lyapunov's function is crucial to obtain solutions. Normally, there is no systematic way to find these functions. Several forms of Lyapunov functions are proposed in the literature (Tanaka et al., 1996; Wang et al., 1996; Tanaka et al., 2003; Chadli et al., 2000; Bernal and Husek, 2005; Mozelli et al., 2009; Nguyen et al., 2016), depending on the nature and complexity of the system.

a. Quadratic Lyapunov function

A quadratic Lyapunov function is of the following shape:

$$V(x(t)) = x^T(t)Px(t) \tag{II.32}$$

with $P = P^T$ is a positive definite matrix.

The quadratic Lyapunov function is used to study a system's stability, which is called quadratic stability. The method based on this type of function consists of searching for the P matrix. The use of a Lyapunov quadratic function can introduce a certain degree of conservatism. However, it is numerically efficient because it leads to convex optimisation problems, and the resulting control laws are of reasonable complexity from a practical point of view.

b. Non-quadratic Lyapunov function

A non-quadratic Lyapunov function is of the following shape:

$$V(x(t)) = \sum_{i=1}^{m} h_i(\theta(t))x(t)^T P_i x(t) \tag{II.33}$$

where $P_i = P_i^T$ is a positive definite matrix and $h_i(\theta(t))$ are activation functions satisfying the conditions (II.7).

The non-quadratic Lyapunov function is a global function including the quadratic case ($P_i = P,\ i = 1, \ldots, m$). The synthesis technique based on this type of Lyapunov function may have a valuable advantage compared to that based on the quadratic function. It considers the variation in speed of the decision variables, which reduces conservatism and gives more relaxed stability conditions. However, this function reduces the overall stability of the non-linear system as it allows to analyse of the stability of each local sub-model separately.

In addition to quadratic and non-quadratic functions, there are other Lyapunov functions such as piecewise quadratic functions, polynomial functions and functions defined by path integrals. These functions will not be covered in this manuscript, but the reader can refer to these references.

II.4.3 Quadratic stability of T-S fuzzy systems

Let us consider the open-loop T-S fuzzy model below:

$$\dot{x}(t) = \sum_{i=1}^{m} h_i(\theta(t))A_i x(t) \tag{II.34}$$

where $h_i(\theta(t)$ are the activation functions defined in section II.2 and verify the conditions (II.7).

The stability of the T-S fuzzy model (II.34) is guaranteed if conditions, in the form of Linear Matrix Inequalities (LMIs) of the following theorem, are fulfilled.

Theorem. II. 4 *(Tanaka et al., 1998) The equilibrium of the T-S fuzzy system described in* (II.34) *is asymptotically stable if there is a common positive definite matrix P such that:*

$$A_i^T P + P A_i < 0, \qquad for\, i = 1, 2 \ldots, m \tag{II.35}$$

Proof. II. 1 *Let the following quadratic function:*

$$V(x(t)) = x^T(t) P x(t), \qquad with\, P > 0 \tag{II.36}$$

The time derivative of $V(x(t))$ is given as follows:

$$\dot{V}(x(t)) = \dot{x}^T(t) P x(t) + x^T(t) P \dot{x}(t) \tag{II.37}$$

$$= x^T(t) \sum_{i=1}^{m} h_i(\theta(t)) A_i^T P x(t) + x^T(t) P \sum_{i=1}^{m} h_i(\theta(t)) A_i x(t) \tag{II.38}$$

$$= x^T(t) \sum_{i=1}^{m} h_i(\theta(t)) \left(A_i^T P + P A_i \right) x(t) \tag{II.39}$$

The open loop system (II.34) *converges to zero if $\dot{V}(x(t)) < 0$ (i.e. if* (II.35) *are satisfied).*

The existence of $P > 0$ depends on the following two conditions:

- Stability of each local model. The eigenvalues of each matrix A_i must belong to the left half-plane of the complex plane (i.e. each A_i must be a Hurwitz matrix).
- Availability of a Lyapunov function common to the r local models. For this, the sum $\sum_{i=1}^{m} A_i$ must be a Hurwitz matrix. The proof can be obtained by summing the LMIs (II.35).

The second condition allows a quick test since if there are two matrices such that their sum $A_i + A_j$ is not stable, it means that there no symmetric matrix $P > 0$ that satisfies the LMIs (II.35). Lemma 2 provides a systematic method to test the non-existence of a common symmetrical matrix $P > 0$.

II.5 Observers for T–S fuzzy systems

In many practical systems, the state variables are sometimes not available and cannot be measured, and sometimes they can be measured by instrumental sensors. However, some constraints are related to using these sensors, such as unreliability, high cost, degradation, loss of signals in certain weather conditions and sometimes unavailability of these sensors. To overcome these challenges, system states can be estimated using only accessible and available measurements.

An observer is designed to reconstruct the state vector of a system from the known inputs, outputs and the dynamic model of the system. In this section, the observer design methods for T-S fuzzy systems are discussed. Before starting the observer design procedure, it is always necessary to ensure that system states can be estimated from

the input and output information. The observability of a system is the property that indicates if the states can be estimated only from the knowledge of the input and output signals.

The necessary and sufficient condition of observability is called the Kalman criterion for observability. The following definition gives it.

Definition. II. 9 *(Meda-Campaña et al., 2020) The T-S fuzzy system described by* (II.5) *is fuzzy observable if its associated observability matrix, given as follows*

$$\mathcal{O} = \begin{bmatrix} C_i^T & (C_iA_i)^T & (C_iA_i^2)^T & \dots & (C_iA_i^{n_x-1})^T \end{bmatrix}^T \in \mathbb{R}^{(n_x \times n_y)n_x}$$

has a full rank for any valid value of the fuzzy weights included in the fuzzy system, i.e., a T-S fuzzy system is fuzzy observable if $rank(\mathcal{O}) = n_x$.

In this section, steps to design observers for continuous fuzzy systems are presented. First, a T-S fuzzy observer structure is proposed, which is a sum of local Luenberger-type observers. The observer with unknown inputs is then studied. The convergence of the estimation error to zero is given by solving a Lyapunov function, which can be formulated as a convex optimisation problem in LMI terms, which has well-established methods and tools for its resolution.

II.5.1 Observer synthesis for T-S fuzzy systems

Let us consider the following non-linear dynamic system represented by T-S fuzzy models:

$$\begin{cases} \dot{x}(t) = \sum_{i=1}^{m} h_i(\theta(t))\{A_ix(t) + B_iu(t)\} \\ y(t) = \sum_{i=1}^{m} h_i(\theta(t))C_ix(t) \end{cases} \tag{II.40}$$

with $x(t) \in \mathbb{R}^{n_x}$, $u(t) \in \mathbb{R}^{n_u}$ and $y(t) \in \mathbb{R}^{n_y}$ are the state vector, the input vector and the output vector of the system, respectively. A_i, B_i and C_i are appropriate dimensional matrices that describe the system dynamics. $h_i(\theta(t))$ are the activation functions of the local models and $\theta(t)$ represents the decision variables that can be state-dependent, output-dependent and/or input-dependent. Here it is assumed that $\theta(t)$ are only dependent on measurable variables.

Like all observer designs, fuzzy observers are required to satisfy

$$x(t) - \hat{x}(t) \to 0, \quad when\ t \to \infty$$

where $\hat{x}(t)$ represents the state estimated by the fuzzy observer.

In order to design a fuzzy observer, each local model is associated with a local observer, and it is assumed that each pair (A_i, C_i) is observable. The overall observer is the sum of local observers weighted by activation functions identical to those used in the fuzzy system (II.40) (Palm and Driankov, 1999).

The following structure defines the fuzzy observer

$$\begin{cases} \dot{\hat{x}}(t) = \sum_{i=1}^{m} h_i(\theta(t))\{A_i\hat{x}(t) + B_i u(t) + L_i(y(t) - \hat{y}(t))\} \\ \hat{y}(t) = \sum_{i=1}^{m} h_i(\theta(t)) C_i \hat{x}(t) \end{cases} \tag{II.41}$$

where $\hat{y}(t) \in \mathbb{R}^{n_y}$ is the estimated output vector and $L_i \in \mathbb{R}^{n_x \times n_y}$ are the gains of local observers. The activation functions $h_i(\theta(t))$ are the same as those of the fuzzy system (II.40) and have the same properties (II.7).

The state estimation error is defined as follows:

$$e_x(t) = x(t) - \hat{x}(t) \tag{II.42}$$

The state estimation error dynamic is given by:

$$\dot{e}_x(t) = \dot{x}(t) - \dot{\hat{x}}(t) \tag{II.43}$$

$$= \sum_{i=1}^{m}\sum_{j=1}^{m} h_i(\theta(t))h_j(\theta(t))\{A_i - L_i C_j\}e_x(t) \tag{II.44}$$

$$= \sum_{i=1}^{m}\sum_{j=1}^{m} h_i(\theta(t))h_j(\theta(t))\tilde{A}_{ij}e_x(t) \tag{II.45}$$

The objective is to determine the gains L_i, such that the estimation error $e_x(t)$ converges to zero. The following theorem proposes a fundamental result for establishing the stability of (II.45).

Theorem. II. 5 *(Tanaka et al., 1998) The estimation error dynamic* (II.45) *is asymptotically stable, if there exist* $Q = Q^T > 0$, *and* $L_i,\ i = 1, 2, \ldots, r$, *such that*

$$\tilde{A}_{ii}^T Q + Q\tilde{A}_{ii} < 0 \quad , i = 1,\ 2,\ \ldots, m \tag{II.46}$$

$$(\tilde{A}_{ij} + \tilde{A}_{ji})^T Q + Q(\tilde{A}_{ij} + \tilde{A}_{ji}) \leq 0 \quad , j = \ i+1,\ i+2, \ldots, m \tag{II.47}$$

with : $\tilde{A}_{ij} = A_i - L_i C_j$

Proof. II. 2 *Let us consider the following quadratic Lyapunov function*

$$V(e_x(t)) = e_x^T(t) Q e_x(t), \qquad with\ Q > 0 \tag{II.48}$$

The derivative of $V(e_x(t))$ *is given as follows*

$$\dot{V}(e_x(t)) = \dot{e}_x^T(t) Q e_x(t) + e_x^T(t) Q \dot{e}_x(t) \tag{II.49}$$

$$= \sum_{i=1}^{m}\sum_{j=1}^{m} h_i(\theta(t))h_j(\theta(t)) e_x^T(t) \left(\tilde{A}_{ij}^T Q + Q\tilde{A}_{ij}\right) e_x(t) \tag{II.50}$$

using Lemma 3, the conditions (II.46)-(II.47) *which ensure that* $\dot{V}(e_x(t)) < 0$ *are obtained.*

The following example shows the construction of an observer using the conditions of Theorem. II.5.

Example. II. 2 *Let us consider the same non-linear system of Example 1. To make the models locally observable, let us assume that* $C(x(t)) = \begin{bmatrix} x_1^2(t) & 1 \end{bmatrix}$. *The equations governing the global observer are as follows:*

$$\begin{cases} \dot{\hat{x}}(t) = \sum_{i=1}^{4} h_i(\theta(t))\{A_i\hat{x}(t) + B_i u(t) + L_i(y(t) - \hat{y}(t))\} \\ \hat{y}(t) = \sum_{i=1}^{4} h_i(\theta(t)) C_i \hat{x}(t) \end{cases} \tag{II.51}$$

To construct the observer gains L_i, *the conditions* (II.46)-(II.47) *are transformed into LMIs using the change of variables* $N_i = QL_i$. *Afterward, the feasibility problem of these LMIs is solved using the LMI toolbox of MATLAB software. Then, the observation gains are as follows:*

$$L_1 = \begin{bmatrix} 0,0290 \\ 0,4254 \end{bmatrix}, \; L_2 = \begin{bmatrix} -0,0102 \\ 0,5582 \end{bmatrix}, \; L_3 = \begin{bmatrix} 0,0496 \\ -0,2067 \end{bmatrix}, \; L_4 = \begin{bmatrix} 0,0300 \\ -0,0912 \end{bmatrix}$$

Assume that $u(t) = 0$ *and consider the initial conditions* $x_0 = \begin{bmatrix} 0,9 & 0,5 \end{bmatrix}^T$ *and* $\hat{x}_0 = \begin{bmatrix} 0,8 & 0,2 \end{bmatrix}^T$.

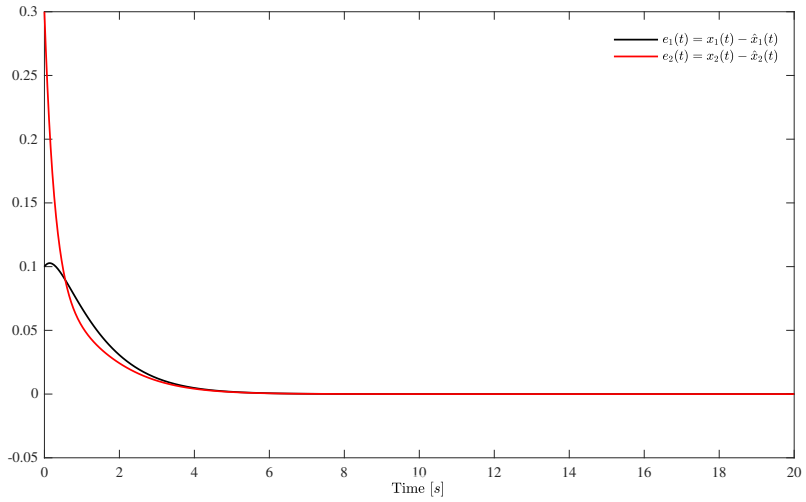

FIGURE II.7: Time evolution of estimation error $e(t)$

The evolution of the estimation error of the system over time is illustrated in the Fig. II.7.

It can be seen that the estimation error clearly converges to zero (see Fig. II.7), which indicates a good agreement between the measured and estimated states over time.

To reduce the conservatism of the conditions (II.46)-(II.47) and to obtain more relaxed results, the authors in (Liu and Zhang, 2003) proposed the following theorem, which is similar to the Theorem. II.(5) with the inclusion of additional decision variables.

Theorem. II. 6 *(Liu and Zhang, 2003) The estimation error dynamic* (II.45) *is asymptotically stable, if there exist matrices* N_i, Q, Y_{ij}, *where* Q *is symmetrical positive definite,* Y_{ii} *are*

symmetrical, $Y_{ji} = Y_{ij}^T$, $i \neq j$, $i, j = 1, 2, \ldots, m$, *satisfy the following LMIs:*

$$A_i^T Q + Q A_i + C_i^T N_i^T + N_i C_i < Y_{ii} \quad , i = 1,\ 2,\ \ldots, m \tag{II.52}$$

$$(A_i + A_j)^T Q + Q(A_i + A_j) + C_j^T N_i^T + N_i C_j + C_i^T N_j^T + N_j C_i \leq Y_{ij} + Y_{ij}^T, \quad j = \ i+1,\ i+2,\ \ldots, m \tag{II.53}$$

$$\begin{bmatrix} Y_{11} & Y_{12} & \ldots & Y_{1r} \\ * & Y_{22} & \ldots & Y_{2r} \\ \vdots & \vdots & \ddots & \vdots \\ * & * & \ldots & Y_{rr} \end{bmatrix} < 0 \tag{II.54}$$

The gains of the fuzzy observer (II.51) *are obtained by:*

$$L_i = Q^{-1} N_i \tag{II.55}$$

II.5.2 Unknown inputs fuzzy observer

Classical state estimation methods can no longer be applied when a system is under unknown inputs. These unknown inputs are typically caused by modelling errors, sensor faults, disturbances, or noises on the system's state or output. In this context, several works in the literature used unknown input observer to estimate either state alone or state and also unknown inputs (Tan and Edwards, 2002; Akhenak et al., 2004b; Chadli et al., 2008; El Youssfi et al., 2019b, 2020b). The synthesis of this type of observers is carried out using different techniques, particularly those that require the elimination of unknown inputs and those that use the sliding mode (Chadli, 2010b; Akhenak et al., 2007). In the following, two different cases are examined. The first is where only the system state is affected by unknown inputs. The second case is where unknown inputs simultaneously affect both system state and output.

a. Unknown inputs only affect the system state

Let us consider a non-linear system affected by unknown inputs, represented by the following T-S fuzzy models:

$$\begin{cases} \dot{x}(t) = \sum_{i=1}^{m} h_i(\theta(t)) \{A_i x(t) + B_i u(t) + E_i v(t) + D_i\} \\ y(t) = Cx(t) \end{cases} \tag{II.56}$$

where $v(t) \in \mathbb{R}^{n_v}$ is the unknown inputs vector assumed to be bounded, $E_i \in \mathbb{R}^{n_x \times n_v}$ are influence matrices of unknown inputs. $D_i \in \mathbb{R}^{n_x}$ represents a vector dependent on the operating point. $h_i(\theta(t))$ are the activation functions and have the same properties (II.7).

Assumption. II. 1 *Matrix* $E_i \in \mathbb{R}^{n_x \times n_v}$ *is full rank (i.e.* $rank(E_i) = n_v$ *with* $n_v < n_y$*).*

Let us consider the following unknown inputs observer structure:

$$\begin{cases} \dot{\eta}(t) = \sum_{i=1}^{m} h_i(\theta(t))\{N_i\eta(t) + M_i u(t) + G_i + L_i y(t)\} \\ \hat{x}(t) = \eta(t) - Hy(t) \end{cases} \tag{II.57}$$

where $N_i \in \mathbb{R}^{n_x \times n_x}$, $M_i \in \mathbb{R}^{n_x \times n_u}$ and $L_i \in \mathbb{R}^{n_x \times n_y}$ are local observer gains, $G_i \in \mathbb{R}^{n_x}$ are constant vectors and $H \in \mathbb{R}^{n_x \times n_y}$ is a transformation matrix. These matrices must be determined to ensure asymptotic convergence of the estimated state $\hat{x}(t)$ to the real state $x(t)$.

By considering the state estimation error (II.42) and the estimated state (II.57), the expression of the error becomes:

$$e_x(t) = (I + HC)x(t) - \eta(t) \tag{II.58}$$

By deriving (II.58) over time and posing $\bar{H} = I + HC$, we obtain the following error dynamics:

$$\begin{aligned} \dot{e}_x(t) = \sum_{i=1}^{m} h_i(\theta(t)) \Big[\bar{H}A_i x(t) + \bar{H}B_i u(t) + \bar{H}E_i v(t) + \bar{H}D_i \Big] \\ - \sum_{i=1}^{m} h_i(\theta(t)) \Big[N_i\eta(t) + M_i u(t) + G_i + L_i y(t) \Big] \end{aligned} \tag{II.59}$$

which can also be written as follows:

$$\begin{aligned} \dot{e}_x(t) = \sum_{i=1}^{m} h_i(\theta(t)) \Big[N_i e(t) + (\bar{H}A_i - N_i\bar{H} - L_i C)x(t) \\ + (\bar{H}B_i - M_i)u(t) + \bar{H}E_i v(t) + \bar{H}D_i - G_i \Big] \end{aligned} \tag{II.60}$$

by setting $Q_i = N_i H + L_i$, the error dynamics $\dot{e}_x(t)$ becomes as follows:

$$\begin{aligned} \dot{e}_x(t) = \sum_{i=1}^{m} h_i(\theta(t)) \Big[N_i e(t) + (\bar{H}A_i - N_i - Q_i C)x(t) \\ + (\bar{H}B_i - M_i)u(t) + \bar{H}E_i v(t) + \bar{H}D_i - G_i \Big] \end{aligned} \tag{II.61}$$

If the following conditions are verified:

$$\bar{H}E_i = 0 \tag{II.62}$$

$$N_i = \bar{H}A_i - Q_i C \tag{II.63}$$

$$M_i = \bar{H}B_i \tag{II.64}$$

$$G_i = \bar{H}D_i \tag{II.65}$$

Then, the dynamics of the state estimation error is reduced to:

$$\dot{e}_x(t) = \sum_{i=1}^{m} h_i(\theta(t)) N_i e(t) \tag{II.66}$$

The asymptotic convergence conditions of the state estimation (II.57) towards the T-S fuzzy model state (II.56) are given by the following theorem.

Theorem. II. 7 *(Akhenak et al., 2003b) The state estimation error between the T-S fuzzy model with unknown inputs* (II.56) *and the fuzzy observer* (II.57) *converges asymptotically to zero, if all pairs (A_i, C) are observable and if there is a symmetrical matrix $X > 0$, such that the following conditions are fulfilled for all $i = 1, 2, \ldots, m$*

$$N_i^T X^T + X N_i < 0 \qquad \text{(II.67)}$$

$$Q_i = N_i H - L_i \qquad \text{(II.68)}$$

$$\bar{H} = I + HC \qquad \text{(II.69)}$$

$$N_i = \bar{H} A_i - Q_i C \qquad \text{(II.70)}$$

$$\bar{H} E_i = 0 \qquad \text{(II.71)}$$

$$M_i = \bar{H} B_i \qquad \text{(II.72)}$$

$$G_i = \bar{H} D_i \qquad \text{(II.73)}$$

Using the equation (II.63), inequality (II.67) becomes:

$$(\bar{H} A_i - Q_i C)^T X^T + X(\bar{H} A_i - Q_i C) < 0 \qquad \text{(II.74)}$$

Inequality (II.74) is non-linear regarding the variables Q_i and X. The approach to solving all the constraints (II.67)-(II.73) is detailed in (Akhenak, 2004).

b. Unknown inputs affect both the system state and output

Let us consider a non-linear system affected by unknown inputs, represented by the following T-S fuzzy models:

$$\begin{cases} \dot{x}(t) = \sum_{i=1}^{m} h_i(\theta(t)) \{A_i x(t) + B_i u(t) + E_i v(t) + D_i\} \\ y(t) = Cx(t) + Fv(t) \end{cases} \qquad \text{(II.75)}$$

where $F \in \mathbb{R}^{n_y \times n_v}$ is influence matrix of unknown inputs on the system output.

Considering the fuzzy observer (II.57), the parameters N_i, L_i, M_i, G_i and H should be determined in order to ensure asymptotic convergence of the estimated state $\hat{x}(t)$ to the real state $x(t)$.

From the estimation error definition (II.42) and replacing $\hat{x}(t)$ by its expression given by (II.57), the expression of the error becomes :

$$e_x(t) = (I + HC)x(t) - \eta(t) + HFv(t) \qquad \text{(II.76)}$$

By using the same previous steps, the time derivative of (II.76) is given as follows:

$$\begin{aligned} \dot{e}_x(t) = \sum_{i=1}^{m} h_i(\theta(t)) \{ & N_i e(t) + (\bar{H} A_i - N_i - Q_i C)x(t) + (\bar{H} B_i - M_i)u(t) \\ & + (\bar{H} E_i - Q_i F)v(t) + \bar{H} D_i - G_i\} + HF\dot{v}(t) \end{aligned} \qquad \text{(II.77)}$$

with: $\bar{H} = I + HC$ and $Q_i = N_i H + L_i$.

If the following conditions are satisfied:

$$HF = 0 \quad \text{(II.78)} \qquad M_i = \bar{H}B_i \quad \text{(II.81)}$$
$$\bar{H}E_i = Q_i F \quad \text{(II.79)} \qquad G_i = \bar{H}D_i \quad \text{(II.82)}$$
$$N_i = \bar{H}A_i - Q_i C \quad \text{(II.80)}$$

Then, the dynamic of the state estimation error takes the form of (II.66). The following theorem gives the conditions of asymptotic convergence of the state estimation (II.57) towards the T-S fuzzy model state (II.75).

Theorem. II. 8 *(Akhenak et al., 2004a) The state estimation error between the fuzzy model with unknown inputs* (II.75) *and the fuzzy observer* (II.57) *converges asymptotically to zero, if all pairs (A_i, C) are observable, the matrix F is full row-column and if there is a symmetrical matrix $X > 0$, such that the following conditions are fulfilled for all $i = 1, 2, \ldots, m$.*

$$N_i^T X^T + X N_i < 0 \quad \text{(II.83)} \qquad \bar{H}E_i = Q_i F \quad \text{(II.87)}$$
$$\bar{H} = I + HC \quad \text{(II.84)} \qquad HF = 0 \quad \text{(II.88)}$$
$$Q_i = N_i H - L_i \quad \text{(II.85)} \qquad M_i = \bar{H}B_i \quad \text{(II.89)}$$
$$N_i = \bar{H}A_i - Q_i C \quad \text{(II.86)} \qquad G_i = \bar{H}D_i \quad \text{(II.90)}$$

Similar to the Theorem. II.7, the approach to solve all the constraints (II.83)-(II.90) is specified in (Akhenak, 2004).

c. Estimation of unknown inputs

Many works have been done to estimate unknown inputs in linear dynamical systems (Maquin et al., 1994; Stotsky and Kolmanovsky, 2001; Akhenak et al., 2007). In (Edwards et al., 2000; Akhenak et al., 2003a), authors have suggested methods based on sliding-mode observers to detect and estimate sensor faults. However, authors in (Liu and Peng, 2002) introduced the estimation of unknown inputs of a linear dynamical system under disturbances with a Luenberger observer. The idea is based on correct state estimation. Since if the asymptotic convergence conditions are satisfied, the state estimation error tends to zero, which allows us to replace $x(t)$ by $\hat{x}(t)$ and $v(t)$ by $\hat{v}(t)$ in the fuzzy T-S model equation (II.75):

$$\begin{cases} \dot{\hat{x}}(t) = \sum_{i=1}^{m} h_i(\theta(t))\{A_i\hat{x}(t) + B_i u(t) + E_i\hat{v}(t) + D_i\} \\ \hat{y}(t) = C\hat{x}(t) + F\hat{v}(t) \end{cases} \quad \text{(II.91)}$$

The observer (II.91) can be rewritten in the following form:

$$\begin{bmatrix} \dot{\hat{x}}(t) \\ \hat{y}(t) \end{bmatrix} = \begin{bmatrix} \sum_{i=1}^{m} h_i(\theta(t))\{A_i\hat{x}(t) + B_i u(t) + D_i\} \\ C\hat{x}(t) \end{bmatrix} + W\hat{v}(t) \tag{II.92}$$

where

$$W = \begin{bmatrix} \sum_{i=1}^{m} h_i(\theta(t))E_i \\ F \end{bmatrix}$$

Assuming that the matrix W is a full row-column matrix. The estimation of unknown input is computed using the pseudo-inverse of matrix W as follows:

$$\hat{v}(t) = (W^T W)^{-1} W^T \begin{bmatrix} \dot{\hat{x}}(t) - \sum_{i=1}^{m} h_i(\theta(t))\{A_i\hat{x}(t) + B_i u(t) + D_i\} \\ y(t) - C\hat{x}(t) \end{bmatrix} \tag{II.93}$$

The estimation of the unknown input can also be done simply if the matrix F is full rank, using the following expression:

$$\hat{v}(t) = (F^T F)^{-1} F^T (y(t) - C\hat{x}(t)) \tag{II.94}$$

II.6 Stabilisation of the T-S fuzzy systems

The fuzzy controller design for the T-S fuzzy systems has been extensively studied in recent years and is generally based on Lyapunov's approach. This approach is inspired by the fact that if a system's energy is continuously dissipated, then the system will reach an equilibrium point. The control laws' development techniques based on Lyapunov's theory involve finding a positive definite symmetrical matrix and its associated quadratic function that guarantees some conditions under the LMI form. Several works have been published in this field (Wang et al., 1996; Tanaka et al., 1998, 2001; Chadli, 2010a; Wang et al., 2018; El Youssfi et al., 2020a). These research works, which have been mainly based on control methods found in literature have addressed control based on state feedback, on static output feedback and estimated state feedback, both with/without uncertainties and/or disturbances.

II.6.1 Stabilisation by state feedback control

To stabilise T-S fuzzy systems, a commonly used control law based on the Parallel Distributed Compensation (PDC) concept (Wang et al., 1996). The principle is to generate a compensator for each rule of the T-S fuzzy model. Then the PDC is made up of linear state feedbacks blended using the same non-linear functions $h_i(\theta(t))$ as the T-S fuzzy model (II.40) (Lendek et al., 2011a). This type of control is of the following form:

$$u(t) = -\sum_{i=1}^{m} h_i(\theta(t))K_i x(t) \tag{II.95}$$

where $K_i \in \mathbb{R}^{n_u \times n_x}$ are the controller gains.

By substituting (II.95) in the T-S fuzzy model (II.40), the closed-loop system becomes as follows:

$$\dot{x}(t) = \sum_{i=1}^{m}\sum_{j=1}^{m} h_i(\theta(t))h_j(\theta(t))G_{ij}x(t) \tag{II.96}$$

with $G_{ij} = A_i - B_iK_j$.

The stability conditions of (II.96) are achieved using the following Lyapunov function:

$$V(x(t)) = x^T(t)Px(t), \qquad P > 0 \tag{II.97}$$

The time derivative of the Lyapunov function over the trajectory of the system (II.96), is given as follows:

$$\dot{V}(x(t)) = \sum_{i=1}^{m}\sum_{j=1}^{m} h_i(\theta(t))h_j(\theta(t))x^T(t)\{G_{ij}^TP + PG_{ij}\}x(t) \tag{II.98}$$

The following theorem provides the conditions for stabilising the T-S fuzzy system (II.40) via the reconstructed control law (II.95).

Theorem. II. 9 *(Tanaka et al., 1998) The closed-loop T-S fuzzy system described by* (II.96) *is asymptotically stable, if there is a positive defined symmetrical matrix P such that*

$$G_{ii}^TP + PG_{ii} < 0, \qquad i = 1, 2, \ldots, m \tag{II.99}$$

$$\left(G_{ij} + G_{ji}\right)^T P + P\left(G_{ij} + G_{ji}\right) \leq 0, \quad i < j \tag{II.100}$$

for any $i, j = 1, 2, \ldots, m$*, except pairs* (i, j) *such that* $h_i(\theta(t))h_j(\theta(t)) = 0$.

The determination of the gains $K_i (i = 1, 2, \ldots, m)$ of the control law then requires the transformation of the conditions of the Theorem. II.9 into an equivalent problem under the form of LMIs which convex optimisation tools can solve (Hindi and Boyd, 1998). This transformation corresponds to simple changes of variables $X = P^{-1}$ and $Y_i = K_iP^{-1}$ by multiplying right and left by the matrix X the inequalities (II.99)-(II.100).

So the inequalities (II.99)-(II.100) can be rewritten as LMIs based on the variables X and Y_i as follows:

$$XA_i^T - Y_i^TB_i^T + A_iX - B_iY_i < 0, \qquad i = 1, 2, \ldots, m \tag{II.101}$$

$$XA_i^T - Y_j^TB_i^T + A_iX - B_iY_j + XA_j^T - Y_i^TB_j^T + A_jX - B_jY_i < 0, \quad i < j \tag{II.102}$$

Then, the fuzzy controller gains are obtained by:

$$K_i = Y_iX^{-1} \tag{II.103}$$

The stability conditions of the Theorem. II.9 are quite conservative because they assume that all cross subsystems are stable. This conservatism can be reduced by applying the relaxation Lemma 4, which only requires that the dominant subsystems are

stable with an additional condition. In this context, other relaxing theorems based on the Theorem. II.9 can be found in these references (Tanaka et al., 1998; Liu and Zhang, 2003; Kruszewski et al., 2008; Tanaka et al., 2001; Chadli et al., 2000).

II.6.2 Stabilisation by observer-based controller

Often in real-world control problems, system states are not always fully accessible. In such cases, it is necessary to design the controller using other methods, such as observer-based control designs. This part of the sub-section presents observer-based control design methods involving state estimation for T-S fuzzy systems. Many authors have studied the case of observer-based control and have formulated stability requirements for the augmented system (Tanaka and Taniguchi, 1999; Wang et al., 2019a; Tuan et al., 2019). In what follows, we describe the observer-based stabilisation briefly for T-S fuzzy systems.

Let us consider the T-S fuzzy model (II.40) and the fuzzy observer (II.41). The structure of the observer-based controller is as follows:

$$u(t) = -\sum_{i=1}^{m} h_i(\theta(t)) K_i \hat{x}(t) \tag{II.104}$$

where $K_i \in \mathbb{R}^{n_u \times n_x}$ are the gains of the controller.

The time derivative of the estimation error $e_x(t) = x(t) - \hat{x}(t)$ is obtained as (II.45), which is reproduced here for convenience:

$$\dot{e}_x(t) = \sum_{i=1}^{m} \sum_{j=1}^{m} h_i(\theta(t)) h_j(\theta(t)) \{A_i - L_i C_j\} e_x(t) \tag{II.105}$$

The closed-loop system using the observer-based fuzzy control law is written as follows:

$$\dot{x}(t) = \sum_{i=1}^{m} \sum_{j=1}^{m} h_i(\theta(t)) h_j(\theta(t)) \left\{ (A_i - B_i K_j) x(t) + B_i K_j e_x(t) \right\} \tag{II.106}$$

By combining the dynamics of the estimation error (II.105) and that of the state (II.106), the following augmented system is obtained:

$$\dot{\bar{x}}(t) = \sum_{i=1}^{m} \sum_{j=1}^{m} h_i(\theta(t)) h_j(\theta(t)) \bar{A}_{ij} \bar{x}(t) \tag{II.107}$$

where

$$\bar{x}(t) = \begin{bmatrix} x(t) \\ e_x(t) \end{bmatrix}, \text{ and } \quad \bar{A}_{ij} = \begin{bmatrix} A_i - B_i K_j & B_i K_j \\ 0 & A_i - L_i C_j \end{bmatrix}$$

The problem with the combination of the observer and the closed-loop system is to determine gains L_i and K_i, $(i = 1, 2, \ldots m)$, such that the augmented system (II.107) is asymptotically stable. The asymptotic stability conditions are presented in the following theorem.

Theorem. II. 10 *(Tanaka and Wang, 2004) The system* (II.107) *is asymptotically stable, if there exist symmetric matrices $P > 0$ and $Q > 0$, and matrices X_i and Y_i, $(i = 1, 2, \ldots, m)$, such that the following LMIs are satisfied*

$$A_iP - B_iX_i + PA_i^T - X_i^TB_i^T < 0, \qquad i = 1, 2, \ldots, m \tag{II.108}$$

$$A_iP - B_iX_j + A_jP - B_jX_i + PA_i^T - X_j^TB_i^T + PA_j^T - X_i^TB_j^T \leq 0, \qquad i < j \tag{II.109}$$

$$QA_i - Y_iC_i + A_i^TQ - C_i^TY_i^T < 0, \qquad i = 1, 2, \ldots, m \tag{II.110}$$

$$QA_i - Y_iC_j + QA_j - Y_jC_i + A_i^TQ - C_j^TY_i^T + A_j^TQ - C_i^TY_j^T \leq 0, \qquad i < j \tag{II.111}$$

The control and the observer gains are achieved in the following way:

$$\begin{aligned} K_i &= X_iP^{-1} \\ L_i &= Q^{-1}Y_i \end{aligned} \tag{II.112}$$

Note that Theorem. II.10 allows us to design the observer and the controller separately, ensuring the stability of the closed-loop system, referred to as the separation concept (Ma et al., 1998). It is also worth mentioning that conditions of Lemma 4 can be included for more relaxing results.

II.6.3 Stabilisation by static output-feedback control

Another method to design the controller without requiring access to system state variables is one that uses static feedback. Several literature works have focused on the design of static output feedback control for T-S fuzzy systems, e.g. (Fang et al., 2006; Kau et al., 2007; Huang and Nguang, 2007; Jeung and Lee, 2014; El Youssfi et al., 2020a). Note that the static output feedback control is the most suitable, as it can be easily implemented at a lower cost.

Let us consider the static output feedback control of the following type:

$$u(t) = -\sum_{i=1}^{m} h_i(\theta(t))F_iy(t) \tag{II.113}$$

where $F_i \in \mathbb{R}^{n_u \times n_y}$ are the control gains.

By inserting (II.113) in the model (II.40), with $C_i = C, \forall i = 1, 2, \ldots, r$, the following closed-loop T-S fuzzy system is obtained:

$$\dot{x}(t) = \sum_{i=1}^{m}\sum_{j=1}^{m} h_i(\theta(t))h_j(\theta(t))H_{ij}x(t) \tag{II.114}$$

with $H_{ij} = A_i - B_iF_jC$.

Here, Theorem. II.9 is still valid, then the synthesis of the static output feedback

control law can be achieved easily by substituting G_{ij} by H_{ij}. Therefore, system stability conditions are as follows:

$$\begin{aligned} &H_{ii}^T P + P H_{ii} < 0, \qquad i = 1, 2, \ldots, m \\ &\left(H_{ij} + H_{ji}\right)^T P + P\left(H_{ij} + H_{ji}\right) \leq 0, \qquad i < j \end{aligned} \tag{II.115}$$

These conditions are non-linear and cannot be linearised using the traditional change of variables, which is the main challenge of stabilisation by static output feedback control. To overcome this difficulty while assuming that C is a full-column row matrix, the authors in (Chadli et al., 2002) proposed a linear formulation of the conditions (II.115).

Theorem. II. 11 *(Chadli et al., 2002) The T-S fuzzy system* (II.114) *is asymptotically stable, if there exist symmetric matrix $P > 0$, and matrices Q and X_i, $(i = 1, 2, \ldots, m)$, such that the following conditions are satisfied*

$$\begin{aligned} &A_i P - B_i X_i C + P A_i^T - C^T X_i^T B_i^T < 0, \qquad i = 1, 2, \ldots, m \\ &A_i P - B_i X_j C + A_j P - B_j X_i C + P A_i^T - C^T X_j^T B_i^T + P A_j^T - C^T X_i^T B_j^T \leq 0, \quad i < j \\ &CP = QC \end{aligned} \tag{II.116}$$

The control gains are obtained as follows:

$$F_i = X_i Y^{-1} \tag{II.117}$$

The constraints obtained by Theorem. II.11 are linear and can be easily implemented. Numerically, these constraints can be simply solved using available tools.

II.7 Conclusion

In this second chapter, a brief outline of T-S fuzzy systems has been described. After defining the T-S fuzzy models, this chapter presented the different techniques to obtain a T-S fuzzy model, particularly the non-linearity sector approach, which allows obtaining a T-S fuzzy model from non-linear system equations. A reminder of the necessary results concerning the stability of a class of non-linear systems represented by the T-S fuzzy model is presented. Some results for the synthesis of fuzzy observers, particularly for the unknown input observers for the T-S fuzzy model, are presented. In the last part of this chapter, the results on sufficient conditions for stabilising the T-S fuzzy model are obtained using different control laws, including control law by reconstructed state feedback, estimated state and static output. For a complete state of the art on the T-S approach, the reader may refer to the references (Wang, 1994; Tanaka and Wang, 2004; Lendek et al., 2011a; Chadli and Borne, 2013; Driankov et al., 2013; Benzaouia and Hajjaji, 2016).

Most of the results presented can be extended to other T-S models, such as systems in descriptor form. These synthesis problems will be discussed in more detail and applied to the non-linear vehicle lateral dynamics system in the following chapters.

Chapter III

Automotive vehicle modelling and lateral mode analysis

III.1 Introduction

Intending to predict or study the vehicle's behaviour in various situations and modifying the design if necessary, there is a method that involves its modelling, which means finding a mathematical representation describing this system. The modelling procedure typically leads to a set of differential equations derived from the mechanical laws. The development of computer tools makes modelling the essential step in the study phase. In recent years, the modelling of automotive vehicles for control purposes has been the subject of extensive scientific research, citing, for example, (Genta, 1997; Rajamani, 2005; Karnopp, 2013; Schramm et al., 2014; Abdullah et al., 2016; Dieter et al., 2018). These books include modelling of several elements such as chassis, suspension, shock absorber, brakes, wheels, steering, engine, and so on, taking into account the influence of tyre/ground contact forces. Automotive vehicles are complex systems composed of many mechanical, electronic, electromechanical and other elements. In general, these elements have non-linear characteristics, and their behaviour can change over time and in different driving situations.

In the literature, a vehicle's behaviour is frequently described along several axes, as indicated in several references (e.g. Young and Reid (1993); Genta (1997); Rill (2011); Rajamani (2012); El Majdoub et al. (2012)). However, its principle is still based on analysing the wheels' forces in longitudinal, lateral and vertical directions. The studies are made to model the vehicle in order to develop robust observers, embedded estimators, driving assistance or individual or combined control strategies of these three modes.

The automotive vehicle is a highly non-linear system, and the tire/road contact description is far from obvious. Indeed, the models used are either too simplified and neglect several phenomena whose actions can be necessary or complex and challenging to identify all the model's parameters. This necessitates the determination of a nominal dynamic model that is useful for simulating the behaviour, observation and control of the automotive vehicle. A nominal model is based on assumptions about

the vehicle structure and its environment. These assumptions reduce the model's complexity while keeping it accurate to reality. The possibility to treat different parts of the vehicle separately reduces the number of state variables and results in a nominal model. In this thesis, the focus is on lateral control assistance. Therefore, only the lateral mode modelling of the automotive vehicle is addressed.

In the rest of this chapter, we outline some of the necessary elements for modelling the automotive vehicle. Afterwards, different vehicle models are presented, including the single-track model and the roll model. Then, special attention is given to the modelling of lateral forces in order to represent them by the T-S fuzzy model. The penultimate section is devoted to the state representation of the vehicle's two lateral dynamics models, the first one without considering roll motion and the second one with it.

III.2 Automotive vehicle components and motions

The comprehension of the automotive vehicle's motions, its main components and the wheel/ground contact forces are key factors that allow for better modelling of the automotive vehicle. This section characterises and defines the motions and the main constituent parts of the automotive vehicle.

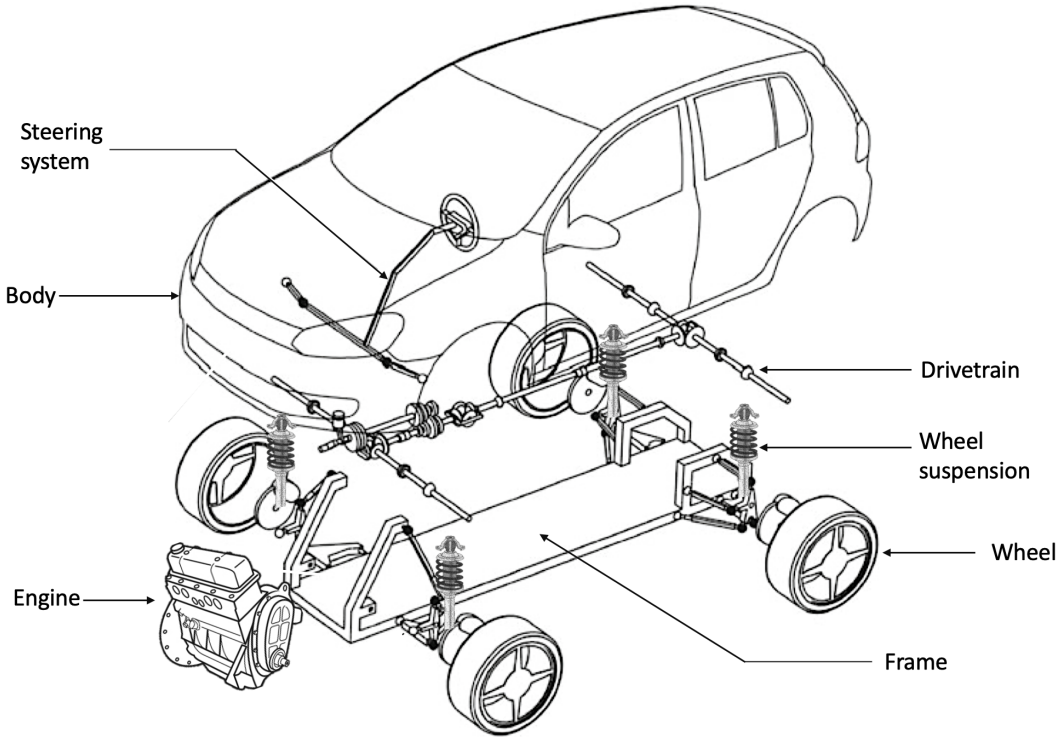

FIGURE III.1: Automotive vehicle components

III.2.1 Automotive vehicle components

The automotive vehicle is a set of mechanical and electronic components connected by several links to ensure the chassis motion and the passengers' comfort. These elements include, as shown in Fig. III.1, the engine, the chassis, the ground linkage system, which itself contains the wheels, the trains, the steering and the suspension. Each device has a specific role that must be understood for modelling reasons.

The automotive vehicle components are described below, including the chassis, drive trains, suspension mechanism, and steering system.

a. Chassis

The chassis consists, as shown in Fig. III.1, of a lower part called "the body", which carries the drive-train, the front and rear axles, the dashboard, the seats, the boot and the tank, and an upper part called "the frame" which supports the roof, the fixed windows, the doors and the bonnets. It is a solid body designed to absorb the forces caused by frequent or exceptional use and absorb impact energy by deforming in an organised manner to preserve the passenger compartment. The chassis is considered a suspended mass, each extremity attached to a wheel by a suspension system. The chassis body is subject to the wheel/ground interaction forces transmitted by the ground linkage system and the vehicle's aerodynamic interaction forces with the wind, which occur mainly in the longitudinal direction, except in crosswind situations. The vehicle reference mark is assumed to be the same as that of the chassis body, which explains why vehicle motion is partly determined by the chassis body's translational and rotational movements.

b. Front and rear axles

All the elements linking the wheels to the chassis can be divided into front and rear axles (see Fig. III.2). The front axle consists of the mechanical components that ensure the suspension and steering of the front wheels, and the rear axle consists of all the components that ensure the suspension and steering of the rear wheels.

The geometry of the train contributes enormously to good road holding both straight and curved roads. The trains are characterised on the one hand by their kinematics determining the position and orientation of the wheel in relation to the ground, which conditions the wheel/ground interaction effort, and on the other hand by their elastokinetics determining the position and orientation of the chassis relative to the train, which is ensured by elastic connecting blocks.

c. Suspension mechanism

The suspension mechanism is an essential part of any vehicle. It consists of a spring-damper assembly located behind each wheel (see Fig. III.3). Its principle is to isolate the vehicle from the vibrations and stresses caused by track irregularities by eliminating unwanted motion frequencies, and consequently, to improve driver comfort.

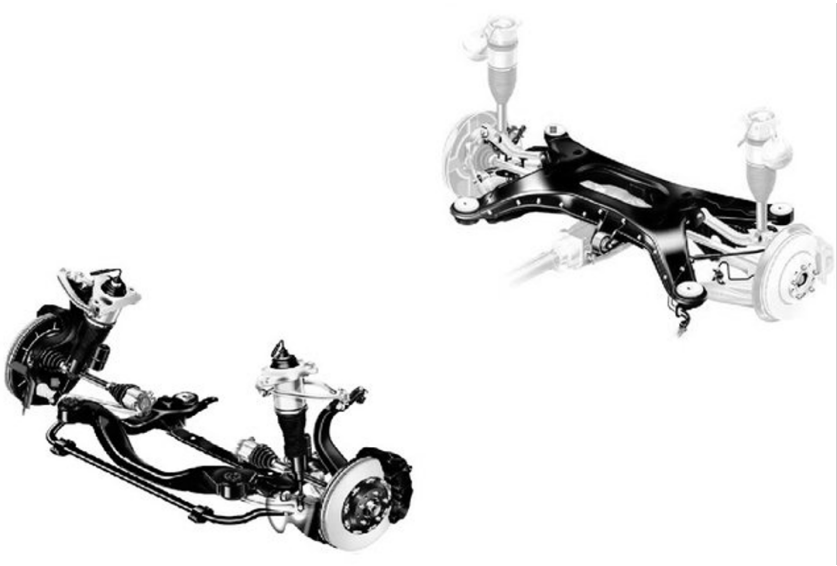

FIGURE III.2: Automotive vehicle's front and rear axles

Suspension systems can be divided according to the different control modes used into conventional passive suspensions, semi-active suspensions that use mechanical principles to adjust the suspension effort according to road behaviour, and more recently, fully controlled active suspensions have appeared, which require high energy input, making them more challenging to install on the vehicle.

Many different types of mechanically independent suspension have been tried out over the years, including, as shown in Fig. III.3 (Živković et al., 2020), the McPherson suspension, double-wishbone suspension and multi-arm suspension. In practice, their use depends mainly on the load to be transported, the manufacturing costs and the vehicle type.

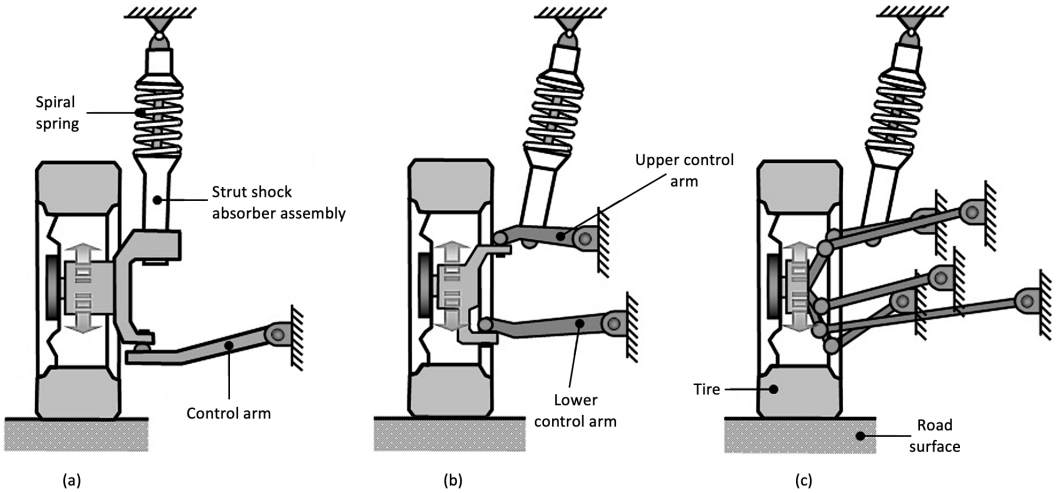

FIGURE III.3: Suspension system types
a) McPherson, b) double-wishbone, c) multi–link

The "spring and damper" part of the suspension is presented by a system consisting of a spring of stiffness k_i and a damper of damping coefficient f_{v_i} and dry friction

f_{s_i}, as shown in the diagram in Fig. III.4 (Khan et al., 2016).

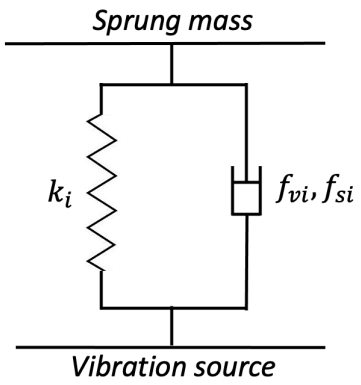

FIGURE III.4: Suspension model

d. Steering system

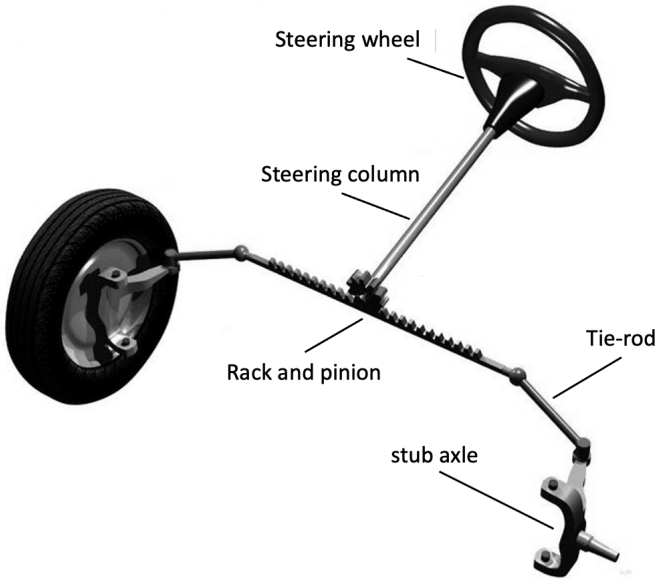

FIGURE III.5: Rack and pinion steering system

The vehicle's steering system operates through the combination of several mechanical elements. The latter's joint action enables the driver to intervene in the direction that he wishes to give to his vehicle's trajectory. In practice, this enables him to negotiate curves and turns safely. A conventional steering system consists, as shown in Fig III.5 (Khan et al., 2016), of:

- Steering wheel.
- Steering column.
- Rack and pinion, which transforms the steering wheel rotation into a translation in order to turn the steered wheels.

– Tie rods, which transfer the force from the rack to the stub axles.

– Stub axles where the wheel is fixed.

The steering wheel's action in the vehicle's steering system is essential because it transforms the driver's small effort into a steering effort. The power steering system facilitates the driver's manoeuvres by assisting the torque applied to the steering wheel.

III.2.2 Automotive vehicle motions: translations and rotations

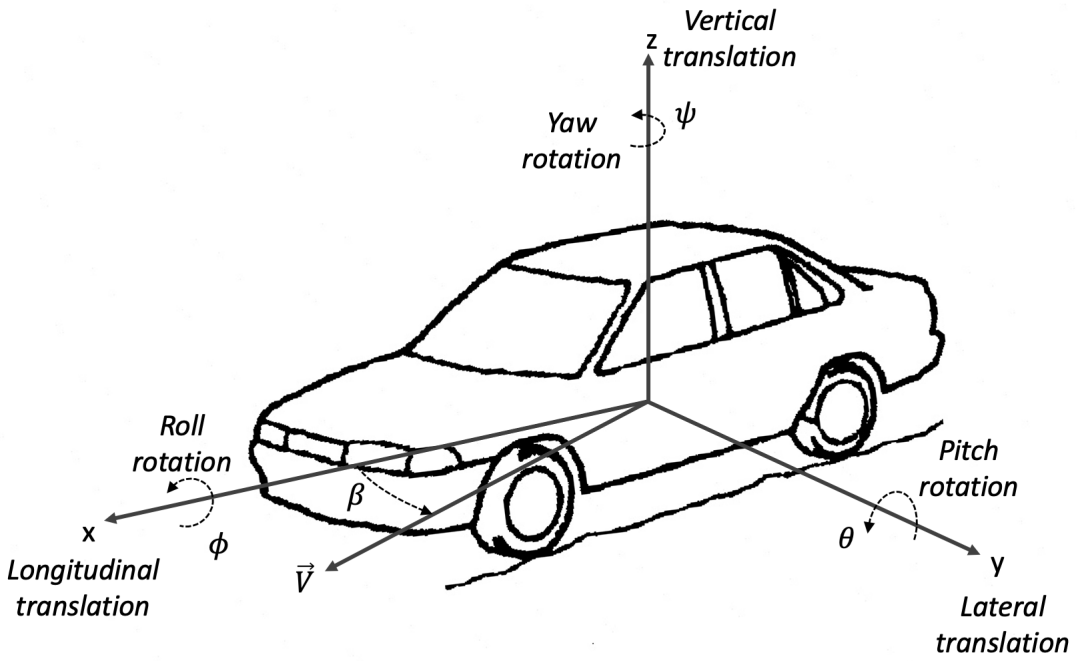

FIGURE III.6: Different vehicle motions

An automotive vehicle moves according to six Degrees of Freedom (Kiencke and Nielsen, 2000), which is a set of three translations and three rotations (Fig. III.6). The x-axis translation indicates the vehicle's longitudinal movement. The lateral movement is on the y-axis. The z-axis translation characterises the bodywork's vertical movement, reflecting the chassis movement via its suspension. Rotation around the z-axis represents the angular yaw movement ψ of the vehicle, which determines its direction. Rotation around the x-axis defines the roll angle ϕ, which is mainly felt when the vehicle moves through a curve or changes track. Lastly, rotation around the y-axis describes the pitch angle θ of the vehicle experienced during acceleration and braking operations. The parameter β is the slip angle, which is the angle between the vehicle heading and the speed vector $\vec{V}$.

As this thesis's main objective is to design robust and fault-tolerant control laws for the system of the lateral dynamics of an automotive vehicle, only the planar study of motions is discussed, vertical movements are not addressed.

III.3 Automotive vehicle dynamics

In motion, automotive vehicles modelled as a rigid body have 6-DoF. In this section, the vehicles are assumed to have only a plane motion parallel to the road surface. The objective is to establish the equations for automotive vehicle dynamics whose only the lateral, roll and yaw motions are considered. It will then be assumed that the vehicle does not perform any pitching motion. Thus, many publications can be found in literature dealing with planar modelling of the automotive vehicle (Sheikholeslam and Desoer, 1992; Lu and Hedrick, 2005; Hamersma and Els, 2014; Knapczyk and Kucybała, 2016).

The four-wheel automotive vehicle model is presented below, which then leads to a more simplified bicycle model. Afterwards, the roll model is described, which introduces the roll behaviour, taking into account the suspension kinematics. For convenience, the parameters used in this section can be found and explained in the list of symbols at the beginning of the document.

III.3.1 Four-wheel automotive vehicle model

The four-wheel model, widely referred to as the two-track model, is mostly used in literature to study and control the vehicle's longitudinal and lateral dynamic behaviour (Furukawa et al., 1989; Wang and Qi, 2001; Zhao et al., 2018). It is a 3-DoF model which has the advantage of displaying all four wheels; it includes the yaw rate $\dot{\psi}$ and both longitudinal and lateral motions. The z-axis movement is not taken into account, and the roll and pitch movements are neglected.

Figure III.7 illustrates the various variables and parameters related to the automotive vehicle's planar dynamics. In this model, the following simplifications are applied:

- Rear steering angles are approximately zero: $\delta_{r_1} \approx 0$ and $\delta_{r_2} \approx 0$
- The direction of the rear tyres is the same as that of the vehicle.
- Front steering angles are assumed to be equal: $\delta_f = \delta_{f_1} = \delta_{f_2}$

The application of the fundamental principle of dynamics to the vehicle's mass m_v in parts, longitudinally, laterally and around the vertical axis z through the CG, neglecting pitching and suspension, produces the following equations (Doumiati et al.,

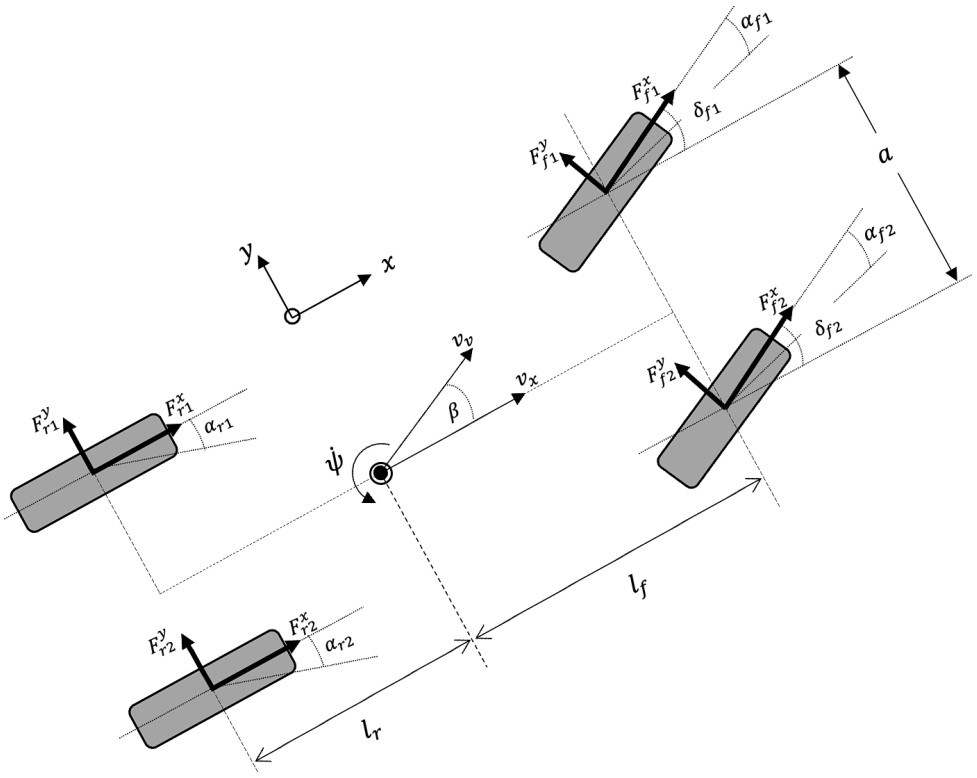

FIGURE III.7: Four-wheel vehicle model

2012):

$$\dot{\beta} = \frac{1}{m_v v_v}\left\{\bar{F}_r^y\cos(\beta) - \bar{F}_r^x\sin(\beta) + \bar{F}_f^y\cos(\delta_f-\beta) + \bar{F}_f^x\sin(\delta_f-\beta)\right\} - \dot{\psi} \tag{III.1}$$

$$\ddot{\psi} = \frac{1}{I_z}\left\{\left(l_f\bar{F}_f^y - \frac{a}{2}\underline{\mathrm{F}}_f^x\right)\cos(\delta_f) + \left(l_f\bar{F}_f^x + \frac{a}{2}\underline{\mathrm{F}}_f^y\right)\sin(\delta_f) - l_r\bar{F}_r^y - \frac{a}{2}\underline{\mathrm{F}}_r^x\right\} \tag{III.2}$$

$$a_x = \frac{1}{m_v}\left\{\bar{F}_f^x\cos(\delta_f) - \bar{F}_f^y\sin(\delta_f) + \bar{F}_r^x\right\} \tag{III.3}$$

$$\dot{v}_x = a_x + v_y\dot{\psi} \tag{III.4}$$

$$a_y = \frac{1}{m_v}\left\{\bar{F}_f^y\cos(\delta_f) + \bar{F}_f^x\sin(\delta_f) + \bar{F}_r^y\right\} \tag{III.5}$$

$$\dot{v}_y = a_y - v_x\dot{\psi} \tag{III.6}$$

$$\dot{v}_v = \frac{1}{m_v}\left\{\bar{F}_f^x\cos(\delta_f-\beta) - \bar{F}_f^y\sin(\delta_f-\beta) + \bar{F}_r^x\cos(\beta) + \bar{F}_r^y\sin(\beta)\right\} \tag{III.7}$$

where I_z is the moment of inertia around the vertical axis and for the sake of simplicity:

$$\begin{aligned} \bar{F}_f^{x,y} &= F_{f1}^{x,y} + F_{f2}^{x,y}, \quad & \bar{F}_r^{x,y} &= F_{r1}^{x,y} + F_{r2}^{x,y} \\ \underline{\mathrm{F}}_f^{x,y} &= F_{f1}^{x,y} - F_{f2}^{x,y}, \quad & \underline{\mathrm{F}}_r^{x,y} &= F_{r1}^{x,y} - F_{r2}^{x,y} \end{aligned} \tag{III.8}$$

Note that the subscript/exponent "f" denotes front tyres and "r" denotes rear tyres, and the subscript "i" is replaced by "1" for left tyres and "2" for right tyres of the vehicle (e.g. F_{r1}^y is the lateral force of the right-left rear wheel).

From Fig. III.7, the velocity of each wheel in its rolling direction can be obtained as follows (Osborn and Shim, 2006; Kiencke and Nielsen, 2000):

$$v_{f1}^{w} = \left(v_x - \frac{a}{2}\dot{\psi}\right)\cos(\delta_f) + \left(v_y + l_f\dot{\psi}\right)\sin(\delta_f) \tag{III.9}$$

$$v_{f2}^{w} = \left(v_x + \frac{a}{2}\dot{\psi}\right)\cos(\delta_f) + \left(v_y + l_f\dot{\psi}\right)\sin(\delta_f) \tag{III.10}$$

$$v_{r1}^{w} = v_x - \frac{a}{2}\dot{\psi} \tag{III.11}$$

$$v_{r2}^{w} = v_x + \frac{a}{2}\dot{\psi} \tag{III.12}$$

Then, the slip angle for all four wheels and the slip angle β at the CG can be calculated as follows:

$$\alpha_{f1} = \delta_f - \arctan\left(\frac{v_y + l_f\dot{\psi}}{v_x - \frac{a\dot{\psi}}{2}}\right) \tag{III.13}$$

$$\alpha_{f2} = \delta_f - \arctan\left(\frac{v_y + l_f\dot{\psi}}{v_x + \frac{a\dot{\psi}}{2}}\right) \tag{III.14}$$

$$\alpha_{r1} = -\arctan\left(\frac{v_y - l_r\dot{\psi}}{v_x - \frac{a\dot{\psi}}{2}}\right) \tag{III.15}$$

$$\alpha_{r2} = -\arctan\left(\frac{v_y - l_r\dot{\psi}}{v_x + \frac{a\dot{\psi}}{2}}\right) \tag{III.16}$$

$$\beta = \arctan\left(\frac{v_y}{v_x}\right) \tag{III.17}$$

III.3.2 Single-track model

The single-track half-vehicle model, also known as the bicycle model, was developed in (Segel, 1956). It is one of the most widely used models to describe the behaviour of the vehicle's lateral dynamics, mainly to evaluate side-slip angles and study lateral accelerations a_y as well as rotation about the vertical axis z (Corno et al., 2015; Rajamani, 2011). It can be seen as a simplification of the four-wheel model, where it is assumed that there is only one wheel for each train, as shown in Fig. III.8, by projecting the two wheels of the train on the central axis of the vehicle (Ungoren et al., 2004). The resulting wheel will have a steering angle equivalent to the steering angle of the two wheels.

In this model, the rear steering angle is zero, vertical motions are ignored, and roll motion is not considered. The simplified model of the bicycle is used in many industrial applications such as ESP, and it has only two degrees of freedom corresponding to lateral and yaw movements. The simplified lateral dynamics model "bicycle" is inspired from equations (III.2)-(III.1), considering the left/right forces of a train are

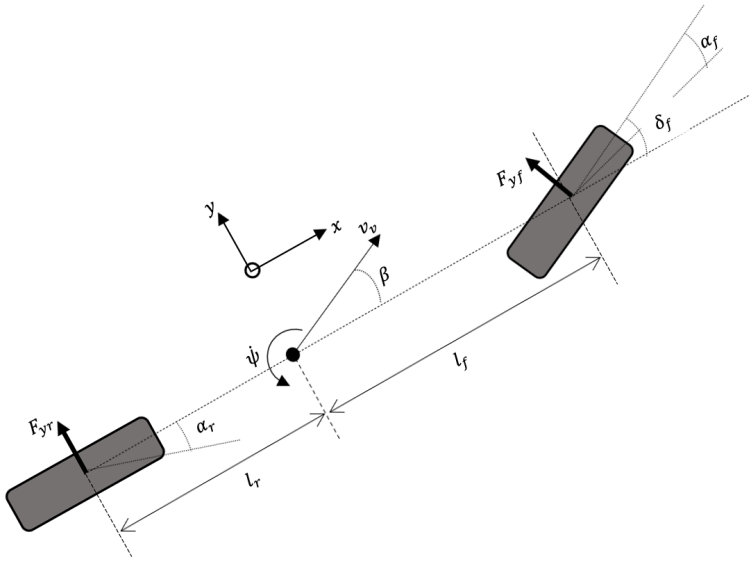

FIGURE III.8: Half-vehicle model

identical. The result is then obtained as follows:

$$\begin{cases} \dot{\beta} = \dfrac{2}{m_v v_v}\left\{F_r^y\cos(\beta) - F_r^x\sin(\beta) + F_f^y\cos(\delta_f-\beta) + F_f^x\sin(\delta_f-\beta)\right\} - \dot{\psi} \\ \ddot{\psi} = \dfrac{2}{I_z}\left\{l_f\left(F_f^y\cos(\delta_f) + F_f^x\sin(\delta_f)\right) - l_r F_r^y\right\} \end{cases} \tag{III.18}$$

Under the hypothesis of small angles, the equation system (III.18) becomes:

$$\begin{cases} \dot{\beta} = \dfrac{2}{m_v v_v}\left(F_r^y + F_f^y\right) - \dot{\psi} \\ \ddot{\psi} = \dfrac{2}{I_z}\left(l_f F_f^y - l_r F_r^y\right) \end{cases} \tag{III.19}$$

and the front and rear tyre side-slip angles are obtained as follows:

$$\alpha_f = \delta_f - \beta - l_f\frac{\dot{\psi}}{v_x} \tag{III.20}$$

$$\alpha_r = -\beta + l_r\frac{\dot{\psi}}{v_x} \tag{III.21}$$

The bicycle model can be used, for example, to study the vehicle's cornering stability as a function of grip potential, the state in which the system is in, and the steering control applied to the wheel (Mammar and Koenig, 2002). The objective is then to define the necessary control law to be applied to the vehicle to remain within the stability zone.

A strategy for stabilising the automotive vehicle's lateral behaviour is to use the chassis moment around the CG as a control variable (Oudghiri et al., 2007). The ABS generate this by applying braking torques to each wheel with different magnitudes.

In this case, the yaw motion equation in (III.19) becomes as follows:

$$\ddot{\psi} = \frac{2}{I_z}\left(l_f F_f^y - l_r F_r^y\right) + \frac{1}{I_z} M_z \tag{III.22}$$

with M_z is the moment around the vehicle's CG.

III.3.3 Automotive vehicle roll dynamics

The suspension system generates roll and pitch movements. These movements affect the essential characteristics of vehicle dynamics and should be addressed. In this subsection, the focus is on the roll movement. Roll is a lateral sway. It is simply the fact that the automotive vehicle inclines about the X-axis when cornering or under lateral wind forces' action. For example, when a vehicle takes a left turn at high speed, it will put more weight on the right wheels outside the turn. Then, as it comes out of the turn, the left wheels will be used instead (Wallentowitz, 2014). The presence of anti-roll bars can mitigate this phenomenon. These connect two opposing axles, thus levelling the suspensions. This minimises mass transfer and improves driving comfort. If a vehicle takes too much roll, the wheels are no longer located in the axis perpendicular to the road, the contact between the ground and the tyre becomes less good. Figure III.9 shows a schematic diagram of the different mechanisms governing the rolling motion (Jin et al., 2019).

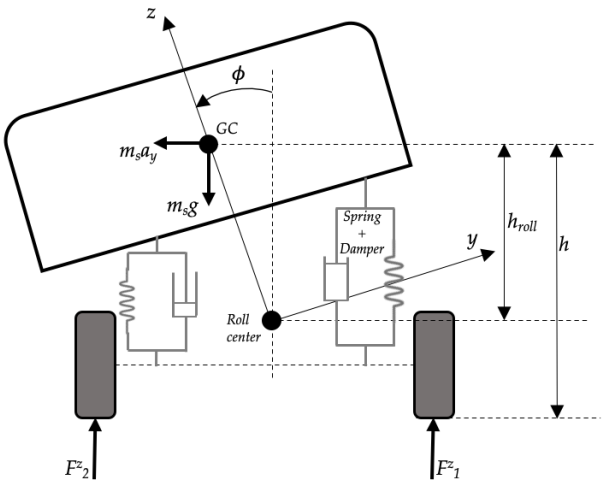

FIGURE III.9: Schematic description of roll dynamics (rear view)

As shown in Fig. III.9, the vehicle is considered to be a two-mass system, consisting of a sprung mass m_s and an unsprung mass m_u. The roll dynamics are caused solely by the sprung mass. The vehicle roll motion concerning the road is produced by the inertial force caused by the lateral acceleration $m_s a_y$, which generates the moment $m_s a_y h_\phi$ around the roll axis. A gravity force component $m_s g \sin(\phi)$ also adds to the roll moment for a significant roll angle. The roll dynamics of the vehicle body can be

defined depending on the torque equilibrium in the roll axis by the following equation (Ding and Massel, 2005):

$$\ddot{\phi} = \frac{m_s h_\phi}{I_x} a_y + \frac{m_s g h_\phi}{I_x} \sin(\phi) - \frac{C_\phi}{I_x}\dot{\phi} - \frac{K_\phi}{I_x}\phi \tag{III.23}$$

This 1-DoF model represents only the roll motion of a vehicle. It is also called the roll plane model. It is used to study the lateral load transfer due to the rolling motion.

III.4 Model of lateral forces

The tyre is a very complex component, which is subject to high forces and temperature variations. It is subject to external forces and moments along the longitudinal, lateral and vertical axes. Physical models of forces are accurate and precise but too complicated to be used to construct control systems for automotive vehicles. In this thesis, only the models of the lateral forces F^y will be presented.

Literature is rich in theoretical developments and tyre behaviour analyses (see for example Livingston and Brown Jr (1969, 1970); Dugoff et al. (1970); Bakker et al. (1989); Gim and Nikravesh (1990); Pacejka et al. (1996)). The model most commonly used by tyre manufacturers and automakers is the Pacejka model, discussed in detail in the following subsection.

III.4.1 Magic formula of Pacejka

To identify lateral forces, the model most commonly used by tyre manufacturers and automakers is the Pacejka model (Pacejka and Bakker, 1992; Pacejka et al., 1996; Pacejka and Besselink, 1997; Pacejka, 2006). It is a semi-empirical model constructed from experimental data by identifying and interpolating parameters and the tyre's physical models. It is also known as the "magic formula" based on a $\sin(\arctan)$, which provides an excellent approximation of the force curves (see Fig. III.10 and Fig.III.11).

The general form of the "magic formula" is given by the following equation:

$$\begin{cases} Y(x) = D \sin\left\{C \arctan\left[Bx - E\left(Bx - \arctan(Bx)\right)\right]\right\} + S_v \\ x = X + S_h \end{cases} \tag{III.24}$$

where Y and X represent output and input, respectively (e.g. lateral force and slip angle). The different parameters and their meanings involved in the formula (III.24) are given in Tab. III.1 and Fig. III.10. According to Schramm et al. (2014), the following relationships are valid:

$$C = 1 \pm \left(1 - \frac{2}{\pi} \arcsin\left(\frac{y_s}{D}\right)\right) \tag{III.25}$$

$$E = \frac{Bx_m - \tan\left(\frac{\pi}{2C}\right)}{Bx_m - \arctan(Bx_m)}, \quad if\ C > 1 \tag{III.26}$$

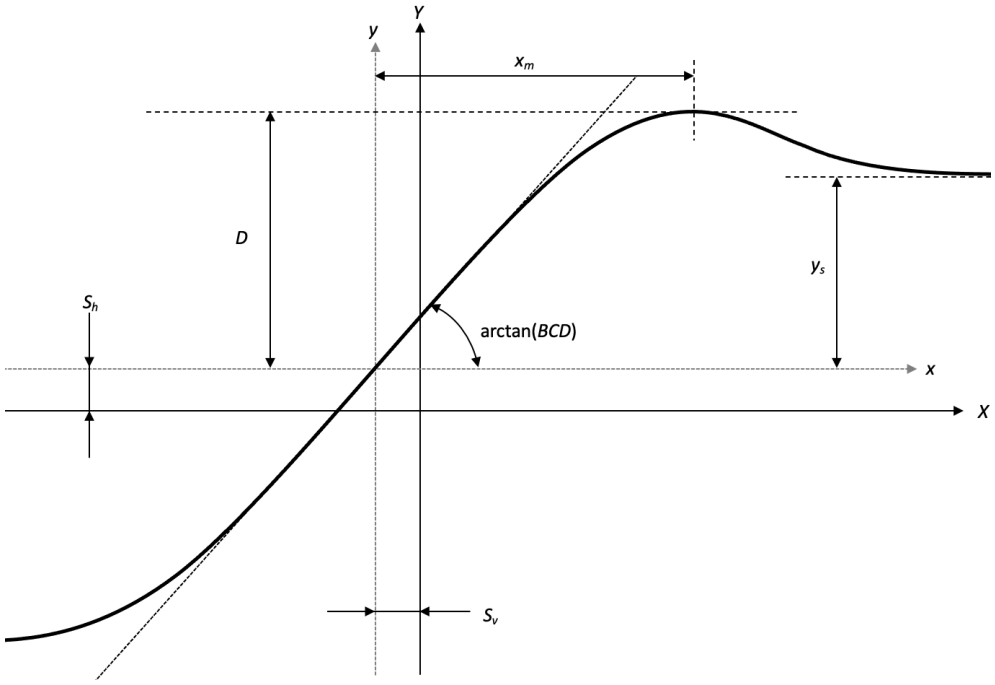

FIGURE III.10: Macro coefficients of the Pacejka model

TABLE III.1: Magic formula parameters

Parameters	Interpretation
B	Stiffness factor (slope at the origin)
D	peak value (maximum of the adhesion curve)
C	form factor (to adjust the shape of the curve)
E	curvature factor
BCD	slope of the characteristic curve at zero slip (stiffness)
S_v	vertical shift of the curvature from the origin
S_h	horizontal shift of the curvature from the origin

Expression of the lateral forces of each wheel without taking into account the effect of longitudinal slip σ_x is given by the following formula (Dandach, 2014):

$$\begin{cases} F^y(x) = D_y \sin\left\{C_y \arctan\left[B_y x - E_y\left(B_y x - \arctan(B_y x)\right)\right]\right\} + S_v^y \\ x = \alpha + S_h^y \end{cases} \tag{III.27}$$

where α represents the tyre slip. The constant parameters with subscript or exponent y appearing in this equation are given as follows:

$$D_y = F^z(a_1F^z + a_2)(1 - a_3v^2) \tag{III.28}$$

$$B_y = \frac{a_4}{C_yD_y}\sin\left(2\arctan\left(\frac{F^z}{a_5}\right)\right)(1 - a_6|v|) \tag{III.29}$$

$$C_y = a_0 \tag{III.30}$$

$$E_y = (a_7F^z + a_8)\left(1 - \left(a_9v + a_{10}\,\text{sign}(\alpha + S_h^y)\right)\right) \tag{III.31}$$

$$S_h^y = a_{11}F^z + a_{12} + a_{13}v \tag{III.32}$$

$$S_v^y = a_{14}F^z + a_{15} + v\left(a_{16}{F^z}^2 + a_{17}F^z\right) \tag{III.33}$$

With the variable v represents the camber angle, the parameters a_i depend on the structures and road conditions as well as on the state of the tyre. These parameters are identified empirically, and the role of each parameter is illustrated in Tab. III.2 (Garcia, 2013).

TABLE III.2: Pacejka lateral force parameters

Parameters	Mission
a_0	Form factor
a_1	Load effect on the coefficient of lateral friction
a_2	Coefficient of lateral friction
a_3	Camber effect on the coefficient of lateral friction
a_4	Stiffness change with slip
a_5	Stiffness/load progressivity change
a_6	Effect of camber on stiffness
a_7	Curvature variation with load
a_8	Curvature factor
a_9	Effect of load on horizontal displacement
a_{10}	Horizontal displacement at : $F^z = 0$ & $v = 0$
a_{11}	Effect of camber on horizontal displacement
a_{12}	Vertical displacement
a_{13}	Vertical displacement at : $F^z = 0$
a_{14}	Effect of camber on vertical displacement versus load
a_{15}	Effect of camber on vertical displacement
a_{16}	Curvature variation with camber
a_{17}	Displacement of the curvature

For a constant load, the relationship between the lateral force and slip angle is initially linear as shown in Fig. III.11, with a constant slope determined by the cornering stiffness C_α. This region of handling is called the linear operating region. As the slip angle grows, eventually, the force starts to saturate due to limited friction on the road, entering the non-linear region. In this area, we can talk about a possible skidding risk. The wheel slip is related to the variables $(\delta_f, \beta, \dot{\psi})$ by static equations, as illustrated in equations (III.20)-(III.21).

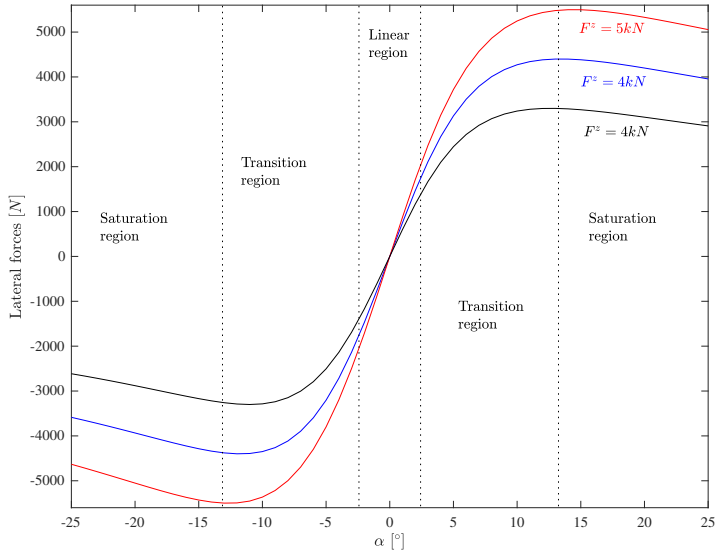

FIGURE III.11: Lateral force versus slip angle for different values of vertical loads F^z (calculated by Pacejka formula)

III.4.2 Linear model of lateral forces

Experimental results show that the lateral force F^y is proportional to small values of the slip angle ($|\alpha| < 2°$) as shown in Fig. III.11. The camber angle υ is neglected. Each vehicle tyre has small values of "α" under normal driving conditions (far from the saturation region) where the lateral acceleration does not exceed the threshold of 3.93 m/s^2 (Gillespie, 1992; Milliken et al., 1995; Jazar, 2017; Lechner, 2002). Under such conditions, the lateral forces are approximately linear functions of the slip angle with a slope equal to the cornering stiffness C_α. Therefore, it is common to use this linear approximation for the tyre forces:

$$F^y(\alpha) = C_\alpha \alpha \tag{III.34}$$

where the coefficient C_α is called the lateral force coefficient or cornering stiffness, its unit is $[N.rad^{-1}]$ and depends on the adhesion of the road surface and the vertical load of the tyre (Gillespie, 1992, chap. 6).

Tyres are highly non-linear over the threshold mentioned above and eventually saturate with subsequent degradation in force capacity (see Fig. III.11). Due to the neglect of force saturation, the tyre forces tend to be overestimated by the linear model, especially when tyre slip is significant. The limiting potential of linear models has been studied in detail in (Lechner, 2002).

III.5 Vehicle T-S fuzzy model representation

In this section, we approximate the non-linear model of the automotive vehicle dynamics given earlier, by T-S fuzzy representation (Takagi and Sugeno, 1985).

It is widely recognised that one of the most critical components of an automotive vehicle is the tyre, as it is the only point of contact with the road. All the forces necessary to control an automotive vehicle's motion are transmitted through the tyre, making the tyre-road interface an important source of dynamic stimulation of the automotive vehicle. Therefore, a detailed understanding of tyre behaviour is necessary to develop safe, comfortable and durable vehicles.

The challenge of achieving a correct automotive model is that the tyre/road contact forces are highly non-linear and difficult to model. The method based on T-S fuzzy models is proposed in several works (e.g. El Hajjaji et al. (2006); Oudghiri et al. (2008); Dahmani et al. (2013); Jin et al. (2017); Tuan and El Hajjaji (2018); El Youssfi et al. (2018c, 2020a,b)). As mentioned in Chapter II, it is a very interesting mathematical representation of non-linear systems that allows representing any non-linear system, whatever its complexity, by a simple structure based on linear models interpolated by positive and bounded non-linear functions. Besides, this method has a simple form with valuable properties that make it easily exploitable from a mathematical point of view, allowing the extension of some results from the linear field to non-linear systems.

The lateral tyre/road contact forces are assumed to be proportional to the slip angle, but this approximation is only valid for a small slip angle $|\alpha| < 0,02\ rad$ (Varrier, 2013). In contrast, a non-linear model must be considered for an increasing slip. To overcome this issue, the idea is to describe the two lateral forces' behaviour (front and rear) by a set of T-S fuzzy rules.

To obtain the T-S fuzzy model, two slip regions are considered: a low slip region and a high slip region (Dahmani et al., 2015b). Then, the front and rear cornering forces can be approximated by the following four-rule system:

$$\begin{aligned}
&\textbf{If } |\alpha_f| \text{ is } \mathcal{M}_{f_1}, \textbf{ Then } F_f^y = \mathcal{C}_{f_1}(\mu)\alpha_f \\
&\textbf{If } |\alpha_f| \text{ is } \mathcal{M}_{f_2}, \textbf{ Then } F_f^y = \mathcal{C}_{f_2}(\mu)\alpha_f \\
&\textbf{If } |\alpha_r| \text{ is } \mathcal{M}_{r_1}, \textbf{ Then } F_r^y = \mathcal{C}_{r_1}(\mu)\alpha_r \\
&\textbf{If } |\alpha_r| \text{ is } \mathcal{M}_{r_2}, \textbf{ Then } F_r^y = \mathcal{C}_{r_2}(\mu)\alpha_r
\end{aligned} \tag{III.35}$$

where $\mathcal{C}_{f_i}$ and $\mathcal{C}_{r_i}$, with $i = 1, 2$, represent the stiffness coefficients of the front and rear wheels, respectively. They depend on the road friction coefficient μ and the vehicle parameters. The variables α_f and α_r are, as shown in Fig. III.8, the slip angles of the front and rear tyres, respectively. They are given by the equations (III.20)-(III.21).

The overall forces are then approximated by:

$$\begin{cases}
F_f^y = \lambda_{f_1}(\alpha_f)\mathcal{C}_{f_1}(\mu)\alpha_f + \lambda_{f_2}(\alpha_f)\mathcal{C}_{f_2}(\mu)\alpha_f \\
F_r^y = \lambda_{r_1}(\alpha_r)\mathcal{C}_{r_1}(\mu)\alpha_r + \lambda_{r_2}(\alpha_r)\mathcal{C}_{r_2}(\mu)\alpha_r
\end{cases} \tag{III.36}$$

which can be rewritten as follows:

$$\begin{cases} F_f^y = \sum_{i=1}^{2} \lambda_{f_i}(\alpha_f)\mathcal{C}_{f_i}(\mu)\alpha_f \\ F_r^y = \sum_{i=1}^{2} \lambda_{r_i}(\alpha_r)\mathcal{C}_{r_i}(\mu)\alpha_r \end{cases} \tag{III.37}$$

where $\lambda_{f_i}(\alpha_f)$ and $\lambda_{r_i}(\alpha_r)$, with $i = 1, 2$, are bell-shaped membership functions associated with the sets $\mathcal{M}_{f_i}$ and $\mathcal{M}_{r_i}$, respectively. They are of the following form:

$$\begin{cases} \lambda_{f_i}(\alpha_f) = \dfrac{\omega_{f_i}(\alpha_f)}{\sum_{i=1}^{2} \omega_{f_i}(\alpha_f)} \\ \\ \lambda_{r_i}(\alpha_r) = \dfrac{\omega_{r_i}(\alpha_r)}{\sum_{i=1}^{2} \omega_{r_i}(\alpha_r)} \end{cases} \tag{III.38}$$

with:

$$\omega_{f_i}(\alpha_f) = \frac{1}{\left(1 + \left|\dfrac{|\alpha_f| - \mathrm{c}_{f_i}}{\mathrm{a}_{f_i}}\right|\right)^{2\mathrm{b}_{f_i}}}, \quad \omega_{r_i}(\alpha_r) = \frac{1}{\left(1 + \left|\dfrac{|\alpha_r| - \mathrm{c}_{r_i}}{\mathrm{a}_{r_i}}\right|\right)^{2\mathrm{b}_{r_i}}} \tag{III.39}$$

Several works in literature assume that angles α_f and α_r have similar values, then fuzzy rules can be suggested based only on α_f. This hypothesis allows us to reduce the number of membership functions and parameters to be identified. However, this assumption remains conventional since, in the real case, these angles have different values. Therefore, they are considered separately here.

The parameters of the fuzzy model membership functions (a_{f_i}, a_{r_i}, b_{f_i}, b_{r_i}, c_{f_i} and c_{r_i}, and the tyre stiffness coefficients ($\mathcal{C}_{f_i}$ and $\mathcal{C}_{r_i}$) are obtained using an identification procedure based on the Levenberg-Marquardt algorithm in combination with the least-squares method (El Hajjaji et al., 2006). This procedure based on the minimisation of the quadratic deviation between the non-linear expressions of the lateral forces given by the magic formula (III.27) and the approximated forces (III.37).

The numerical values for the stiffness coefficients and membership function parameters are reported in Tab. III.3.

TABLE III.3: Values of stiffness coefficients and membership function parameters

$\mathcal{C}_{f_1}$	86477	a_{f_1}	0,0969	b_{f_1}	1,4407	c_{f_1}	−0,0130
$\mathcal{C}_{f_2}$	0794	a_{f_2}	0,1298	b_{f_2}	0,7962	c_{f_2}	0,0753
$\mathcal{C}_{r_1}$	50696	a_{r_1}	0,5384	b_{r_1}	1,8307	c_{r_1}	0,2941
$\mathcal{C}_{r_2}$	0383	a_{r_2}	0,7068	b_{r_2}	2,5565	c_{r_2}	1,2334

A comparison between Pacejka's non-linear model and T-S fuzzy model of the front and rear lateral forces, for a road friction coefficient $\mu = 0.7$, is depicted in Fig. III.12. It can be clearly seen that the T-S fuzzy model (III.37) follows the non-linear model (III.27) accurately for the two lateral forces (front and rear). The curves of the

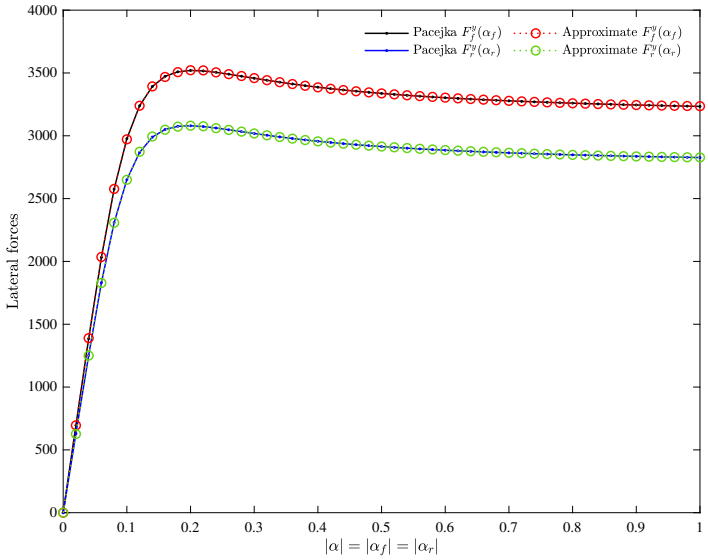

FIGURE III.12: Difference between the lateral forces obtained by the non-linear system and those obtained by the T-S fuzzy model (for a road friction coefficient $\mu = 0,7$)

membership functions $\lambda_{f_i}(\alpha)$ and $\lambda_{r_i}(\alpha)$ are computed over the considered range of slip angle and are presented in Fig. III.13.

III.5.1 State representation of vehicle lateral dynamics without roll motion

By substituting in the non-linear equations of the simplified model of the automotive vehicle lateral dynamics (bicycle model), the front and rear lateral forces by their fuzzy expressions (III.37), and taking into account the equations of front and rear tyre side-slip angles (III.20)-(III.21), the equation system (III.19) can be re-written for small angle β (to consider $v_v \approx v_x$) as follows:

$$\begin{cases} \dot{\beta} = \dfrac{2}{m_v v_x} \sum\limits_{i=1}^{4} h_i(\alpha_f, \alpha_r) \left[-\sigma_i \beta + \dfrac{\rho_i}{v_x} \dot{\psi} + \nu_i \delta_f \right] - \dot{\psi} \\ \ddot{\psi} = \dfrac{2}{I_z} \sum\limits_{i=1}^{4} h_i(\alpha_f, \alpha_r) \left[\rho_i \beta - \dfrac{\tau_i}{v_x} \dot{\psi} + l_f \nu_i \delta_f \right] \end{cases} \tag{III.40}$$

with:

$$\sigma_1 = \mathcal{C}_{f_1} + \mathcal{C}_{r_1}, \quad \sigma_2 = \mathcal{C}_{f_1} + \mathcal{C}_{r_2}, \quad \sigma_3 = \mathcal{C}_{f_2} + \mathcal{C}_{r_1}, \quad \sigma_4 = \mathcal{C}_{f_2} + \mathcal{C}_{r_2}$$

$$\rho_1 = l_r \mathcal{C}_{r_1} - l_f \mathcal{C}_{f_1}, \quad \rho_2 = l_r \mathcal{C}_{r_2} - l_f \mathcal{C}_{f_1}, \quad \rho_3 = l_r \mathcal{C}_{r_1} - l_f \mathcal{C}_{f_2}, \quad \rho_4 = l_r \mathcal{C}_{r_2} - l_f \mathcal{C}_{f_2}$$

$$\tau_1 = l_f^2 \mathcal{C}_{f_1} + l_r^2 \mathcal{C}_{r_1}, \quad \tau_2 = l_f^2 \mathcal{C}_{f_1} + l_r^2 \mathcal{C}_{r_2}, \quad \tau_3 = l_f^2 \mathcal{C}_{f_2} + l_r^2 \mathcal{C}_{r_1}, \quad \tau_4 = l_f^2 \mathcal{C}_{f_2} + l_r^2 \mathcal{C}_{r_2}$$

$$\nu_1 = \nu_2 = \mathcal{C}_{f_1}, \quad \nu_3 = \nu_4 = \mathcal{C}_{f_2}$$

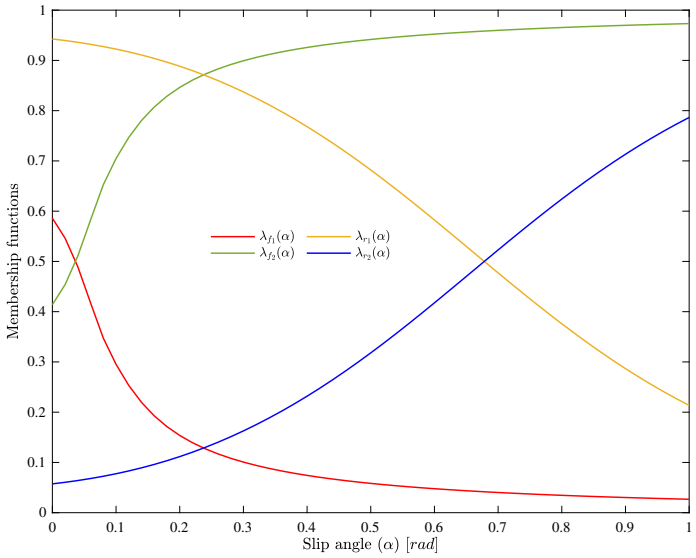

FIGURE III.13: Representative curves of membership functions

The membership functions $h_i(\alpha_f, \alpha_r)$ are given as follows:

$$h_1(\alpha_f, \alpha_r) = \lambda_{f_1}(\alpha_f) \times \lambda_{r_1}(\alpha_r) \tag{III.41}$$

$$h_2(\alpha_f, \alpha_r) = \lambda_{f_1}(\alpha_f) \times \lambda_{r_2}(\alpha_r) \tag{III.42}$$

$$h_3(\alpha_f, \alpha_r) = \lambda_{f_2}(\alpha_f) \times \lambda_{r_1}(\alpha_r) \tag{III.43}$$

$$h_4(\alpha_f, \alpha_r) = \lambda_{f_2}(\alpha_f) \times \lambda_{r_2}(\alpha_r) \tag{III.44}$$

Then, the equation system of the lateral dynamics of the automotive vehicle (III.40) can be represented by the following state representation:

$$\dot{x}(t) = \sum_{i=1}^{4} h_i(\alpha_f, \alpha_r) \left[A_i x(t) + B_{fi} \delta_f(t) \right] \tag{III.45}$$

The state vector is defined by the following:

$$x = \begin{bmatrix} \beta & \dot{\psi} \end{bmatrix}^T$$

and the matrices that describe the dynamics of the system are:

$$A_i = \begin{bmatrix} -2\dfrac{\sigma_i}{m_v v_x} & 2\dfrac{\rho_i}{m_v v_x^2} - 1 \\ \\ 2\dfrac{\rho_i}{I_z} & -2\dfrac{\tau_i}{I_z v_x} \end{bmatrix}, \quad B_{fi} = \begin{bmatrix} 2\dfrac{\nu_i}{m_v v_x} \\ \\ 2\dfrac{l_f \nu_i}{I_z} \end{bmatrix}$$

Under the front wheel steering angle shown in Fig. III.14 and the main values of the vehicle parameters shown in Tab. III.4 (Rahimi and Naraghi, 2018). The simulation

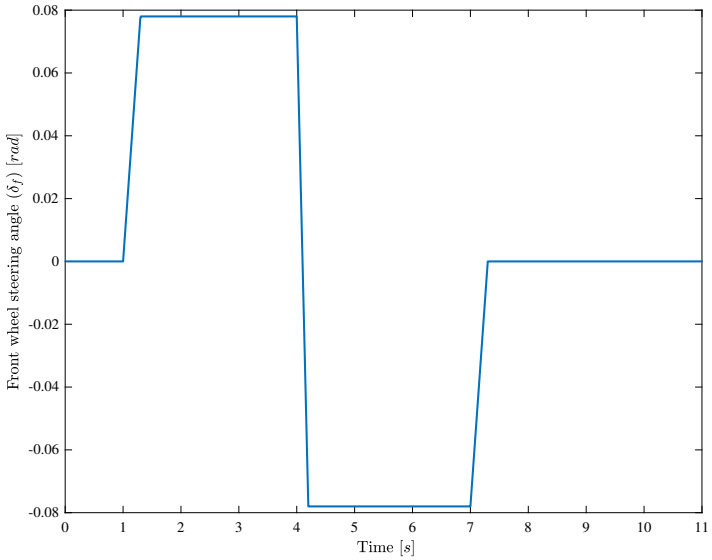

FIGURE III.14: Steering angle given by driver

TABLE III.4: Parameters for the vehicle simulation

Parameter	m_v	I_z	l_f	l_r
Value	1712	2488	1,18	1,77

runs for linear, non-linear, and fuzzy models of the vehicle lateral dynamics system. The results of the comparison are displayed in Fig. III.15.

It is clear from Fig. III.15 that the T-S fuzzy model follows with a good approximation the non-linear model of the vehicle's lateral dynamics throughout the trajectory. However, for a considerable slip angle, the linear model deviates from it. This demonstrates the T-S fuzzy representation's ability to describe the non-linear behaviour of the vehicle's lateral dynamics.

The following sub-section deals with the 3-DoF model, representing the yaw, lateral and roll motions of an automotive vehicle and its T-S fuzzy representation.

III.5.2 State representation of vehicle lateral dynamics with roll motion

The model presented here is used in most of our work and corresponds to the vehicle's lateral and roll dynamics. It is obtained by considering the well-known single-track model (bicycle) represented in sub-section III.3.2 with consideration of 1-DoF corresponding to the roll motion (illustrated in sub-section III.3.3). So this model consists of 3-DoF representing the yaw, lateral and roll motions (see figure III.16) (Ryu et al., 2007; Zhao and Liu, 2014).

Under the assumption of small angles, the 3-DoF model with consideration of the

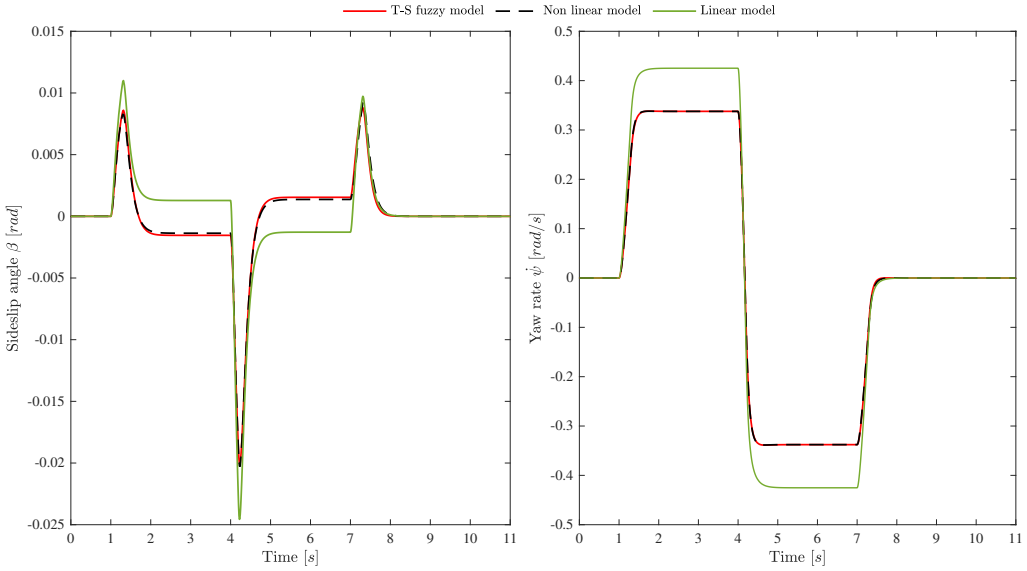

FIGURE III.15: Side-slip angle and yaw rate variations

bank angle of the road can be described by the following differential equations (Kidane et al., 2006; Dahmani et al., 2015b):

$$\begin{cases} \dot{\beta} = \dfrac{2}{m_v v_x}\left(F_r^y + F_f^y\right) + \dfrac{m_s h_\phi}{m_v v_x}\ddot{\phi} - \dfrac{m_s g}{m_v v_x}\varphi - \dot{\psi} \\ \ddot{\psi} = \dfrac{2}{I_z}\left(l_f F_f^y - l_r F_r^y\right) \\ \ddot{\phi} = \dfrac{m_s v_v h_\phi}{\mathcal{I}_x}\left(\dot{\beta} + \dot{\psi}\right) + \dfrac{m_s g h_\phi}{\mathcal{I}_x}(\phi + \varphi) - \dfrac{K_\phi}{\mathcal{I}_x}\phi - \dfrac{C_\phi}{\mathcal{I}_x}\dot{\phi} \end{cases} \tag{III.46}$$

with:

$$\mathcal{I}_x = I_x + m_s h_\phi^2$$

where ψ, ϕ and φ are yaw, roll and road bank angles, respectively. For a detailed explanation of the parameters appearing in this model of the lateral and roll dynamics of the automotive vehicle, refer to the list of symbols.

By replacing in the non-linear model of the automotive vehicle lateral dynamics, with consideration of roll motion, the front and rear lateral forces by their fuzzy expressions (III.37), and taking into account the equations of the lateral slip angles of the front and rear tyres (III.20)-(III.21), the system of equations (III.46) can be rewritten as

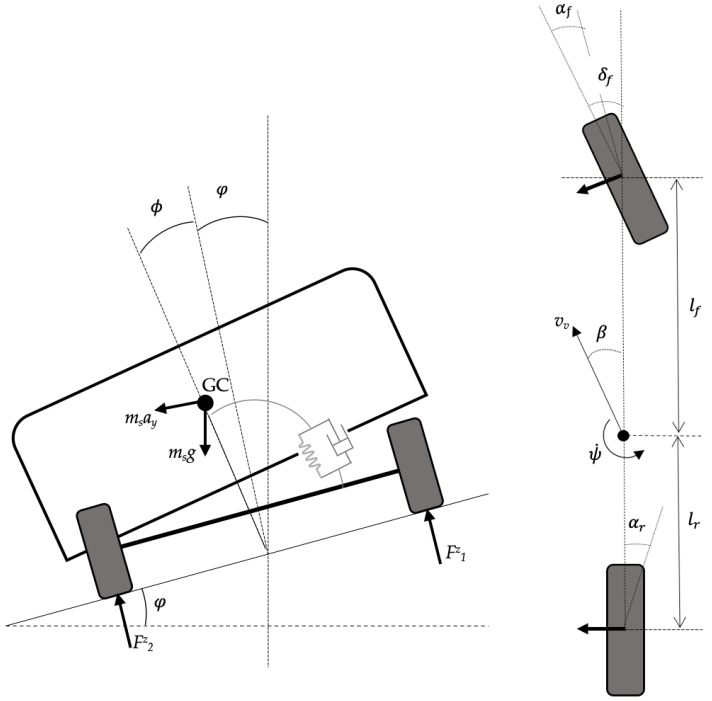

FIGURE III.16: Automotive vehicle lateral and roll dynamics model

follows:

$$\begin{cases} \dot{\beta} = & \frac{2(1+\kappa)}{m_v v_x} \sum_{i=1}^{4} h_i(\alpha_f, \alpha_r)\vartheta_i + \frac{r_{s/v} h_\phi \Lambda}{v_x}\phi - \frac{r_{s/v} h_\phi C_\phi}{v_x \bar{\jmath}_x}\dot{\phi} - \frac{r_{s/v} g}{v_x \bar{\jmath}_x}\left(M h_\phi^2 - \bar{\jmath}_x\right)\varphi - \dot{\psi} \\ \ddot{\psi} = & \frac{2}{I_z}\sum_{i=1}^{4} h_i(\alpha_f, \alpha_r)\varpi_i \\ \ddot{\phi} = & \frac{2 r_{s/v} h_\phi}{\bar{\jmath}_x}\sum_{i=1}^{4} h_i(\alpha_f, \alpha_r)\vartheta_i + \Lambda\phi - \frac{C_\phi}{\bar{\jmath}_x}\dot{\phi} + \frac{M g h_\phi}{\bar{\jmath}_x}\varphi \end{cases} \tag{III.47}$$

In order to reduce the size of the equations, the parameters included are as follows:

$$\vartheta_i = -\sigma_i\beta + \frac{\rho_i}{v_x}\dot{\psi} + \nu_i\delta_f, \quad \varpi_i = \rho_i\beta - \frac{\tau_i}{v_x}\dot{\psi} + l_f\nu_i\delta_f, \quad \Lambda = \frac{m_s g h_\phi - K_\phi}{\bar{\jmath}_x}$$

$$M = m_s(1 - r_{s/v}), \qquad \bar{\jmath}_x = I_x + M h_\phi^2, \qquad r_{s/v} = \frac{m_s}{m_v}, \qquad \kappa = r_{s/v}\frac{m_s h_\phi^2}{\bar{\jmath}_x}$$

with membership functions $h_i(\alpha_f, \alpha_r)$ and parameters δ_i, ρ_i, τ_i and ν_i are identical to those defined in the previous sub-section.

Then, the equation system (III.47) of the lateral dynamics of the automotive vehicle, with consideration of roll motion, can be represented by the following state representation:

$$\dot{x}(t) = \sum_{i=1}^{4} h_i(\alpha_f, \alpha_r) \left[A_i x(t) + B_{fi}\delta_f(t) + B_\varphi \varphi(t) \right] \tag{III.48}$$

The state vector is defined by the following:

$$x = \begin{bmatrix} \beta & \phi & \dot{\psi} & \dot{\phi} \end{bmatrix}^T$$

and the matrices that describe the dynamics of the system are:

$$A_i = \begin{bmatrix} -2\dfrac{(1+\kappa)\sigma_i}{m_v v_x} & \dfrac{r_{s/v} h_\phi \left(m_s g h_\phi - K_\phi\right)}{v_x \bar{J}_x} & 2\dfrac{(1+\kappa)\rho_i}{m_v v_x^2} - 1 & -\dfrac{r_{s/v} h_\phi C_\phi}{v_x} \\ 0 & 0 & 0 & 1 \\ 2\dfrac{\rho_i}{I_z} & 0 & -2\dfrac{\tau_i}{v_x I_z} & 0 \\ -2\dfrac{r_{s/v} h_\phi \sigma_i}{\bar{J}_x} & \dfrac{m_s g h_\phi - K_\phi}{\bar{J}_x} & 2\dfrac{r_{s/v} h_\phi \rho_i}{v_x \bar{J}_x} & -\dfrac{C_\phi}{\bar{J}_x} \end{bmatrix}$$

$$B_{fi} = \begin{bmatrix} 2\dfrac{(1+\kappa)\nu_i}{m_v v_x} \\ 0 \\ 2\dfrac{l_f \nu_i}{I_z} \\ 2\dfrac{r_{s/v} h_\phi \nu_i}{\bar{J}_x} \end{bmatrix}, \quad B_\varphi = \begin{bmatrix} -\dfrac{r_{s/v} g}{v_x \bar{J}_x}\left(M h_\phi^2 - \bar{J}_x\right) \\ 0 \\ 0 \\ \dfrac{M g h_\phi}{\bar{J}_x} \end{bmatrix}$$

The model of the lateral dynamics of the automotive vehicle with consideration of roll movement has been widely discussed and has been the subject of many publications. Among these, the following bibliographic references use T-S fuzzy models: (Rabhi et al., 2009; Daraoui et al., 2012; Oudghiri et al., 2014; Dahmani et al., 2015a, 2013, 2015b; Aouaouda et al., 2014a, 2015; El Youssfi et al., 2017, 2018a,b,c, 2019b; El Youssfi and El Bachtiri, 2020).

III.6 Conclusion

In this third chapter, the automotive vehicle's movements and main components are first characterised and defined. Then, the automotive vehicle dynamics models are discussed. In the beginning, the four-wheel vehicle model, which, with a set of assumptions, leads to a more simplified bicycle model. Then, the roll dynamics model.

Afterwards, two lateral force models are presented. The first one is based on the Pacejka magic formula, it is accurate and more realistic, but it requires the empirical determination of many factors and constants. The second one is simple linear but overestimates the forces. Furthermore, to avoid the non-linearity of the lateral forces, a T-S fuzzy representation of the tyre model is considered. This approximation allowed us to obtain a T-S fuzzy model representing the automotive vehicle's lateral dynamics with/without taking into account roll motion.

Chapter IV

Fault/state estimation for automotive vehicle lateral dynamics

IV.1 Introduction

Driver errors or bad reflexes cause most accidents. For this reason, automotive industries and researchers in this area have worked hard to develop and produce intelligent, reliable, relaxed, and safe vehicles (Bishop, 2000; Christensen and Bastien, 2015; Hussain and Zeadally, 2018). Since the 1970s, many solutions have been proposed to introduce and develop advanced passive security devices like airbags and driver-assisted active security devices such as ACC, ABS, and ESP (Rajamani, 2005; Jarašūniene and Jakubauskas, 2007; Falcone et al., 2007; Winner et al., 2014; Chamraz and Balogh, 2018). These depend on the service provided by electronic systems for various vehicle activities in dangerous driving situations. In case of deviation in an undesirable direction, the computer makes immediate decisions to respond with appropriate corrective actions to ensure the vehicle's stability.

The processes mentioned above are mainly monitored with known and unknown entries. Their operation and effectiveness need detailed knowledge of the automotive vehicle dynamics parameters (Plancke, 2009; El Youssfi et al., 2018a, 2019b). These parameters' measurements sometimes do not provide complete system details because of some state measurements' unavailability. Furthermore, the number of sensors is reduced due to cost reasons and can sometimes be also unavailable.

The idea is to use a software sensor, called an observer, able to reconstruct the unmeasurable and measurable states accurately from measurable ones. Thus, it should build unknown inputs of the system from the model and calculated parameters. Different estimation techniques have been applied in this context to solve problems of observer design. Among these techniques, the classical Luenberger observer, which uses static gain synthesis to make the observer states converge to the real system states and stabilise the estimation error (Monot et al., 2018; Van Dong et al., 2019). Nevertheless, disturbances in the system often lead to lousy reconstruction and instability. In (Katzfuss et al., 2016; Reina and Messina, 2019), Kalman filter has been used, which is robust to measurement noise. In (Liu et al., 2018; El Youssfi et al., 2018a), a sliding

mode observer is used to achieve asymptotic convergence of the state estimation error to zero despite uncertainties in the input and non-linearities.

These observers may not be practical when the system dynamics are subject to the influence of unknown inputs. Usually, these unknown inputs come from faults, modelling errors, disturbances or noise. The problem of designing observers for standard and descriptor systems with unknown inputs has received considerable attention in recent years (Mammar et al., 2006; Hashemi et al., 2017; Nguyen et al., 2019b,a; Du et al., 2019; El Youssfi et al., 2019b, 2020b). These observers allow reconstruction of system states even in the presence of unknown inputs, and are often involved in diagnosis, for the detection and estimation of faults affecting the system. Two types of observers are developed in this chapter for the purpose of simultaneously estimating the automotive vehicle lateral dynamics system states and the faults that affect it. The first one allows to estimate faults/states of T-S fuzzy descriptor systems under the influence of actuator faults and external disturbances. This observer will be used to design a fault-tolerant control law for descriptor systems in the next chapter. These types of systems appear in a variety of physical systems such as power systems, electrical circuits, vehicle systems and many other systems that can be modelled by dynamic equations (Yuan and Zhang, 2010). These systems, also known as differential algebraic systems or singular systems, are much tighter than the state-space expression to represent real independent parametric perturbations (Taniguchi et al., 2000). While, the second observer is the unknown input observer for estimating faults/states of T-S fuzzy standard uncertain systems in the presence of sensor/actuator faults.

Our main objective in this chapter is to accurately estimate faults and states of the automotive vehicle lateral dynamics in the presence of uncertainties, disturbances and/or faults. The model used to explain the lateral movements of the automotive vehicle is the bicycle model shown in Fig III.8. The asymptotic stability of the estimation error is ensured by Lyapunov's method. Its sufficient conditions are provided in the form of Linear Matrix Inequalities (LMIs), which can be resolved using LMI optimisation techniques. The results are improved using some lemmas (see Appendix).

This chapter is structured in the following way: Second section deals with the fault/state estimation method, using descriptor approach, for T-S fuzzy system of an automotive vehicle under varied disturbances and actuator faults. The third section is devoted to fault/state estimation by an unknown input observer for uncertain T-S fuzzy system of an automotive vehicle with simultaneous sensor and actuator faults. These two sections are divided into the following sub-sections: the first one presents a brief description of the problem. Then, the second presents the design of the observer to estimate the system states and faults jointly. Then, the stability analysis of the estimation error appeared in the third sub-section. At the end of each section, an application to the automotive vehicle lateral dynamics is given. The conclusion is included in the last section.

IV.2 Fault/state estimation approach using descriptor approach

Using the descriptor approach, this section addresses the problem of fault and state estimation of an automotive vehicle's lateral dynamics represented by the T-S fuzzy model affected by faults and actuator disturbances.

IV.2.1 Issue description

In practice, automotive vehicle lateral dynamics can be affected by faults and/or disturbances, considered as additional inputs, such as actuator fault. To cope with this problem, actuator faults and appropriate disturbances must therefore be implemented. Using the descriptor approach in this section, the observer mentioned above is used to estimate fault/state for the automotive vehicle lateral dynamics system, represented by the T-S fuzzy model, affected by both actuator faults and disturbances.

Consider the following T-S fuzzy descriptor system fitted to the vehicle system (III.40):

$$\begin{cases} E\dot{x}(t) = \sum_{i=1}^{4} h_i(\alpha_f, \alpha_r) \left[A_i x(t) + B_{fi}(\delta_f(t) + f(t)) + D_i d(t) \right] \\ y(t) = Cx(t) \end{cases} \tag{IV.1}$$

where $x(t)$, $\delta_f(t)$ and $y(t)$ are descriptor state, input and output vectors, respectively. $f(t)$ and $d(t)$ are actuator faults and external disturbances, respectively. The matrices A_i, B_i, C and D_i are known matrices with suitable dimensions. Matrix E may be rank deficient, i.e., $rank(E) = r_e \leq n_x$.

Using the descriptor approach and considering the actuator fault $f(t)$ as an additional state, an extended system can be written as follows:

$$\begin{cases} \bar{E}\dot{\bar{x}}(t) = \sum_{i=1}^{4} h_i(\alpha_f, \alpha_r) \left[\bar{A}_i \bar{x}(t) + \bar{B}_i \delta_f(t) + \bar{D}_i d(t) + \bar{F}\dot{f}(t) \right] \\ y(t) = \bar{C}\bar{x}(t) \end{cases} \tag{IV.2}$$

where

$$\bar{E} = \begin{bmatrix} E & 0 \\ 0 & I \end{bmatrix}, \ \bar{A}_i = \begin{bmatrix} A_i & B_{fi} \\ 0 & 0 \end{bmatrix}, \ \bar{B}_i = \begin{bmatrix} B_{fi} \\ 0 \end{bmatrix}, \ \bar{D}_i = \begin{bmatrix} D_i \\ 0 \end{bmatrix}, \ \bar{F} = \begin{bmatrix} 0 \\ I \end{bmatrix}, \ \bar{C} = \begin{bmatrix} C & 0 \end{bmatrix}$$

The regularity and non-impulsiveness of a singular continuous system play important roles in analysing the singular system. Therefore, it is essential to develop conditions that guarantee that the nominal singular system is regular and impulse-free and not only stable.

Definition. IV. 1 *(Dai et al., 1989; Yuan and Zhang, 2010) The matrix pencil* $(E, \sum_{i=1}^{m} h_i A_i)$ *is regular if* $\det(sE - \sum_{i=1}^{m} h_i A_i)$ *is not identically zero.*

Definition. IV. 2 *(Dai et al., 1989; Yuan and Zhang, 2010) The matrix pencil* $(E, \sum_{i=1}^{m} h_i A_i)$ *is impulse-free if* $deg(\det(sE - \sum_{i=1}^{m} h_i A_i)) = rank(E)$.

Definition. IV. 3 *System* (IV.1) *is admissible if it is regular, impulse-free and stable.*

The fault $f(t)$ and the state $x(t)$ can be estimated by employing the augmented system $\bar{x}(t)$. The challenge then is to design an observer for the system (IV.2). It should be noted that working with the augmented system (IV.2) which contains the system states as well as an auxiliary fault states vector instead of system (IV.1) help us to estimate the fault afterwards and not only to detect it. Estimating and detecting the fault gives us the possibility to easily build up a fault-tolerant control (in Chapter V). This is not allowed with system (IV.1).

Before going on, the following assumptions are considered in the remainder of this section.

Assumption. IV. 1 *System* (IV.1) *is assumed to be admissible.*

Assumption. IV. 2 *(Jia et al., 2015)* $\bar{E}$ *and* $\bar{C}$ *matrices satisfy the conditions of rank according to the following:*

$$rank \begin{bmatrix} \bar{E} \\ \bar{C} \end{bmatrix} = n_x \tag{IV.3}$$

Remark. IV. 1 *Note that the constructed observer* (IV.4) *necessitates the conditions of Assumption. IV.2.*

IV.2.2 Observer design

In this part, the design of an observer estimating the state system and actuator faults is considered. So, let us consider the following observer:

$$\begin{cases} \dot{\eta}(t) = \sum_{i=1}^{4} h_i(\alpha_f, \alpha_r) \Big[T\bar{A}_i \hat{\bar{x}}(t) + T\bar{B}_i \delta_f(t) + L_i(y(t) - \hat{y}(t)) \Big] \\ \hat{\bar{x}}(t) = \eta(t) + Hy(t) \\ \hat{y}(t) = \bar{C}\hat{\bar{x}}(t) \end{cases} \tag{IV.4}$$

where $\eta(t)$ and $\hat{\bar{x}}(t)$ are the observer states and the estimated states, respectively. $\hat{y}(t)$ is the estimated output. T, H and L_i are matrices to be determined.

Remark. IV. 2 *The observer structure* (IV.4) *used in this study is widely used in physical applications, and many works show its capability not only to detect the faults, but also to estimate their amplitude (Rodrigues et al., 2014; Wang et al., 2015, 2019b). Furthermore, using the observer structure* (IV.4) *imply looking for gains* T, H, *and* L_i *which is different to the traditional ones, and this give some flexibility to the observer structure. Moreover, looking for the variables* T, H, *and* L_i *together need some simplification and assumptions.*

IV.2.3 Stability analysis

Let us define the error between the augmented system (IV.2) and the observer (IV.4) as follows:

$$\bar{e}_x(t) = \bar{x}(t) - \hat{\bar{x}}(t) \tag{IV.5}$$

$$= (I - H\bar{C})\bar{x}(t) - \eta(t) \tag{IV.6}$$

According to references (Aouaouda et al., 2013; Bouarar et al., 2013; Kharrat et al., 2018; Wang et al., 2015; Rodrigues et al., 2014), Assumption. IV.2 means that there are non-singular matrices T and H, such that

$$T\bar{E} + H\bar{C} = I \tag{IV.7}$$

So, estimation error can be described as follows:

$$\bar{e}_x(t) = T\bar{E}\bar{x}(t) - \eta(t) \tag{IV.8}$$

The dynamics of the estimation error is expressed by the following

$$\dot{\bar{e}}_x(t) = T\bar{E}\dot{\bar{x}}(t) - \dot{\eta}(t) \tag{IV.9}$$

$$\dot{\bar{e}}_x(t) = \sum_{i=1}^{4} h_i(\alpha_f, \alpha_r) \left\{ \left(T\bar{A}_i - L_i\bar{C}\right) \bar{e}_x(t) + T\bar{D}_i d(t) + T\bar{F}\dot{f}(t) \right\} \tag{IV.10}$$

and the fault estimation error is defined as follows

$$e_f(t) = C_f \bar{e}_x(t) \tag{IV.11}$$

where $C_f = \begin{bmatrix} 0 & I \end{bmatrix}$.

Under Assumption. IV.1, the following theorem presents a sufficient condition that satisfies the asymptotic convergence of the fuzzy observer (IV.4) to the augmented system (IV.2).

Theorem. IV. 1 *(El Youssfi et al., 2021c) Under Assumption. IV.2, the fuzzy observer* (IV.4) *asymptotically converges to the system* (IV.2)*, if there exist two positive scalars γ_1 and γ_2, and positive symmetric matrix P, and matrices X, Y_i, such that the following inequality is satisfied for i=1,...,4.*

$$\begin{bmatrix} \Xi_i & P\mathcal{D}_{1i} + X\mathcal{D}_{2i} & P\mathcal{F}_1 + X\mathcal{F}_2 \\ * & -\gamma_1 I & 0 \\ * & * & -\gamma_2 I \end{bmatrix} < 0 \tag{IV.12}$$

where

$$\Xi_i = P\mathcal{A}_{1i} + \mathcal{A}_{1i}^T P + X\mathcal{A}_{2i} + \mathcal{A}_{2i}^T X^T - Y_i\bar{C} - \bar{C}^T Y_i^T + C_f^T C_f \tag{IV.13}$$

The gains of observers can be determined as follows

$$L_i = P^{-1}Y_i \tag{IV.14}$$

Proof. IV. 1 *The proof is divided in two part, one part is dedicated on how to obtain the matrices T and H and second part is the proof of Theorem. IV.1.*

From equation (IV.7)*, one can write*

$$\begin{bmatrix} T & H \end{bmatrix} \begin{bmatrix} \bar{E} \\ \bar{C} \end{bmatrix} = I \tag{IV.15}$$

By using Lemma 8, we can get the solution of (IV.15) *as*

$$\begin{bmatrix} T & H \end{bmatrix} = \begin{bmatrix} \bar{E} \\ \bar{C} \end{bmatrix}^{\dagger} + W \left\{ I - \begin{bmatrix} \bar{E} \\ \bar{C} \end{bmatrix} \begin{bmatrix} \bar{E} \\ \bar{C} \end{bmatrix}^{\dagger} \right\} \tag{IV.16}$$

where W is an arbitrary matrix with appropriate dimensions.

From equation (IV.16)*, the matrices T and H are respectively obtained as*

$$\begin{cases} T = \Delta^{\dagger} M + W \left\{ I - \Delta\Delta^{\dagger} \right\} M \\ H = \Delta^{\dagger} N + W \left\{ I - \Delta\Delta^{\dagger} \right\} N \end{cases} \tag{IV.17}$$

with Δ*, M and N are given by*

$$\Delta = \begin{bmatrix} \bar{E} \\ \bar{C} \end{bmatrix}, \quad M = \begin{bmatrix} I \\ 0 \end{bmatrix}, \quad N = \begin{bmatrix} 0 \\ I_{(n_y)} \end{bmatrix}$$

In order to proof Theorem. IV.1, we select the Lyapunov functional described as follows

$$V(\bar{e}_x(t)) = \bar{e}_x^T(t) P \bar{e}_x(t) \tag{IV.18}$$

where P is a symmetrical positive matrix defined with an adequate dimension.

The derivative of $V(\bar{e}_x(t))$ *a long the trajectory of* $\bar{e}_x(t)$ *corresponds to*

$$\dot{V}(\bar{e}_x(t)) = \bar{e}_x^T(t) P \dot{\bar{e}}_x(t) + \dot{\bar{e}}_x^T(t) P \bar{e}_x(t) \tag{IV.19}$$

Considering real positive scalars $\gamma_1 > 0$ *and* $\gamma_2 > 0$*. The fault estimation error* $e_f(t)$ *is robust against external disturbances and fault variations (Wang et al., 2015), i.e.*

$$\|e_f(t)\|_2 \leq \sqrt{\gamma_1^2 \|d(t)\|_2 + \gamma_2^2 \|\dot{f}(t)\|_2} \tag{IV.20}$$

So, defining the following criterion function

$$J = \int_0^t \left[e_f^T(\tau) e_f(\tau) - \gamma_1 d^T(\tau) d(\tau) - \gamma_2 \dot{f}^T(\tau) \dot{f}(\tau) \right] d\tau \tag{IV.21}$$

It is known from different works in literature that (IV.20) *and* (IV.21) *are equivalent. So, under zero initial condition, we have:*

$$J \leq \int_0^t \left[e_f^T(\tau)e_f(\tau) - \gamma_1 d^T(\tau)d(\tau) - \gamma_2 \dot{f}^T(\tau)\dot{f}(\tau)\right]d\tau + V(\bar{e}_x(t)) - V(\bar{e}_x(0)) \quad \text{(IV.22)}$$

$$J \leq \int_0^t \left[\dot{V}(\bar{e}_x(\tau)) + e_f^T(\tau)e_f(\tau) - \gamma_1 d^T(\tau)d(\tau) - \gamma_2 \dot{f}^T(\tau)\dot{f}(\tau)\right]d\tau \quad \text{(IV.23)}$$

$$J \leq \int_0^t \Omega^T(\tau)\Pi_i\Omega(\tau)d\tau \quad \text{(IV.24)}$$

where

$$\Omega(t) = \begin{bmatrix} \bar{e}_x(t) \\ d(t) \\ \dot{f}(t) \end{bmatrix}, \quad \Pi_i = \begin{bmatrix} PTA_i + A_i^T T^T P - PL_i\bar{C} - \bar{C}^T L_i^T P & PT\bar{D}_i & P\bar{F} \\ * & -\gamma_1 I & 0 \\ * & * & -\gamma_2 I \end{bmatrix}$$

Taking into account the exchange of variables $PW = X$ *and* $PL_i = Y_i$*, and the following expressions:*

$$T\bar{A}_i = \mathcal{A}_{1i} + W\mathcal{A}_{2i} \quad \text{(IV.25)}$$

$$T\bar{D}_i = \mathcal{D}_{1i} + W\mathcal{D}_{2i} \quad \text{(IV.26)}$$

$$T\bar{F} = \mathcal{F}_1 + W\mathcal{F}_2 \quad \text{(IV.27)}$$

Then, by using Schur complement, we obtain (IV.12)*. So, if conditions* (IV.12) *are satisfied, that means* $J < 0$*. This implies that the fuzzy observer* (IV.4) *is asymptotically converged to the system* (IV.2) *with the performance* (IV.20)*. This accomplished the proof.*

Remark. IV. 3 *Theorem. IV.1 is provided with two setting parameters, namely* $\gamma_1 > 0$ *and* $\gamma_2 > 0$ *which reflect the effect of noise and fault derivative on the fault estimation error, respectively. The problem is how these parameters can be combined to give a feasible solution for the LMIs* (IV.12)*. The easiest way to solving this problem is to proceed by trial and error.*

Remark. IV. 4 *The proposed observer* (IV.4) *is different to that used in (Wu and Dong, 2016; Bouattour et al., 2009; Do et al., 2018), because the authors assume that* $\dot{f}(t) \approx 0$*. This assumption is outdated in this study. Furthermore, it deals with the problem of estimating time-varying faults* $\hat{f}(t)$ *which is simplicity computed by* $\hat{f}(t) = C_f\hat{\bar{x}}(t)$*.*

Remark. IV. 5 *It should be noted that, the design technique applied in this study overcome the equality problem used in the results of (Kharrat et al., 2018).*

IV.2.4 Numerical illustration and simulation results

In order to demonstrate the effectiveness of the proposed observer in estimating fault/state of the lateral dynamics system without consideration of roll motion, some simulations have been performed using Matlab software. For that, the longitudinal velocity is taken as constant $v_x = 25\ m/s$, the steering angle is shown in Fig. IV.1 is considered,

and the parameters' values are listed in the Tab. III.4. It should be mentioned that the simulated results are obtained assuming that the yaw moment is zero ($M_z(t) = 0$).

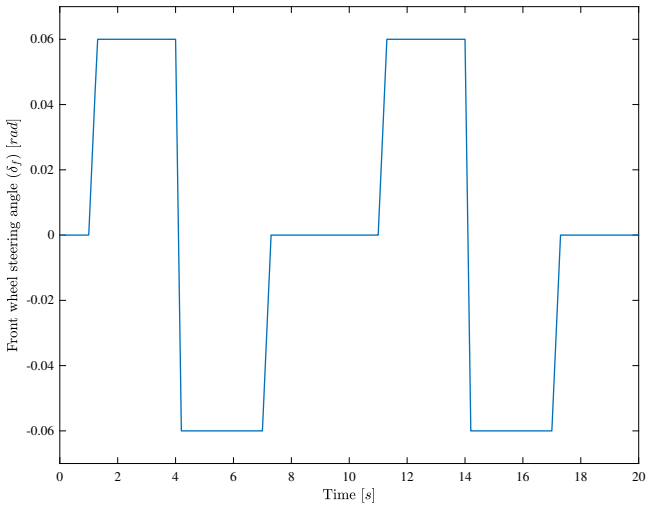

FIGURE IV.1: Steering angle profile given by the driver

The numerical values of the faulty system matrices of the automotive vehicle lateral dynamics are as follows:

$$A_1 = \begin{bmatrix} -10,5597 & -0,9435 \\ 7,8176 & -16,2867 \end{bmatrix}, \quad A_2 = \begin{bmatrix} -6,0290 & -1,4598 \\ -63,5932 & -8,1492 \end{bmatrix}$$

$$A_3 = \begin{bmatrix} -5,9721 & -0,4982 \\ 69,4073 & -10,3087 \end{bmatrix}, \quad A_4 = \begin{bmatrix} -1,4413 & -1,0145 \\ -2,0035 & -2,1712 \end{bmatrix}$$

$$B_{f1} = B_{f2} = \begin{bmatrix} 5,4347 \\ 72,9608 \end{bmatrix}, \quad B_{f3} = B_{f4} = \begin{bmatrix} 0,8470 \\ 11,3712 \end{bmatrix}$$

$$C = \begin{bmatrix} 0 & 1 \end{bmatrix}, \quad D_1 = D_2 = D_3 = D_4 = \begin{bmatrix} 0.5 \\ 0.5 \end{bmatrix}, \quad E = \begin{bmatrix} 1 & 0 \\ 0 & 1 \end{bmatrix}$$

Remark. IV. 6 *In the general case, matrix E is supposed to be singular non invertible. A special case of E equal to an identity is introduced in this application.*

By using Matlab LMI Toolbox (Gahinet et al., 1994; Erkus and Lee, 2004) and choosing $\gamma_1 = 0,2$, $\gamma_2 = 0,15$, Theorem. IV.1 optimization problem can be easily solved. We obtain the following observer gains and matrices:

$$L_1 = \begin{bmatrix} 3,1638 \\ -3,0785 \\ 10,4204 \end{bmatrix}, \quad L_2 = \begin{bmatrix} -59,7551 \\ -7,1105 \\ 15,3116 \end{bmatrix}, \quad L_3 = \begin{bmatrix} 35,5790 \\ 5,1189 \\ 2,9669 \end{bmatrix}, \quad L_4 = \begin{bmatrix} -27,3335 \\ 1,0953 \\ 7,8577 \end{bmatrix}$$

$$T = \begin{bmatrix} 0,9577 & 0 & -0,0423 \\ 0,1800 & 1,0000 & 0,1800 \\ 0,0324 & 0 & 1,0324 \end{bmatrix}, \quad H = \begin{bmatrix} -0,0423 \\ 0,1800 \\ 0,0324 \end{bmatrix}$$

Considering the unknown disturbance $d(t)$ with band-limited white noise and the fault $f(t)$ of the following form:

$$f(t) = \begin{cases} 0,023t - 0,1 & 0 \leq t < 5 \\ 0,05 & 5 \leq t < 10 \\ 0,05\sin(3t) & t \geq 10 \end{cases} \tag{IV.28}$$

Figures IV.2 and IV.3 display the response of the system states and their estimates under the influence of actuator fault $f(t)$ and Fig. IV.4 shows the actuator fault scenario $f(t)$ and its estimation.

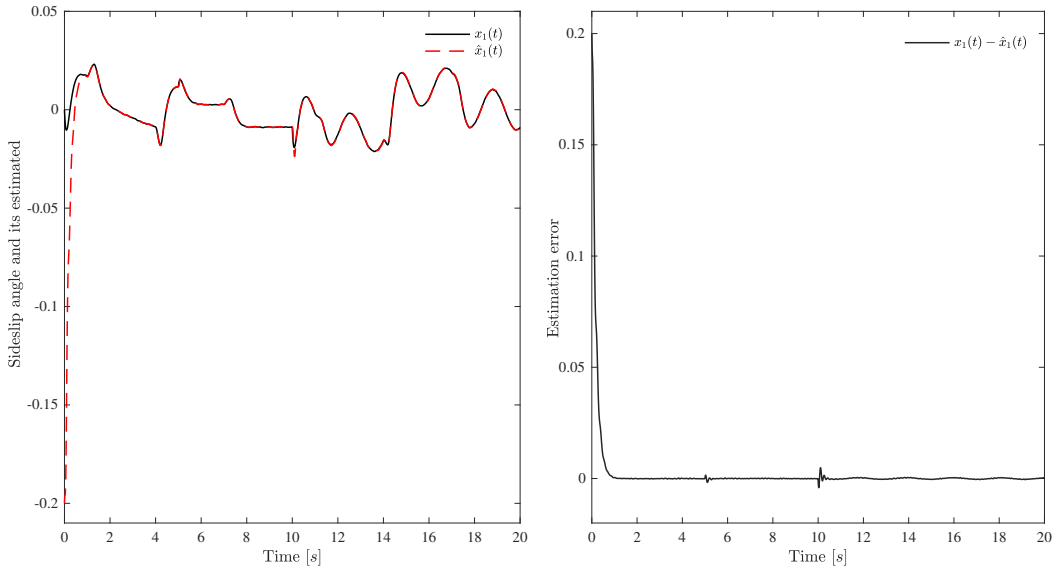

FIGURE IV.2: Time evolution of side-slip angle and its estimated (left) Estimation error (right)

It is clear from all figures IV.2-IV.4 that the estimate converges closely with the measurement, both for actuator faults and system states. This shows the proposed observer's ability to accurately estimate the system parameters or even faults, despite the presence of external disturbances.

It can be seen from Figures IV.2 and IV.3 that, after the system fails, the vehicle loses its performance and its states have reached unacceptable values. This problem can be overcome by applying a fault-tolerant control law (see Chapter V).

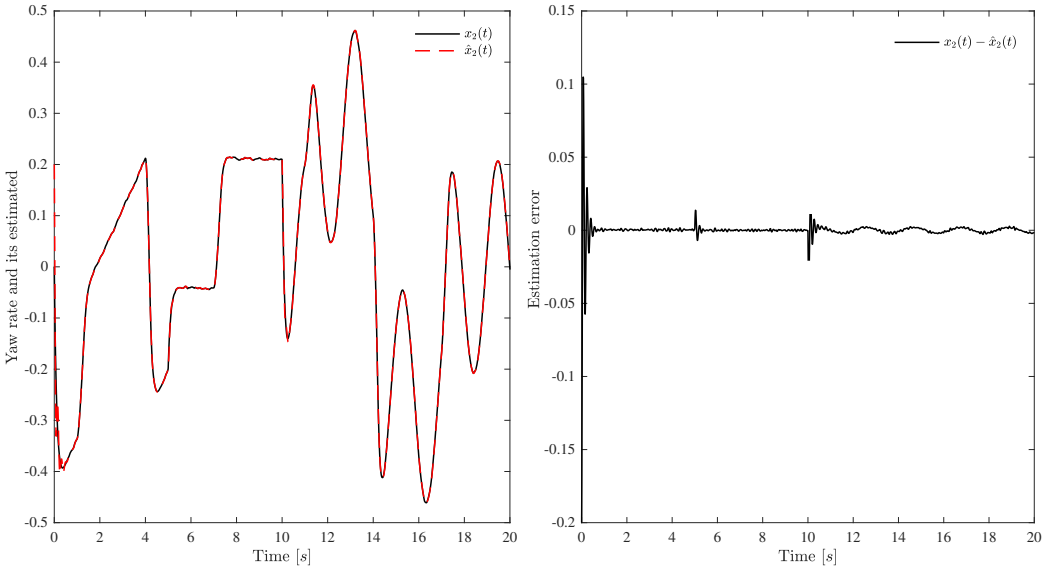

FIGURE IV.3: Time evolution of yaw rate and its estimated (left) Estimation error (right)

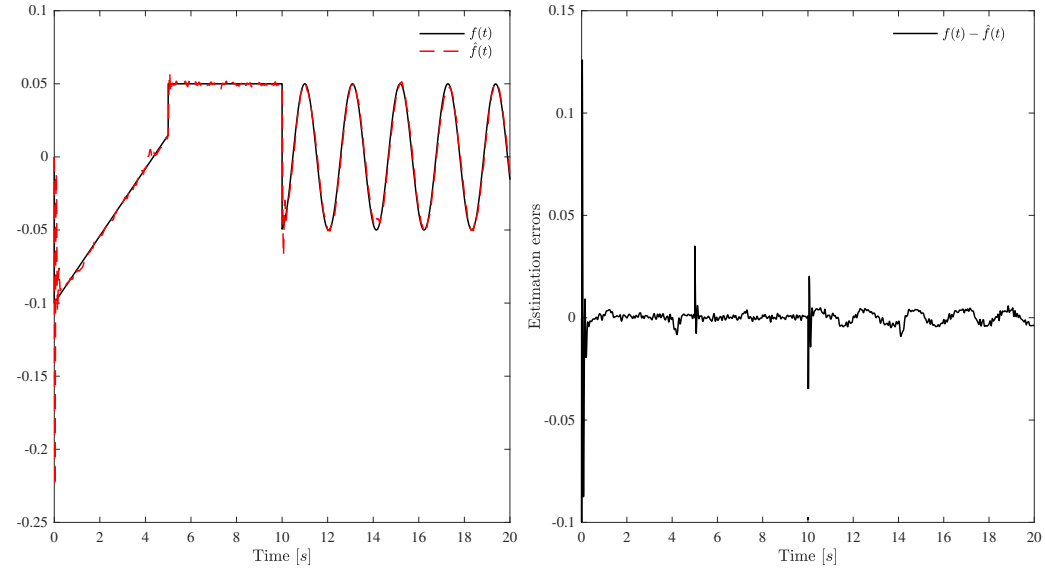

FIGURE IV.4: Time evolution of fault and its estimated (left) Estimation error (right)

IV.3 Fault/state estimation using unknown input observer

This section deals with an unknown input observer's design by considering a property of the time derivatives of membership functions for an automotive vehicle lateral dynamics represented by the T-S fuzzy model with uncertainties.

IV.3.1 Issue description

Automotive vehicle lateral dynamics may show unexpected dangerous behaviour in the presence of unusual external conditions such as lateral wind force, the variation of the road adhesion coefficient, and others. So to deal with this problem, sensor/actuator faults and appropriate uncertainties have to be implemented.

Let us consider the following uncertain system with sensor/actuator faults:

$$\begin{cases} \dot{x}(t) = \sum_{i=1}^{4} h_i(\alpha_f, \alpha_r) \left[(A_i + \Delta A_i(t))x(t) + (B_{fi} + \Delta B_{fi}(t))\delta_f(t) + F_{1i} f(t) \right] \\ y(t) = Cx(t) + F_2 f(t) \end{cases} \tag{IV.29}$$

where $x(t)$, $y(t)$ and $\delta_f(t)$ denote state, output and input vectors, respectively. $h_i(\alpha_f, \alpha_r)$ are the membership functions which are defined in Chapter III. A_i, B_i and C are state, input and output matrices, respectively. $f(t)$ are faults assigned to both actuator and sensors. F_{1i} and F_2 are constant matrices with compatible dimensions. $\Delta A_i(t)$ and $\Delta B_{fi}(t)$ are matrices functions that represent time-varying parameter uncertainties affecting the state and the input, respectively, and are constructed as follows:

$$\Delta A_i(t) = E\Delta\tilde{A}_i(t), \;\; \Delta B_{fi}(t) = E\Delta\tilde{B}_{fi}(t), \tag{IV.30}$$

where E is a full column rank matrix.

Based on the uncertainties form (IV.30), the T-S fuzzy model (IV.29) can be rewritten as follows:

$$\begin{cases} \dot{x}(t) = \sum_{i=1}^{4} h_i(\alpha_f, \alpha_r) \Big[A_i x(t) + B_i u(t) + E\omega_i(t) + F_{1i} f(t) \Big] \\ y(t) = Cx(t) + F_2 f(t) \end{cases} \tag{IV.31}$$

with:

$$\omega_i(t) = \tilde{A}_i(t)x(t) + \tilde{B}_{fi}(t)\delta_f(t) \tag{IV.32}$$

The augmented system formed by the system (IV.31) and the fault dynamics can be described as follows:

$$\begin{cases} \dot{\bar{x}}_a(t) = \sum_{i=1}^{4} h_i(\alpha_f, \alpha_r) \Big[\bar{A}_i \bar{x}_a(t) + \bar{B}_i u(t) + \bar{E}\bar{\omega}_i(t) \Big] \\ y(t) = \bar{C}\bar{x}_a(t) \end{cases} \tag{IV.33}$$

where

$$\bar{x}_a(t) = \begin{bmatrix} x(t) \\ f(t) \end{bmatrix}, \; \bar{\omega}_i(t) = \begin{bmatrix} \omega_i(t) \\ \dot{f}(t) \end{bmatrix}, \; \bar{A}_i = \begin{bmatrix} A_i & F_{1i} \\ 0 & 0 \end{bmatrix}, \; \bar{B}_i = \begin{bmatrix} B_i \\ 0 \end{bmatrix}, \; \bar{E} = \begin{bmatrix} E & 0 \\ 0 & I \end{bmatrix}, \; \bar{C} = \begin{bmatrix} C & F_2 \end{bmatrix}$$

Before proceeding to the design of the augmented system observer (IV.33), to estimate states and faults in the coming subsection, the following assumptions are necessary.

Assumption. IV. 3 *(Vu and Do, 2018) The matrices $\bar{C}$ and $\bar{E}$ are full row and full column rank, respectively.*

An effective way to further reduce conservatism is to select the fuzzy Lyapunov function dependent on the weighting (Zhao et al., 2012), i.e.

$$P = \sum_{i=1}^{m} h_i(\xi(t))P_i > 0 \tag{IV.34}$$

Since the time derivative of (IV.34) needs that of $h_i(\xi(t))$, the following assumption is taken into consideration.

Assumption. IV. 4 *(Tanaka et al., 2003)*

$$\begin{cases} |\dot{h}_k(\xi(t))| \leq a_k \\ a_k \geq 0 \end{cases} \tag{IV.35}$$

Remark. IV. 7 *Assumption. IV.4 means that the state variables describing the membership functions have bounded variations, and the parameters a_k are upper bounds on the derivative of the membership functions. Note that in most practical applications, membership functions in priors usually depend on one or two state variables (Jadbabaie, 1999).*

IV.3.2 Unknown input observer design

There are several practical problems in automotive vehicle production in the real world that prevent the use of sensors, especially lateral velocity and yaw rate sensors, which include high cost, signal degradation or loss under some circumstances and others. The observer theory can be used to overcome this problem. The block diagram shown in Fig. IV.5 presents the concept of the unknown input observer, where $\delta_f(t)$ is the input, $f(t)$ is the fault signal, $\hat{x}(t)$ and $\hat{f}(t)$ are the state and fault estimation, respectively, and $y(t)$ is the system output.

This subsection aims to design an unknown input observer to simultaneously estimate the system states and the sensor/actuator faults under uncertainties affecting both state and input matrices.

Let us consider the following observer that has the same structure as the previous T-S fuzzy system:

$$\begin{cases} \dot{z}(t) = \sum\limits_{i=1}^{4} h_i(\alpha_f, \alpha_r)\Big[N_i z(t) + G_i u(t) + L_i y(t)\Big] \\ \hat{\hat{x}}_a(t) = z(t) - Hy(t) \end{cases} \tag{IV.36}$$

where N_i, G_i, L_i and H are the observer parameters to be determined. $z(t)$ and $\hat{\hat{x}}_a(t)$ are the observer states and the estimate of the augmented system, respectively.

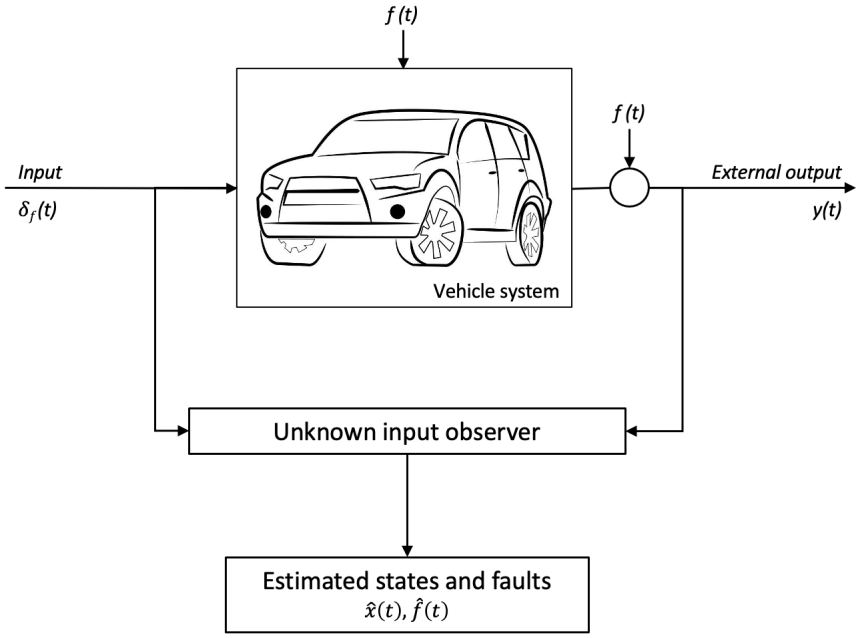

FIGURE IV.5: Scheme of the approach for state/fault estimation

IV.3.3 Stability analysis

Let us define the estimation error between the faulty augmented system (IV.33) and the observer (IV.36) as follows:

$$e_x(t) = \bar{x}_a(t) - \hat{\bar{x}}_a(t) \tag{IV.37}$$

Putting:

$$M = I + H\bar{C} \tag{IV.38}$$

Error (IV.37) can be rewritten as follows:

$$e_x(t) = M\bar{x}_a(t) - z(t) \tag{IV.39}$$

The dynamics of the estimation error $e_x(t)$ is written as follows:

$$\dot{e}_x(t) = M\dot{\bar{x}}_a(t) - \dot{z}(t) \tag{IV.40}$$

Substituting $\dot{\bar{x}}_a(t)$ and $\dot{z}(t)$ by their expressions (IV.33) and (IV.36) respectively, we obtain:

$$\dot{e}_x(t) = \sum_{i=1}^{4} h_i(\alpha_f, \alpha_r)\Big[(M\bar{A}_i - L_i\bar{C} - N_iH\bar{C})\bar{x}_a(t) + (M\bar{B}_i - G_i)u(t) + M\bar{E}\bar{\omega}_i(t) - N_i\hat{\bar{x}}_a(t)\Big] \tag{IV.41}$$

Adding and subtracting $N_i\bar{x}_a(t)$, we get:

$$\dot{e}_x(t) = \sum_{i=1}^{4} h_i(\alpha_f, \alpha_r)\Big[(M\bar{A}_i - L_i\bar{C} - N_iM)\bar{x}_a(t) + (M\bar{B}_i - G_i)u(t) + M\bar{E}\bar{\omega}_i(t) + N_ie_x(t)\Big] \tag{IV.42}$$

If the following conditions are met:

$$M\bar{A}_i - L_i\bar{C} - N_iM = 0 \tag{IV.43}$$
$$M\bar{B}_i - G_i = 0 \tag{IV.44}$$
$$M\bar{E} = 0 \tag{IV.45}$$

Then (IV.42) becomes as follows:

$$\dot{e}_x(t) = \sum_{i=1}^{4} h_i(\alpha_f, \alpha_r)N_ie_x(t) \tag{IV.46}$$

The following theorem presents the conditions for the estimation error dynamics (IV.46) to be asymptotically stable.

Theorem. IV. 2 *(Vu and Do, 2018) Under assumptions 3-4 and for a given positive constant a_k, the observer* (IV.36) *tends asymptotically to the augmented system* (IV.33) *if there exist positive symmetric matrices P_j and matrices N_i, G_i, L_i, H, such that the following conditions are satisfied for $i, j = 1, \ldots, 4$.*

$$M = I + H\bar{C} \tag{IV.47}$$
$$M\bar{A}_i - L_i\bar{C} - N_iM = 0 \tag{IV.48}$$
$$G_i = M\bar{B}_i \tag{IV.49}$$
$$M\bar{E} = 0 \tag{IV.50}$$
$$\sum_{k=1}^{4} a_kP_k + N_i^TP_j + P_jN_i < 0 \tag{IV.51}$$

Proof. IV. 2 *Let us consider the following Lyapunov function candidate*

$$V(e_x(t)) = \sum_{i=1}^{4} h_i(\alpha_f, \alpha_r)e_x^T(t)P_ie_x(t) \tag{IV.52}$$

where $P_i = P_i^T > 0$.

The time derivative of (IV.52) *is as follows*

$$\dot{V}(e_x(t)) = \sum_{i=1}^{4} \dot{h}_i(\alpha_f, \alpha_r)e_x^T(t)P_ie_x(t) + \sum_{i=1}^{4} h_i(\alpha_f, \alpha_r)\left\{\dot{e}_x^T(t)P_ie_x(t) + e_x^T(t)P_i\dot{e}_x(t)\right\} \tag{IV.53}$$

Using Assumption. IV.4, we can write

$$\dot{V}(e_x(t)) \leq \sum_{i=1}^{4} h_i(\alpha_f, \alpha_r) \left\{ \sum_{k=1}^{4} a_k e_x^T(t) P_k e_x(t) + \dot{e}_x^T(t) P_i e_x(t) + e_x^T(t) P_i \dot{e}_x(t) \right\} \quad \text{(IV.54)}$$

Substituting (IV.46) *into* (IV.54), *gives*

$$\dot{V}(e_x(t)) \leq \sum_{i=1}^{4} \sum_{j=1}^{4} h_i(\alpha_f, \alpha_r) h_j(\alpha_f, \alpha_r) e_x^T(t) \left\{ \sum_{k=1}^{4} a_k P_k + N_i^T P_j + P_j N_i \right\} e_x(t) \quad \text{(IV.55)}$$

Then, if condition (IV.51) *of Theorem. IV.2 holds, then* $\dot{V}(t) < 0$. *This means that the estimation error* $e_x(t)$ *tends asymptotically to zero.*

Remark. IV. 8 *The Lyapunov function* (IV.52) *is well defined to study the stability of T-S fuzzy systems (Tanaka et al., 2003).*

IV.3.4 Transformation into LMI using Finsler's lemma

According to Theorem. IV.2, it is difficult to find the matrices N_i and P_j with the given coefficient a_k to check the condition (IV.51). However, to overcome this challenge, Theorem. IV.7 illustrates the procedure of transforming (IV.51) into a linear matrix inequality, based on Finsler's lemma, that Matlab LMI Toolbox will easily solve.

Theorem. IV. 3 *(El Youssfi et al., 2021b) For a given positive scalar* a_k, *the states and faults of the system* (IV.33) *are estimated asymptotically with the observer* (IV.36) *if there exist the matrices* V, $\bar{Y}$, $\bar{Q}_i$ *and positive symmetric matrix* P_i *such that the following conditions hold for* $i, j = 1, \ldots, 4$.

$$\begin{bmatrix} \sum_{k=1}^{m} a_k P_k + \gamma(\Pi_i + \Pi_i^T) & \Theta_{ij} \\ * & -V - V^T \end{bmatrix} < 0 \quad \text{(IV.56)}$$

where

$$\Pi_i = V\bar{R}_i - \bar{Q}_i\bar{C} + \bar{Y}\bar{S}_i \quad \text{(IV.57)}$$

$$\Theta_{ij} = P_j - \gamma V + \bar{R}_i^T V^T - \bar{C}^T \bar{Q}_i^T + \bar{S}_i^T \bar{Y}^T \quad \text{(IV.58)}$$

$$\bar{R}_i = (I + \Psi\bar{C})\bar{A}_i \quad \text{(IV.59)}$$

$$\bar{S}_i = \Phi\bar{C}\bar{A}_i \quad \text{(IV.60)}$$

$$\Psi = -\bar{E}(\bar{C}\bar{E})^+ \quad \text{(IV.61)}$$

$$\Phi = I - (\bar{C}\bar{E})(\bar{C}\bar{E})^+ \quad \text{(IV.62)}$$

$$(\bar{C}\bar{E})^+ = ((\bar{C}\bar{E})^T(\bar{C}\bar{E}))^{-1}(\bar{C}\bar{E})^T \quad \text{(IV.63)}$$

The existence of V, $\bar{Y}$, and $\bar{Q}_i$ satisfies the correctness of equations (IV.64)-(IV.65). *Furthermore, the linearity of our matrix inequality formulation is guaranteed.*

$$Y = V^{-1}\bar{Y} \tag{IV.64}$$

$$Q_i = V^{-1}\bar{Q}_i \tag{IV.65}$$

So, the observer gains can be derived as follows:

$$H = \Psi + Y\Phi \tag{IV.66}$$

$$N_i = M\bar{A}_i - Q_i\bar{C} \tag{IV.67}$$

$$G_i = M\bar{B}_i \tag{IV.68}$$

$$L_i = Q_i(I + \bar{C}H) - M\bar{A}_iH \tag{IV.69}$$

Proof. IV. 3 *According to IV.38 and IV.45, we can write:*

$$H(\bar{C}\bar{E}) = -\bar{E} \tag{IV.70}$$

By using the same notation given in Lemma 6, where $\mathbb{X} = H$, $\mathbb{W} = \bar{C}\bar{E}$ and $\mathbb{Y} = -\bar{E}$, the general solution of (IV.70) *according to Assumption. IV.3 and Lemma 6 is:*

$$H = \Psi + Y\Phi \tag{IV.71}$$

where $\Psi = -\bar{E}(\bar{C}\bar{E})^{+}$, $\Phi = I - (\bar{C}\bar{E})(\bar{C}\bar{E})^{+}$ and Y is an arbitrary matrix of compatible dimension.

Let us put

$$Q_i = L_i + N_iH \tag{IV.72}$$

Substituting (IV.72) *into* (IV.43), *we obtain*

$$N_i = M\bar{A}_i - Q_i\bar{C} \tag{IV.73}$$

According to (IV.72) *and* (IV.73), *we get*

$$L_i = Q_i(I + \bar{C}H) - M\bar{A}_iH \tag{IV.74}$$

By combining (IV.38) *with* (IV.73) *and replacing H with its expression* (IV.71), *the following formula can be given:*

$$N_i = \bar{R}_i + Y\bar{S}_i - Q_i\bar{C} \tag{IV.75}$$

where

$$\bar{R}_i = (I + \Psi\bar{C})\bar{A}_i, \qquad \bar{S}_i = \Phi\bar{C}\bar{A}_i$$

The estimation error $e_x(t)$ tends asymptotically to zero if the right side of the inequality (IV.54) *is less than zero. Then, we can write*

$$\bar{e}_x^T \bar{P}_{ik} \bar{e}_x < 0 \tag{IV.76}$$

where

$$\bar{P}_{ik} = \begin{bmatrix} \sum_{k=1}^{4} a_k P_k & P_i \\ P_i & 0 \end{bmatrix}, \quad \bar{e}_x = \begin{bmatrix} e_x(t) \\ \dot{e}_x(t) \end{bmatrix} \tag{IV.77}$$

From (IV.46)*, we have*

$$\Omega \bar{e}_x = 0, \quad with \;\; \Omega = \begin{bmatrix} N_i & -I \end{bmatrix} \quad and \;\; \Omega\Omega_\perp = 0 \tag{IV.78}$$

$\Omega_\perp$ is the orthogonal complement of Ω.

According to (IV.76)-(IV.78) *and based on Finsler's Lemma 7, the following condition is satisfied*

$$\begin{bmatrix} \sum_{k=1}^{4} a_k P_k & P_i \\ P_i & 0 \end{bmatrix} + \begin{bmatrix} U \\ V \end{bmatrix} \begin{bmatrix} N_i & -I \end{bmatrix} + \begin{bmatrix} N_i^T \\ -I \end{bmatrix} \begin{bmatrix} U^T & V^T \end{bmatrix} < 0 \tag{IV.79}$$

which is equivalent to this inequality

$$\begin{bmatrix} \sum_{k=1}^{4} a_k P_k + UN_i + N_i^T U^T & P_j - U + N_i^T V^T \\ * & -V - V^T \end{bmatrix} < 0 \tag{IV.80}$$

It should be noted that equation (IV.80) *is a Bilinear Matrix Inequality (BMI). However, the obtained condition can not be solved since it could provide a non-unique solution. Furthermore, we can not provide any simulation test since the obtained condition does not have any constant matrix. So, new development is needed.*

Equation (IV.80) *can be transformed into a LMI by considering $U = \gamma V$ and the variable change $\bar{N}_i = VN_i$. Now, by replacing N_i by its expression in* (IV.75)*, equation* (IV.80) *can be rewritten as follows:*

$$\begin{bmatrix} \sum_{k=1}^{4} a_k P_k + \bar{\Pi}_i + \bar{\Pi}_i^T & \bar{\Theta}_{ij} \\ * & -V - V^T \end{bmatrix} < 0 \tag{IV.81}$$

where

$$\bar{\Pi}_i = U\bar{R}_i - UQ_i\bar{C} + UY\bar{S}_i \tag{IV.82}$$

$$\bar{\Theta}_{ij} = P_j - U + \bar{R}_i^T V^T - \bar{C}^T Q_i^T V^T + \bar{S}_i^T Y^T V^T \tag{IV.83}$$

By substituting $U = \gamma V$, $\bar{Y} = VY$ and $\bar{Q}_i = VQ_i$, the inequality of the linear matrix (IV.56) *can be determined. This completes the proof.*

In Theorem. IV.3, we have tackled free slack variables as a method to improve the result. Consequently, the matrix V has been involved as slack to obtain less conservative results and get good states/fault estimation for automotive vehicle lateral dynamics.

Remark. IV. 9 *The given γ is determined according to Finsler's Lemma 7. The choice of γ is made arbitrarily so that the conditions of Theorem. IV.3 are feasible and take into account the quality of simulation results.*

IV.3.5 Relaxed unknown input observer

In this subsection, relaxing stability conditions of the estimation error (IV.37) are presented. Based on the Lyapunov function approach and the introduction of some relaxed variables, sufficient conditions for the unknown input observer design are formulated as Linear Matrix Inequalities (LMIs).

The following theorem provides the conditions for the asymptotic stability of the estimation error in (IV.37).

Theorem. IV. 4 *(El Youssfi et al., 2020b) Under assumptions 3-4 and for a given positive constant a_k, the observer* (IV.36) *tends asymptotically to the augmented system* (IV.33) *if there exist positive symmetric matrices P_j and matrices N_i, G_i, L_i, H, such that the following conditions are satisfied for $i, j = 1, \ldots, 4$ and $i < j$.*

$$M = I + H\bar{C} \tag{IV.84}$$

$$M\bar{A}_i - L_i\bar{C} - N_iM = 0 \tag{IV.85}$$

$$G_i = M\bar{B}_i \tag{IV.86}$$

$$M\bar{E} = 0 \tag{IV.87}$$

$$\sum_{k=1}^{4} a_kP_k + N_i^TP_i + P_iN_i < \Lambda_{ii} \tag{IV.88}$$

$$2\sum_{k=1}^{4} a_kP_k + N_i^TP_j + P_jN_i + N_j^TP_i + P_iN_j \leq \Lambda_{ij} + \Lambda_{ij}^T \tag{IV.89}$$

$$\begin{bmatrix} \Lambda_{11} & \Lambda_{12} & \Lambda_{13} & \Lambda_{14} \\ * & \Lambda_{22} & \Lambda_{23} & \Lambda_{24} \\ * & * & \Lambda_{33} & \Lambda_{34} \\ * & * & * & \Lambda_{44} \end{bmatrix} < 0 \tag{IV.90}$$

Proof. IV. 4 *Following the same steps of proof 2 and applying Lemma 4 on* (IV.55)*, we obtain*

$$\begin{aligned} \dot{V}(t) \leq & \sum_{i=1}^{4} h_i^2(\alpha_f, \alpha_r) e_x^T(t) \left\{ \sum_{k=1}^{4} a_kP_k + N_i^TP_i + P_iN_i \right\} e_x(t) \\ & + \sum_{i=1}^{4}\sum_{j>i}^{4} h_i(\alpha_f, \alpha_r)h_j(\alpha_f, \alpha_r) e_x^T(t) \left\{ 2\sum_{k=1}^{4} a_kP_k + N_i^TP_j + P_jN_i + N_j^TP_i + P_iN_j \right\} e_x(t) \end{aligned} \tag{IV.91}$$

If conditions in (IV.88), (IV.89) *and* (IV.90) *are satisfied, this means that* $\dot{V}(t) < 0$ *and this completes the proof.*

The result in Theorem. IV.4 provides an improved extension of the work presented in (Vu and Do, 2018). The results of our study are less conservative, thanks to the relaxation matrices involved via Lemma 4. Moreover, if we put $\Lambda_{ij} = 0$, we obtain the same conditions as (Vu and Do, 2018). Thus, the proposed theorem is a general case.

As with Theorem. IV.2, in Theorem. IV.4 it is difficult to find the matrices N_i and P_j with the given coefficient a_k to verify the conditions (IV.88)-(IV.90). However, to overcome this challenge, the following theorem illustrates the procedure for transforming (IV.88)-(IV.90) into linear matrix inequalities that the Matlab LMI Toolbox will easily solve.

Theorem. IV. 5 *(El Youssfi et al., 2020b) For a given positive scalar* a_k*, the states and faults of the system* (IV.33) *are estimated asymptotically with the observer* (IV.36) *if there exist the matrices* N_i*,* G_i*,* L_i*,* H*,* R*,* $\bar{Y}$*,* $\bar{Q}_i$ *and positive symmetric matrix* P_i *such that the following linear matrix inequalities hold for* $i, j = 1, \ldots, 4$ *and* $i < j$*.*

$$\begin{bmatrix} \Delta_{ii} & P_i - Z + \Gamma_i \\ * & -Z - Z^T \end{bmatrix} < 0 \tag{IV.92}$$

$$\begin{bmatrix} \Delta_{ij} + \Delta_{ji} & P_j - Z + \Gamma_i & P_i - Z + \Gamma_j & -Z_1 \\ * & -Z - Z^T & -Z & -Z_2 \\ * & * & -Z - Z^T & -Z_1 - Z^T \\ * & * & * & -Z_2 - Z_2^T \end{bmatrix} \leq 0 \tag{IV.93}$$

$$\begin{bmatrix} \Lambda_{11} & \Lambda_{12} & \Lambda_{13} & \Lambda_{14} \\ * & \Lambda_{22} & \Lambda_{23} & \Lambda_{24} \\ * & * & \Lambda_{33} & \Lambda_{34} \\ * & * & * & \Lambda_{44} \end{bmatrix} < 0 \tag{IV.94}$$

where

$$\Delta_{ij} = \sum_{k=1}^{m} a_k P_k - \Lambda_{ij} + Z\bar{R}_i + \bar{R}_j^T Z^T + \bar{Y}\bar{S}_i + \bar{S}_j^T \bar{Y}^T - \bar{C}^T \bar{Q}_i^T - \bar{Q}_j \bar{C} \tag{IV.95}$$

$$\Gamma_i = \bar{R}_i^T Z^T + \bar{S}_i^T \bar{Y}^T - \bar{C}^T \bar{Q}_i^T \tag{IV.96}$$

$$\bar{R}_i = (I + \Psi\bar{C})\bar{A}_i \tag{IV.97}$$

$$\bar{S}_i = \Phi\bar{C}\bar{A}_i \tag{IV.98}$$

$$\Psi = -\bar{E}(\bar{C}\bar{E})^+ \tag{IV.99}$$

$$\Phi = I - (\bar{C}\bar{E})(\bar{C}\bar{E})^+ \tag{IV.100}$$

$$(\bar{C}\bar{E})^+ = ((\bar{C}\bar{E})^T(\bar{C}\bar{E}))^{-1}(\bar{C}\bar{E})^T \tag{IV.101}$$

The existence of Z, $\bar{Y}$, and $\bar{Q}_i$ satisfies the correctness of the following equations

$$Y = Z^{-1}\bar{Y} \tag{IV.102}$$
$$Q_i = Z^{-1}\bar{Q}_i \tag{IV.103}$$

Furthermore, the linearity of our matrix inequality formulation is guaranteed and the observer gains are obtained as follows:

$$H = \Psi + Y\Phi \tag{IV.104}$$
$$M = I + H\bar{C} \tag{IV.105}$$
$$N_i = M\bar{A}_i - Q_i\bar{C} \tag{IV.106}$$
$$G_i = M\bar{B}_i \tag{IV.107}$$
$$L_i = Q_i(I + \bar{C}H) - M\bar{A}_iH \tag{IV.108}$$

Proof. IV. 5 *Following the same procedure as the proof 3 up to equation* (IV.75).

If conditions (IV.88) *in Theorem. IV.II.52 are hold. By applying Lemma 5, we obtain directly the following*

$$\begin{bmatrix} \sum_{k=1}^{4} a_k P_k - \Lambda_{ii} + N_i^T Z^T + Z N_i & P_i - Z + N_i^T Z^T \\ * & -Z - Z^T \end{bmatrix} < 0 \tag{IV.109}$$

By replacing N_i by its expression (IV.75), *conditions* (IV.92) *are obtained.*

The conditions (IV.93) *are obtained by using Lemma 5 twice. In the first step, we define variables indicated in Lemma 5 as follows*

$$\Theta_{ijk} = 2\sum_{k=1}^{4} a_k P_k + N_j^T P_i + P_i N_j - \Lambda_{ij} - \Lambda_{ij}^T \tag{IV.110}$$

if conditions (IV.89) *hold, that means is equivalent to the following conditions*

$$\begin{bmatrix} \Theta_{ijk} + N_i^T Z^T + Z N_i & P_j - Z + N_i^T Z^T \\ * & -Z - Z^T \end{bmatrix} < 0 \tag{IV.111}$$

In the second step, the condition (IV.111) *can be written as follows*

$$\tilde{\Theta}_{ijk} + \tilde{N}_j^T \tilde{P}_i + \tilde{P}_i \tilde{N}_j < 0 \tag{IV.112}$$

where

$$\tilde{\Theta}_{ijk} = \begin{bmatrix} 2\sum_{k=1}^{4} a_k P_k - \Lambda_{ij} - \Lambda_{ij}^T + N_i^T Z^T + Z N_i & P_j - Z + N_i^T Z^T \\ * & -Z - Z^T \end{bmatrix}$$

$$\tilde{N}_j = \begin{bmatrix} N_j & 0 \\ 0 & 0 \end{bmatrix}, \qquad \tilde{P}_i = \begin{bmatrix} P_i & 0 \\ 0 & 0 \end{bmatrix}$$

Applying the Lemma 5, we obtain the following conditions

$$\begin{bmatrix} \tilde{\Theta}_{ijk} + \tilde{N}_j^T \tilde{Z}^T + \tilde{Z}\tilde{N}_j & \tilde{P}_i - \tilde{Z} + \tilde{N}_j^T \tilde{Z}^T \\ * & -\tilde{Z} - \tilde{Z}^T \end{bmatrix} < 0 \tag{IV.113}$$

where

$$\tilde{Z} = \begin{bmatrix} Z & Z_1 \\ Z & Z_2 \end{bmatrix}$$

Replacing N_i by its expression (IV.75) *and taking into account the $\bar{Y} = ZY$ and $\bar{Q}_i = ZQ_i$, give the linear matrix inequalities* (IV.92)-(IV.94)*. This complete the proof.*

Remark. IV. 10 *The bounds on the time derivative of the membership functions must be chosen in advance. The main drawback of this method is that it is not obvious how to choose these bounds in a systematic way other than by using trial and error methods (Jadbabaie, 1999). So, the choice of a_k is made arbitrarily so that the conditions of previous theorems are feasible and take into account the quality of simulation results.*

Remark. IV. 11 *Compared with some works in the literature (Zhang et al., 2018; Gómez-Peñate et al., 2019; Martínez-García et al., 2020), which just focus on sensor faults or actuator faults, we have concentrated in this study on the problem of estimating actuator and sensor faults together.*

IV.3.6 Numerical illustration and simulation results

In order to demonstrate the effectiveness of the proposed observer in estimating the sensor/actuator faults and states of the lateral dynamics system without consideration of roll motion, some simulations have been performed using Matlab software. For that, the same vehicle system employed in sub-section IV.2.4 is used here.

Assuming that the fault $f(t)$ affecting the actuator and the outputs of the system is of the following form:

$$f(t) = \begin{cases} 0,46t - 2 & 0 \leq t < 5 \\ 1 & 5 \leq t < 10 \\ \sin(3t) & t \geq 10 \end{cases} \tag{IV.114}$$

The numerical values of the faulty uncertain system matrices of the automotive vehicle lateral dynamics (IV.31) are as follows: The numerical values of the matrices appearing in the faulty uncertain system of the automotive vehicle lateral dynamics (IV.31) are as follows (for A_i and B_{fi} are the same as the previous section):

$$C = \begin{bmatrix} 1 & 0 \\ 0 & 1 \end{bmatrix}, \quad F_{21} = F_{22} = F_{23} = F_{24} = \begin{bmatrix} 0.5 \\ 0.5 \end{bmatrix}, \quad E = \begin{bmatrix} 0.1 \\ 0.1 \end{bmatrix}, \quad F_2 = \begin{bmatrix} 0 \\ 0.5 \end{bmatrix}$$

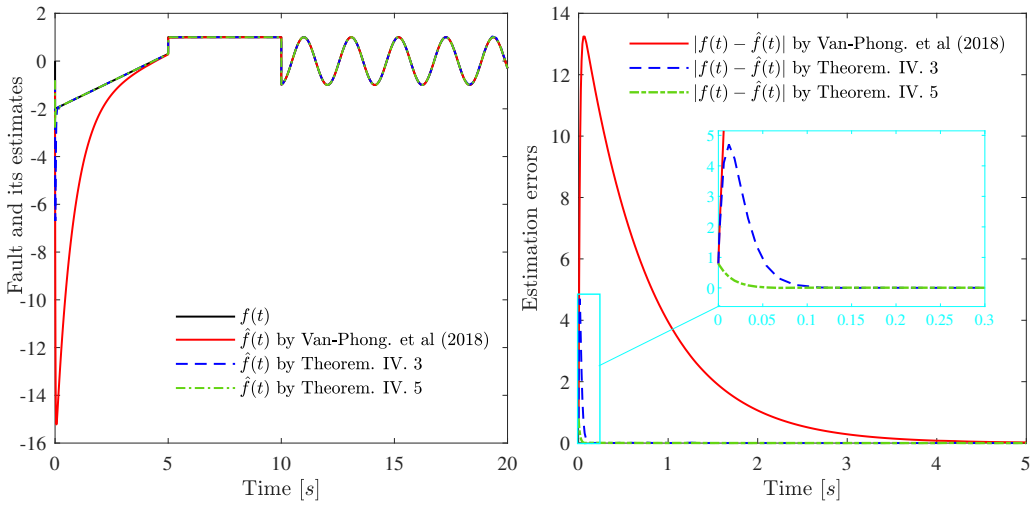

FIGURE IV.6: Time evolution of fault and its estimates (left) Estimation errors (right)

Solving the LMIs of previous theorems, using the LMI toolbox of Matlab (Gahinet et al., 1994; Erkus and Lee, 2004), we recover the following observer gains displayed in Tab. IV.1 by selecting $a_1 = 2,5$, $a_2 = 0,4$, $a_3 = 1,5$ and $a_4 = 0,3$.

The automotive vehicle lateral dynamics system was simulated by choosing the following initial conditions:

$$x(0) = \begin{bmatrix} 0 & 0 \end{bmatrix}^T, \quad \hat{z}(0) = \begin{bmatrix} -0,8 & 0,8 & 0 \end{bmatrix}^T$$

Figure IV.6 shows in its left part the fault scenario $f(t)$ and its estimations, using different methods, and in its right part the evolution of the estimation errors.

The automotive vehicle lateral dynamics system was simulated by including the fault shown in red in Fig. IV.6. It is clear that the estimation by the observer's gains obtained by Theorem. IV.5 converges very quickly to the fault, just after its appearance, against the result obtained by Theorem. IV.3 which itself presents some rapidity compared to Theorem 2 of (Vu and Do, 2018). This can be seen in the estimation errors' evolution (dotted green converges rapidly to zero compared to dotted blue and subsequently to solid red).

The left-hand sides of figures IV.7 and IV.8 show respectively the side-slip angle $\beta(t)$ and yaw rate $\dot{\psi}(t)$ with their estimates, by different approaches, under influence of sensor/actuator faults $f(t)$ and their right-hand sides show the evolution of the estimation errors.

The two figures IV.7 and IV.8 clearly show a relaxed estimation of the states despite uncertainties and faults. It is noticeable that the gains obtained by Theorem. IV.5 present the quickness and efficiency compared to Theorem. IV.3 which itself represents certain swiftness compared to the gains obtained by Theorem 2 of (Vu and Do, 2018), when estimating the states of the vehicle lateral dynamics system. This is clearly visible in the evolution of the estimation errors (dotted green converges rapidly to zero

TABLE IV.1: Gains obtained by different theorems

Gains	Theorem. IV.3	Theorem. IV.5
N_1	$\begin{bmatrix} -4,7452 & 0,0001 & 0,0000 \\ -0,0001 & -7,2483 & 5,0060 \\ 0,0000 & 5,0060 & -14,7573 \end{bmatrix}$	$\begin{bmatrix} -32,8643 & -1,5653 & -0,7827 \\ 36,0558 & -24,4520 & -6,1569 \\ -71,4496 & 22,2424 & -1,0171 \end{bmatrix}$
N_2	$\begin{bmatrix} -4,7452 & 0,0001 & 0,0000 \\ -0,0003 & -5,6193 & 1,7482 \\ 0,0003 & 1,7482 & -8,2417 \end{bmatrix}$	$\begin{bmatrix} -32,8643 & -1,5653 & -0,7827 \\ -47,3571 & -14,9468 & -6,1569 \\ 95,3763 & 3,2319 & -1,0171 \end{bmatrix}$
N_3	$\begin{bmatrix} -4,7452 & 0,0001 & 0,0000 \\ -0,0001 & -6,0539 & 2,6173 \\ 0,0000 & 2,6173 & -9,9798 \end{bmatrix}$	$\begin{bmatrix} -32,8643 & -1,5653 & -0,7827 \\ 85,4924 & -19,6536 & -6,1569 \\ -170,3228 & 12,6456 & -1,0171 \end{bmatrix}$
N_4	$\begin{bmatrix} -4,7452 & 0,0001 & 0,0000 \\ -0,0001 & -4,4250 & -0,6406 \\ -0,0000 & -0,6406 & -3,4641 \end{bmatrix}$	$\begin{bmatrix} -32,8643 & -1,5653 & -0,7827 \\ 2,0795 & -10,1484 & -6,1569 \\ -3,4969 & -6,3648 & -1,0171 \end{bmatrix}$
L_1	$\begin{bmatrix} 0,0000 & -0,0000 \\ 7,7267 & 0,9864 \\ -15,4534 & -1,9729 \end{bmatrix}$	$\begin{bmatrix} 0,0000 & -0,0000 \\ 3,6359 & -1,6491 \\ -7,2717 & 3,2981 \end{bmatrix}$
L_2	$\begin{bmatrix} 0,0000 & -0,0000 \\ -63,6351 & 0,9864 \\ 127,2701 & -1,9729 \end{bmatrix}$	$\begin{bmatrix} 0,0000 & -0,0000 \\ -54,5971 & -1,6491 \\ 109,1942 & 3,2981 \end{bmatrix}$
L_3	$\begin{bmatrix} 0,0000 & -0,0000 \\ 69,3351 & 0,9864 \\ -138,6703 & -1,9729 \end{bmatrix}$	$\begin{bmatrix} 0,0000 & -0,0000 \\ 65,7837 & -1,6491 \\ -131,5675 & 3,2981 \end{bmatrix}$
L_4	$\begin{bmatrix} -0,0000 & -0,0000 \\ -2,0266 & 0,9864 \\ 4,0533 & -1,9729 \end{bmatrix}$	$\begin{bmatrix} 0,0000 & -0,0000 \\ 7,5508 & -1,6491 \\ -15,1015 & 3,2981 \end{bmatrix}$
H	$\begin{bmatrix} -1,0000 & 0 \\ -0,0136 & 0 \\ 0,0271 & -2,0000 \end{bmatrix}$	$\begin{bmatrix} -1,0000 & 0 \\ -2,6491 & 0 \\ 5,2981 & -2,0000 \end{bmatrix}$
G_1	$\begin{bmatrix} -0,0000 & 72,8871 & -145,7741 \end{bmatrix}^T$	$\begin{bmatrix} -0,0000 & 58,5640 & -117,1280 \end{bmatrix}^T$
G_2	$\begin{bmatrix} -0,0000 & 72,8871 & -145,7741 \end{bmatrix}^T$	$\begin{bmatrix} -0,0000 & 58,5640 & -117,1280 \end{bmatrix}^T$
G_3	$\begin{bmatrix} -0,0000 & 11,3597 & -22,7193 \end{bmatrix}^T$	$\begin{bmatrix} -0,0000 & 9,1274 & -18,2547 \end{bmatrix}^T$
G_4	$\begin{bmatrix} -0,0000 & 11,3597 & -22,7193 \end{bmatrix}^T$	$\begin{bmatrix} -0,0000 & 9,1274 & -18,2547 \end{bmatrix}^T$

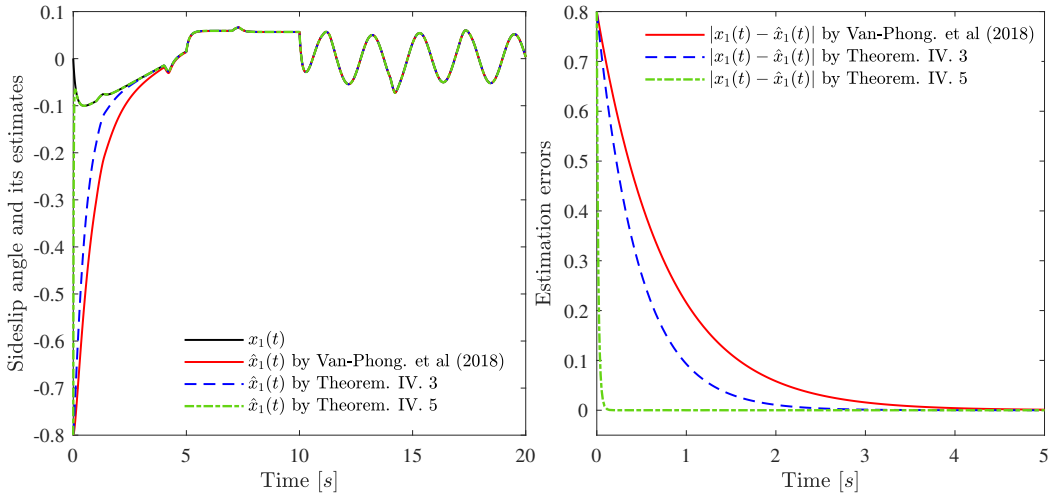

FIGURE IV.7: Time evolution of side-slip angle and its estimates (left) Estimation errors (right)

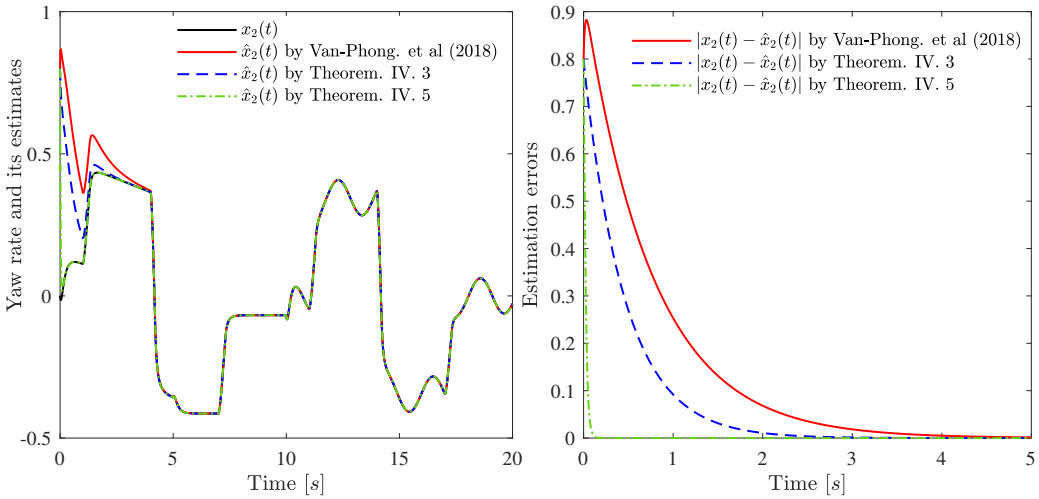

FIGURE IV.8: Time evolution of yaw rate and its estimates (left) Estimation errors (right)

compared to dotted blue and subsequently to solid red).

As mentioned in Remark. IV.11, some works in the literature focus either on actuator or sensor faults and not both simultaneously. So in this study, both types of faults are investigated. However, this study's limitations are reflected in the fact that an identical fault affects the actuator and the sensors at the same time, which is unusual in real systems, including the automotive vehicle lateral dynamics system.

IV.4 Conclusion

In this chapter, we have addressed the problem of fault and state estimation for an automotive vehicle lateral dynamics represented by T-S fuzzy model. In the first part of this chapter, an observer was designed, using descriptor approach, to estimate the fault/state for vehicle system affected by both actuator faults and various disturbances. In the second part, an observer with unknown inputs was proposed to estimate the fault/state of an uncertain system of vehicle affected by sensor/actuator faults. In general, convergence of the estimation error to zero is studied with the Lyapunov approach, which is reformulated as an LMIs problem. The simulations on the lateral dynamics system of an automotive vehicle were performed and the results obtained highlight the effectiveness of the proposed approaches for fault/state estimation.

In the next chapter, based on observers' information, robust control laws against faults are designed to overcome the performance deterioration caused by these faults.

Chapter V

Fault-tolerant control for automotive vehicle lateral dynamics

V.1 Introduction

Nowadays, the concern to improve passenger safety has led to increasingly efficient automotive vehicle control systems (ESP, ABS, TCS, ACC, etc.). Conventional control in the current automotive vehicle can hardly achieve all the objectives in case of disturbances or faults that can degrade its behaviour or even destabilise it. For this reason, the introduction of robustness against disturbances and the consideration of the possible occurrence of faults in the control laws used for automotive vehicle dynamics control systems has become indispensable. These types of controls are known as Fault-Tolerant Controls (FTCs) (Rodrigues, 2005; Oudghiri, 2008; Bezzaoucha, 2013; Zhang, 2017). As discussed in the first chapter, this type of control can be classified into passive or active approaches. Passive approaches use robust control techniques to ensure that the closed-loop system remains insensitive to some faults with constant controllers and without online fault information on the system. They are designed to keep the system reliable in terms of its stability and performance in the nominal and predefined fault cases (Kanev, 2004; Noura et al., 2009; Picó and Adam, 2015; Stetter et al., 2020). Active approaches differ from passive methods by using fault detection and diagnosis unit and an online synthesis of the controller (Amin and Hasan, 2019). Several works have been published concerning the robust control of automotive vehicle dynamics represented by the T-S fuzzy model. Among them, we cite these references and those that contain (Aouaouda et al., 2014b; Oudghiri et al., 2014; Ichalal et al., 2016; El Youssfi et al., 2019a; El Youssfi and El Bachtiri, 2020).

As discussed in the introduction of the previous chapter, driver assistance systems depend on the service provided by the electronic systems for various vehicle activities in critical driving situations. If the vehicle deviates in an undesirable direction, the computer makes immediate decisions to respond with corrective actions to ensure the stability of the automotive vehicle. The synthesis of controllers inspired by control techniques found in the literature has been actively considered in recent years, and many studies have been published in this area (Wang and Longoria, 2009; Rajamani, 2011; El Youssfi et al., 2017, 2021a). The states of the automotive vehicle system are not

always fully measurable. Therefore, it is necessary to design a controller using other methods. Note that the most appropriate control is based on static output feedback because, at a lower cost, it can be easily implemented. Besides, stabilisation through static output feedback control of vehicle dynamics systems is rarely studied, although, in practice, it is important and useful (Jing et al., 2016; El Youssfi et al., 2020a). However, this type of control remains passive and is sensitive to various faults.

On the other hand, the dependence of the driver assistance system control on actuator and sensor components is becoming increasingly complex. The automotive vehicle dynamics system can typically be exposed to the actuator and/or the sensor faults. It is well known that conventional control strategies are unable to adjust when these faults occur. So, fault-tolerant control laws must be designed to ensure the rigorous stability of the system, even in case of faults. Several works concerning this type of control have been published in the literature, including (Oudghiri, 2008; Aouaouda et al., 2013; Hernandez-Alcantara et al., 2018).

In this chapter, our objective is to design fault-tolerant relaxant control laws to ensure the stability of the automotive vehicle lateral dynamics, limit the effect of faults either at the actuator or sensor side and compensate for the impact of disturbances. The stability of the T-S fuzzy model is studied using the Lyapunov function. The appropriate conditions for controller and observer design are given as Linear Matrix Inequalities (LMIs) that can be solved easily by specific tools (Matlab LMI toolbox or YALMIP) (Gahinet and Apkarian, 1994; Lofberg, 2004). The model of the automotive vehicle used in this chapter is the so-called "bicycle" model with an additional degree of freedom corresponding to roll motion.

V.2 H_∞ static output-feedback control for automotive vehicle lateral dynamics

In this section, a H_∞ static output-feedback control law robust against external disturbances is proposed to improve the automotive vehicle's lateral stability and drive performance and avoid skidding in critical conditions.

V.2.1 Issue description and static output-feedback control design

Let us consider the T-S fuzzy model of automotive vehicle lateral dynamics, including roll motion, described in Chapter III, as affected by external disturbances. Thus, the T-S fuzzy system (III.48) becomes:

$$\begin{cases} \dot{x}(t) = \sum_{i=1}^{4} h_i(\alpha_f, \alpha_r) \left[A_i x(t) + B_{fi} u(t) + E_i d(t) \right] \\ y(t) = \sum_{i=1}^{4} h_i(\alpha_f, \alpha_r) \left[C_{yi} x(t) + F_i d(t) \right] \\ z(t) = \sum_{i=1}^{4} h_i(\alpha_f, \alpha_r) \left[C_{zi} x(t) + D_i u(t) \right] \end{cases} \tag{V.1}$$

where $x(t)$ and $y(t)$ are state and measured output of the system, respectively. In vehicle lateral motion control, it is not only the handling but also the vehicle stability should be addressed. Thus, controlled output $z(t)$ is considered. $d(t)$ is external disturbances. $u(t)$ is an assistant steering angle added to the driver's steering angle. A_i, B_{fi}, E_i, F_i, D_i, C_{yi} and C_{zi} are constant matrices with compatible dimensions.

The vehicle side-slip angle and roll angle are generally difficult to measure with inexpensive sensors. In this section, the vehicle yaw rate $\dot{\psi}$, roll rate $\dot{\phi}$ and lateral acceleration a_y are taken as measured outputs.

Let us consider the following control law expression based on static output-feedback:

$$u(t) = -\sum_{i=1}^{4} h_i(\alpha_f, \alpha_r) G_i y(t) \tag{V.2}$$

where G_i are the control gains.

By replacing (V.2) in (V.1), the perturbed system of automotive vehicle lateral dynamics can be rewritten as follows:

$$\begin{cases} \dot{x}(t) = \sum\limits_{i=1}^{4}\sum\limits_{j=1}^{4}\sum\limits_{k=1}^{4} h_i h_j h_k [\bar{A}_{ijk} x(t) + \bar{B}_{ijk} d(t)] \\ z(t) = \sum\limits_{i=1}^{4}\sum\limits_{j=1}^{4}\sum\limits_{k=1}^{4} h_i h_j h_k [\bar{C}_{ijk} x(t) + \bar{D}_{ijk} d(t)] \end{cases} \tag{V.3}$$

where

$$\begin{gathered} \bar{A}_{ijk} = A_i - B_{fi} G_j C_{yk}, \qquad \bar{B}_{ijk} = E_i - B_{fi} G_j F_k, \\ \bar{C}_{ijk} = C_{zi} - D_i G_j C_{yk}, \qquad \bar{D}_{ijl} = -D_i G_j F_k \\ h_i = h_i(\alpha_f, \alpha_r), \quad h_j = h_j(\alpha_f, \alpha_r), \quad h_k = h_k(\alpha_f, \alpha_r) \end{gathered}$$

To simplify equations in the remainder of this section, these simplifications are considered:

$$\begin{aligned} \bar{A} &= \sum_{i=1}^{4}\sum_{j=1}^{4}\sum_{k=1}^{4} h_i h_j h_k \bar{A}_{ijk}, \qquad \bar{B} = \sum_{i=1}^{4}\sum_{j=1}^{4}\sum_{k=1}^{4} h_i h_j h_k \bar{B}_{ijk}, \\ \bar{C} &= \sum_{i=1}^{4}\sum_{j=1}^{4}\sum_{k=1}^{4} h_i h_j h_k \bar{C}_{ijk}, \qquad \bar{D} = \sum_{i=1}^{4}\sum_{j=1}^{4}\sum_{k=1}^{4} h_i h_j h_k \bar{D}_{ijk} \end{aligned} \tag{V.4}$$

V.2.2 Main results

In this subsection, sufficient stability conditions for the closed-loop system and the design of H_∞ static output-feedback control are given.

Theorem. V. 1 *(Chaibi et al., 2019) Consider a scalar $\gamma > 0$, the closed-loop T-S fuzzy system* (V.3) *is asymptotically stable and satisfies the H_∞ performances if there exist symmetric matrix*

$P > 0$, and matrices U and V, such that the following LMI is satisfied.

$$\Lambda = \begin{bmatrix} -U - U^T & \Lambda_{12} & U\bar{B} & 0 \\ * & \Lambda_{22} & V\bar{B} & \bar{C}^T \\ * & * & -\gamma^2 I & \bar{D}^T \\ * & * & * & -I \end{bmatrix} < 0, \quad with \quad \begin{cases} \Lambda_{12} = P + U\bar{A} - V^T \\ \Lambda_{22} = V\bar{A} + \bar{A}^T V^T \end{cases} \tag{V.5}$$

Proof. V. 1 *Let us consider the following matrix:*

$$\Sigma = \begin{bmatrix} 0 & P & 0 \\ P & \bar{C}^T\bar{C} & \bar{C}^T\bar{D} \\ 0 & \bar{D}^T\bar{C} & -\gamma^2 I + \bar{D}^T\bar{D} \end{bmatrix} \tag{V.6}$$

By using the Schur complement, (V.5) *is equivalent to the following:*

$$\Sigma + sym(X^T Y Z) < 0 \tag{V.7}$$

where

$$X = I,\ Y = \begin{bmatrix} U^T & V^T & 0 \end{bmatrix}^T,\ Z = \begin{bmatrix} -I & \bar{A} & \bar{B} \end{bmatrix}$$

Selecting $Z^{\perp} = \begin{bmatrix} \bar{A} & \bar{B} \\ I & 0 \\ 0 & I \end{bmatrix}$ *and applying Lemma 10. Through some manipulations, we obtain:*

$$\begin{bmatrix} \bar{A} & \bar{B} \\ I & 0 \end{bmatrix}^T \begin{bmatrix} 0 & P \\ P & 0 \end{bmatrix} \begin{bmatrix} \bar{A} & \bar{B} \\ I & 0 \end{bmatrix} + \begin{bmatrix} \bar{C}^T\bar{C} & \bar{C}^T\bar{D} \\ \bar{D}^T\bar{C} & \bar{D}^T\bar{D} - \gamma^2 I \end{bmatrix} < 0 \tag{V.8}$$

which is similar to

$$\begin{bmatrix} P\bar{A} + \bar{A}^T P & P\bar{B} \\ \bar{B}^T P & 0 \end{bmatrix} + \begin{bmatrix} \bar{C}^T\bar{C} & \bar{C}^T\bar{D} \\ \bar{D}^T\bar{C} & \bar{D}^T\bar{D} - \gamma^2 I \end{bmatrix} < 0 \tag{V.9}$$

Let us consider the following Lyapunov function

$$V(x(t)) = x^T(t) P x(t) \tag{V.10}$$

Its derivative can be written as follows:

$$\dot{V}(x(t)) = \dot{x}^T(t) P x(t) + x^T(t) P \dot{x}(t) \tag{V.11}$$

If (V.9) *holds, it can be easily checked that*

$$\dot{V}(x(t)) + z^T(t) z(t) - \gamma^2 d^T(t) d(t) < 0 \tag{V.12}$$

Integration of inequality (V.12) *on both sides from 0 to ∞ gives*

$$\int_0^{\infty} \left[\dot{V}(x(t)) + z^T(t) z(t) - \gamma^2 d^T(t) d(t)\right] dt = V(x(\infty)) - V(x(0)) + \int_0^{\infty} \left[z^T(t) z(t) - \gamma^2 d^T(t) d(t)\right] dt < 0 \tag{V.13}$$

Thus, under a zero initial condition, we have

$$\int_0^\infty z^T(t)z(t)dt < \gamma^2 \int_0^\infty d^T(t)d(t)dt \tag{V.14}$$

The proof is completed.

In the following theorem, new LMI conditions are presented to guarantee the asymptotic stability of the closed-loop T-S fuzzy system (V.3) with the H_∞ static output-feedback control.

Theorem. V. 2 *(El Youssfi et al., 2020a) Consider a scalar $\gamma > 0$, the closed-loop fuzzy system* (V.3) *is asymptotically stable and satisfies the H_∞ performances, if for known scalar parameter α there exist symmetrical positive matrices P and R and other matrices U, V, W, M, and N_i, such that the following LMIs hold.*

$$\begin{bmatrix} \Xi_{iii} & \Delta_{iii} \\ * & \Omega \end{bmatrix} < 0, \qquad i = 1, \ldots, 4 \tag{V.15}$$

$$\begin{bmatrix} \Xi_{iij} + \Xi_{iji} + \Xi_{jii} & \Delta_{iij} & \Delta_{iji} & \Delta_{jii} \\ * & \Omega & 0 & 0 \\ * & * & \Omega & 0 \\ * & * & * & \Omega \end{bmatrix} < 0, \qquad i, j = 1, 2, \ldots, 4, \qquad i \neq j \tag{V.16}$$

$$\begin{bmatrix} \Xi_{ijk} + \Xi_{ikj} + \Xi_{jik} + \Xi_{jki} + \Xi_{kij} + \Xi_{kji} & \Delta_{ijk} & \Delta_{ikj} & \Delta_{jik} & \Delta_{jki} & \Delta_{kij} & \Delta_{kji} \\ * & \Omega & 0 & 0 & 0 & 0 & 0 \\ * & * & \Omega & 0 & 0 & 0 & 0 \\ * & * & * & \Omega & 0 & 0 & 0 \\ * & * & * & * & \Omega & 0 & 0 \\ * & * & * & * & * & \Omega & 0 \\ * & * & * & * & * & * & \Omega \end{bmatrix} < 0 \tag{V.17}$$

$$i = 1, 2, \qquad j = 2, 3, \qquad k = 3, 4$$

where

$$\Xi_{ijk} = \begin{bmatrix} -U - U^T & P + UA_i - V^T + B_{fi}N_jC_{yk} & UE_i + B_{fi}N_jF_k & 0 \\ * & sym\{VA_i + B_{fi}N_jC_{yk}\} & VE_i + B_{fi}N_jF_k & C_{zi}^T W^T + C_{yk}^T N_j^T D_i^T \\ * & * & -\gamma^2 I & F_k^T N_j^T D_i^T \\ * & * & * & I - W - W^T \end{bmatrix}$$

$$\Delta_{ijk} = \begin{bmatrix} 0 & UB_{fi} - B_{fi}M \\ C_{yk}^T N_j^T & VB_{fi} - B_{fi}M \\ F_k^T N_j^T & 0 \\ 0 & WD_i - D_iM \end{bmatrix}, \quad \Omega = \begin{bmatrix} -R & 0 \\ 0 & \alpha^2 R - \alpha M - \alpha M^T \end{bmatrix}$$

Furthermore, the static output-feedback control gain matrices are given by

$$G_i = M^{-1}N_i, \qquad i = 1, 2, \ldots, 4 \tag{V.18}$$

Proof. V. 2 . *Assume that the inequality* (V.15) *holds, that means that $I - W - W^T < 0$ and $\alpha^2 R - \alpha M - \alpha M^T < 0$ (with $\alpha^2 R > 0$), which guarantees the non singularity of the matrices*

M and W. From (V.15)-(V.17), *we have*

$$\sum_{i=1}^{4}\sum_{j=1}^{4}\sum_{k=1}^{4} h_i h_j h_k \Psi_{ijk} < 0 \tag{V.19}$$

where

$$\Psi_{ijl} = \begin{bmatrix} \Xi_{ijl} & \theta_{ijl} \\ * & \Gamma \end{bmatrix} \tag{V.20}$$

From Lemma 12 and the exploitation of the Schur complement, the inequality (V.19) *ensures that*

$$\bar{\Psi}_{ijk} = \Xi_{ijk} + \begin{bmatrix} 0 \\ C_{yk}^T N_j^T \\ F_k^T N_j^T \\ 0 \end{bmatrix} R^{-1} \begin{bmatrix} 0 \\ C_{yk}^T N_j^T \\ F_k^T N_j^T \\ 0 \end{bmatrix}^T + \begin{bmatrix} UB_{fi} - B_{fi}M \\ VB_{fi} - B_{fi}M \\ 0 \\ WD_i - D_iM \end{bmatrix} (M^T R^{-1} M)^{-1} \begin{bmatrix} UB_{fi} - B_{fi}M \\ VB_{fi} - B_{fi}M \\ 0 \\ WD_i - D_iM \end{bmatrix}^T < 0 \tag{V.21}$$

By using Lemma 11 and defining $N_j = MG_j$, *we can check that* (V.21) *is equivalent to*

$$\bar{\Psi}_{ijk} = \Xi_{ijk} + \begin{bmatrix} UB_{fi} - B_{fi}M \\ VB_{fi} - B_{fi}M \\ 0 \\ WD_i - D_iM \end{bmatrix} \begin{bmatrix} 0 \\ C_{yk}^T G_j^T \\ F_k^T G_j^T \\ 0 \end{bmatrix}^T + \begin{bmatrix} 0 \\ C_{yk}^T G_j^T \\ F_k^T G_j^T \\ 0 \end{bmatrix} \begin{bmatrix} UB_{fi} - B_{fi}M \\ VB_{fi} - B_{fi}M \\ 0 \\ WD_i - D_iM \end{bmatrix}^T < 0 \tag{V.22}$$

By replacing Ξ_{ijk} *by its expression, we obtain the following inequality:*

$$\bar{\Psi}_{ijk} = \begin{bmatrix} -U - U^T & P + UA_i - V^T + UB_{fi}G_jC_{yk} & UE_i + UB_{fi}G_jF_k & 0 \\ * & sym\{VA_i + VB_{fi}G_jC_{yk}\} & VE_i + VB_{fi}G_jF_k & C_{zi}^T W^T + C_{yk}^T G_j^T D_i^T W^T \\ * & * & -\gamma^2 I & F_k^T G_j^T D_i^T W^T \\ * & * & * & I - W - W^T \end{bmatrix} < 0 \tag{V.23}$$

In view of the fact that $-(V-X)X^{-1}(V-X)^T \leq 0,\ X > 0$ *implies* $-VX^{-1}V^T \leq -V - V^T + X$.

Pre-post multiplying both sides of (V.23) *by* $diag\{I, I, I, W^{-1}\}$ *and its transpose, and replacing* $\bar{A}$, $\bar{B}$, $\bar{C}$ *and* $\bar{D}$ *by their expressions in* (V.4), *we get the inequality in* (V.5). *This completes the proof.*

V.2.3 Numerical illustration and simulation results

A test illustrating a critical driving situation is performed under MATLAB software to show the efficiency of the H_∞ static output-feedback control for perturbed automotive vehicle lateral dynamics system (III.46) represented by T-S fuzzy model (V.1). The parameters of the vehicle are shown in Tab. V.1 (Rahimi and Naraghi, 2018).

TABLE V.1: Parameters for vehicle simulation

Parameter	m_v	m_s	v_x	I_x	I_z	l_r	l_f	h	C_ϕ	K_ϕ
Value	1712	1592	25	614	2488	1,77	1,18	1,00	6000	48000

By solving LMIs (V.15)-(V.17), we obtain for $\alpha = 1$ the lower bound of the H_∞ level $\gamma_{min} = 0,0801$ and the following controller gains:

$$G_1 = \begin{bmatrix} -0,0076 & -0,5990 & -0,1254 \end{bmatrix}, \quad G_2 = \begin{bmatrix} -0,0079 & -0,6767 & -0,1253 \end{bmatrix}$$
$$G_3 = \begin{bmatrix} -0,0088 & -0,5064 & -0,1536 \end{bmatrix}, \quad G_4 = \begin{bmatrix} -0,0091 & -0,5885 & -0,1510 \end{bmatrix}$$

The simulations are carried out with the front steering angle profile given in Fig. V.1. In this scenario, a critical driving situation is induced at time $t = 10s$ to test the proposed control law.

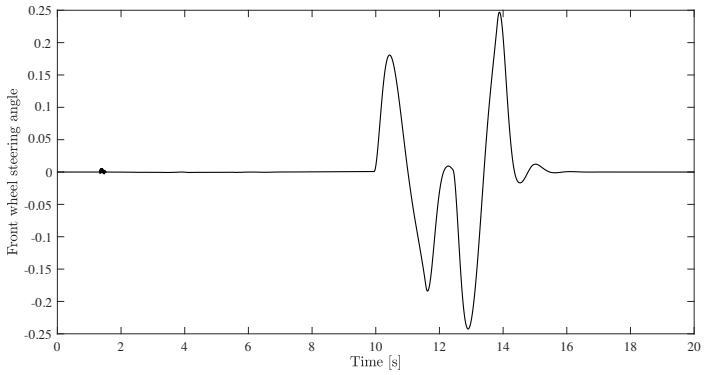

FIGURE V.1: Front wheel steering angle $\delta_f(t)$ $[rad]$

By applying the front wheel steering angle shown in Fig. V.1 and the control law (V.2) to the system (V.1), we obtain the system responses shown in Fig. V.2. Figure V.3 shows the performance of the proposed algorithm to eliminate disturbances. We choose $d(t) = 0.5\sin(2\pi t)$ in these simulations.

It can be seen from Fig. V.2 that the proposed control law is able to maintain and improve the stability and safety of the automotive vehicle under difficult driving conditions. It can also be noted that the external disturbances have been successfully rejected.

From Fig. V.3, it can be seen that the attenuation disturbance performances are satisfactory, and the H_∞ requirement on (V.14) is achieved.

The results presented in this section belong to the so-called passive fault-tolerant control techniques where their fault tolerance capability is limited to low amplitude faults. While in the following sections, active fault-tolerant control strategies are presented.

V.3 Sensor fault-tolerant control for automotive vehicle lateral dynamics

This section deals with the sensor fault-tolerant control approach for the T-S fuzzy system of automotive vehicle lateral dynamics with roll motion consideration (represented in Section III.5). This technique is based on a bank of Luenberger observers to

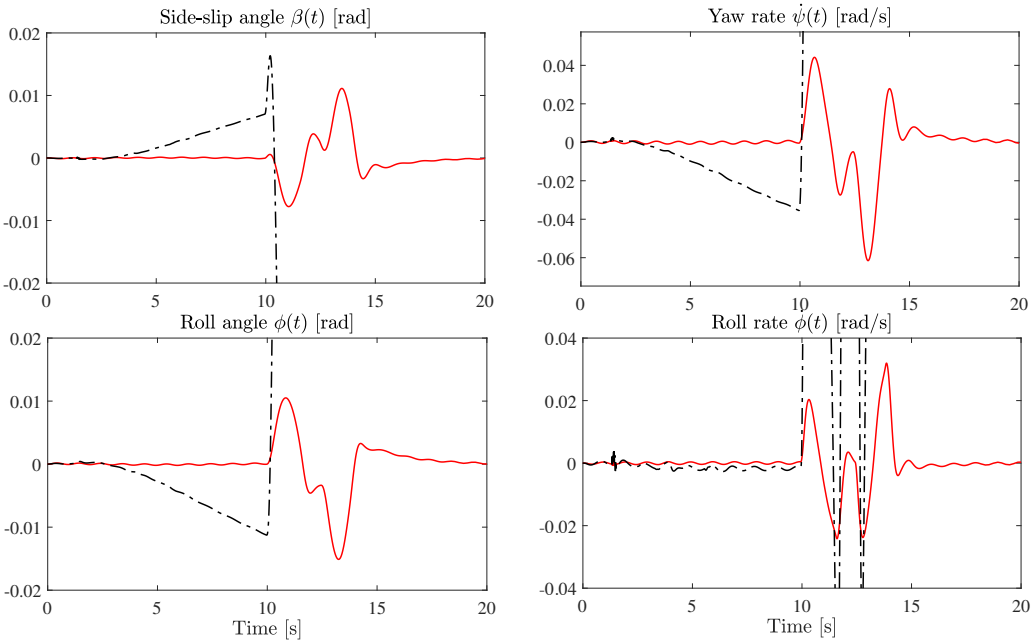

FIGURE V.2: System responses without (black dotted) and with (red) control

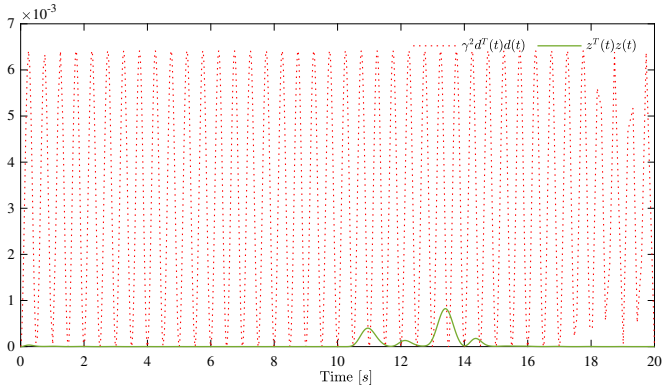

FIGURE V.3: Disturbance attenuation performance with H_∞ control

switch between them, which allows to detect the fault and adapt the control law to minimise the impact of the faults while keeping the vehicle stability and the nominal performances.

V.3.1 H_∞ observer-based control

Consider the perturbed T-S fuzzy model of the lateral dynamics of the automotive vehicle, including roll motion, described in (V.1), with matrices $F_i (i = 1, \ldots, 4)$ and $D_i (i = 1, \ldots, 4)$ being zero. An observer-based control law is considered that shares the same membership functions as (V.1):

$$u(t) = -\sum_{i=1}^{4} h_i(\alpha_f, \alpha_r) K_i \hat{x}(t) \tag{V.24}$$

where $\hat{x}(t)$ is the estimated state and K_i are the controller gains to be determined.

Let us take the following T-S fuzzy observer:

$$\begin{cases} \dot{\hat{x}}(t) = \sum_{i=1}^{4} h_i(\alpha_f, \alpha_r)\left[A_i\hat{x}(t) + B_{fi}u(t) + L_i(y(t) - \hat{y}(t))\right] \\ \hat{y}(t) = \sum_{i=1}^{4} h_i(\alpha_f, \alpha_r)C_{yi}\hat{x}(t) \end{cases} \tag{V.25}$$

where $\hat{y}(t)$ is the estimated output and L_i are the observer gains to be determined.

As a result, the closed loop of T-S fuzzy system (V.1) becomes as follows:

$$\dot{x}(t) = \sum_{i=1}^{4}\sum_{j=1}^{4} h_i(\alpha_f, \alpha_r)h_j(\alpha_f, \alpha_r)\left[(A_i - B_{fi}K_j)x(t) + B_{fi}K_j e(t) + E_i d(t)\right] \tag{V.26}$$

where $e(t) = x(t) - \hat{x}(t)$ is the estimation error.

The time derivative of the estimation error can be written as follows:

$$\dot{e}(t) = \sum_{i=1}^{4}\sum_{j=1}^{4} h_j(\alpha_f, \alpha_r)h_i(\alpha_f, \alpha_r)\left[(A_i - L_iC_{yj})e(t) + E_i d(t)\right] \tag{V.27}$$

From (V.26)-(V.27), we can write:

$$\dot{x}_a(t) = \sum_{i=1}^{4}\sum_{j=1}^{4} h_j(\alpha_f, \alpha_r)h_i(\alpha_f, \alpha_r)\left[\bar{A}_{ij}x_a(t) + \bar{E}_i(t)d(t)\right] \tag{V.28}$$

where:

$$x_a(t) = \begin{bmatrix} x(t) \\ e(t) \end{bmatrix}, \quad \bar{A}_{ij} = \begin{bmatrix} A_i - B_{fi}K_j & B_{fi}K_j \\ 0 & A_i - L_iC_{yj} \end{bmatrix}, \quad \bar{E}_i = \begin{bmatrix} E_i \\ E_i \end{bmatrix}$$

The asymptotic stability of the T-S fuzzy augmented system (V.28) is outlined in the following theorem.

Theorem. V. 3 *(Lin et al., 2005) The asymptotic stability of the T-S fuzzy augmented system* (V.28) *with H_∞ performance is guaranteed for γ attenuation via the control law* (V.24)*, if there exist matrices $P = P^T > 0$, $Q = Q^T > 0$, X_i, Y_i, Γ_{ij} and Λ_{ij} with Γ_{ii} and Λ_{ii} are symmetrical,*

such that the following LMIs are verified for $i = 1, \ldots, 4$ and $i < j$:

$$PA_i^T + A_iP + X_i^T B_{fi}^T + B_{fi}X_i + \gamma^{-2}E_iE_i^T - \Gamma_{ii} < 0 \tag{V.29}$$

$$A_i^T Q + QA_i + C_{yi}^T Y_i^T + Y_i C_{yi} - \Lambda_{ii} < 0 \tag{V.30}$$

$$P(A_i + A_j)^T + (A_i + A_j)P + X_i^T B_{fj}^T + B_{fj}X_i + X_j^T B_{fi}^T + B_{fi}X_j + \gamma^{-2}(E_iE_j^T + E_jE_i^T) - \Gamma_{ij} - \Gamma_{ij}^T \leq 0 \tag{V.31}$$

$$(A_i + A_j)^T Q + Q(A_i + A_j) + C_{yi}^T Y_j^T + Y_i C_{yj} + C_{yj}^T Y_i + Y_j C_{yi} - \Lambda_{ij} - \Lambda_{ij}^T \leq 0 \tag{V.32}$$

$$\begin{bmatrix} \Gamma_{11} & \Gamma_{12} & \Gamma_{13} & \Gamma_{14} & PC_{zi}^T \\ * & \Gamma_{22} & \Gamma_{23} & \Gamma_{24} & PC_{zi}^T \\ * & * & \Gamma_{33} & \Gamma_{34} & PC_{zi}^T \\ * & * & * & \Gamma_{44} & PC_{zi}^T \\ * & * & * & * & -I \end{bmatrix} < 0 \tag{V.33}$$

$$\begin{bmatrix} \Lambda_{11} & \Lambda_{12} & \Lambda_{13} & \Lambda_{14} \\ * & \Lambda_{22} & \Lambda_{23} & \Lambda_{24} \\ * & * & \Lambda_{33} & \Lambda_{34} \\ * & * & * & \Lambda_{44} \end{bmatrix} < 0 \tag{V.34}$$

The controller and observer gains are determined by:

$$K_i = X_i P^{-1} \tag{V.35}$$

$$L_i = Q^{-1} Y_i \tag{V.36}$$

Proof. V. 3 *The demonstration can be found in (Lin et al., 2005).*

V.3.2 Fault-tolerant control strategy

The detection and isolation of faults are important before they have a significant impact on vehicle performances. In this subsection, a fault-tolerant control model for the automotive vehicle lateral dynamics system is presented, based on the detection and isolation block to sequester the healthy sensors from the faulty ones.

This method uses three observers as shown in Fig. V.4, each of them linked to the output of one sensor. The purpose of the "Decision & switching" block is to analyse the residual signals to detect faults and identify the faulty sensors. Then, using the switching system, the state variables are reconstructed from the output of a healthy sensor. The system output vector includes lateral acceleration, yaw rate and roll rate sensors. Then three observer-based controllers can be conceived.

Let $C_{yi}^n (n = 1, 2, 3)$ be the n^{th} row of the matrix C_{yi}. Under the observability assumption of each pair (A_i, C_{yi}^n), the state can be estimated via first, second or third output. Sensor faults are modelled as additive signals to the output:

$$y(t) = C_{yi}x(t) + Ff(t) \tag{V.37}$$

where $f(t)$ represents the faults and the matrix F represents the fault location (e.g. $F = \begin{pmatrix} 1 & 0 & 0 \end{pmatrix}^T$ if only the first sensor is faulty).

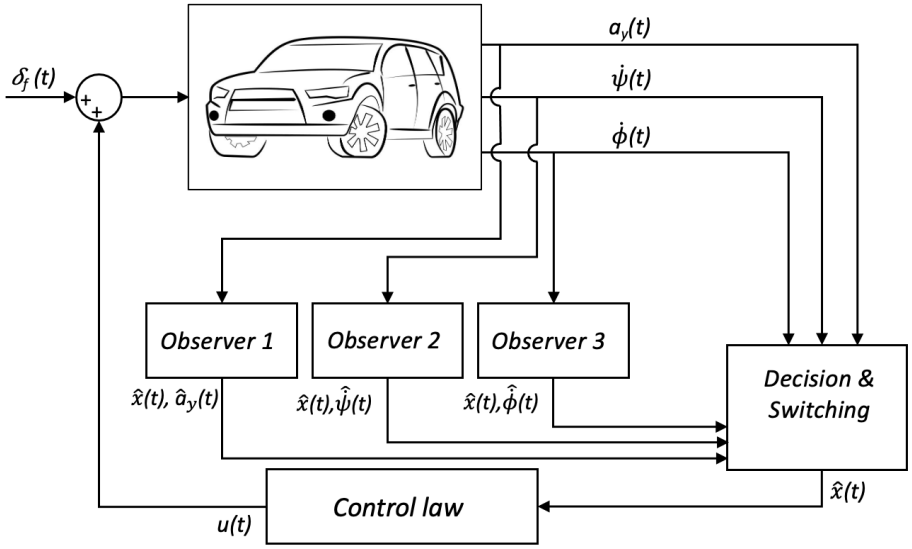

FIGURE V.4: Block diagram of sensor fault-tolerant control

The control law becomes as follows:

$$u(t) = -\sum_{i=1}^{4} h_i(\alpha_f, \alpha_r) K_i \hat{x}^n(t) \tag{V.38}$$

with $\hat{x}^n(t)$ is the estimated state via a healthy sensor and has the following form:

$$\begin{cases} \dot{\hat{x}}^n(t) = \sum\limits_{i=1}^{4} h_i(\alpha_f, \alpha_r)\left[A_i \hat{x}^n(t) + B_{fi} u(t) + L_i^n (y^n(t) - \hat{y}^n(t))\right] \\ \hat{y}^n(t) = \sum\limits_{i=1}^{4} h_i(\alpha_f, \alpha_r) C_{yi}^n \hat{x}(t) \end{cases} \tag{V.39}$$

V.3.3 Numerical illustration and simulation results

As a demonstration of the efficiency of the fault-tolerant control based on the observer bank, some simulations have been performed using the lateral dynamics model of the automotive vehicle with roll motion consideration and MATLAB software. For that, the same vehicle system employed in sub-section V.2.3 is used here.

By solving stability conditions (V.29)-(V.34) using the LMI Toolbox (Gahinet et al., 1994; Erkus and Lee, 2004), we obtain the lower bound of the H_∞ level $\gamma_{min} = 0,217$ and the following gains:

$$K_1 = \begin{bmatrix} 2,1535 & 09053 & -0,9338 & 0,1111 \end{bmatrix}, \; K_2 = \begin{bmatrix} 1,9532 & 0,7878 & -0,7801 & 0,0988 \end{bmatrix}$$
$$K_3 = \begin{bmatrix} 2,4498 & 1,1420 & -1,1955 & 0,1405 \end{bmatrix}, \; K_4 = \begin{bmatrix} 2,1993 & 0,9942 & -1,0026 & 0,1250 \end{bmatrix}$$
$$L_1^1 = \begin{bmatrix} -0,0513 \\ 0,0287 \\ -0,0534 \\ -0,1434 \end{bmatrix}, \; L_2^1 = \begin{bmatrix} -0,0488 \\ 0,0312 \\ -0,0303 \\ -0,0684 \end{bmatrix}, \; L_3^1 = \begin{bmatrix} -0,0479 \\ 0,0295 \\ -0,0771 \\ -0,1041 \end{bmatrix}, \; L_4^1 = \begin{bmatrix} -0,0450 \\ 0,0323 \\ -0,0507 \\ -0,0167 \end{bmatrix}$$

$$L_1^2 = \begin{bmatrix} 63,5756 \\ -18,9325 \\ 15,8397 \\ 131,9472 \end{bmatrix}, \quad L_2^2 = \begin{bmatrix} 70,4725 \\ -20,8292 \\ 16,1965 \\ 148,0536 \end{bmatrix}, \quad L_3^2 = \begin{bmatrix} 42,7156 \\ -13,2024 \\ 11,6816 \\ 82,9924 \end{bmatrix}, \quad L_4^2 = \begin{bmatrix} 49,6125 \\ -15,0992 \\ 12,0384 \\ 99,0988 \end{bmatrix}$$

$$L_1^3 = 10^3. \begin{bmatrix} 0,5120 \\ -0,1962 \\ -1,9744 \\ 0,0094 \end{bmatrix}, \quad L_2^3 = 10^3. \begin{bmatrix} 0,4635 \\ -0,1734 \\ -1,6900 \\ 0,0111 \end{bmatrix}, \quad L_3^3 = 10^3. \begin{bmatrix} 0,4166 \\ -0,1585 \\ -1,6412 \\ 0,0087 \end{bmatrix}, \quad L_4^3 = 10^3. \begin{bmatrix} 0,3682 \\ -0,1358 \\ -1,3569 \\ 0,0103 \end{bmatrix}$$

In this study the simulations are done without and with the proposed approach to show its efficiency. The three sensors are assumed to be under the impact of faults shown in Fig. V.5. The simulation results for the system states of automotive vehicle

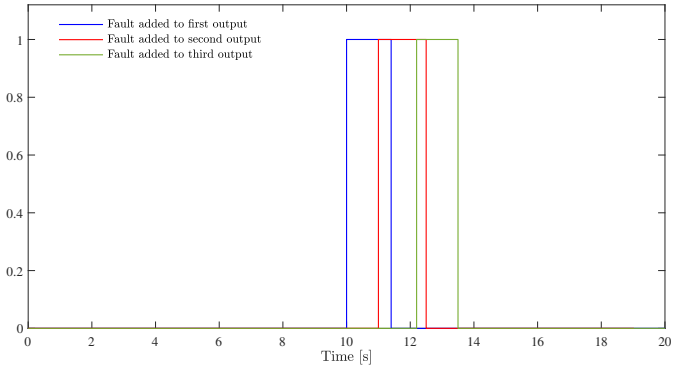

FIGURE V.5: Signals added to sensor outputs

lateral dynamics with consideration of roll motion are displayed in Fig. V.6 without using any switch block and in Fig. V.7 with using switching block.

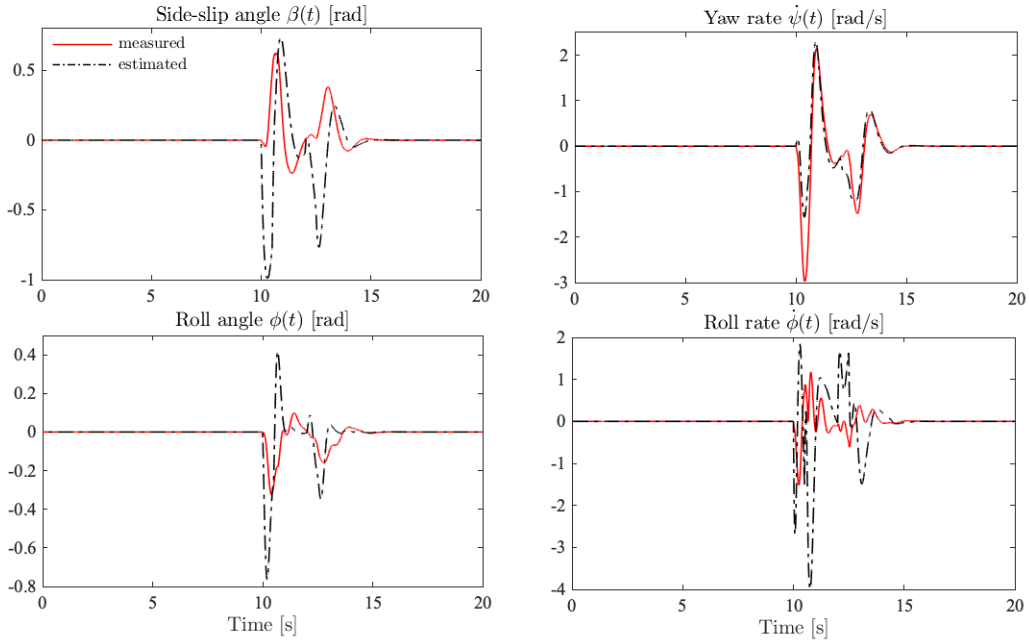

FIGURE V.6: Estimated and measured vehicle response without FTC

It can be seen in Fig. V.6, that between $10\,s$ and $14,5\,s$, the vehicle performance degrades to unacceptable values just after only one sensor becomes faulty. Furthermore, a bad estimation of the states in this range is remarked.

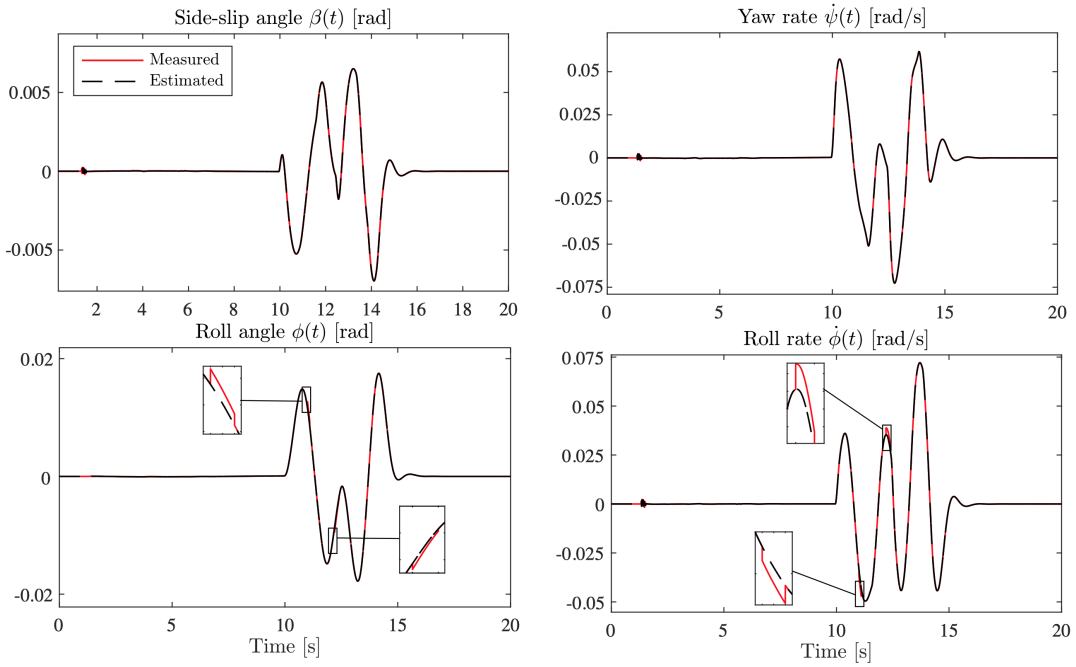

FIGURE V.7: Estimated and measured vehicle response with FTC

It can be seen in Fig. V.7, that when the control law is based on three observers bank with the switching block, the vehicle system remains stable throughout the simulation without losing its performance despite the presence of faults on its sensors. This demonstrates the effectiveness of the fault-tolerant control strategy applied.

Figure V.8 shows the performance of our algorithm in eliminating disturbances. In these simulations, disturbances are of the following sinusoidal form $d(t) = \sin(2\pi t)$.

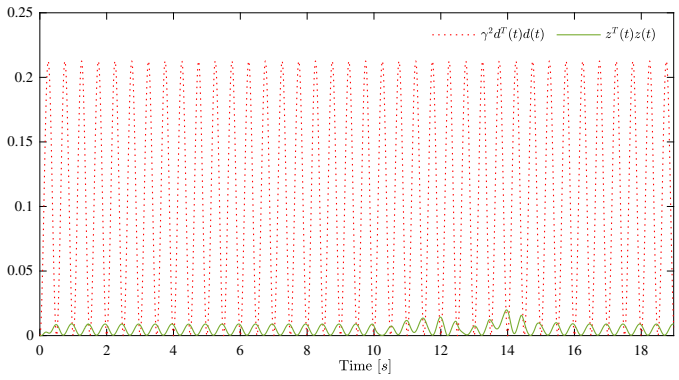

FIGURE V.8: Disturbance attenuation performance with H_∞ fault-tolerant control

From Fig. V.8, it can be seen that the attenuation disturbance performance is satisfactory and H_∞ requirement is reached, so the added disturbances have been successfully rejected.

Remark. V. 1 *The approach proposed in this section is an improvement over the one used in (Oudghiri et al., 2008; El Youssfi et al., 2017, 2018b; Abzi et al., 2020), because authors use a two-degree-of-freedom vehicle model and assume that two faults cannot appear at the same time. This assumption is outdated in this study. Moreover, this approach addresses the problem of fault-tolerant control for lateral acceleration and yaw rate sensors as well as roll rate sensor.*

In this section, a sensor fault-tolerant active control technique is proposed for automotive vehicle lateral dynamics system. As discussed in the first chapter, faults can also affect the actuators, so the following section is devoted to the actuator fault-tolerant active control.

V.4 Actuator fault-tolerant control for automotive vehicle lateral dynamics

This section presents fault-tolerant control methods for the automotive vehicle lateral dynamics system. These approaches focus on actuator faults, which requires knowledge of system parameters and occurring faults. For this reason, observers appropriate for simultaneous estimation of system states and actuator faults are required. This section breaks down into two sub-sections: the first presents a fault-tolerant control method based on the tracking error, and the second technique is based on the descriptor approach.

V.4.1 Observer and tracking based fault-tolerant control

In this sub-section and after designing a faulty T-S fuzzy model for the automotive vehicle lateral dynamics system. A fuzzy observer is shaped to estimate system states and actuator faults. Subsequently, a fault-tolerant control law is developed based on the information provided by this observer.

a. Faulty system description and observer design

Let us consider the following faulty system of automotive vehicle lateral dynamics:

$$\begin{cases} \dot{x}_f(t) = \sum\limits_{i=1}^{4} h_i(\alpha_f, \alpha_r)\Big[A_i x_f(t) + B_{fi}\big(u_{_{FTC}}(t) + f(t)\big)\Big] \\ y_f(t) = \sum\limits_{i=1}^{4} h_i(\alpha_f, \alpha_r) C_{yi} x_f(t) \end{cases} \tag{V.40}$$

where $x_f(t)$ and $y_f(t)$ are state and output vectors of the faulty system, respectively. $u_{_{FTC}}(t)$ is control law to be designed later, it is considered to be equivalent to a fault-tolerant control law added to the front wheel steering angle given by the driver. $f(t)$ is actuator fault.

Let us consider the following overall fuzzy observer, which shares the same membership functions as the T-S fuzzy system (V.40).

$$\begin{cases} \dot{\hat{x}}_f(t) = \sum_{i=1}^{4} h_i(\alpha_f, \alpha_r)\Big[A_i\hat{x}_f(t) + B_{fi}\big(u_{_{FTC}}(t) + \hat{f}(t)\big) + L_i\big(y_f(t) - \hat{y}_f(t)\big)\Big] \\ \hat{y}_f(t) = \sum_{i=1}^{4} h_i(\alpha_f, \alpha_r)C_{fi}\hat{x}_f(t) \\ \dot{\hat{f}}(t) = \sum_{i=1}^{4} h_i(\alpha_f, \alpha_r)G_i\left(y_f(t) - \hat{y}_f(t)\right) \end{cases} \tag{V.41}$$

where $\hat{x}_f(t)$, $\hat{y}_f(t)$ and $\hat{f}(t)$ are respectively the state vector, output vector and fault vector estimates. L_i and G_i are the observer gains to be determined.

The output error between faulty T-S fuzzy systems (V.40) and T-S fuzzy observer (V.41) is given as follows

$$e_y(t) = y_f(t) - \hat{y}_f(t) \tag{V.42}$$

$$= \sum_{i=1}^{4} h_i(\alpha_f, \alpha_r)C_{yi}(x_f(t) - \hat{x}_f(t)) \tag{V.43}$$

$$= \sum_{i=1}^{4} h_i(\alpha_f, \alpha_r)C_{yi}e_x(t) \tag{V.44}$$

where $e_x(t) = x_f(t) - \hat{x}_f(t)$ is the state estimation error. Its dynamics can be written as follows

$$\dot{e}_x(t) = \sum_{i=1}^{4}\sum_{j=1}^{4} h_i(\alpha_f, \alpha_r)h_j(\alpha_f, \alpha_r)\Big[(A_i - L_iC_{yj})e_x(t) + B_{fi}e_f(t)\Big] \tag{V.45}$$

where $e_f(t) = f(t) - \hat{f}(t)$ is the fault estimation error.

Let us consider the tracking error $e_t(t)$ defined as follows:

$$e_t(t) = x(t) - x_f(t) \tag{V.46}$$

where $x(t)$ is the state vector of the faultless system.

The time derivative of the tracking error (V.46) can be written as follows:

$$\dot{e}_t(t) = \sum_{i=1}^{4} h_i(\alpha_f, \alpha_r)\Big[A_ie_t(t) + B_{fi}(u(t) - u_{_{FTC}}(t)) - B_{fi}f(t)\Big] \tag{V.47}$$

b. Observer-based fault-tolerant control design

A fault-tolerant control is suggested to disregard the fault influence and maintain the stability of the faulty automotive vehicle lateral dynamic system. The proposed control procedure is outlined in Fig. V.9, (Ichalal et al., 2010).

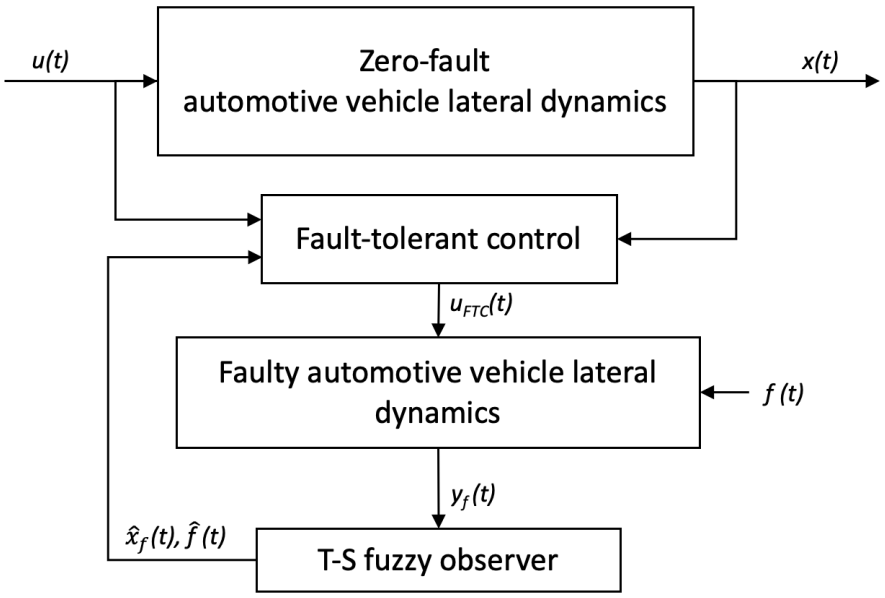

FIGURE V.9: Observer-based fault-tolerant control scheme

Let us consider the following control law

$$u_{FTC}(t) = -\sum_{i=1}^{4} h_i(\alpha_f, \alpha_r) F_i \left(x(t) - \hat{x}_f(t)\right) + u(t) - \hat{f}(t) \tag{V.48}$$

where F_i are the control gains.

By replacing the equation (V.48) in (V.47), we get the following:

$$\dot{e}_t(t) = \sum_{i=1}^{4}\sum_{j=1}^{4} h_i(\alpha_f, \alpha_r) h_j(\alpha_f, \alpha_r) \Big[(A_i + B_{fi}F_j)e_t(t) + B_{fi}F_j e_x(t) - B_{fi}e_f(t)\Big] \tag{V.49}$$

Assuming that $\dot{f}(t) = 0$, the dynamics of the fault estimation error $e_f(t)$ is as follows

$$\dot{e}_f(t) = -\sum_{i=1}^{4}\sum_{j=1}^{4} h_i(\alpha_f, \alpha_r) h_j(\alpha_f, \alpha_r) G_i C_{yj} e_x(t) \tag{V.50}$$

Let us consider the following augmented system:

$$\dot{\bar{e}}(t) = \sum_{i=1}^{4}\sum_{j=1}^{4} h_i(\alpha_f, \alpha_r) h_j(\alpha_f, \alpha_r) \bar{A}_{ij} \bar{e}(t) \tag{V.51}$$

with $\bar{e} = \begin{bmatrix} e_t(t) \\ e_x(t) \\ e_f(t) \end{bmatrix}$, and $\bar{A}_{ij} = \begin{bmatrix} A_i + B_{fi}F_j & B_{fi}F_j & -B_{fi} \\ 0 & A_i - L_i C_{yj} & B_{fi} \\ 0 & -G_i C_{yj} & 0 \end{bmatrix}$

The observer-based fault-tolerant control (V.48) stabilizes the faulty system (V.40) and the observer (V.41) estimates state and fault of the T-S fuzzy system (V.40), if the conditions of the following theorem are fulfilled.

Theorem. V. 4 *(El Youssfi and El Bachtiri, 2020) The state $\bar{e}(t)$ of the augmented system* (V.51) *converges asymptotically to zero if there exist positive scalar ρ, symmetrical matrices $P > 0$, $Q_2 > 0$, $Y > 0$, and Υ_{ii}, as well as other matrices with appropriate dimensions U_i, V_i, and Υ_{ij}. such that the following conditions are satisfied for $i = 1, 2, 3, 4$, and $i < j$.*

$$\Delta_{ii} < \Upsilon_{ii} \tag{V.52}$$

$$\Delta_{ij} + \Delta_{ji} \leq \Upsilon_{ij} + \Upsilon_{ij}^T \tag{V.53}$$

$$\begin{bmatrix} \Upsilon_{11} & \Upsilon_{12} & \Upsilon_{13} & \Upsilon_{14} \\ * & \Upsilon_{22} & \Upsilon_{23} & \Upsilon_{24} \\ * & * & \Upsilon_{33} & \Upsilon_{34} \\ * & * & * & \Upsilon_{44} \end{bmatrix} < 0 \tag{V.54}$$

where

$$\Delta_{ij} = \begin{bmatrix} A_i P + P A_i^T + B_{fi} V_j + V_j^T B_{fi}^T & B_{fi} \bar{X}_j & 0 \\ * & -2\rho Y & \rho I \\ * & * & Q_2 \bar{A}_i + \bar{A}_i^T Q_2 - U_i \bar{C}_{yj} - \bar{C}_{yj}^T U_i^T \end{bmatrix} \tag{V.55}$$

with $\bar{X}_j = \begin{bmatrix} V_j & -Z \end{bmatrix}$, *and* $Y = \begin{bmatrix} P & 0 \\ 0 & Z \end{bmatrix}$

Observer and control gains are calculated from the following:

$$F_i = V_i P^{-1}, \quad \bar{E}_i = \begin{bmatrix} L_i \\ G_i \end{bmatrix} = Q_2^{-1} U_i \tag{V.56}$$

Proof. V. 4 *The gains L_i, G_i and F_i are calculated by analysing the system stability outlined in differential equation* (V.51) *by using the Lyapunov method with a quadratic function.*

Let us select the following quadratic Lyapunov function

$$V(\bar{e}(t)) = \bar{e}^T(t) Q \bar{e}(t) \tag{V.57}$$

where Q is a positive definite matrix divided as follows

$$Q = \begin{bmatrix} Q_1 & 0 \\ 0 & Q_2 \end{bmatrix}$$

The time derivative of $V(t) = V(\bar{e}(t))$ can be expressed as follows

$$\dot{V}(t) = \bar{e}^T(t) Q \dot{\bar{e}}(t) + \dot{\bar{e}}^T(t) Q \bar{e}(t) \tag{V.58}$$

$$= \sum_{i=1}^{4} \sum_{j=1}^{4} h_i(\alpha_f, \alpha_r) h_j(\alpha_f, \alpha_r) \bar{e}^T(t) \Big(Q \bar{A}_{ij} + \bar{A}_{ij}^T Q \Big) \bar{e}(t) \tag{V.59}$$

The predefined matrix $\bar{A}_{ij}$ *can be rewritten as follows:*

$$\bar{A}_{ij} = \begin{bmatrix} A_i + B_{fi}F_j & B_{fi}\bar{F}_j \\ 0 & \bar{A}_i - \bar{E}_i\bar{C}_{yj} \end{bmatrix} \tag{V.60}$$

where

$$\bar{F}_j = \begin{bmatrix} F_j & -I \end{bmatrix}, \ \bar{A}_i = \begin{bmatrix} A_i & B_{fi} \\ 0 & 0 \end{bmatrix}, \ \bar{C}_{yi} = \begin{bmatrix} C_{yi} & 0 \end{bmatrix}, \ \textit{and} \ \bar{E}_i = \begin{bmatrix} L_i \\ G_i \end{bmatrix}$$

The formula (V.59) *is negative if the following conditions are satisfied*

$$\dot{V}(t) = \sum_{i=1}^{4}\sum_{j=1}^{4} h_i(\alpha_f, \alpha_r)h_j(\alpha_f, \alpha_r)\Lambda_{ij} < 0 \tag{V.61}$$

with

$$\Lambda_{ij} = \begin{bmatrix} Q_1A_i + A_i^TQ_1 + Q_1B_{fi}F_j + F_j^TB_{fi}^TQ_1 & Q_1B_{fi}\bar{F}_j \\ B_{fi}\bar{F}_j^TQ_1 & Q_2\bar{A}_i + \bar{A}_i^TQ_2 - Q_2\bar{E}_i\bar{C}_{yj} - \bar{C}_{yj}^T\bar{E}_i^TQ_2 \end{bmatrix} \tag{V.62}$$

using the lemma of congruence, we have

$$\Lambda_{ij} < 0 \Longleftrightarrow X\Lambda_{ij}X^T < 0 \tag{V.63}$$

with: $X = \begin{bmatrix} Q_1^{-1} & 0 \\ 0 & Y \end{bmatrix}$, $Y = \begin{bmatrix} Q_1^{-1} & 0 \\ 0 & Z \end{bmatrix}$, *and* $Z = Z^T > 0$

Then, the inequality (V.61) *can be rewritten as follows:*

$$\begin{bmatrix} A_iQ_1^{-1} + Q_1^{-1}A_i^T + B_{fi}F_jQ_1^{-1} + Q_1^{-1}F_j^TB_{fi}^T & B_{fi}\bar{F}_jY \\ YB_{fi}\bar{F}_j^T & YS_{ij}Y \end{bmatrix} < 0 \tag{V.64}$$

The negativity of (V.64) *enforces that*

$$S_{ij} < 0$$

where $S_{ij} = Q_2\bar{A}_i + \bar{A}_i^TQ_2 - Q_2\bar{E}_i\bar{C}_j - \bar{C}_j^T\bar{E}_i^TQ_2$

which can be analysed using the following property

$$(Y + \rho S_{ij}^{-1})^T S_{ij}(Y + \rho S_{ij}^{-1}) \leq 0 \Longleftrightarrow YS_{ij}Y \leq -\rho(Y + Y^T) - \rho^2 S_{ij}^{-1} \tag{V.65}$$

Accordingly, (V.64) *can then be delineated as follows*

$$\begin{bmatrix} A_iQ_1^{-1} + Q_1^{-1}A_i^T + B_iF_jQ_1^{-1} + Q_1^{-1}F_j^TB_i^T & B_i\bar{F}_jY & 0 \\ * & -2\rho Y & \rho I \\ * & * & Q_2\bar{A}_i + \bar{A}_i^TQ_2 - Q_2\bar{E}_i\bar{C}_j - \bar{C}_j^T\bar{E}_i^TQ_2 \end{bmatrix} < 0 \tag{V.66}$$

Using Lemma 9, and with some manipulations, we can obtain easily (V.52)-(V.54). *This completes the proof.*

Remark. V. 2 *Notice that in this study, the resolution of the LMIs of Theorem V.4 and the computation of the observer and the controller gains are performed in one step.*

c. Numerical illustration and simulation results

A numerical test is done by considering the fault-tolerant control law (V.48) to show the effectiveness of the proposed approach in neglecting actuator fault effects on the performance of our system. The simulations are performed with the front steering angle profile given in Fig. V.1, which is in the form of a sequence of right and left turns between instants $10\,s$ and $15\,s$ representing a severe driving situation.

The resolution of the LMIs of Theorem V.4, using the LMI toolbox (Gahinet et al., 1994; Erkus and Lee, 2004), and selecting $\rho = 0,612$, gives the following gains:

$$F_1 = \begin{bmatrix} 8,5603 & -0,5456 & -2,8434 & -0,2578 \end{bmatrix}, F_2 = \begin{bmatrix} 16,8392 & -1,2540 & -6,8566 & -0,6293 \end{bmatrix}$$
$$F_3 = \begin{bmatrix} 30,8589 & -2,2266 & -11,9023 & -1,0710 \end{bmatrix}, F_4 = \begin{bmatrix} 8,7415 & -0,4866 & -2,9362 & -0,2454 \end{bmatrix}$$

$$L_1 = \begin{bmatrix} 0,0429 & 56,0255 & -6,0486 \\ 0,0013 & 1,1625 & -68,3723 \\ 0,0946 & -9,4038 & 4,6495 \\ 1,0117 & 6,4926 & -8,6963 \end{bmatrix}, \quad L_2 = \begin{bmatrix} 0,0403 & -56,1168 & 18,0389 \\ 0,0007 & -18,2472 & -64,1047 \\ 0,0919 & 5,8916 & 50,8970 \\ 1,0117 & 51,4663 & -8,3851 \end{bmatrix}$$

$$L_3 = \begin{bmatrix} 0,0419 & 111,4690 & -39,0730 \\ 0,0012 & 19,3850 & -61,2003 \\ 0,0981 & -14,9635 & -46,2076 \\ 1,0117 & -44,8045 & -8,1695 \end{bmatrix}, \quad L_4 = \begin{bmatrix} 0,0375 & -0,6634 & -14,9859 \\ 0,0003 & -0,0201 & -56,9327 \\ 0,0954 & 0,4388 & 0,0871 \\ 1,0116 & 0,1221 & -7,8583 \end{bmatrix}$$

$$G_1 = \begin{bmatrix} -0,0284 & 84,2490 & 96,1124 \end{bmatrix}, \quad G_2 = \begin{bmatrix} -0,0294 & 34,1801 & 105,3823 \end{bmatrix}$$
$$G_3 = \begin{bmatrix} -0,0287 & 50,7472 & -8,3714 \end{bmatrix}, \quad G_4 = \begin{bmatrix} -0,0305 & 0,6835 & 0,8977 \end{bmatrix}$$

The simulations in this study are done with the proposed approach to show its effectiveness. The actuator is assumed to be under the fault impact shown in Fig. V.10. The

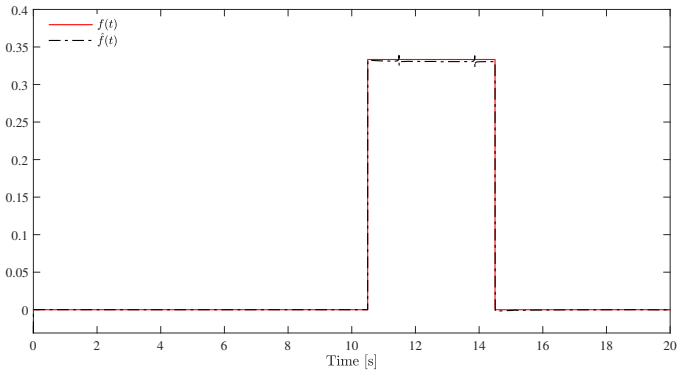

FIGURE V.10: Actuator fault and its estimated

time evolution of the actuator fault $f(t)$ and its estimation $\hat{f}(t)$ is shown in Fig. V.10. It can be noticed that the estimated fault follows nearly the added fault, which shows the good efficiency of the proposed observer to estimate the fault.

The response of the system states simultaneously with its estimates in the presence of actuator fault and with the application of the mentioned approach is shown in Fig. V.11.

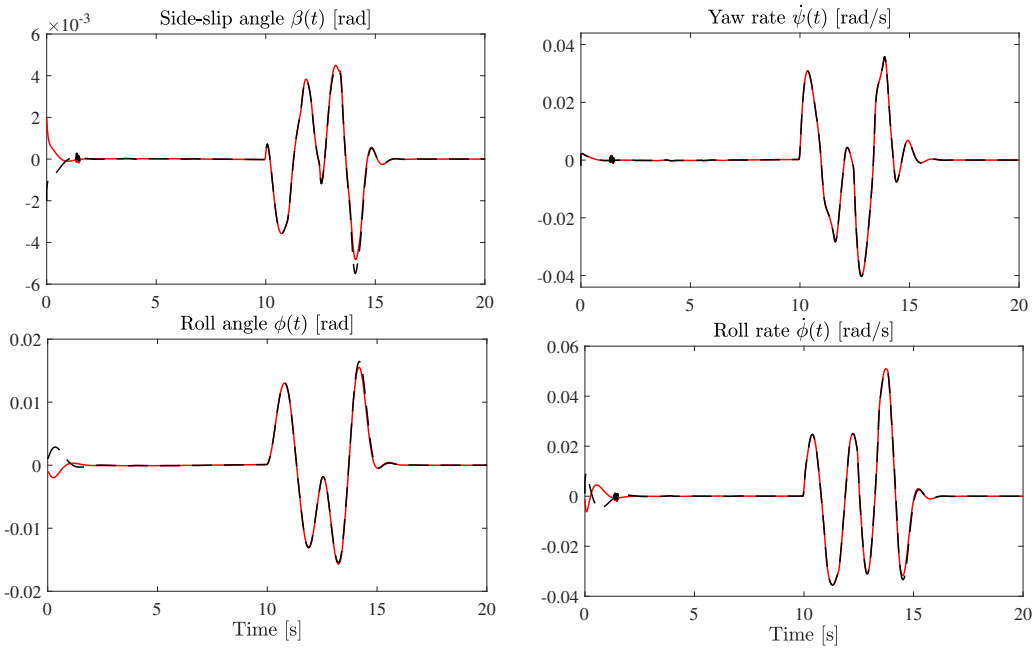

FIGURE V.11: Estimated and measured vehicle response with FTC

In Fig. V.11, simulations of the faulty system state in the presence of the proposed fault-tolerant control show significantly that the vehicle remains stable throughout the simulation without losing its performance despite the presence of actuator faults, demonstrating the success of the proposed method.

d. Discussion

In this subsection, a fault-tolerant control scheme is proposed to reform states of the automotive vehicle lateral dynamics system when it becomes faulty at the actuator part. The mentioned strategy is based on using a reference model and the information provided by the T-S fuzzy observer. This control law is developed to reduce the deviation of the faulty system from the reference; it uses steering angle, estimation error and tracking error. The stability of the whole system is studied in one step with Lyapunov theory and by solving LMI constraints. The automotive vehicle simulations demonstrate that the designed fault-tolerant control is very efficient and can be adapted to specific driving situations.

V.4.2 Observer-based fault-tolerant control using descriptor approach

By considering descriptor system and observer given in Section IV.2 of Chapter IV, this sub-section addresses the problem of actuator fault-tolerant control design of the perturbed automotive vehicle lateral dynamics system (IV.1) using descriptor approach.

Remark. V. 3 *In Chapter IV, the aim is to design control-free observers for the lateral dynamics system of the automotive vehicle. It requires that the system be stable at the beginning, so a stable two-degree-of-freedom model is considered. However, an additional degree of freedom corresponding to roll motion will be considered in the present to expand the application range of the proposed controls.*

a. H_∞ Fault-tolerant control design

The objective is to develop a control based on the fault and state information reconstructed by the observer (IV.4) for the augmented system (IV.2).

Let us consider the following control scheme

$$u_{FTC}(t) = -\sum_{i=1}^{4} h_i(\alpha_f, \alpha_r) K_i \hat{x}(t) - \hat{f}(t) \tag{V.67}$$

where K_i represents the controller gain matrices to be determined.

As a result, the closed loop of T-S descriptor system (IV.2) becomes as follows

$$E\dot{x}(t) = \sum_{i=1}^{4}\sum_{j=1}^{4} h_i(\alpha_f, \alpha_r) h_j(\alpha_f, \alpha_r) \Big[A_i x(t) - B_i K_j \hat{x}(t) - B_i \hat{f}(t) + B_i f(t) + D_i d(t) \Big] \tag{V.68}$$

After some simple handling, (V.68) becomes as follows:

$$E\dot{x}(t) = \sum_{i=1}^{4}\sum_{j=1}^{4} h_i(\alpha_f, \alpha_r) h_j(\alpha_f, \alpha_r) \Big[(A_i - B_i K_j) x(t) + B_i K_j e_x(t) + B_i e_f(t) + D_i d(t) \Big] \tag{V.69}$$

Let us consider the following definition.

Definition. V. 1 *(Lin et al., 2005) Considering real positive scalar $\gamma_3 > 0$, and defined positive matrix Q. The H_∞ norm of the fuzzy system* (IV.2) *is defined as follows*

$$\int_0^\infty z^T(s) Q z(s) ds \leq \gamma_3^2 \int_0^\infty d^T(s) Q d(s) ds \tag{V.70}$$

The observer-based fault-tolerant control (V.67) and observer (IV.4) stabilize and observe the state of the T-S descriptor system (IV.2), if the following theorem is satisfied.

Theorem. V. 5 *(El Youssfi et al., 2021c) For positive scalar parameters $\gamma_p > 0$, $(\forall p = 1, 2, 3)$, the control law* (V.67) *and the observer* (IV.4) *stabilize and observe the T-S descriptor system states* (IV.2)*, if there exist symmetric matrices $R > 0$, $P > 0$, $Q > 0$, and other matrices U, X, Z_i, Y_i $(\forall i = 1, \ldots, r)$, as well as known scalar parameters λ_q, $(\forall q = 1, 2, 3)$,*

such that the following LMIs hold for all $i, j = 1,2,3,4$ and $i < j$.

$$\begin{bmatrix} \bar{\Upsilon}_{ii} - \Theta_{ii} & \lambda_1\Gamma_i + \bar{Z}_i^T \\ & -\lambda_1 U - \lambda_1 U^T \end{bmatrix} < 0 \tag{V.71}$$

$$\begin{bmatrix} \bar{\Upsilon}_{ij} + \bar{\Upsilon}_{ji} - \Theta_{ij} - \Theta_{ij}^T & \lambda_2\Gamma_i + \bar{Z}_j^T & \lambda_3\Gamma_j + \bar{Z}_i^T \\ & -\lambda_2 U - \lambda_2 U^T & 0 \\ * & * & -\lambda_3 U - \lambda_3 U^T \end{bmatrix} \leq 0 \tag{V.72}$$

$$\begin{bmatrix} \Theta_{11} & \Theta_{12} & \Theta_{13} & \Theta_{14} \\ * & \Theta_{22} & \Theta_{23} & \Theta_{24} \\ * & * & \Theta_{33} & \Theta_{34} \\ * & * & \dots & \Theta_{44} \end{bmatrix} < 0 \tag{V.73}$$

where

$$\bar{\Upsilon}_{ij} = \begin{bmatrix} \Omega_i & 0 & RD_i & 0 \\ * & \Xi_i & P\mathcal{D}_{1i} + X\mathcal{D}_{2i} & P\mathcal{F}_1 + X\mathcal{F}_2 \\ * & * & -\gamma_1 I - \gamma_3^2 Q & \\ * & * & * & -\gamma_2 I \end{bmatrix}, \; \Gamma_i = \begin{bmatrix} -RB_i \\ 0 \\ 0 \\ 0 \end{bmatrix}, \; \bar{Z}_i^T = \begin{bmatrix} Z_i \\ \begin{bmatrix} Z_i^T & U \end{bmatrix}^T \\ 0 \\ 0 \end{bmatrix}$$

with

$$\begin{aligned} \Omega_i &= RA_i + A_i^T R + C_{zi}^T Q C_{zi} \\ \Xi_i &= P\mathcal{A}_{1i} + \mathcal{A}_{1i}^T P + X\mathcal{A}_{2i} + \mathcal{A}_{2i}^T X^T - \Upsilon_i\bar{C} - \bar{C}^T\Upsilon_i^T + C_f^T C_f \end{aligned}$$

The controller and observer gain matrices can be determined through the following:

$$K_i = U^{-1}Z_i \tag{V.74}$$

$$L_i = P^{-1}\Upsilon_i \tag{V.75}$$

Proof. V. 5 *Let be the Lyapunov function candidate in the following format*

$$\bar{V}(t) = V(t) + V_e(t) \tag{V.76}$$

where $V_e(t) = V(\bar{e}_x(t))$ given by the equation (IV.18) *and $V(t)$ is given as follows:*

$$V(t) = (Ex(t))^T Rx(t), \qquad R > 0 \tag{V.77}$$

The time derivative of $V(t)$ is calculated as

$$\dot{V}(t) = x^T(t)RE\dot{x}(t) + (E\dot{x}(t))^T Rx(t) \tag{V.78}$$

By replacing (IV.2) *in* (V.78)*, the following expression is obtained*

$$\dot{V}(t) = 2x^T(t)R\Big[(A_i - B_iK_j)x(t) + B_iK_je_x(t) + B_ie_f(t) + D_id(t)\Big] \tag{V.79}$$

Thus, by defining the following criterion function

$$J_2 = J_1 + \int_0^t \{z(\tau)^T Q z(\tau) - \gamma_3^2 d^T(\tau) Q d(\tau)\} d\tau \tag{V.80}$$

Under zero initial condition, we have

$$J_2 \leq J_1 + \int_0^t \{z(\tau)^T Q z(\tau) - \gamma_3^2 d^T(\tau) Q d(\tau)\} d\tau + \bar{V}(t) - \bar{V}(0) \tag{V.81}$$

$$\leq J_1 + \int_0^t \{z(\tau)^T Q z(\tau) - \gamma_3^2 d^T(\tau) Q d(\tau) + \dot{\bar{V}}(\tau)\} d\tau \tag{V.82}$$

$$\leq \int_0^t \{\Omega^T(\tau) \Pi \Omega(\tau) + \dot{V}(\tau) + z(\tau)^T Q z(\tau) - \gamma_3^2 d^T(\tau) Q d(\tau)\} d\tau \tag{V.83}$$

By substituting (V.79) *in* (V.81)*, it gives*

$$J_2 \leq \int_0^t \{\Phi^T(\tau) \Upsilon \Phi(\tau)\} d\tau \tag{V.84}$$

where

$$\Upsilon = \begin{bmatrix} \Omega & R\bar{B}\tilde{K} & R\bar{D} & 0 \\ * & \Xi & P\bar{\mathcal{D}}_1 + X\bar{\mathcal{D}}_2 & P\mathcal{F}_1 + X\mathcal{F}_2 \\ * & * & -\gamma_1 I - \gamma_3^2 Q & 0 \\ * & * & * & -\gamma_2 I \end{bmatrix}, \quad \Phi(t) = \begin{bmatrix} x(t) \\ \bar{e}_x(t) \\ d(t) \\ \dot{f}(t) \end{bmatrix} \tag{V.85}$$

with $\Omega = \sum_{i=1}^{4} \mu_i \Omega_i, \quad \Xi = \sum_{i=1}^{4} \mu_i \Xi_i, \quad \bar{K} = \sum_{i=1}^{4} \mu_i K_i, \quad \tilde{K} = \begin{bmatrix} \bar{K} & I \end{bmatrix}$

Using Lemma B.4, the following expression can be given.

$$\Upsilon = \sum_{i=1}^{4} h_i^2(\alpha_f, \alpha_r) \Upsilon_{ii} + \sum_{i=1}^{4} \sum_{i<j}^{4} h_i(\alpha_f, \alpha_r) h_j(\alpha_f, \alpha_r) (\Upsilon_{ij} + \Upsilon_{ji}) \tag{V.86}$$

Then, the control law (V.67) *and the observer* (IV.4) *stabilise and observe, respectively, the states of the system* (IV.2)*, if the following conditions are fulfilled.*

$$\begin{aligned} &\Upsilon_{ii} < 0 && i = 1, 2, 3, 4 \\ &\Upsilon_{ij} + \Upsilon_{ji} < 0 && 1 \leq i < j \leq 4 \end{aligned} \tag{V.87}$$

According to Lemma B.4, there exist matrices $\Theta_{ii} = \Theta_{ii}^T$ *and* Θ_{ij}*, such that the following conditions are satisfied.*

$$\begin{aligned} &\Upsilon_{ii} < \Theta_{ii} && i, j = 1, 2, 3, 4 \\ &\Upsilon_{ij} + \Upsilon_{ji} \leq \Theta_{ij} + \Theta_{ij}^T && 1 \leq i < j \leq 4 \end{aligned} \tag{V.88}$$

Furthermore, Υ_{ij} *matrices can be re-written as follows:*

$$\Upsilon_{ij} = \bar{\Upsilon}_{ij} + sym\left\{\Gamma_i \underbrace{\begin{bmatrix} K_j & \begin{bmatrix} K_j & I \end{bmatrix} & 0 & 0 \end{bmatrix}}_{\Lambda_j}\right\} \tag{V.89}$$

By substituting (V.89) *in* (V.88)*, the following inequalities are obtained.*

$$\begin{aligned} &\bar{\Upsilon}_{ii} - \Theta_{ii} + sym\left\{\Gamma_i \Lambda_i\right\} < 0 && i = 1,2,3,4 \\ &\bar{\Upsilon}_{ij} + \bar{\Upsilon}_{ji} - \Theta_{ij} - \Theta_{ij}^T + sym\left\{\Gamma_i \Lambda_j + \Gamma_j \Lambda_i\right\} \leq 0 && 1 \leq i < j \leq 4 \end{aligned} \tag{V.90}$$

Using Lemma B.9 and replacing UK_i *by* Z_i*, the LMIs* (V.71)-(V.73) *of Theorem V.5 are achieved. This completes the proof.*

Remark. V. 4 *The LMIs* (V.71)-(V.72) *are given with the parameters* λ_q*,* $(q = 1,2,3)$ *known a priory. In the literature, these parameters are obtained using a numerical optimisation algorithm, such as the "fminsearch" function in the MATLAB optimisation toolbox. In this study, the variables* λ_q*,* $(q = 1,2,3)$ *are chosen arbitrarily in order to obtain feasibility and increase system performance, where the effect of optimising these parameters leads to a more efficient result.*

b. Numerical illustration and simulation results

In order to demonstrate the effectiveness of the proposed fault-tolerant control law, some simulations have been performed using MATLAB software. The same vehicle system used throughout this chapter is employed here.

Using MATLAB LMI toolbox and choosing the following parameter values $\gamma_1 = 0,3$, $\gamma_2 = 5$, and $\gamma_3 = 0,05$, the optimization problem of Theorem V.5 can be conveniently resolved. The following controller and observer gains are obtained.

$$K_1 = \begin{bmatrix} 0,4920 & 0,3553 & 0,0638 & 0,0480 \end{bmatrix}, \quad K_2 = \begin{bmatrix} 0,4670 & 0,3499 & 0,0492 & 0,0489 \end{bmatrix}$$
$$K_3 = \begin{bmatrix} 0,2160 & 0,1412 & 0,0016 & 0,0155 \end{bmatrix}, \quad K_4 = \begin{bmatrix} 0,1033 & 0,0720 & 0,0237 & 0,0043 \end{bmatrix}$$

$$L_1 = \begin{bmatrix} 0,2579 & 0,0167 \\ -0,5838 & -0,0072 \\ -0,1494 & 0,4071 \\ 36,9352 & 18,8010 \\ -0,8739 & 4,6831 \end{bmatrix}, \quad L_2 = \begin{bmatrix} 0,8765 & 0,1099 \\ 0,0920 & -0,0570 \\ -0,0783 & 0,4202 \\ -0,0011 & 21,6544 \\ 28,8426 & 2,3968 \end{bmatrix}$$

$$L_3 = \begin{bmatrix} 0,4807 & -0,0101 \\ -0,5811 & 0,0023 \\ -0,1759 & 1,0642 \\ 37,2438 & 18,7868 \\ -29,6901 & 3,5937 \end{bmatrix}, \quad L_4 = \begin{bmatrix} 1,0687 & 0,0830 \\ 0,0932 & -0,0479 \\ -0,1050 & 1,0481 \\ 0,3582 & 21,6384 \\ 0,0410 & 1,3056 \end{bmatrix}$$

To illustrate the ability of the proposed control to eliminate the fault effects on the system performances, two fault scenarios are studied. The first fault $f_1(t)$ is chosen as an intermittent that occurs during an extreme change of direction between the instants

10.5 s and 14.5 s. While the second fault $f_2(t)$ is chosen as a strong sinusoidal variation from instant 4 s. The evolution of these two faults $f_1(t)$ and $f_2(t)$ as well as their estimates are shown in Fig. V.12 and Fig. V.14, respectively. The response of the system states with the application of the control law (V.67) and their estimates under the influence of the two actuator faults $f_1(t)$ and $f_2(t)$, respectively, are shown in Fig. V.13 and Fig. V.15.

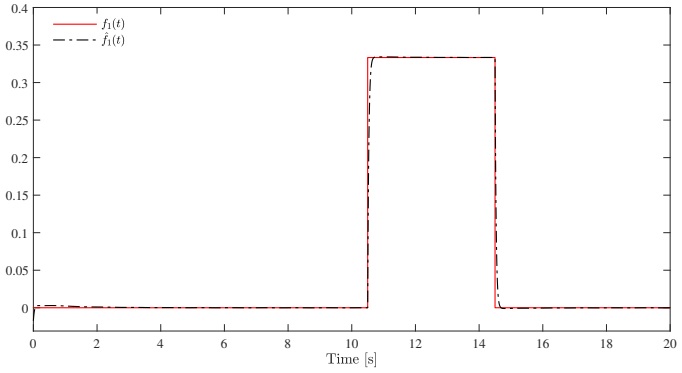

FIGURE V.12: Fault $f_1(t)$ and its estimated

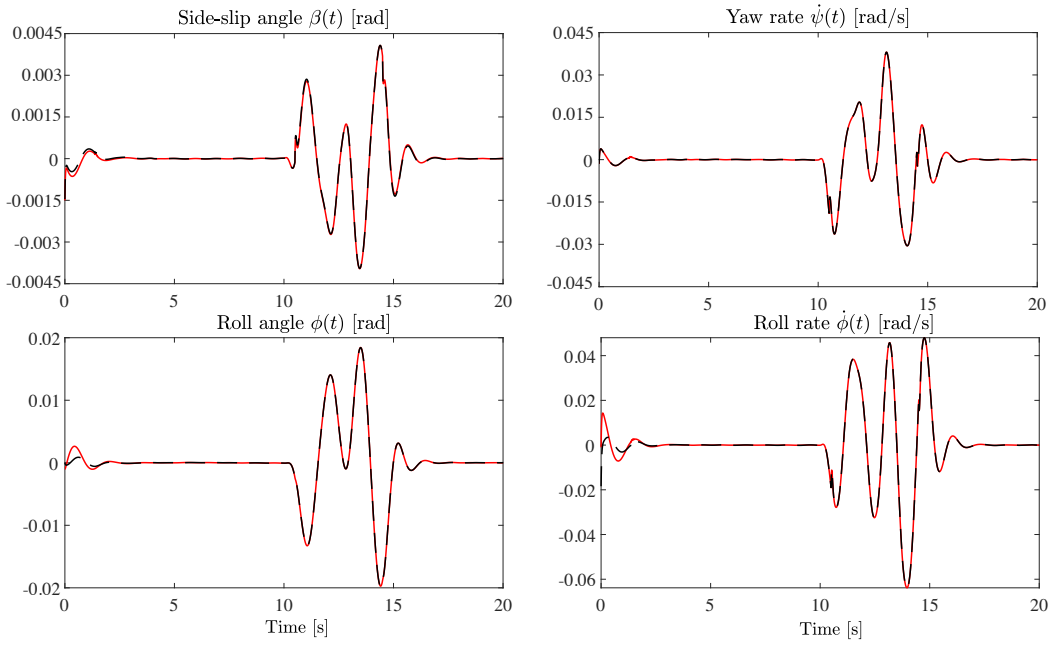

FIGURE V.13: System state responses when a fault $f_1(t)$ occurs using the proposed control

It is clear from all figures V.12-V.15 that the estimation converges closely with the measurement for actuator faults and system states. This shows the ability of the suggested observer to accurately estimate the system parameters and even the faults, despite the presence of external disturbances.

It can be seen from Fig. V.13 and Fig. V.15, respectively, that after the system becomes faulty by $f_1(t)$ or $f_2(t)$ and with the implementation of the proposed control

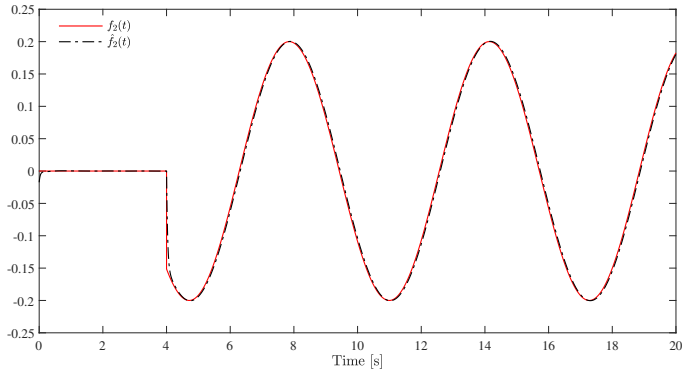

FIGURE V.14: Fault $f_2(t)$ and its estimated

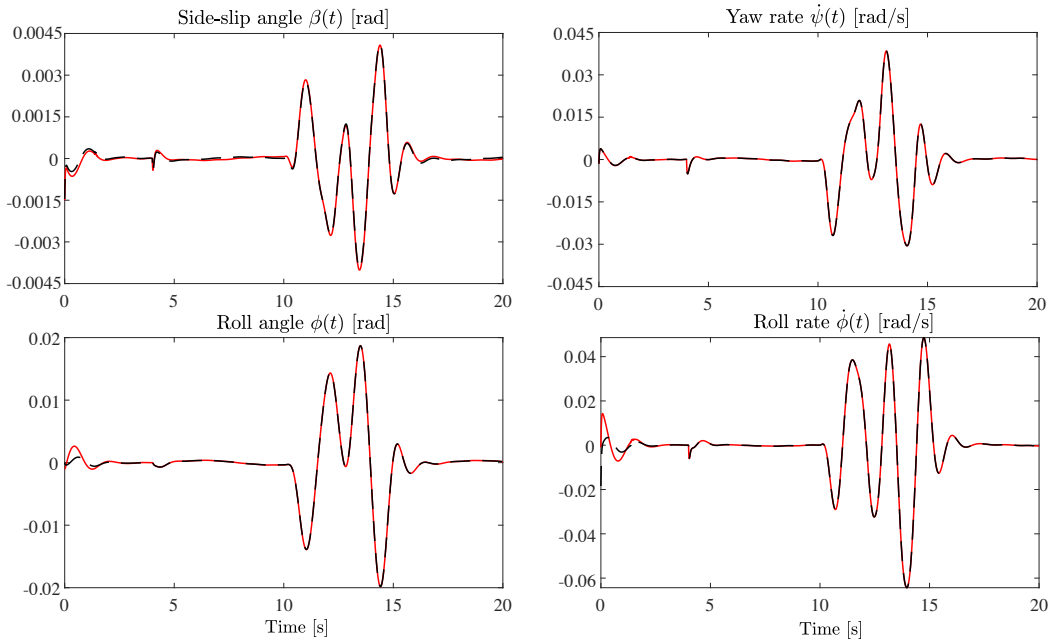

FIGURE V.15: System state responses when a fault $f_2(t)$ occurs using the proposed control

law, the automotive vehicle lateral dynamics system stays stable throughout the simulation without losing its performance despite the presence of actuator faults. This demonstrates the validity of the suggested control law.

c. Discussion

In this sub-section, the fault-tolerant control problem for the automotive vehicle lateral dynamics system using the descriptor approach is addressed. First of all, the augmented system (IV.2) and the observer (IV.4) from Chapter IV have been used here to simultaneously estimate the system states and the actuator faults. Based on the information provided by the observer, a robust control against actuator faults is designed in order to overcome the performance deterioration caused by these faults. The proposed approach is reformulated as linear matrix inequalities (LMIs) problem.

Simulation results highlight the effectiveness of the proposed approach in estimating faults and states as well as constructing a fault-tolerant control law capable of maintaining the stability of the system despite the presence of faults and rapidly varying external disturbances.

V.5 Conclusion

In this chapter, different control laws have been proposed for the automotive vehicle lateral dynamics system, with consideration of roll motion, represented by the T-S fuzzy model. Firstly, a H_∞ control method based on static output-feedback is elaborated. This is a disturbance robust passive control that uses the information provided by the system output. Then, using the information provided by the observers, control strategies and laws are designed to overcome the performance deterioration caused by faults and make our system relatively insensitive to faults either at the sensor or actuator sides. In each section, the overall system's stability is studied using the quadratic Lyapunov function, and the appropriate conditions for the existence of these control laws are analysed. Their conceptions are expressed in the form of Linear Matrix Inequalities (LMIs). The simulation results highlight in each section the effectiveness and the ability of the proposed control laws to maintain the stability of the system in a critical driving situation and in the presence of faults and external disturbances.

General conclusion

This thesis issue was the application of theoretical results of state/fault estimation and Fault-Tolerant Control (FTC) to the non-linear system of automotive lateral dynamics. The latter has been represented using Takagi-Sugeno (T-S) fuzzy models. An overview of Fault Detection (FD) and FTC techniques has been proposed in the first chapter in order to provide the context for our contribution. First, we have recalled some terminologies and classifications of faults. Then, we have described some approaches to residue generation and fault isolation. After that, some important specific FTC methods were discussed and classified into active and passive ones.

A T-S fuzzy model is a well-adapted tool for the modelisation of non-linear systems, allowing them to be represented by a finite number of local linear sub-systems in different regions of operation. As we have seen in the second chapter, fundamental results of the T-S fuzzy model for continuous systems have been presented. Initially, a definition of this type of system and the process to obtain it were offered. After that, a set of definitions and theorems concerning the stability concept was pointed out. In addition, stability analysis of T-S fuzzy models using the Lyapunov method was documented. Furthermore, the design of observers for T-S fuzzy systems has been introduced. Finally, we have reported some results on the quadratic stabilisation of T-S fuzzy systems with different control laws, including state feedback, static output feedback and estimated state feedback.

The third chapter was dedicated to the modelling of the lateral dynamics of the automotive vehicle. In a first step, we have presented some components necessary to the modelling of the vehicle, as well as its main movements. Next, a four-wheel model was introduced, which, based on a set of assumptions, leads to a simplified extended bicycle model for describing the lateral motion. Then, we have introduced an additional degree of freedom associated with rolling to have a model of the lateral dynamics that considers the kinematics of the suspension. After that, two lateral force models have been presented. The first one is based on the magic formula of Pacejka, it is accurate and more realistic, but it requires the empirical determination of many factors and constants. The second one is simple linear but overestimates the forces. To cope with this situation, a T-S fuzzy representation of the tire model was included. This approximation allowed us to obtain T-S fuzzy models representing the lateral dynamics of the automotive vehicle with/without taking into account roll motion. These models can be used to design steering control systems for lateral trajectory maintenance. They can also be extended for use in yaw stability control, rollover control and other vehicle control applications.

In the fourth chapter, significant initial contributions of this thesis to state/fault estimation have been introduced. It includes two observer-based methods developed for the automotive vehicle lateral dynamics system. The first one uses the descriptor approach to simultaneously estimate the states and actuator faults that affect a perturbed vehicle system. The second is the unknown input observer that can simultaneously estimate the states and faults of an uncertain vehicle system affected by sensor and actuator faults. The simulation results obtained highlight the effectiveness of the proposed approaches for state/fault estimation.

In the fifth and last chapter, the main contributions of the thesis have been developed. We have proposed three different control laws for the automotive vehicle lateral dynamics system, with the consideration of roll motion, in order to compensate for the effects of faults and for driving assistance. In a first step, we have employed an H_∞ control based on static output-feedback, which is a disturbance-robust passive control that uses the information provided by the system output. Then, we have implemented an active FTC strategy to compensate for sensor faults. In this approach, a fault detection and identification block consisting of an observer bank and a decision block was used to select the appropriate control law to maintain the correct lateral behavior of the automotive vehicle. Lastly, we have developed active FTC laws for actuator faults that require a good knowledge of the vehicle parameters and the faults that occur. For this purpose, we have used appropriate observers for the simultaneous estimation of system states and actuator faults. Two methods have been studied in this context. The first one is based on the tracking error, and the second on the descriptor approach developed in the fourth chapter. The simulation results obtained by these different strategies have shown that it is possible to maintain the correct behaviour of an automotive vehicle despite the presence of disturbances, sensor or actuator faults.

The work carried out is a significant advance and can be a good starting point for any analysis and control of the automotive vehicle dynamic system. However, there are still many avenues to explore. In brief, here are some perspectives that would be interesting for future work:

- Develop a fault-tolerant control algorithm based on adaptive event triggering for autonomous vehicle lateral dynamics in non-secure communication networks and integration of tracking control and direct yaw moment control to achieve better lateral dynamic performance.

- Consider an uncertain vehicle dynamics model by accounting for the network-induced communication delay, which is a continuous time-varying function with a known upper bound.

- Concerning the vehicle model, it is very interesting to consider a complete model with more freedom degrees, including lateral dynamics, longitudinal dynamics, and even suspension dynamics.

It would also be very interesting to validate these different control algorithms on an industrial simulator using real measurements and subsequently on an automotive vehicle.

Appendix

System and LMI analysis lemmas

The objective of this appendix is to present some lemmas useful for the analysis of T-S systems and LMIs.

Lemma 1 *(Morere, 2001) Let $f(z(t)) : \mathbb{R} \rightarrow \mathbb{R}$ a function bounded on $[-z_2, z_1]$, with $(z_1, z_2) \in \mathbb{R}^{2+}$. Then, there exist two functions $N_1(z(t)) \geq 0$ and $N_2(z(t)) \geq 0$ such as:*

$$\begin{cases} f(z(t)) = \alpha N_1(z(t)) + \beta N_2(z(t)) \\ N_1(z(t)) + N_2(z(t)) = 1 \end{cases} \tag{91}$$

with α and β are two scalars.

Proof 1 *Assuming that the function $f(z(t))$ is bounded such that $\alpha \leq f(z(t)) \leq \beta$, it is therefore possible to write:*

$$f(z(t)) = \alpha N_1(z(t)) + \beta N_2(z(t)) \tag{92}$$

with:

$$\begin{aligned} \alpha &= \min_{z \in [-z_2, z_1]} (f(z(t))), & \beta &= \max_{z \in [-z_2, z_1]} (f(z(t))) \\ N_1(z(t)) &= \frac{f(z(t)) - \alpha}{\beta - \alpha}, & N_2(z(t)) &= \frac{\beta - f(z(t))}{\beta - \alpha} \end{aligned} \tag{93}$$

Lemma 2 *(Boyd et al., 1994) Determining if a matrix $P > 0$ verifying* (II.35) *does not exist is equivalent to finding not all null Q_i matrices such that:*

$$\begin{cases} Q_i \geq 0, \ \forall i = 1, \ldots, r \\ \sum_{i=1}^{m} \left(Q_i A_i^T + A_i Q_i \right) \geq 0 \end{cases} \tag{94}$$

Lemma 3 *(Tanaka and Sano, 1994) Let $\mathcal{X}_{ij}$ be matrices of the appropriate dimensions.*

$$\sum_{i=1}^{r} \sum_{j=1}^{r} h_i(z(t)) h_j(z(t)) \mathcal{X}_{ij} < 0 \tag{95}$$

is verified if the two following conditions are fulfilled

$$\mathcal{X}_{ii} < 0, \qquad i = 1,\ 2,\ ...,r \tag{96}$$

$$\mathcal{X}_{ij} + \mathcal{X}_{ji} \leq 0,\ \ i,j = 1,\ 2,\ ...,r; i < j \tag{97}$$

Lemma 4 *(Xiaodong and Qingling, 2003; Bede, 2013) Let the matrices $\mathcal{X}_{ij}$ and the condition be*

$$\begin{aligned}\sum_{i=1}^{r}\sum_{j=1}^{r} h_i(z(t))h_j(z(t))\mathcal{X}_{ij} = &\sum_{i=1}^{r} h_i^2(z(t))\mathcal{X}_{ii} \\ &+ \sum_{i=1}^{r}\sum_{i<j}^{r} h_i(z(t))h_j(z(t))\left(\mathcal{X}_{ij} + \mathcal{X}_{ji}\right) < 0\end{aligned} \tag{98}$$

Equation (98) *is true if there exists matrices $\mathcal{Y}_{ii}$ and $\mathcal{Y}_{ij}$ such that the following conditions are fulfilled:*

$$\mathcal{X}_{ii} < \mathcal{Y}_{ii}, \qquad i = 1,\ 2,\ ...,r \tag{99}$$

$$\mathcal{X}_{ij} + \mathcal{X}_{ji} \leq \mathcal{Y}_{ij} + \mathcal{Y}_{ij}^T,\ \ i,j = 1,\ 2,\ ...,r;\ \ i < j \tag{100}$$

$$\begin{bmatrix} \mathcal{Y}_{11} & \mathcal{Y}_{12} & \dots & \mathcal{Y}_{1r} \\ * & \mathcal{Y}_{22} & \dots & \mathcal{Y}_{2r} \\ \vdots & \vdots & \ddots & \vdots \\ * & * & \dots & \mathcal{Y}_{rr} \end{bmatrix} < 0 \tag{101}$$

Lemma 5 *(Bede, 2013) Let A, Υ, P, and Θ be matrices with proper sizes. The following two inequalities are equivalent:*

$$\Theta + A^T P + PA < 0 \tag{102}$$

$$\begin{bmatrix} A^T\Upsilon^T + \Upsilon A + \Theta & P - \Upsilon + A^T\Upsilon^T \\ * & -\Upsilon - \Upsilon^T \end{bmatrix} < 0 \tag{103}$$

Lemma 6 *(Bærentzen et al., 2012) Consider the matrix $\mathbb{W} \in \mathfrak{R}^{n\times m}$, with $n \geq m$, and matrix $\mathbb{Y} \in \mathfrak{R}^{n\times k}$, the matrix $\mathbb{X}$ with the form*

$$\mathbb{X} = \mathbb{Y}\mathbb{W}^+ + \mathbb{U}(I - \mathbb{W}\mathbb{W}^+)$$

is a solution of $\mathbb{X}\mathbb{W} = \mathbb{Y}$ when the condition $\mathbb{Y}\mathbb{W}^+\mathbb{W} = \mathbb{Y}$ holds. $\mathbb{U} \in \mathfrak{R}^{k\times m}$ is an arbitrary matrix and $\mathbb{W}^+$ is the Moore-Penrose pseudo-inverse of $\mathbb{W}$ which is denoted

$$\mathbb{W}^+ = (\mathbb{W}^T\mathbb{W})^{-1}\mathbb{W}^T$$

Lemma 7 *(Finsler's Lemma) (de Oliveira and Skelton, 2001) Let $\zeta \in \mathbb{R}^n$, $\mathbb{Z} \in \mathbb{R}^{n\times n}$ and $\Sigma \in \mathbb{R}^{m\times n}$ with $rank(\Sigma) < n$ and $(\Sigma)_\perp$ such that $\Sigma\Sigma_\perp = 0$. Then, the following conditions*

are equivalent:

$$\zeta^T \mathbb{Z} \zeta < 0, \forall \zeta \neq 0 : \Sigma \zeta = 0 \tag{104}$$

$$\Sigma_\perp^T \mathbb{Z} \Sigma_\perp < 0 \tag{105}$$

$$\exists \mu \in \mathbb{R} : \mathbb{Z} - \mu \Sigma^T \Sigma < 0 \tag{106}$$

$$\exists \mathbb{Q} \in \mathbb{R}^{n \times m} : \mathbb{Z} + \mathbb{Q}\Sigma + \Sigma^T \mathbb{Q}^T < 0 \tag{107}$$

Lemma 8 *(Wang et al., 2015) For the matrices $\mathcal{Q}$, $\mathcal{G}$ and $\mathcal{Z}$ with suitable dimensions.*

$$\mathcal{Q} = \mathcal{Z}\mathcal{G}^\dagger + \mathcal{S}\left[I - \mathcal{G}\mathcal{G}^\dagger\right] \tag{108}$$

is the general solution to the following equation

$$\mathcal{Q}\mathcal{G} = \mathcal{Z} \tag{109}$$

with $\mathcal{S}$ is an arbitrary matrix. In this paper, the sign $\dagger$ indicates the pseudo-inverse of a matrix.

Lemma 9 *(Chang et al., 2015) For appropriately dimensioned matrices* $\mathbf{S}$, $\mathbf{R}$, *and* $\mathbf{W}$, *and scalar λ. The inequality*

$$\mathbf{S} + \mathbf{R}\mathbf{A} + \mathbf{A}^T \mathbf{R}^T < 0 \tag{110}$$

is achieved if the following condition is satisfied

$$\begin{bmatrix} \mathbf{S} & \lambda \mathbf{R} + \mathbf{A}^T \mathbf{W}^T \\ * & -\lambda \mathbf{W} - \lambda \mathbf{W}^T \end{bmatrix} < 0 \tag{111}$$

Lemma 10 *(Gahinet and Apkarian, 1994) Given a symmetric matrix $\Sigma \in \mathbb{R}^{p \times p}$ and two matrices X, Z of column dimension p, there exists a matrix Y such that the LMI*

$$\Sigma + sym\{X^T Y Z\} < 0 \tag{112}$$

holds if and only if the following two projection inequalities with respect to Y are satisfied:

$$X^{\perp^T} \Sigma X^\perp < 0, \quad Z^{\perp^T} \Sigma Z^\perp < 0. \tag{113}$$

where $X^\perp$ and $Z^\perp$ are arbitrary matrices whose columns form a basis of the null spaces of X and Z, respectively.

Lemma 11 *(Jeung and Lee, 2014) For a positive definite matrix $R \in \mathbb{R}^{n \times n}$, matrices X and Y with appropriate dimensions, the following inequality holds:*

$$X^T Y + Y^T X \leq X^T R X + Y^T R^{-1} Y$$

Lemma 12 *(Jeung and Lee, 2014) For a positive definite matrix $R \in \mathbb{R}^{n\times n}$, a square matrix $X \in \mathbb{R}^{n\times n}$, and a scalar α, the following inequality holds:*

$$-X^T R^{-1} X \leq \alpha^2 R \pm \alpha X \pm \alpha X^T$$

Bibliography

Abdullah, M., Jamil, J., and E. Mohan, A. (2016). *Vehicle Dynamics Modeling & Simulation*. Centre for Advanced Research on Energy (CARe), Faculty of Mechanical Engineering, Universiti Teknikal Malaysia Melaka.

Abzi, I., Kabbaj, M. N., and Benbrahim, M. (2020). Fault tolerant control of vehicle lateral dynamic using a new pneumatic forces multiple model. *Actuators*, 9(4):120.

Achbi, M. S. (2012). *Commande tolérante aux défauts en utilisant les Réseaux de Neurones Artificiels et les Systèmes d'Inférence Floue*. PhD thesis, Université Mohamed Khider-Biskra.

Akhenak, A. (2004). *Conception d'observateurs non linéaires par approche multimodèle: application au diagnostic*. PhD thesis, Institut National Polytechnique de Lorraine.

Akhenak, A., Chadli, M., Maquin, D., and Ragot, J. (2003a). Sliding mode multiple observer for fault detection and isolation. In *42nd IEEE International Conference on Decision and Control (IEEE Cat. No. 03CH37475)*, volume 1, pages 953–958. IEEE.

Akhenak, A., Chadli, M., Maquin, D., and Ragot, J. (2003b). State estimation via multiple observer with unknown inputs: Application to the three tank system. In *5th IFAC Symposium on Fault Detection, Supervision and Safety for Technical Processes, Safeprocess' 2003*, pages 1227–1232.

Akhenak, A., Chadli, M., Ragot, J., and Maquin, D. (2004a). Conception d'un observateur flou à entrées inconnues. *Rencontres francophones sur la Logique Floue et ses Applications, Nantes, France*, pages 18–19.

Akhenak, A., Chadli, M., Ragot, J., and Maquin, D. (2004b). Estimation d'état et d'entrées inconnues d'un système non linéaire représenté sous forme multi-modèle. In *Conférence Internationale Francophone d'Automatique, CIFA*.

Akhenak, A., Chadli, M., Ragot, J., and Maquin, D. (2007). Design of sliding mode unknown input observer for uncertain Takagi-Sugeno model. In *2007 Mediterranean Conference on Control & Automation*, pages 1–6. IEEE.

Alrowaie, F. A. (2015). *Fault isolation and alarm design in non-linear stochastic systems*. PhD thesis, University of British Columbia.

Alwi, H., Edwards, C., and Tan, C. P. (2011). *Fault detection and fault-tolerant control using sliding modes*. Springer Science & Business Media.

Aly, A. A., Zeidan, E.-S., Hamed, A., Salem, F., et al. (2011). An antilock-braking systems (abs) control: A technical review. *Intelligent Control and Automation*, 2(03):186.

Amin, A. A. and Hasan, K. M. (2019). A review of fault tolerant control systems: advancements and applications. *Measurement*, 143:58–68.

Andry, A., Shapiro, E., and Chung, J. (1983). Eigenstructure assignment for linear systems. *IEEE transactions on aerospace and electronic systems*, AES-19(5):711–729.

Aouaouda, S., Bouarar, T., and Bouhali, O. (2014a). Fault tolerant tracking control using unmeasurable premise variables for vehicle dynamics subject to time varying faults. *Journal of the Franklin Institute*, 351(9):4514–4537.

Aouaouda, S., Chadli, M., Boukhnifer, M., and Karimi, H.-R. (2015). Robust fault tolerant tracking controller design for vehicle dynamics: A descriptor approach. *mechatronics*, 30:316–326.

Aouaouda, S., Chadli, M., Cocquempot, V., and Tarek Khadir, M. (2013). Multi-objective h_- / h_∞ fault detection observer design for Takagi–Sugeno fuzzy systems with unmeasurable premise variables: descriptor approach. *International Journal of Adaptive Control and Signal Processing*, 27(12):1031–1047.

Aouaouda, S., Chadli, M., and Karimi, H.-R. (2014b). Robust static output-feedback controller design against sensor failure for vehicle dynamics. *IET Control Theory & Applications*, 8(9):728–737.

Babuška, R. (2012). *Fuzzy modeling for control*, volume 12. Springer Science & Business Media.

Bærentzen, J. A., Gravesen, J., Anton, F., and Aanæs, H. (2012). *Guide to computational geometry processing: foundations, algorithms, and methods*. Springer Science & Business Media.

Bakker, E., Pacejka, H. B., and Lidner, L. (1989). A new tire model with an application in vehicle dynamics studies. *SAE transactions*, pages 101–113.

Basseville, M., Nikiforov, I. V., et al. (1993). *Detection of abrupt changes: theory and application*, volume 104. prentice Hall Englewood Cliffs.

Bede, B. (2013). *Mathematics of Fuzzy Sets and Fuzzy Logic*. Studies in Fuzziness and Soft Computing. Springer, Berlin.

Benzaouia, A. and Hajjaji, A. E. (2016). *Advanced Takagi-Sugeno Fuzzy Systems*. Springer.

Bernal, M. and Husek, P. (2005). Non-quadratic performance design for Takagi-Sugeno fuzzy systems. *International Journal of Applied Mathematics and Computer Science*, 15(3):383.

Bezzaoucha, S. (2013). *Commande tolérante aux défauts de systemes non linéaires représentés par des modeles de Takagi-Sugeno*. PhD thesis, Université de Lorraine.

Bhiri, B. (2017). *Stabilité et stabilisation en temps fini des systèmes dynamiques*. PhD thesis, Université de Lorraine.

Bishop, R. (2000). A survey of intelligent vehicle applications worldwide. In *Proceedings of the IEEE Intelligent Vehicles Symposium 2000 (Cat. No. 00TH8511)*, pages 25–30. IEEE.

Blanke, M., Izadi-Zamanabadi, R., Bøgh, S. A., and Lunau, C. P. (1997). Fault-tolerant control systems—a holistic view. *Control Engineering Practice*, 5(5):693–702.

Blanke, M., Kinnaert, M., Lunze, J., Staroswiecki, M., and Schröder, J. (2006). *Diagnosis and fault-tolerant control*, volume 2. Springer.

Bodson, M. and Groszkiewicz, J. E. (1997). Multivariable adaptive algorithms for reconfigurable flight control. *IEEE transactions on control systems technology*, 5(2):217–229.

Bouarar, T., Marx, B., Maquin, D., and Ragot, J. (2013). Fault-tolerant control design for uncertain Takagi–Sugeno systems by trajectory tracking: a descriptor approach. *IET Control Theory & Applications*, 7(14):1793–1805.

Bouattour, M., Chadli, M., El Hajjaji, A., and Chaabane, M. (2009). State and faults estimation for TS models and application to fault diagnosis. *IFAC Proceedings Volumes*, 42(8):492–497.

Boyd, S., El Ghaoui, L., Feron, E., and Balakrishnan, V. (1994). *Linear matrix inequalities in system and control theory*. SIAM.

Caglayan, A., Allen, S., and Wehmuller, K. (1988). Evaluation of a second generation reconfiguration strategy for aircraft flight control systems subjected to actuator failure/surface damage. In *Proceedings of the IEEE 1988 national aerospace and electronics conference*, pages 520–529. IEEE.

Casavola, A., Famularo, D., and Franzè, G. (2005). A robust deconvolution scheme for fault detection and isolation of uncertain linear systems: an LMI approach. *Automatica*, 41(8):1463–1472.

Chadli, M. (2010a). Chaotic systems reconstruction. In *Evolutionary Algorithms and Chaotic Systems*, pages 237–264. Springer.

Chadli, M. (2010b). An LMI approach to design observer for unknown inputs Takagi-Sugeno fuzzy models. *Asian Journal of Control*, 12(4):524–530.

Chadli, M., Akhenak, A., Maquin, D., and Ragot, J. (2008). Fuzzy observer for fault detection and reconstruction of unknown input fuzzy models. *International Journal of Modelling, Identification and Control*, 3(2):193–200.

Chadli, M. and Borne, P. (2013). Multiple models approach in automation. In *Takagi-Sugeno Fuzzy Systems*. Wiley Online Library.

Chadli, M. and Coppier, H. (2013). *Command-control for Real-time Systems*. Wiley Online Library.

Chadli, M., Maquin, D., and Ragot, J. (2000). Relaxed stability conditions for Takagi-Sugeno fuzzy systems. In *Smc 2000 conference proceedings. 2000 ieee international conference on systems, man and cybernetics.'cybernetics evolving to systems, humans, organizations, and their complex interactions'(cat. no. 0*, volume 5, pages 3514–3519. IEEE.

Chadli, M., Maquin, D., and Ragot, J. (2002). An LMI formulation for output feedback stabilization in multiple model approach. In *Proceedings of the 41st IEEE Conference on Decision and Control, 2002.*, volume 1, pages 311–316. IEEE.

Chaibi, R., Er Rachid, I., Tissir, E. H., and Hmamed, A. (2019). Finite-frequency static output feedback H_∞ control of continuous-time t–s fuzzy systems. *Journal of Circuits, Systems and Computers*, 28(02):1950023.

Chamraz, S. and Balogh, R. (2018). Two approaches to the adaptive cruise control (acc) design. In *2018 Cybernetics & Informatics (K&I)*, pages 1–6. IEEE.

Chang, X.-H., Zhang, L., and Park, J. H. (2015). Robust static output feedback $\mathcal{H}_\infty$ control for uncertain fuzzy systems. *Fuzzy Sets and Systems*, 273:87–104.

Chen, J. and Patton, R. J. (2012). *Robust model-based fault diagnosis for dynamic systems*, volume 3. Springer Science & Business Media.

Christensen, J. and Bastien, C. (2015). *Nonlinear optimization of vehicle safety structures: Modeling of structures subjected to large deformations*. Butterworth-Heinemann.

Corno, M., Panzani, G., and Savaresi, S. M. (2015). Single-track vehicle dynamics control: state of the art and perspective. *IEEE/asme transactions on mechatronics*, 20(4):1521–1532.

Dahmani, H., Chadli, M., Rabhi, A., and El Hajjaji, A. (2013). Road curvature estimation for vehicle lane departure detection using a robust Takagi–Sugeno fuzzy observer. *Vehicle System Dynamics*, 51(5):581–599.

Dahmani, H., Chadli, M., Rabhi, A., and El Hajjaji, A. (2015a). Detection of impending vehicle rollover with road bank angle consideration using a robust fuzzy observer. *International Journal of Automation and Computing*, 12(1):93–101.

Dahmani, H., Pagès, O., and El Hajjaji, A. (2015b). Observer-based state feedback control for vehicle chassis stability in critical situations. *IEEE Transactions on control systems technology*, 24(2):636–643.

Dai, L. et al. (1989). *Singular control systems*, volume 118. Springer.

Danancher, M., Roth, M., Lesage, J.-J., and Litz, L. (2011). A comparative study of three model-based FDI approaches for discrete event systems. In *2011 3rd International Workshop on Dependable Control of Discrete Systems*, pages 29–34. IEEE.

Dandach, H. (2014). *Prédiction de l'espace navigable par l'approche ensembliste pour un véhicule routier*. PhD thesis, Compiègne.

Danglot, B., Preux, P., Baudry, B., and Monperrus, M. (2018). Correctness attraction: a study of stability of software behavior under runtime perturbation. *Empirical Software Engineering*, 23(4):2086–2119.

Daraoui, N., Pagès, O., and El Hajjaji, A. (2012). Robust roll and yaw control systems using fuzzy model of the vehicle dynamics. In *2012 IEEE International Conference on Fuzzy Systems*, pages 1–6. IEEE.

de Oliveira, M. C. and Skelton, R. E. (2001). Stability tests for constrained linear systems. In *Perspectives in robust control*, pages 241–257. Springer.

Dieter, S., Hiller, M., and Baradini, R. (2018). Vehicle dynamics: Modeling and simulation.

Ding, E. and Massel, T. (2005). Estimation of vehicle roll angle. *IFAC Proceedings Volumes*, 38(1):122–127.

Do, M.-H., Koenig, D., and Theilliol, D. (2018). Robust $\mathcal{H}_\infty$ proportional-integral observer for fault diagnosis: Application to vehicle suspension. *IFAC-PapersOnLine*, 51(24):536–543.

Doumiati, M., Charara, A., Victorino, A., and Lechner, D. (2012). *Vehicle dynamics estimation using Kalman filtering: experimental validation*. John Wiley & Sons.

Driankov, D., Hellendoorn, H., and Reinfrank, M. (2013). *An introduction to fuzzy control*. Springer Science & Business Media.

Du, D., Cocquempot, V., and Jiang, B. (2019). Robust fault estimation observer design for switched systems with unknown input. *Applied Mathematics and Computation*, 348:70–83.

Du, D., Jiang, B., and Shi, P. (2015). Active fault tolerant control for switched systems with time delay. In *Fault Tolerant Control for Switched Linear Systems*, pages 119–134. Springer.

Dugoff, H., Fancher, P. S., and Segel, L. (1970). An analysis of tire traction properties and their influence on vehicle dynamic performance. *SAE transactions*, pages 1219–1243.

Edwards, C., Spurgeon, S. K., and Patton, R. J. (2000). Sliding mode observers for fault detection and isolation. *Automatica*, 36(4):541–553.

El Hajjaji, A., Chadli, M., Oudghiri, M., and Pages, O. (2006). Observer-based robust fuzzy control for vehicle lateral dynamics. In *2006 American Control Conference*, pages 6–pp. IEEE.

El Majdoub, K., Giri, F., Ouadi, H., Dugard, L., and Chaoui, F. Z. (2012). Vehicle longitudinal motion modeling for nonlinear control. *Control Engineering Practice*, 20(1):69–81.

El Youssfi, N. and El Bachtiri, R. (2020). TS fuzzy observers to design actuator fault-tolerant control for automotive vehicle lateral dynamics. In *Building Transportation, Traffic and Engineering Systems*. IntechOpen.

El Youssfi, N., El Bachtiri, R., Chaibi, R., and Tissir, E. H. (2020a). Static output-feedback H_∞ control for T–S fuzzy vehicle lateral dynamics. *SN Applied Sciences*, 2(1):101.

El Youssfi, N., El Bachtiri, R., and El Aiss, H. (2021a). T-S fuzzy observers design and actuator fault tolerant control applied to vehicle lateral dynamics. *International Journal of Digital Signals and Smart Systems*, 5(2):105–124.

El Youssfi, N., El Bachtiri, R., Zoulagh, T., and El Aiss, H. (2020b). Relaxed state and fault estimation for vehicle lateral dynamics represented by T–S fuzzy systems. *Journal of Control Science and Engineering*, 2020.

El Youssfi, N., El Bachtiri, R., Zoulagh, T., and El Aiss, H. (2021b). Unknown input observer design for vehicle lateral dynamics described by T–S fuzzy systems. *Manuscript submitted for publication*.

El Youssfi, N., Oudghiri, M., Aitouche, A., and El Bachtiri, R. (2018a). Fuzzy sliding-mode observer for lateral dynamics of vehicles with consideration of roll motion. In *2018 26th Mediterranean Conference on Control and Automation (MED)*, pages 861–866. IEEE.

El Youssfi, N., Oudghiri, M., and El Bachtiri, R. (2017). Observer-based fault tolerant control for vehicle lateral dynamics. In *2017 14th International Multi-Conference on Systems, Signals & Devices (SSD)*, pages 70–75. IEEE.

El Youssfi, N., Oudghiri, M., and El Bachtiri, R. (2018b). Control design and sensors fault tolerant for vehicle dynamics (a selected paper from ssd'17). *International Journal of Digital Signals and Smart Systems*, 2(1):50–67.

El Youssfi, N., Oudghiri, M., and El Bachtiri, R. (2019a). Actuator fault estimation and fault tolerant control for vehicle lateral dynamics. *AIP Conference Proceedings*, 2074(1):020027.

El Youssfi, N., Oudghiri, M., and El Bachtiri, R. (2019b). Vehicle lateral dynamics estimation using unknown input observer. *Procedia computer science*, 148:502–511.

El Youssfi, N., Oudghiri, M., El Bachtiri, R., and Chafouk, H. (2018c). H_∞ yaw and roll sensors fault-tolerant control for vehicle lateral dynamics. In *2018 International Conference on Electronics, Control, Optimization and Computer Science (ICECOCS)*, pages 1–6. IEEE.

El Youssfi, N., Zoulagh, T., El Aiss, H., El Bachtiri, R., and Zhiguang, F. (2021c). T–S fuzzy observer and actuator fault-tolerant controller designs for descriptor systems. *Manuscript submitted for publication*.

Erkus, B. and Lee, Y. (2004). Linear matrix inequalities and matlab LMI toolbox. In *University of Southern California Group Meeting Report, Los Angeles, California*.

Falcone, P., Borrelli, F., Asgari, J., Tseng, H. E., and Hrovat, D. (2007). Predictive active steering control for autonomous vehicle systems. *IEEE Transactions on control systems technology*, 15(3):566–580.

Fang, C.-H., Liu, Y.-S., Kau, S.-W., Hong, L., and Lee, C.-H. (2006). A new LMI-based approach to relaxed quadratic stabilization of TS fuzzy control systems. *IEEE Transactions on fuzzy systems*, 14(3):386–397.

Farmer, C. M. (2004). Effect of electronic stability control on automobile crash risk. *Traffic injury prevention*, 5(4):317–325.

Frank, P. M. (1996). Analytical and qualitative model-based fault diagnosis–a survey and some new results. *European Journal of control*, 2(1):6–28.

Furukawa, Y., Yuhara, N., Sano, S., Takeda, H., and Matsushita, Y. (1989). A review of four-wheel steering studies from the viewpoint of vehicle dynamics and control. *Vehicle system dynamics*, 18(1-3):151–186.

Gahinet, P. and Apkarian, P. (1994). A linear matrix inequality approach to H_∞ control. *International journal of robust and nonlinear control*, 4(4):421–448.

Gahinet, P., Nemirovskii, A., Laub, A. J., and Chilali, M. (1994). The LMI control toolbox. In *Proceedings of 1994 33rd IEEE Conference on Decision and Control*, volume 3, pages 2038–2041. IEEE.

Gao, Z. and Antsaklis, P. J. (1991). Stability of the pseudo-inverse method for reconfigurable control systems. *international Journal of Control*, 53(3):717–729.

Gao, Z. and Antsaklis, P. J. (1992). Reconfigurable control system design via perfect model following. *International Journal of Control*, 56(4):783–798.

Garcia, A. (2013). Pacejka '94 parameters explained – a comprehensive guide. `https://www.edy.es/dev/docs/pacejka-94-parameters-explained-a-comprehensive-guide/`, Sidst set 16/03/2021.

Gasso, K. (2000). *Identification des systèmes dynamiques non-linéaires: approche multi-modèle*. PhD thesis, Institut National Polytechnique de Lorraine.

Gasso, K., Mourot, G., Boukhriss, A., and Ragot, J. (1999). Optimisation de la structure d'un modèle de Takagi-Sugeno. *Actes des rencontres francophones (LFA)*.

Genta, G. (1997). *Motor vehicle dynamics: modeling and simulation*, volume 43. World Scientific.

Gertler, J. (1992). Structured residuals for fault isolation, disturbance decoupling and modelling error robustness. *IFAC Proceedings Volumes*, 25(4):15–23.

Gertler, J. (1998). Fault detection and diagnosis in engineering systems marcel dekker. *New York*.

Gillespie, T. D. (1992). *Fundamentals of vehicle dynamics*, volume 400. Society of automotive engineers Warrendale, PA.

Gim, G. and Nikravesh, P. E. (1990). An analytical model of pneumatic tyres for vehicle dynamic simulations. part 1: pure slips. *International Journal of vehicle design*, 11(6):589–618.

Gómez-Peñate, S., Valencia-Palomo, G., López-Estrada, F.-R., Astorga-Zaragoza, C.-M., Osornio-Rios, R. A., and Santos-Ruiz, I. (2019). Sensor fault diagnosis based on a sliding mode and unknown input observer for Takagi-Sugeno systems with uncertain premise variables. *Asian Journal of Control*, 21(1):339–353.

Guelton, K., Delprat, S., and Guerra, T.-M. (2008). An alternative to inverse dynamics joint torques estimation in human stance based on a takagi–sugeno unknown-inputs observer in the descriptor form. *Control Engineering Practice*, 16(12):1414–1426.

Guilbot, M. (2014). Aides à la conduite, véhicule connecté et protection des données personnelles. In *APVP14 - 5ème Atelier Protection de la Vie privée*, page 6p, Cabourg, France.

Håland, Y. (2006). The evolution of the three point seat belt from yesterday to tomorrow. In *IRCOBI Conference*.

Hamersma, H. A. and Els, P. S. (2014). Longitudinal vehicle dynamics control for improved vehicle safety. *Journal of Terramechanics*, 54:19–36.

Han, H., Yang, Y., Li, L., and Ding, S. X. (2018). Observer-based fault detection for uncertain nonlinear systems. *Journal of the Franklin Institute*, 355(3):1278–1295.

Hashemi, A. and Pisu, P. (2011). Adaptive threshold-based fault detection and isolation for automotive electrical systems. In *2011 9th World Congress on Intelligent Control and Automation*, pages 1013–1018. IEEE.

Hashemi, E., Zarringhalam, R., Khajepour, A., Melek, W., Kasaiezadeh, A., and Chen, S.-K. (2017). Real-time estimation of the road bank and grade angles with unknown input observers. *Vehicle system dynamics*, 55(5):648–667.

Hernandez-Alcantara, D., Amezquita-Brooks, L., Morales-Menendez, R., Sename, O., and Dugard, L. (2018). The cross-coupling of lateral-longitudinal vehicle dynamics: Towards decentralized fault-tolerant control schemes. *Mechatronics*, 50:377–393.

Hindi, H. and Boyd, S. (1998). Analysis of linear systems with saturation using convex optimization. In *Proceedings of the 37th IEEE Conference on Decision and Control (Cat. No. 98CH36171)*, volume 1, pages 903–908. IEEE.

Huang, C. Y. and Stengel, R. F. (1990). Restructurable control using proportional-integral implicit model following. *Journal of Guidance, Control, and Dynamics*, 13(2):303–309.

Huang, D. and Nguang, S. K. (2007). Static output feedback controller design for fuzzy systems: An LMI approach. *Information Sciences*, 177(14):3005–3015.

Hussain, R. and Zeadally, S. (2018). Autonomous cars: Research results, issues, and future challenges. *IEEE Communications Surveys & Tutorials*, 21(2):1275–1313.

Ichalal, D. (2009). *Estimation et diagnostic de systèmes non linéaires décrits par un modèle de Takagi-Sugeno*. PhD thesis, Institut National Polytechnique de Lorraine. Thèse de doctorat dirigée par Maquin, Didier et Ragot, José Automatique, traitement du signal et des images, génie informatique Vandoeuvre-les-Nancy, INPL 2009.

Ichalal, D., Marx, B., Ragot, J., Mammar, S., and Maquin, D. (2016). Sensor fault tolerant control of nonlinear Takagi–Sugeno systems. application to vehicle lateral dynamics. *International Journal of Robust and Nonlinear Control*, 26(7):1376–1394.

Ichalal, D., Marx, B., Ragot, J., and Maquin, D. (2010). Observer based actuator fault tolerant control for nonlinear Takagi-Sugeno systems: an LMI approach. In *18th Mediterranean Conference on Control and Automation, MED'10*, pages 1278–1283. IEEE.

Ikeda, K., Shin, S., and Kitamori, T. (1993). Fault tolerance of decentralized adaptive control. In *Proceedings ISAD 93: International Symposium on Autonomous Decentralized Systems*, pages 275–281. IEEE.

Isermann, R. (2005). Model-based fault-detection and diagnosis–status and applications. *Annual Reviews in control*, 29(1):71–85.

Isermann, R. (2006). *Fault-diagnosis systems: an introduction from fault detection to fault tolerance*. Springer Science & Business Media.

Isermann, R. and Ballé, P. (1997). Trends in the application of model-based fault detection and diagnosis of technical processes. *Control Engineering Practice*, 5(5):709 – 719.

Jadbabaie, A. (1999). A reduction in conservatism in stability and 52 gain analysis of Takagi-Sugeno fuzzy systems via linear matrix inequalities. *IFAC Proceedings Volumes*, 32(2):5451–5455.

Jain, T., Yamé, J. J., and Sauter, D. (2018). *Active Fault-Tolerant Control Systems: A Behavioral System Theoretic Perspective*. Springer International Publishing, 1 edition.

Jarašūniene, A. and Jakubauskas, G. (2007). Improvement of road safety using passive and active intelligent vehicle safety systems. *Transport*, 22(4):284–289.

Jazar, R. N. (2017). *Vehicle dynamics: theory and application*. Springer.

Jensen, T. H. (2007). Assessing mathematical modelling competency. *Mathematical modeling (ICTMA 12) education, engineering and economic*, pages 141–148.

Jeong, H., Park, B., Park, S., Min, H., and Lee, S. (2019). Fault detection and identification method using observer-based residuals. *Reliability Engineering & System Safety*, 184:27–40.

Jeung, E. T. and Lee, K. R. (2014). Static output feedback control for continuous-time TS fuzzy systems: an LMI approach. *International Journal of Control, Automation and Systems*, 12(3):703–708.

Jia, Q., Chen, W., Zhang, Y., and Li, H. (2015). Fault reconstruction and fault-tolerant control via learning observers in Takagi–Sugeno fuzzy descriptor systems with time delays. *IEEE Transactions on industrial electronics*, 62(6):3885–3895.

Jiang, J. and Yu, X. (2012). Fault-tolerant control systems: A comparative study between active and passive approaches. *Annual Reviews in control*, 36(1):60–72.

Jin, X., Yin, G., and Chen, N. (2019). Advanced estimation techniques for vehicle system dynamic state: A survey. *Sensors*, 19(19):4289.

Jin, X., Yin, G., and Wang, J. (2017). Robust fuzzy control for vehicle lateral dynamic stability via Takagi-Sugeno fuzzy approach. In *2017 American Control Conference (ACC)*, pages 5574–5579. IEEE.

Jing, H., Wang, R., Hu, C., Wang, J., Yan, F., and Chen, N. (2016). Vehicle lateral motion control considering network-induced delay and tire force saturation. In *2016 American Control Conference (ACC)*, pages 6881–6886. IEEE.

Joshi, S. and Talange, D. (2016). Fault tolerant control of an auv using periodic output feedback with multi model approach. *International Journal of System Dynamics Applications (IJSDA)*, 5(2):41–62.

Jung, B., Kim, Y., and Ha, C. (2009). Fault tolerant flight control system design using a multiple model adaptive controller. *Proceedings of the Institution of Mechanical Engineers, Part G: Journal of Aerospace Engineering*, 223(1):39–50.

Kanev, S. K. (2004). *Robust fault-tolerant control*. FEBO-DRUK.

Karnopp, D. (2013). *Vehicle dynamics, stability, and control*. CRC Press.

Katzfuss, M., Stroud, J. R., and Wikle, C. K. (2016). Understanding the ensemble kalman filter. *The American Statistician*, 70(4):350–357.

Kau, S.-W., Lee, H.-J., Yang, C.-M., Lee, C.-H., Hong, L., and Fang, C.-H. (2007). Robust h_∞ fuzzy static output feedback control of TS fuzzy systems with parametric uncertainties. *Fuzzy sets and systems*, 158(2):135–146.

Kawamoto, S., Tada, K., Ishigame, A., and Taniguchi, T. (1992). An approach to stability analysis of second order fuzzy systems. In *[1992 Proceedings] IEEE International Conference on Fuzzy Systems*, pages 1427–1434. IEEE.

Khalil, H. K. and Grizzle, J. W. (2002). *Nonlinear systems*, volume 3. Prentice hall Upper Saddle River, NJ.

Khan, L., Qamar, S., and Khan, U. (2016). Adaptive PID control scheme for full car suspension control. *Journal of the Chinese Institute of Engineers*, 39(2):169–185.

Kharrat, D., Gassara, H., El Hajjaji, A., and Chaabane, M. (2018). Adaptive observer and fault tolerant control for T–S descriptor nonlinear systems with sensor and actuator faults. *International Journal of Control, Automation and Systems*, 16(3):972–982.

Kidane, S., Alexander, L., Rajamani, R., Starr, P., and Donath, M. (2006). Road bank angle considerations in modeling and tilt stability controller design for narrow commuter vehicles. In *2006 American control conference*, pages 6–pp. IEEE.

Kiencke, U. and Nielsen, L. (2000). Automotive control systems: for engine, driveline, and vehicle.

Klir, G. and Yuan, B. (1995). *Fuzzy sets and fuzzy logic*, volume 4. Prentice hall New Jersey.

Knapczyk, J. and Kucybała, P. (2016). Simplified planar model of a car steering system with rack and pinion and mcpherson suspension. *IOP Conference Series: Materials Science and Engineering*, 148(1):012011.

Konstantopoulos, I. K. and Antsaklis, P. J. (1996). Eigenstructure assignment in reconfigurable control systems. *ISIS*, 96:001.

Kruszewski, A., Wang, R., and Guerra, T.-M. (2008). Nonquadratic stabilization conditions for a class of uncertain nonlinear discrete time ts fuzzy models: A new approach. *IEEE Transactions on Automatic Control*, 53(2):606–611.

Lechner, D. (2002). *Analyse du comportement dynamique des véhicules routiers légers: développement d'une méthodologie appliquée à la sécurité primaire*. PhD thesis, Ecole Centrale de Lyon.

Leine, R. I. (2010). The historical development of classical stability concepts: Lagrange, poisson and lyapunov stability. *Nonlinear Dynamics*, 59(1):173–182.

Lendek, Z., Guerra, T. M., Babuška, R., and De Schutter, B. (2011a). *Stability Analysis of TS Fuzzy Systems*, pages 25–48. Springer Berlin Heidelberg, Berlin, Heidelberg.

Lendek, Z., Guerra, T. M., Babuška, R., and Schutter, B. (2011b). *Stability analysis and nonlinear observer design using Takagi-Sugeno fuzzy models*. Springer.

Li, L. (2016). *Fault detection and fault-tolerant control for nonlinear systems*. Springer.

Li, L., Ding, S., and Peng, X. (2020). Optimal observer-based fault detection and estimation approaches for TS fuzzy systems. *IEEE Transactions on Fuzzy Systems*.

Li, L., Ding, S. X., Qiu, J., Yang, Y., and Xu, D. (2016). Fuzzy observer-based fault detection design approach for nonlinear processes. *IEEE Transactions on Systems, Man, and Cybernetics: Systems*, 47(8):1941–1952.

Li, R. and Yang, Y. (2020). Fault detection for ts fuzzy singular systems via integral sliding modes. *Journal of the Franklin Institute*, 357(17):13125–13143.

Lin, C., Wang, Q.-G., and Lee, T. H. (2005). Improvement on observer-based H_∞ control for T–S fuzzy systems. *Automatica*, 41(9):1651–1656.

Lin, S.-Y. and Horng, S.-C. (2006). A classification-based fault detection and isolation scheme for the ion implanter. *IEEE transactions on semiconductor manufacturing*, 19(4):411–424.

Liu, C.-S. and Peng, H. (2002). Inverse-dynamics based state and disturbance observers for linear time-invariant systems. *J. Dyn. Sys., Meas., Control*, 124(3):375–381.

Liu, M., Zhang, L., Shi, P., and Zhao, Y. (2018). Fault estimation sliding-mode observer with digital communication constraints. *IEEE Transactions on Automatic Control*, 63(10):3434–3441.

Liu, X. and Zhang, Q. (2003). New approaches to h-infinity controller designs based on fuzzy observers for TS fuzzy systems via LMI. *Automatica*, 39(9):1571–1582.

Livingston, D. and Brown Jr, J. (1969). Physics of the slipping wheel. i. force and torque calculations for various pressure distributions. *Rubber chemistry and technology*, 42(4):1014–1027.

Livingston, D. and Brown Jr, J. (1970). Physics of the slipping wheel. ii. slip under both tractive and lateral forces. *Rubber chemistry and technology*, 43(2):244–261.

Lofberg, J. (2004). Yalmip: A toolbox for modeling and optimization in matlab. In *2004 IEEE international conference on robotics and automation (IEEE Cat. No. 04CH37508)*, pages 284–289. IEEE.

Lu, X.-Y. and Hedrick, J. K. (2005). Heavy-duty vehicle modelling and longitudinal control. *Vehicle System Dynamics*, 43(9):653–669.

Luenberger, D. (1977). Dynamic equations in descriptor form. *IEEE Transactions on Automatic Control*, 22(3):312–321.

Ma, X.-J., Sun, Z.-Q., and He, Y.-Y. (1998). Analysis and design of fuzzy controller and fuzzy observer. *IEEE Transactions on fuzzy systems*, 6(1):41–51.

Mackenroth, U. (2013). *Robust control systems: theory and case studies*. Springer Science & Business Media.

Mamdani, E. H. and Assilian, S. (1975). An experiment in linguistic synthesis with a fuzzy logic controller. *International journal of man-machine studies*, 7(1):1–13.

Mammar, S., Glaser, S., and Netto, M. (2006). Vehicle lateral dynamics estimation using unknown input proportional-integral observers. In *2006 American control conference*, pages 6–pp. IEEE.

Mammar, S. and Koenig, D. (2002). Vehicle handling improvement by active steering. *Vehicle system dynamics*, 38(3):211–242.

Maquin, D., Gaddouna, B., and Ragot, J. (1994). Estimation of unknown inputs in linear systems. In *Proceedings of 1994 American Control Conference-ACC'94*, volume 1, pages 1195–1197. IEEE.

Markovsky, I., Willems, J. C., Van Huffel, S., and De Moor, B. (2006). *Exact and approximate modeling of linear systems: A behavioral approach*. SIAM.

Marsden, G., McDonald, M., and Brackstone, M. (2001). Towards an understanding of adaptive cruise control. *Transportation Research Part C: Emerging Technologies*, 9(1):33–51.

Martínez-García, C., Puig, V., Astorga-Zaragoza, C.-M., Madrigal-Espinosa, G., and Reyes-Reyes, J. (2020). Estimation of actuator and system faults via an unknown input interval observer for Takagi–Sugeno systems. *Processes*, 8(1):61.

Martinez-Guerra, R. and Mata-Machuca, J. L. (2016). *Fault detection and diagnosis in nonlinear systems*. Springer.

Mawhin, J. (2005). Alexandr mikhailovich lyapunov, thesis on the stability of motion (1892). In *Landmark Writings in Western Mathematics 1640-1940*, pages 664–676. Elsevier.

Maybeck, P. S. and Pogoda, D. L. (1989). Multiple model adaptive controller for the stol f-15 with sensor/actuator failures. In *Proceedings of the 28th IEEE Conference on Decision and Control,*, pages 1566–1572. IEEE.

Meda-Campaña, J., Rubio, J. d. J., Aguilar-Ibañez, C., Tapia-Herrera, R., Gonzalez-Salazar, R., Rodriguez-Manzanarez, R., Lopez-Contreras, G., Hernandez-Monterrosas, J., Elias, I., and Cruz, D. (2020). General controllability and observability tests for Takagi-Sugeno fuzzy systems. *Evolving Systems*, 11(2):349–358.

Meskin, N. and Khorasani, K. (2011). *Fault detection and isolation: Multi-vehicle unmanned systems*. Springer Science & Business Media.

Methnani, S. (2012). *Diagnosis and sensors and actuators fault reconstruction : application to WWTPs*. Theses, Université de Toulon.

Milliken, W. F., Milliken, D. L., et al. (1995). *Race car vehicle dynamics*, volume 400. Society of Automotive Engineers Warrendale, PA.

Monot, N., Moreau, X., Benine-Neto, A., Rizzo, A., and Aioun, F. (2018). Comparison of observers for vehicle yaw rate estimation. In *2018 IEEE Intelligent Vehicles Symposium (IV)*, pages 1925–1930. IEEE.

Morere, Y. (2001). *Mise en oeuvre de lois de commande pour les modèles flous de type Takagi-Sugeno*. PhD thesis, Valenciennes.

Mozelli, L. A., Palhares, R. M., and Avellar, G. S. (2009). A systematic approach to improve multiple lyapunov function stability and stabilization conditions for fuzzy systems. *Information Sciences*, 179(8):1149–1162.

Najim, K., Ikonen, E., and Daoud, A.-K. (2004). *Stochastic processes: estimation, optimisation and analysis*. Elsevier.

Nguyen, A.-T., Guerra, T.-M., and Campos, V. (2019a). Simultaneous estimation of state and unknown input with l_∞ guarantee on error-bounds for fuzzy descriptor systems. *IEEE Control Systems Letters*, 3(4):1020–1025.

Nguyen, A.-T., Guerra, T.-M., Sentouh, C., and Zhang, H. (2019b). Unknown input observers for simultaneous estimation of vehicle dynamics and driver torque: Theoretical design and hardware experiments. *IEEE/ASME Transactions on Mechatronics*, 24(6):2508–2518.

Nguyen, A.-T., Laurain, T., Palhares, R., Lauber, J., Sentouh, C., and Popieul, J.-C. (2016). LMI-based control synthesis of constrained Takagi–Sugeno fuzzy systems subject to l_2 or l_∞ disturbances. *Neurocomputing*, 207:793–804.

Noura, H., Theilliol, D., Ponsart, J.-C., and Chamseddine, A. (2009). *Fault-tolerant control systems: Design and practical applications*. Springer Science & Business Media, 1 edition.

Ohtake, H., Tanaka, K., and Wang, H. O. (2003). Fuzzy modeling via sector nonlinearity concept. *Integrated Computer-Aided Engineering*, 10(4):333–341.

Orjuela, R., Marx, B., Ragot, J., and Maquin, D. (2009). Une approche multimodele pour le diagnostic des systemes non linéaires. In *2ème Workshop Surveillance, Sûreté et Sécurité des Grands Systèmes, 3SGS'09*.

Osborn, R. P. and Shim, T. (2006). Independent control of all-wheel-drive torque distribution. *Vehicle system dynamics*, 44(7):529–546.

Oudghiri, M. (2008). *Commande multi-modèles tolérante aux défauts: Application au contrôle de la dynamique d'un véhicule automobile.* PhD thesis, Université de Picardie Jules Verne.

Oudghiri, M., Chadli, M., and El Hajjaji, A. (2007). Vehicle yaw control using a robust H_∞ observer-based fuzzy controller design. In *2007 46th IEEE Conference on Decision and Control*, pages 3895–3900. IEEE.

Oudghiri, M., Chadli, M., and El Hajjaji, A. (2008). Robust observer-based fault-tolerant control for vehicle lateral dynamics. *International Journal of vehicle design*, 48(3-4):173–189.

Oudghiri, M., Rabhi, A., and Elhajjaji, A. (2014). h_∞ robust observer-based control for vehicle rollover. In *22nd Mediterranean Conference on Control and Automation*, pages 43–48. IEEE.

Pacejka, H. (2006). Tire and vehicle dynamics. sae edition. *Society of Automative Engineers, Inc*.

Pacejka, H. and Besselink, I. (1997). Magic formula tyre model with transient properties. *Vehicle system dynamics*, 27(S1):234–249.

Pacejka, H. B. and Bakker, E. (1992). The magic formula tyre model. *Vehicle system dynamics*, 21(S1):1–18.

Pacejka, H. B. et al. (1996). The tyre as a vehicle component. In *26th FISITA Congress, 16-13 June 1996, Prague, Czechoslovakia*.

Palm, R. and Driankov, D. (1999). Towards a systematic analysis of fuzzy observers. In *18th International Conference of the North American Fuzzy Information Processing Society-NAFIPS (Cat. No. 99TH8397)*, pages 179–183. IEEE.

Patan, K. (2014). Neural network-based model predictive control: Fault tolerance and stability. *IEEE Transactions on Control Systems Technology*, 23(3):1147–1155.

Patton, R. and Chen, J. (1991). A review of parity space approaches to fault diagnosis. *IFAC Proceedings Volumes*, 24(6):65 – 81. IFAC/IMACS Symposium on Fault Detection, Supervision and Safety for Technical Processes (SAFEPROCESS'91), Baden-Baden, Germany, 10-13 September 1991.

Patton, R. J. and Chen, J. (1994). Review of parity space approaches to fault diagnosis for aerospace systems. *Journal of Guidance, Control, and Dynamics*, 17(2):278–285.

Patton, R. J. and Chen, J. (1997). Observer-based fault detection and isolation: Robustness and applications. *Control Engineering Practice*, 5(5):671–682.

Patton, R. J., Frank, P. M., and Clark, R. N. (2013). *Issues of fault diagnosis for dynamic systems*. Springer Science & Business Media.

Picó, M. F. and Adam, E. J. (2015). FTC with observers bank in a cstr. In *2015 XVI Workshop on Information Processing and Control (RPIC)*, pages 1–6. IEEE.

Plancke, S. (2009). *Estimation temps réel des états dynamiques d'un véhicule automobile*. PhD thesis, Université Paris Sud-Paris XI.

Rabhi, A., Chadli, M., El Hajjaji, A., and Bosche, J. (2009). Robust observer for prevention of vehicle rollover. In *2009 International Conference on Advances in Computational Tools for Engineering Applications*, pages 627–632. IEEE.

Rahimi, S. and Naraghi, M. (2018). Design of an integrated control system to enhance vehicle roll and lateral dynamics. *Transactions of the Institute of Measurement and Control*, 40(5):1435–1446.

Rajamani, R. (2005). Mechanical engineering series, vehicle dynamics and control.

Rajamani, R. (2011). *Vehicle dynamics and control*. Springer Science & Business Media.

Rajamani, R. (2012). Lateral vehicle dynamics. In *Vehicle Dynamics and control*, pages 15–46. Springer.

Reina, G. and Messina, A. (2019). Vehicle dynamics estimation via augmented extended kalman filtering. *Measurement*, 133:383–395.

Rill, G. (2011). *Road vehicle dynamics: fundamentals and modeling*. Crc Press.

Rodrigues, M. (2005). *Diagnostic et commande active tolérante aux défauts appliqués aux systèmes décrits par des multi-modèles linéaires*. PhD thesis, Université Henri Poincaré-Nancy I.

Rodrigues, M., Hamdi, H., Braiek, N. B., and Theilliol, D. (2014). Observer-based fault tolerant control design for a class of lpv descriptor systems. *Journal of the Franklin Institute*, 351(6):3104–3125.

Ryu, J., Moshchuk, N. K., and Chen, S.-K. (2007). Vehicle state estimation for roll control system. In *2007 American Control Conference*, pages 1618–1623. IEEE.

Saini, V. and Saini, R. (2014). Driver drowsiness detection system and techniques: a review. *International Journal of Computer Science and Information Technologies*, 5(3):4245–4249.

Sallem, F. (2013). *Détection et isolation de défauts actionneurs basées sur un modèle de l'organe de commande*. PhD thesis, Université de Toulouse, Université Toulouse III-Paul Sabatier. 2013TOU30140.

Sami, M. and Patton, R. J. (2013). Active fault tolerant control for nonlinear systems with simultaneous actuator and sensor faults. *International Journal of Control, Automation and Systems*, 11(6):1149–1161.

Sastry, S. (2013). *Nonlinear systems: analysis, stability, and control*, volume 10. Springer Science & Business Media.

Sauter, D., Boukhobza, T., and Hamelin, F. (2006). Decentralized and autonomous design for FDI/FTC of networked control systems. *IFAC Proceedings Volumes*, 39(13):138–143.

Schoukens, J. and Pintelon, R. (2014). *Identification of linear systems: a practical guideline to accurate modeling*. Elsevier.

Schramm, D., Hiller, M., and Bardini, R. (2014). Vehicle dynamics. In *Modeling and simulation*, page 151. Springer.

Segel, L. (1956). Theoretical prediction and experimental substantiation of the response of the automobile to steering control. *Proceedings of the Institution of Mechanical Engineers: Automobile Division*, 10(1):310–330.

Seron, M. M., Zhuo, X. W., De Doná, J. A., and Martínez, J. J. (2008). Multisensor switching control strategy with fault tolerance guarantees. *Automatica*, 44(1):88–97.

Sheikholeslam, S. and Desoer, C. A. (1992). Combined longitudinal and lateral control of a platoon of vehicles. In *1992 American Control Conference*, pages 1763–1767. IEEE.

Shen, Q., Jiang, B., and Shi, P. (2017). *Fault diagnosis and fault-tolerant control based on adaptive control approach*, volume 91. Springer.

Sobhani-Tehrani, E. and Khorasani, K. (2009). *Fault diagnosis of nonlinear systems using a hybrid approach*, volume 383. Springer Science & Business Media.

Staroswiecki, M. (2005). Fault tolerant control: the pseudo-inverse method revisited. *Ifac proceedings volumes*, 38(1):418–423.

Stengel, R. F. (1991). Intelligent failure-tolerant control. *IEEE Control Systems Magazine*, 11(4):14–23.

Stetter, R., Stetter, and Ditzinger (2020). *Fault-Tolerant Design and Control of Automated Vehicles and Processes*. Springer.

Stotsky, A. and Kolmanovsky, I. (2001). Simple unknown input estimation techniques for automotive applications. In *Proceedings of the 2001 American Control Conference.(Cat. No. 01CH37148)*, volume 5, pages 3312–3317. IEEE.

Sugeno, M. and Kang, G. (1988). Structure identification of fuzzy model. *Fuzzy sets and systems*, 28(1):15–33.

Takagi, T. and Sugeno, M. (1985). Fuzzy identification of systems and its applications to modeling and control. *IEEE transactions on systems, man, and cybernetics*, SMC-15(1):116–132.

Tan, C. P. and Edwards, C. (2002). Sliding mode observers for detection and reconstruction of sensor faults. *Automatica*, 38(10):1815–1821.

Tanaka, K., Hori, T., and Wang, H. O. (2001). A fuzzy lyapunov approach to fuzzy control system design. In *Proceedings of the 2001 American Control Conference.(Cat. No. 01CH37148)*, volume 6, pages 4790–4795. IEEE.

Tanaka, K., Hori, T., and Wang, H. O. (2003). A multiple lyapunov function approach to stabilization of fuzzy control systems. *IEEE Transactions on fuzzy systems*, 11(4):582–589.

Tanaka, K., Ikeda, T., and Wang, H. O. (1996). Robust stabilization of a class of uncertain nonlinear systems via fuzzy control: quadratic stabilizability, H_∞ control theory, and linear matrix inequalities. *IEEE Transactions on Fuzzy systems*, 4(1):1–13.

Tanaka, K., Ikeda, T., and Wang, H. O. (1998). Fuzzy regulators and fuzzy observers: relaxed stability conditions and LMI-based designs. *IEEE Transactions on fuzzy systems*, 6(2):250–265.

Tanaka, K. and Ohtake, H. (2001). Fuzzy modeling via sector nonlinearity concept. *Transactions of the Society of Instrument and Control Engineers*, 37(4):372–378.

Tanaka, K. and Sano, M. (1994). A robust stabilization problem of fuzzy control systems and its application to backing up control of a truck-trailer. *IEEE Transactions on Fuzzy systems*, 2(2):119–134.

Tanaka, K. and Taniguchi, T. (1999). Fuzzy observer-based control via LMIs. *Transactions of the Society of Instrument and Control Engineers*, 35(3):422–427.

Tanaka, K. and Wang, H. O. (2004). *Fuzzy control systems design and analysis: a linear matrix inequality approach*. John Wiley & Sons.

Taniguchi, T., Tanaka, K., and Wang, H. O. (2000). Fuzzy descriptor systems and nonlinear model following control. *IEEE Transactions on Fuzzy Systems*, 8(4):442–452.

Tao, G., Chen, S., and Joshi, S. M. (2002). An adaptive control scheme for systems with unknown actuator failures. *automatica*, 38(6):1027–1034.

Tuan, V. L. B. and El Hajjaji, A. (2018). Robust observer-based control for TS fuzzy models application to vehicle lateral dynamics. In *2018 26th Mediterranean Conference on Control and Automation (MED)*, pages 1–6. IEEE.

Tuan, V. L. B., El Hajjaji, A., and Naami, G. (2019). Robust TS-fuzzy observer-based control for quadruple-tank system. In *2019 12th Asian Control Conference (ASCC)*, pages 307–312. IEEE.

Ungoren, A. Y., Peng, H., and Tseng, H. (2004). A study on lateral speed estimation methods. *International Journal of Vehicle Autonomous Systems*, 2(1-2):126–144.

Van Dong, N., Thai, P. Q., Duc, P. M., and Thuan, N. V. (2019). Estimation of vehicle dynamics states using luenberger observer. *International Journal of Mechanical Engineering and Robotics Research*, 8(3).

Varrier, S. (2013). *Détection de situations critiques et commande robuste tolérante aux défauts pour l'automobile*. PhD thesis, Université de Grenoble.

Vu, V.-P. and Do, T. D. (2018). Fault/state estimation observer synthesis for uncertain TS fuzzy systems. *IEEE Access*, 7:358–369.

Wallentowitz, H. (2014). Automotive engineering ii lateral vehicle dynamics.

Wang, D. and Qi, F. (2001). Trajectory planning for a four-wheel-steering vehicle. In *Proceedings 2001 ICRA. IEEE International Conference on Robotics and Automation (Cat. No. 01CH37164)*, volume 4, pages 3320–3325. IEEE.

Wang, D., Shi, P., and Wang, W. (2013). *Robust filtering and fault detection of switched delay systems*, volume 445. Springer.

Wang, H. O., Tanaka, K., and Griffin, M. F. (1996). An approach to fuzzy control of nonlinear systems: Stability and design issues. *IEEE transactions on fuzzy systems*, 4(1):14–23.

Wang, J., Liang, J., and Dobaie, A. M. (2018). Dynamic output-feedback control for positive roesser system under the switched and TS fuzzy rules. *Information Sciences*, 422:1–20.

Wang, J. and Longoria, R. G. (2009). Coordinated and reconfigurable vehicle dynamics control. *IEEE Transactions on Control Systems Technology*, 17(3):723–732.

Wang, L.-X. (1994). *Adaptive fuzzy systems and control: design and stability analysis*. Prentice-Hall, Inc.

Wang, Y., Zheng, L., Zhang, H., and Zheng, W. X. (2019a). Fuzzy observer-based repetitive tracking control for nonlinear systems. *IEEE Transactions on Fuzzy Systems*.

Wang, Z., Rodrigues, M., Theilliol, D., and Shen, Y. (2015). Actuator fault estimation observer design for discrete-time linear parameter-varying descriptor systems. *International Journal of Adaptive Control and Signal Processing*, 29(2):242–258.

Wang, Z., Shi, P., and Lim, C.-C. (2019b). Robust fault estimation observer in the finite frequency domain for descriptor systems. *International Journal of Control*, 92(7):1590–1599.

Wen, J. T. (1990). A unified perspective on robot control: The energy lyapunov function approach. In *29th IEEE Conference on Decision and Control*, pages 1968–1973. IEEE.

Winner, H., Hakuli, S., Lotz, F., and Singer, C. (2014). *Handbook of driver assistance systems*. Springer International Publishing Amsterdam, The Netherlands:.

Wu, Y. and Dong, J. (2016). Fault estimation and fault tolerant control for TS fuzzy systems. In *2016 3rd International Conference on Informative and Cybernetics for Computational Social Systems (ICCSS)*, pages 97–102. IEEE.

Xiaodong, L. and Qingling, Z. (2003). New approaches to h_∞ controller designs based on fuzzy observers for TS fuzzy systems via LMI. *Automatica*, 39(9):1571–1582.

Yang, Z., Izadi-Zamanabadi, R., and Blanke, M. (2000). On-line multiple-model based adaptive control reconfiguration for a class of nonlinear control systems. *IFAC Proceedings Volumes*, 33(11):729–734.

Yoon, S. and MacGregor, J. F. (2000). Statistical and causal model-based approaches to fault detection and isolation. *AIChE Journal*, 46(9):1813–1824.

You, S.-H., Cho, Y. M., and Hahn, J.-O. (2017). Model-based fault detection and isolation in automotive yaw moment control system. *International Journal of Automotive Technology*, 18(3):405–416.

Youmin Zhang and Jin Jiang (2001). Fault tolerant control systems design with consideration of performance degradation. In *Proceedings of the 2001 American Control Conference. (Cat. No.01CH37148)*, volume 4, pages 2694–2699 vol.4.

Young, G. and Reid, K. (1993). Lateral and longitudinal dynamic behavior and control of moving webs. *Journal of Dynamic Systems, Measurement, and Control*.

Yuan, Y. and Zhang, G. (2010). Observer-based reliable controller designs for TS fuzzy descriptor systems with time-delay. In *2010 Seventh International Conference on Fuzzy Systems and Knowledge Discovery*, volume 1, pages 248–253. IEEE.

Zak, S. H. (2003). *Systems and control*, volume 198. Oxford University Press New York.

Zhang, C. (2017). *Fault-tolerant control system design*. PhD thesis, Imperial College London.

Zhang, H., Han, J., Wang, Y., and Liu, X. (2018). Sensor fault estimation of switched fuzzy systems with unknown input. *IEEE Transactions on Fuzzy Systems*, 26(3):1114–1124.

Zhang, K., Jiang, B., and Shi, P. (2012). *Observer-based fault estimation and accomodation for dynamic systems*, volume 436. Springer.

Zhang, X., Polycarpou, M. M., and Parisini, T. (2002). A robust detection and isolation scheme for abrupt and incipient faults in nonlinear systems. *IEEE transactions on automatic control*, 47(4):576–593.

Zhang, Y. and Jiang, J. (2000). Design of proportional-integral reconfigurable control systems via eigenstructure assignment. In *Proceedings of the 2000 American Control Conference. ACC (IEEE Cat. No. 00CH36334)*, volume 6, pages 3732–3736. IEEE.

Zhang, Y. and Jiang, J. (2008). Bibliographical review on reconfigurable fault-tolerant control systems. *Annual reviews in control*, 32(2):229–252.

Zhao, L., Gao, H., and Karimi, H. R. (2012). Robust stability and stabilization of uncertain T–S fuzzy systems with time-varying delay: an input–output approach. *IEEE Transactions on fuzzy systems*, 21(5):883–897.

Zhao, L. and Liu, Z. (2014). Vehicle velocity and roll angle estimation with road and friction adaptation for four-wheel independent drive electric vehicle. *Mathematical Problems in Engineering*, 2014.

Zhao, W., Qin, X., and Wang, C. (2018). Yaw and lateral stability control for four-wheel steer-by-wire system. *IEEE/ASME transactions on mechatronics*, 23(6):2628–2637.

Zhou, K. and Doyle, J. C. (1998). *Essentials of robust control*, volume 104. Prentice hall Upper Saddle River, NJ.

Živković, V., Nedić, B., and Đurić, S. (2020). Manufacturing specificity of vehicle's independent suspension system parts. *Vehicle Vozila i*, 31:31.